Université de Montréal

Mécanisme(s) d'action de l'insuline dans la prévention de l'hypertension et la progression de la tubulopathie dans le diabète: Rôle de hnRNP F, Nrf2 et Bmf

Par

Anindya Ghosh

Programme de science biomédcales

Faculté de Médecine

Thèse présentée à la faculté des études supérieures

en vue de l'obtention du grade de docteur docteur en philosophie (Ph.D)

en science biomédicales

Août 2018

Université de Montréal

Mécanisme(s) d'action de l'insuline dans la prévention de l'hypertension et la progression de la tubulopathie dans le diabète: Rôle de hnRNP F, Nrf2 et Bmf

par Anindya Ghosh

a été évaluée par un jury composé des personnes suivantes :

Dre Jolanta Gutkowska
Présidente rapporteuse

Dr John S.D. Chan
Directeur de recherche

Dre Shao-Ling Zhang
Codirectrice de recherche

Ashok Srivastava
Membre du jury

Jun-Li Liu
Examinateur externe

Daniel Bichet
Représentant de la doyenne

Résumé

Le diabète sucré est un trouble métabolique complexe qui se caractérise par une homéostasie anormale du glucose résultant en une concentration plasmatique trop élevée en glucose et due à un déficit absolu ou relatif de la production de l'insuline ou de son action. Les patients souffrant de diabète sont plus à risque de développer diverses complications comme la néphropathie diabétique (DN), qui demeure la principale cause de maladie rénale en phase terminale (ESRD) et est associée à une morbidité et mortalité cardiovasculaire accrue. Bien que les diabètes de type I et de type II (T1D et T2D) se développent par le biais de mécanismes différents, il n'existe pas de différences pathophysiologiques majeures entre la progression de la DN et ESRD pour les deux types de diabète.

La tubulopathie, qui comprend à la fois l'apoptose/atrophie tubulaire et la fibrose tubulo-interstitielle, est déjà bien acceptée comme marqueur final de la progression de la DN. Et quoique l'hyperglycémie et le stress oxydant soient tous deux associés à l'hypertension et aux lésions tubulaires, leurs mécanismes moléculaires précis d'action demeurent incertains. Pour les patients T1D, le traitement intensif à l'insuline par le biais d'injections quotidiennes demeure la thérapie la plus efficace mais est associé à de nombreux inconvénients, dont l'hypoglycémie. Le but de cette thèse est d'identifier des gènes ou molécules en aval de l'action de l'insuline comme nouvelles cibles thérapeutiques pour contrer la progression de la DN.

Dans un premier temps, nous avons examiné si l'insuline peut affecter l'expression rénale de Nrf2 dans le T1D et étudié les mécanismes sous-jacents. Le traitement avec l'insuline chez les souris Akita a permis de normaliser l'hyperglycémie, l'hypertension, le stress oxydant et les dommages rénaux; l'inhibition de l'expression rénale de Nrf2 et Agt et l'augmentation de l'expression de hnRNP F/K (ribonucléoprotéines nucléaires hétérogènes F et K) ont également été demontrées. In vitro en condition HG, l'insuline réprime la transcription de Nrf2 et Agt, mais stimule celle de hnRNP F/K via la signalisation p44/42 MAPK (p44/42 mitogen-activated protein kinase) dans les RPTCs. L'inhibition de p44/42 MAPK, hnRNP F ou hnRNP K au moyen de siRNA permet de renverser l'inhibition de la transcription de Nrf2 par l'insuline. Un élément de réponse a l'insuline (IRE) a également été identifié dans le promoteur du gène Nrf2 de rat auquel peuvent se lier hnRNP F/K. Dans des études réalisées sur des souris

hyperinsulinémiques-euglycémiques, l'expression de Nrf2 et Agt était diminuée alors que celle de hnRNP F/K était augmentée, indiquant que les effets de l'insuline sur l'expression de Nrf2 et Agt le sont principalement indépendamment de son effet hypoglycémiant.

Finalement, les mécanismes sous-jacents de l'action de l'insuline sur la prévention de l'apoptose des RPTCs ont été élucidés. Nous avons créé une souris Tg surexprimant le gène Bcl2-modifying factor (Bmf) humain, spécifiquement dans les RPTCs, et caractérisé ce modèle. Les mécanismes moléculaires de l'action de l'insuline dans la prévention de l'apoptose des RPTCs induite par Bmf et la perte des RPTCs dans des souris diabétiques ont également été étudiés. Afin de démontrer l'effet de l'insuline sur l'expression de Bmf, des souris Akita traitées avec des implants d'insuline, ainsi que des souris surexprimant hnRNP F spécifiquement au niveau des RPTCs ont été utilisées. Les souris Bmf-Tg présentent une augmentation de la pression systolique (SBP), du ratio albumine-créatinine urinaire (ACR), de l'apoptose des RPTCs et un plus grand nombre de RPTCs urinaires que les souris non-Tg. Le traitement avec l'insuline et la surexpression de hnRNP F dans les souris Akita permet de supprimer l'expression de Bmf des RPTCs et leur apoptose. In vitro dans les RPTCs en culture, l'insuline inhibe l'expression du gène Bmf induite par le HG via la voie de signalisation p44/42 MAPK. La transfection de siRNA contre hnRNP F prévient l'inhibition de la transcription de Bmf par l'insuline. HnRNP F inhibe la transcription de Bmf via un élément sensible à hnRNP F localisé dans le promoteur du gène Bmf.

En résumé, ces études ont permis de démontrer que l'activation chronique de Nrf2 par l'hyperglycémie aggrave la dysfonction rénale par le biais de l'augmentation de l'expression intrarénale de l'Agt et l'activation du système rénine-angiotensine dans le diabète. Nous avons montré que l'insuline stimule l'expression de hnRNP F et hnRNP K dans les RPTCs afin d'inhiber l'expression de Agt, Nrf2 et Bmf, et ultérieurement atténue l'hypertension et les dommages rénaux chez les souris diabétiques Akita. Les travaux présentés dans cette thèse ont donc permis d'identifier hnRNP F/K, Nrf2 et Bmf comme cibles potentielles pour le traitement de l'hypertension et de la maladie rénale dans le diabète.

Mots-clés : Rein, système rénine-angiotensine, angiotensinogène, catalase, hypertension, Bmf, néphropathie diabétique, apoptose, fibrose tubulo-interstitielle, espèces réactives de l'oxygène

Abstract

Diabetes mellitus is a complex metabolic disorder characterized by abnormal glucose homeostasis, resulting in higher plasma glucose due to an absolute or relative deficit in insulin production or action. People with diabetes have an increased risk of developing complications including diabetic nephropathy (DN), which is the major cause of developing end stage renal disease (ESRD) and is associated with increased cardiovascular morbidity and mortality. Although, type I and type II diabetes (T1D and T2D) are developed by different mechanisms, there is no major pathophysiological difference between nephropathy progression and ESRD in both diabetes.

Tubulopathy including tubular apoptosis/atrophy and tubule-interstitial fibrosis is known to be final marker for DN progression. Hyperglycemia and oxidative stress are associated with hypertension and tubular injury; their precise molecular mechanisms remain unclear. Intensive insulin treatment for T1D patients, including daily insulin injections is the most effective therapy but is associated with drawbacks such as hypoglycemia. The aim of this thesis is to identify downstream target genes or molecules of insulin action as potential therapeutic targets to counter DN progression.

Firstly, we investigated whether insulin affects renal Nrf2 expression in T1D and studied its underlying mechanism and reported that insulin treatment normalized hyperglycemia, hypertension, oxidative stress, and renal injury; inhibited renal Nrf2 and Agt gene expression; and upregulated heterogeneous nuclear ribonucleoprotein F and K (hnRNP F/K) expression in Akita mice. In vitro, insulin suppressed Nrf2 and Agt but stimulated hnRNP F/K gene transcription in HG via p44/42 mitogen-activated protein kinase (p44/42 MAPK) signalling in RPTCs. Inhibition with siRNAs of p44/42 MAPK, hnRNP F, or hnRNP K, reversed insulin inhibition of Nrf2 gene transcription. We further identified an insulin-responsive element (IRE) in rat Nrf2 promoter that binds to hnRNP F/K. In hyperinsulinemic-euglycemic clamp studies, renal Nrf2 and Agt expression were downregulated, whereas hnRNP F/K expression was upregulated, indicating insulin-mediated effects on Nrf2 and Agt expression largely occur independently of its glucose-lowering effect.

Secondly, the underlying mechanism of insulin action on preventing RPTC apoptosis was studied. In the present study, a Tg mouse overexpressing human Bcl2-modifying factor (Bmf) in RPTs was created and characterized. Furthermore, the molecular mechanism(s) of insulin action on preventing Bmf-induced RPTC apoptosis and loss in diabetic mice were investigated. To study the effect of insulin on Bmf expression, Akita mice implanted with insulin, specifically those overexpressing hnRNP F in their RPTCs, were used. Bmf-Tg mice exhibited higher systolic blood pressure (SBP), urinary albumin-creatinine ratio (ACR), RPTC apoptosis and more urinary RPTCs than non-Tg mice. Insulin treatment and hnRNP F-overexpression in Akita mice suppressed RPTC Bmf expression and apoptosis. In vitro, insulin inhibited HG-induced Bmf gene expression in RPTCs via p44/42 MAPK signaling. Transfection of hnRNP F siRNA prevented insulin inhibition of Bmf transcription. HnRNP F inhibited Bmf transcription via hnRNP F-responsive element in the Bmf promoter.

In summary, this thesis demonstrated that chronic Nrf2 activation by hyperglycemia aggravates renal dysfunction via enhanced intrarenal Agt expression and RAS activation in diabetes. It was demonstrated that insulin inhibits Agt, Nrf2, and Bmf expression in RPTCs via hnRNP F and hnRNP K expression and, subsequently, attenuates hypertension and kidney injury in Akita mice. This study identifies renal hnRNP F/K, Nrf2 and Bmf as potential targets for the treatment of hypertension and kidney injury in diabetes.

Keywords: Kidney, renin-angiotensin system, angiotensinogen, catalase, hypertension, diabetic nephropathy, Bmf, apoptosis, tubulointerstitial fibrosis, reactive oxygen species.

Table of Contents

Résumé iii
Abstract v
Table of Contents vii
List of Tables xii
List of Figures xiii
List of Abbreviations xvi
Acknowledgements xx
Chapter 1: Introduction 1
1.1 Diabetes Mellitus 2
1.1.1 A Brief History of Diabetes Mellitus: From Ants to Analogues 2
1.1.2 Types of Diabetes Mellitus 3
1.1.2.1 Type 1 Diabetes Mellitus (T1D) 3
1.1.2.2 Type 2 Diabetes Mellitus (T2D) 3
1.1.2.3 Gestational Diabetes Mellitus (GDM) 4
1.1.3 Prevalence of diabetes. 4
1.1.4 Pathogenesis of Diabetes 5
1.2 Role of Kidney and Homeostasis 7
1.2.1 Renal Physiology 7
1.2.2 Renal Histology 7
1.2.2.1 The Nephron 7
1.2.2.2 The Glomerulus 9
1.2.2.2 Glomerular Filtration Barrier 9
1.2.2.3 Podocytes 11
1.2.2.4 Proximal Tubules 12
1.2.2.6 Loop of Henle 14
1.2.2.6 Distal Tubules 15
1.2.2.5 Juxtaglomerular Apparatus 15
1.2.2.6 Tubuloglomerular Feedback 15

1.3 Chronic Kidney Disease (CKD) 18
1.3.1 Prevalence of Chronic Kidney Disease 19
1.3.2. Laboratory Measurements for CKD 19
1.4 Diabetic Nephropathy 20
1.4.1 The Pathogenesis and Progression of DN 20
1.4.2 Pathomechanisms of DN 22
1.4.2.1 Hyperglycemia and DN 23
1.4.2.2 Glycosylation and DN 24
1.4.2.3 Protein Kinase C and DN 26
1.4.2.4 Aldose Reductase Pathway and DN 27
1.4.2.5 Hypertension and DN 28
1.4.2.6 TGF-β and DN 30
1.5 ROS and Oxidative Stress 32
1.5.1 ROS Generation and ROS Sources in the Kidney 33
1.5.1.1 Mitochondrial ROS and DN 33
1.5.1.2 NADPH Oxidases and DN: 36
1.5.2 Antioxidants 40
1.5.2.1 Dietary antioxidant supplement: 40
1.5.2.2 Superoxide dismutase 40
1.5.2.3 Catalase 41
1.5.3 Nrf2-Keap1 system 42
1.5.3.1 Structure and Function of Nrf2 42
1.5.3.2 Regulation of Nrf2 43
1.5.3.3 Nrf2 activator Oltipraz 45
1.5.4.5 Nrf2 inhibitor Trigonelline 46
1.6 Renin-Angiotensin System (RAS) 47
1.6.1 Classical RAS 47
1.6.2 Local RAS 48
1.6.2.1 Intrarenal RAS 48
1.6.3 Components of intrarenal RAS 49
1.6.3.1 Prorenin and Renin 49

1.6.3.2 Angiotensinogen (Agt) 49
1.6.3.3 Angiotensin II (AngII) 50
1.6.3.4 ACE 51
1.6.3.5 ACE2 51
1.6.3.6 Angiotensin Receptors 52
1.6.4 Clinical trials with RAS blockers 54
1.7 Apoptosis 56
1.7.1 Mechanism involved in apoptotic cell death 56
1.7.1.1 Extrinsic apoptosis 56
1.7.1.2 Intrinsic apoptosis 58
1.7.2 Regulation of Apoptosis by Bcl-2 Family Proteins: The Sentinels of Life and Death 58
1.7.2.1 The BH3-only protein Bmf 61
1.8 The Heterogenous Ribonucleoproteins 64
1.8.1 hnRNP K 66
1.8.2 hnRNP F 66
1.9 Insulin Signaling in the Kidney 68
1.9.1 Insulin Receptors 68
1.9.2 Insulin Signaling Pathways 69
1.10 Animal model of Diabetic Nephropathy 72
1.10.1 Mouse Model of Type 1 Diabetes 72
1.10.1.1 Streptozotocin (STZ)-Induced Diabetes 72
1.10.1.2 Akita *Ins2*$^{+/C96Y}$ mutant mice 73
1.10.2 Mouse models of type 2 diabetes 73
1.10.2.1 db/db mouse model 73
1.10.2.2 High fat diet model 73
1.11 Objective and hypothesis of the present study 75
Chapter 2: Article 1 78
Abstract 80
Introduction 81
Materials and Methods 82

Results 87
Discussion 92
Acknowledgements 96
Disclosure 97
Abbreviations 98
Figure Legends 99
Chapter 3: Article 2 119
Abstract 121
Introduction 122
Results 124
Discussion 130
Materials and Methods 134
Acknowledgements 140
Figure Legends 142
Chapter 4: Discussion 159
4.1 Genetically Modified Akita Mice Model (T1D) 161
4.2 Antioxidant Therapies for DKD 163
4.3 Effect of Catalase Overexpression in Diabetic Mice. 163
4.4 Nrf2 Activation: The Double-Edged Sword 165
4.5 Akita Mice Treated with Insulin 170
4.6 Insulin Signaling and Nrf2 172
4.7 Promoter Studies and IREs 173
4.8 Insulin on Gene Expression is Independent of Glucose Lowering Effect 175
4.8.1 Hyperinsulinemic Euglycemic Clamp 175
4.8.2 Studies with SGLT2 inhibitor 175
4.9 Potential Activator of hnRNP F/K: Hordenine 176
4.10 Transgenic mice overexpressing hBMF in the RPTC 177
4.11 Effect of Bmf Overexpression in RPTC 178
4.12 Regulation of Bmf by Insulin 180
4.13 Regulation of Bmf by Nrf2 182
4.14 Limitations of the study 183

4.14.1 Limitations of Akita mice model 183
4.14.2 hnRNP F/K Knockout Mice 183
4.14.3 Role of Other BH3-only Proteins in Diabetic Kidneys 184
4.15 Conclusion 184
Chapter 5: Unpublished Results and Research Perspectives 186
5.1 Generation of Nrf2 transgenic mice 187
5.2 Bmf Promoter analysis 189
5.3 Role of Nrf2 in the regulation of Bmf 191
5.4 Adminstration of SGLT2 Inhibitor Canagliflozin in Akita mice 192
5.5 Future Experiments 195
5.5.1 Generation of Nrf2KO: KAP2-rNrf2-Tg Mice 195
5.5.2 Generation of Akita-Erk1$^{-/-}$:Pax8-Cre-Erk2$^{-/-}$ Mice 196
Chapter 6: References 198
Annex 1: List of Publications i

List of Tables

Table 1-1: Substances secreted or reabsorbed in the nephron and their locations…….17
Table 1-2: Prognosis of CKD by GFR and albuminuria category. 18
Table 1-3: Pathological classification of diabetic nephropathy 22
Table 1-4: Action of angiotensin receptors in kidney and vasculature..... 54
Table 1-5: Summary of major trials with RAS blockers. 55
Table 1- 6: Animal models of DN… 74
Table 2-1: Article 2: Table 1-Primer sequences……..…..……..…….103
Table 2-2: Article 2: Table 2-Antibodies..……..…….104
Table 2-3: Article 2: Table 3-Physiological Measurements……..105
Table 2-4: Article 2: Supplementary Table 1……....116
Table 3-1: Article 3: Table 1-Physiological Measurements……..……147
Table 3-2: Article 3: Supplementary Table 1……...…….157
Table 3-3: Article 3: Supplementary Table 2…….……..158
Table 5-1: Physiological parameters …….....192

List of Figures

Figure 1-1: Estimated diabetes-related deaths and healthcare expenditure in 2017 6
Figure 1-2: Estimated number of people with diabetes worldwide 6
Figure 1-3: Diagram of kidney, juxtaglomerular nephron and superficial nephron. 8
Figure 1-4: Anatomy of glomerulus.. 8
Figure 1-5: Transmission electron micrograph of the glomerular capillary cell wall. 10
Figure 1-6: Podocyte foot process effacement..... 11
Figure 1- 7: Schematic location and ultrastructure of proximal tubular S_1–S_3 segments. 13
Figure 1-8: Proximal tubule markers of different segments.. 14
Figure 1-9: Proposed mechanism of tubuloglomerular feedback (TGF). 16
Figure 1-10: Pathological lesions of DKD. 21
Figure 1-11: Pathophysiology and progression of DN 21
Figure 1-12: Consequences of AGEs formation in the diabetic kidney. 25
Figure 1-13: Physiological effects and cellular mechanisms of DAG–PKC activation induced by hyperglycemia 27
Figure 1-14: Polyol pathway and aldose reductase. 28
Figure 1-15: Pathophysiology of hypertension 29
Figure 1-16: Overview of oxidative stress mediators involved in the pathogenesis of DKD...32
Figure 1-17: Various intracellular sources of ROS. 33
Figure 1-18: Factors associated with mitochondrial dysfunction and ROS generation in DN 34
Figure 1-19: Classical components of NOX 37
Figure 1-20: Function of Nox4 in different renal cells. 38
Figure 1-21: Domain structures of Nrf2 and repressor Keap1 42
Figure 1- 22: Regulation of Nrf2 by different pathways. 44
Figure 1-23: Components of RAS. 47
Figure 1- 24: Pathways of cellular apoptosis 57
Figure 1- 25: Domain organization of various Bcl2 family members. 59
Figure 1-26: The two alternative models for Bax/Bak activation. 61
Figure 1-27: Function and regulation of Bmf. 62
Figure 1-28: Different cytoplasmic and nuclear function of hnRNPs 64

Figure 1- 29: Domain structure of the hnRNP family members. 65
Figure 1-30: Insulin signaling pathways. 71
Figure 1-31 Proposed hypothesis for the current study 77
Figure 2-1: Article 2: Figure 1 106
Figure 2-2: Article 2: Figure 2 107
Figure 2-3: Article 2: Figure 3 108
Figure 2-4: Article 2: Figure 4 109
Figure 2-5: Article 2: Figure 5 110
Figure 2-6: Article 2: Figure 6 111
Figure 2-7: Article 2: Figure 7 112
Figure 2-8: Article 2: Supplementary Figure 1 113
Figure 2-9: Article 2: Supplementary Figure 2 114
Figure 2-10: Article 2: Supplementary Figure 3 115
Figure 2-11: Article 2: Supplementary Figure 4 116
Figure 2-12: Article 2: Supplementary Figure 5 117
Figure 2-13: Article 2: Supplementary Figure 6 118
Figure 3-1: Article 3: Figure 1 148
Figure 3-2: Article 3: Figure 2 149
Figure 3-3: Article 3: Figure 3 150
Figure 3-4: Article 3: Figure 4 151
Figure 3-5: Article 3: Figure 5 152
Figure 3-6: Article 3: Figure 6 153
Figure 3-7: Article 3: Figure 7 154
Figure 3-8: Article 3: Figure 8 155
Figure 3-9: Article 3: Supplementary Figure 1 156
Figure 4-1: Proposed Model 185
Figure 5-1: Generation of KAP2-rNRF2-Tg mice 187
Figure 5-2: Gene expression pattern in rNRF2-Tg mice 188
Figure 5-3: Bmf promoter analysis 189
Figure 5-4: Rat Bmf promoter analysis 190
Figure 5-5: Role of Nrf2 in Bmf expression 191

Figure 5-6: Physiological Measurements…….192
Figure 5-7: Nrf2 and Agt expression ……193
Figure 5-8: Caspase 3 and Bmf expression……...194
Figure 5-9: Diagram to generate Nrf2KO:KAP2-rNrf2-Tg mice…… 195
Figure 5-10: Diagram to generate Akita-Erk1$^{-/-}$:Pax8-Cre-Erk2$^{-/-}$ Mice……..196
Figure 5-11: hnRNP F/K expression in ERK1 KO and Pax8-Cre-Erk2 KO mice ……...197

List of Abbreviations

ACE	Angiotensin converting enzymes.
ACE2	Angiotensin-converting enzyme-2
ACEi	ACE inhibitors.
ACR	Albumin/creatinine ratio
AGEs	Advanced glycosylation end products.
Agt	Angiotensinogen
Ang I	Angiotensin I
Ang II	Angiotensin II
Ang IV	Angiotensin IV
Ang1–7	Angiotensin 1-7
APS	Pleckstrin homology.
AR	Aldose reductase.
ARBs	Angiotensin receptor blockers.
ARE	Antioxidant response element.
AT1R	Angiotensin II type 1 receptor.
AT2R	Angiotensin II type 2 receptor.
Bmf	Bcl2-modifying factor
Cat	Catalase
CKD	Chronic kidney disease
CNC	Cap ‘n’ collar
CTGF	Connective tissue growth factor
Cul3	Cullin 3
DAG	Diacylglycerol.
DM	Diabetes mellitus.
DN	Diabetic nephropathy
ECM	Extracellular matrix.
eGFR	Estimated glomerular filtration rate
eIF4E	Eukaryotic translation initiation factor 4E
EMSA	Electrophorretic mobility shift assay
ER	Endoplasmic reticulum
ERK	Extracellular-signal-regulated kinases
ESRD	End stage of renal disease
GBM	Glomerular basement membrane
GDM	Gestational diabetes Mellitus
GFR	Glomerular filtration rate
Grb2	Growth factor receptor binder-2.
GSH	Glutathione
GSHPx	Glutathion Peroxidase.
gsk3	Glycogen synthase kinase-3.
GTFs	General transcription factors.
H&E	Hematoxylin and eosin
H2O2	Hydrogen peroxide.
HG	High glucose
hnRNP F	Heterogenous nuclear ribonucleoprotein F

hnRNPK	Heterogenous nuclear ribonucleoprotein K
hnRNPs	Heterogenous nuclear ribonucleoproteins
HO-1	Hemoxygenase-1
hrACE2	Human recombinant ACE2
IDF	Diabetes federation.
IGF-1	Insulin-like growth factor 1
IL-6	Interleukin-6
IR	Insulin receptor
IRE	Insulin-responsive element
IRR	Insulin receptor-related
IRSs	Insulin receptor substrates
JGA	Juxtaglomerular apparatus
KDOQI	Kidney disease outcomes quality initiative
Keap1	Kelch-like ECH-associated protein 1
MAPK	Mitogen-activated protein kinase.
Mapkk	Map kinase kinase.
Mapkkk	Map kinase kinase kinase.
MAS	Mas oncogene receptor
MAU	Microalbuminuria
NF-κB	Nuclear transcription factor κappa B.
NKF	National kidney foundation
NO	Nitric oxide.
NOD	The non-obese diabetic.
NOS	Nitric oxide synthase
NQO1	Quinone oxidoreductase 1.
Nrf1	Nuclear respiratory factor 1
Nrf2	Erythroid 2-related factor 2
PAS	Periodic acid schiff
PDK1	Phosphoinositide-dependant Kinase1.
PI3K	Phosphoatidylinositol 3-kinase.
PKC	Protein kinase C.
RAGE	Receptor of advanced glycosylation end products
RAS	Renin-Angiotensin System
RBPs	RNA-binding proteins
RE	Response Element
rMLC-2	Rat myosin light chain-2.
RNA Pol II	RNA polymerase II
ROS	Reactive oxygen species
RPTCs	Renal proximal tubular cells
SBP	Systolic blood pressure
SDH	Sorbitol dehydrogenase.
SH2	Src homology2.
siRNA	Small interfering RNA
SOD	Superoxide dismutases.
ssDNA	Single strand DNA
STZ	Streptozotocin

T1D	Type 1 diabetes mellitus
T2D	Type 2 diabetes mellitus.
TBM	Tubular basement membrane.
TBP	TATA-binding protein
TF	Transcription factors
TFBSs	Transcription factors binding sites
TGF-β	Transforming growth factor.
TNF-α	Tumor necrosis factor- α
TSS	Transcriptional start site.
UTR	Untranslated region.
Vitamin C	Ascorbic acid

But Mousie, thou art no thy-lane,
In proving foresight may be vain:
The best laid schemes o' Mice an' Men
Gang aft agley,
An' lea'e us nought but grief an' pain,
For promis'd joy!

— Robert Burns (To a Mouse)

Acknowledgements

Foremost, I would like to express my sincere gratitude to my advisor Dr. Chan for the continuous support of my Ph.D. study and research, for his patience, motivation, enthusiasm and immense knowledge. His guidance helped me in all my time of research and writing of this thesis. I could not have imagined a better mentor for my study. Besides my advisor, I would like to thank my co-director Dr. Shao-Ling Zhang for her insightful encouragements and valueable guidance.

In addition, I would like to thank the rest of the thesis committee: Dr. Jolanta Gutkowska, Dr. Ashok Srivastava, Dr. Jun-Li Liu, and Dr. Daniel Bichet, for serving as my committee members and for their encouragement, insightful comments and hard questions.

A very special gratitude goes to Ms. Isabelle Chénier, whose help and advice are impossible to overestimate. Her helpful attitude, organizational skills, continuous support to all lab members and her bright ideas make our lab effective and efficient.

My sincere thanks go to Dr. Chao-Sheng Lo and Ms. Shuiling Zhao, who helped me everyday immensely with their valueable suggestions and technical expertise. I would like to thank all the lab members of our laboratory, Henry Nchienzia, Min-Chun Liao, Dr. Shiao-Ying Chang, Xinping Zhao, Dr. Shaaban Abdo, Dr. Yixuan Shi, Abouzar Otoukesh and Yessoufou Aliou, for their patience and valueable suggestions. Working with them and learning from them was a real pleasure and a valueable experience.

With all my gratitude I would like to thank my fellow mates in the CRCHUM, specially Ju Jing Tan, Henry Leung, Laura Sognigbé, Paul Tan, Estelle Simo, Ashish Jain for all of your support and encouragements.

Finally, I would like to thank my Maa and my brothers Liton and Rony. I thank you with all of my heart for your love and support.

Chapter 1: Introduction

1.1 Diabetes Mellitus

1.1.1 A Brief History of Diabetes Mellitus: From Ants to Analogues

The earliest description of diabetes was found in 'Ebers Papyrus' which was written around 1550 BC and describes various remedies to treat "too great emptying of urine" which probably refers to a polyuric state (1). Around the same time, ancient Hindu writings described people with 'a mysterious and deadly disease that caused intense thirst, enormous urine output and wasting away of the body'. Hindu healers observed that flies and ants were attracted to the urine of the victims which can be described as the first clinical test of diabetes. They termed the condition 'madhumeha' or honey urine (2). Apollonius of Memphis probably used the Greek term 'diabetes' for the first time around 230 BC, which means 'to go through' or siphon as the disease drained patients of more fluids than they could consume. Gradually, the latin term for honey 'mellitus' was attributed to diabetes due to its link with sweet urine. In the fifth century AD, the Hindu physicians Charaka and Sushruta, were probably the first to differentiate between two types of diabetes mellitus by observing thin individuals who develop diabetes at a younger age in contrast to heavier individuals who develop the disease later and can live longer after diagnosis. (1, 3).

It was only in 1815 that Eugene Chevreul of Paris proved that the sugar present in the urine of diabetic patient was glucose (1, 4). Claude Bernard, a professor of physiology at Sorbonne University, discovered liver glycolysis and linked glycogen metabolism with diabetes and hypothesized that excess sugar secretion from liver glycogen into the blood leads to diabetes (5). In 1869, Paul Langerhans, a German medical student found islet cells in the pancreas and in 1893, French scientist Gustave–Edouard Laguesse suggested that islets of Langerhans might secrete the substrate that controls glucose. Later in 1909, Belgian physician Jean de Mayer named the presumed substance produced by the islets of Langerhans as "insulin" (1, 6, 7).

In 1921, the key breakthrough came from the findings of Frederick Grant Banting when he started working with John James Rickard Macleod, Charles Best and James Collip at the University of Toronto. On January 11, 1922, after successful experiments on animals with pancreatic extract, they injected Leonard Thompson, a 14-year-old patient, weighted 64 lb, with their extract. Although early results were very disappointing, a few weeks later, a second

injection with Collip's refined "isletin" showed astonishing results. Leonard's blood glucose fell from 520 to 120 mg/dl within 24h and urinary ketones disappeared. He gained weight and lived a relatively healthy life for 13 years but died of pneumonia at the age of 27. In 1923, their work was awarded by Nobel prize for the discovery of insulin (8). In 1978, with the emergence of recombinant DNA technology, production of the first recombinant insulin was announced and in July 1996, the FDA approved the first recombinant DNA human insulin analogue, lispro (Humalog). Today, more than 300 insulin analogues are available including about 70 from animal species, 80 chemically modified insulins and 150 biosynthetic insulins (2, 9).

1.1.2 Types of Diabetes Mellitus

Diabetes mellitus, or diabetes is a chronic condition that occurs when the blood glucose level or glycemia increases because the body cannot produce any or enough insulin or use insulin effectively. There are mainly three types of diabetes, type 1 diabetes, type 2 diabetes and gestational diabetes (10).

1.1.2.1 Type 1 Diabetes Mellitus (T1D)

T1D is caused by an autoimmune disease where antigen-specific T cells selectively destroy insulin producing pancreatic β-cells. As a result, no or very little insulin is produced by the body, leading to hyperglycemia. Although 5%-10% of people with diabetes have T1D, it remains a serious, life-threatening disease. It develops more frequently in children and adolescents and is considered the third most common disorder during childhood. The cause of T1D is not fully understood but multiple environmental and genetic risk factors (eg. HLA haplotypes) have been implicated (11). People with T1D need daily insulin injection to survive.

1.1.2.2 Type 2 Diabetes Mellitus (T2D)

T2D, also known as non-insulin dependent diabetes, is characterized by chronic insulin resistance and a progressive decline in pancreatic β-cell function leading to hyperglycemia. This whole process contributes to develop insulin resistance in liver, muscle and adipose tissue. To compensate for insulin resistance, β-cells start producing more insulin which might exceed maximum capacity resulting in β-cell failure (12). T2D accounts for 90% of all cases of diabetes. It is mostly seen in older people, but it is now seen increasingly in children, adolescents and

younger adults due to the rising prevalence of obesity, physical inactivity and poor diet. The cause of T2D is not completely understood but overweight and obesity, old age as well as genetics or family history have been linked with it (13).

1.1.2.3 Gestational Diabetes Mellitus (GDM)

One of the most common complications in pregnancy is GDM, which affects 14% of pregnancies worldwide. Mild hyperglycemia that is first detected during pregnancy is classified as GDM. Women with considerably higher blood glucose during pregnancy are classified as women with hyperglycemia in pregnancy. GDM usually exists as a transient disorder affecting pregnant women typically around the 2^{nd} and 3^{rd} trimesters of their pregnancy and resolves after delivery. However, pregnant women with hyperglycemia have at least a seven-fold higher risk of developing GDM in subsequent pregnancies and half of them later develop T2D. Offspring born to mothers with GDM develop increased lifelong risks of developing obesity, T2D and metabolic syndrome (13-16).

1.1.3 Prevalence of diabetes.

Today, even with the most advanced pharmaceutical interventions and preventive health care system, the epidemic of diabetes is on the rise across the globe and the cure continues to elude us. Improved diagnosis, the rapid population growth, aging, urbanization, increased prevalence of obesity and physical inactivity are some of the main reasons for today's diabetes epidemic. Current and future quantification of the prevalence of diabetes and affected people will allow rational planning and allocation of resources (17).

According to the International Diabetes federation (IDF) statistics, in 2017, 424.9 million people worldwide, or 8.8% of adults 20-79 years, were estimated to have diabetes. The number would increase to 451 million if the age group was extended to 18-99 years. The IDF anticipates this number will rise to 629 million of people by 2045. This could mean that one in every10 people will have the disease by 2045 (13). As a result, individuals with diabetes will be at higher risk for several complications such as myocardial infarction, stroke, blindness, lower limb amputation, and end stage renal disease (kidney failure, ESDR). According to IDF, 4 million adults (20-79 years) died due to diabetic complications worldwide in 2017. In 2017, North

America alone spent almost 52% (383 billion) of the total amount spent globally on diabetes. Figure1-1 summarizes worldwide diabetes related death and expenditure (13).

The good news is that we have learned a lot in past decades about preventive care for diabetes. Around 25 years ago, the Diabetes Control and Complications Trial (DCCT) showed that intensive glycemic control could reduce the risk of diabetes complications including diabetic nephropathy (18). Although the prevalence of obesity, a major cause of T2D, remains high, it has nonetheless remained stable between 2003-04 and 2009-10 in the United States (US) due to the focus given to public healthcare efforts on obesity (19). In the US, the rate of diabetic complications has declined during the past two decades (1990-2010) including cardiovascular events, but not ESRD. In fact, ESRD increased among older patients. A huge burden of disease still persists in the US because of the overall continued increase in the prevalence of diabetes (20). However, the largest increase will take place in developing countries with poor economy. According to the IDF estimates, by 2045, people with diabetes in South and Central America will increase by 61%, South East Asia by 81%, Middle East and North Africa by 110% and Africa by 156% (figure 1-2) (13). Asia became the "diabetes epicenter" of the world, characterized by a rapid increase in prevalence over a short period and onset at a relatively young age due to the presence of a metabolic obese phenotype (21). These alarming estimates indicate the need for urgent improvements in the performance of the health care system for people with diabetes in poorer economic countries.

1.1.4 Pathogenesis of Diabetes

Diabetes is a group of diverse and complex diseases characterized by chronic hyperglycemia. Without proper glycemic control, all types of diabetes can lead to complication in different parts of body, resulting in hospitalization and mortality. Usually, the injurious effects of hyperglycemia can be separated into microvascular and macrovascular disease (22). The microvascular complications are due to damage to small blood vessels and include diabetic retinopathy, nephropathy and neuropathy, whereas macrovascular complications affect larger blood vessels and cause cardiovascular diseases (CVD) including coronary artery disease (CAD) leading to myocardial infraction, peripheral artery disease contributing to stroke, diabetic encephalopathy and diabetic foot (13). In addition, diabetes had also been associated with other disease such as cancer (23), physical disability (24) and depression (25).

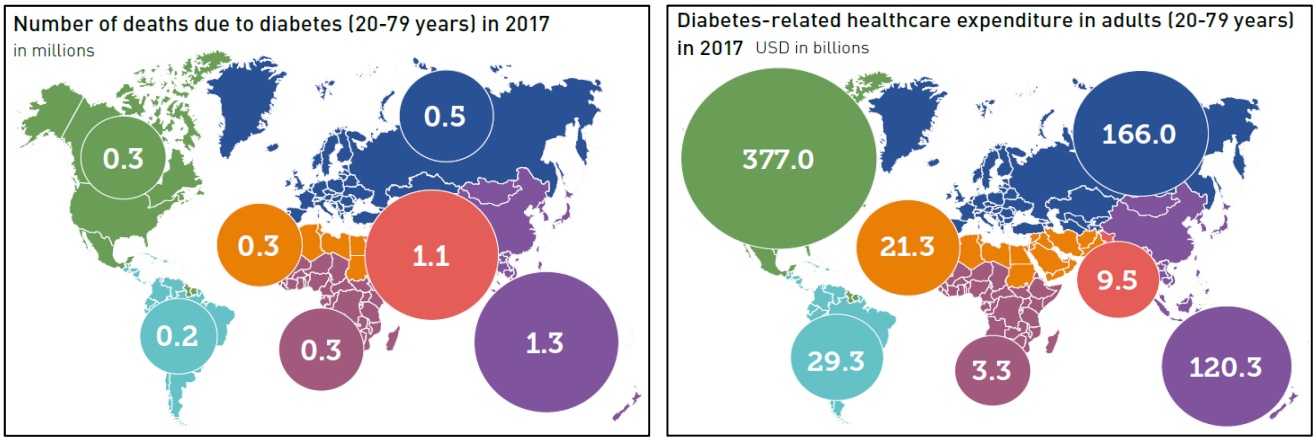

Figure 1-1: Estimated diabetes-related deaths and healthcare expenditure in adults (20-79 years) worldwide in 2017 (13).

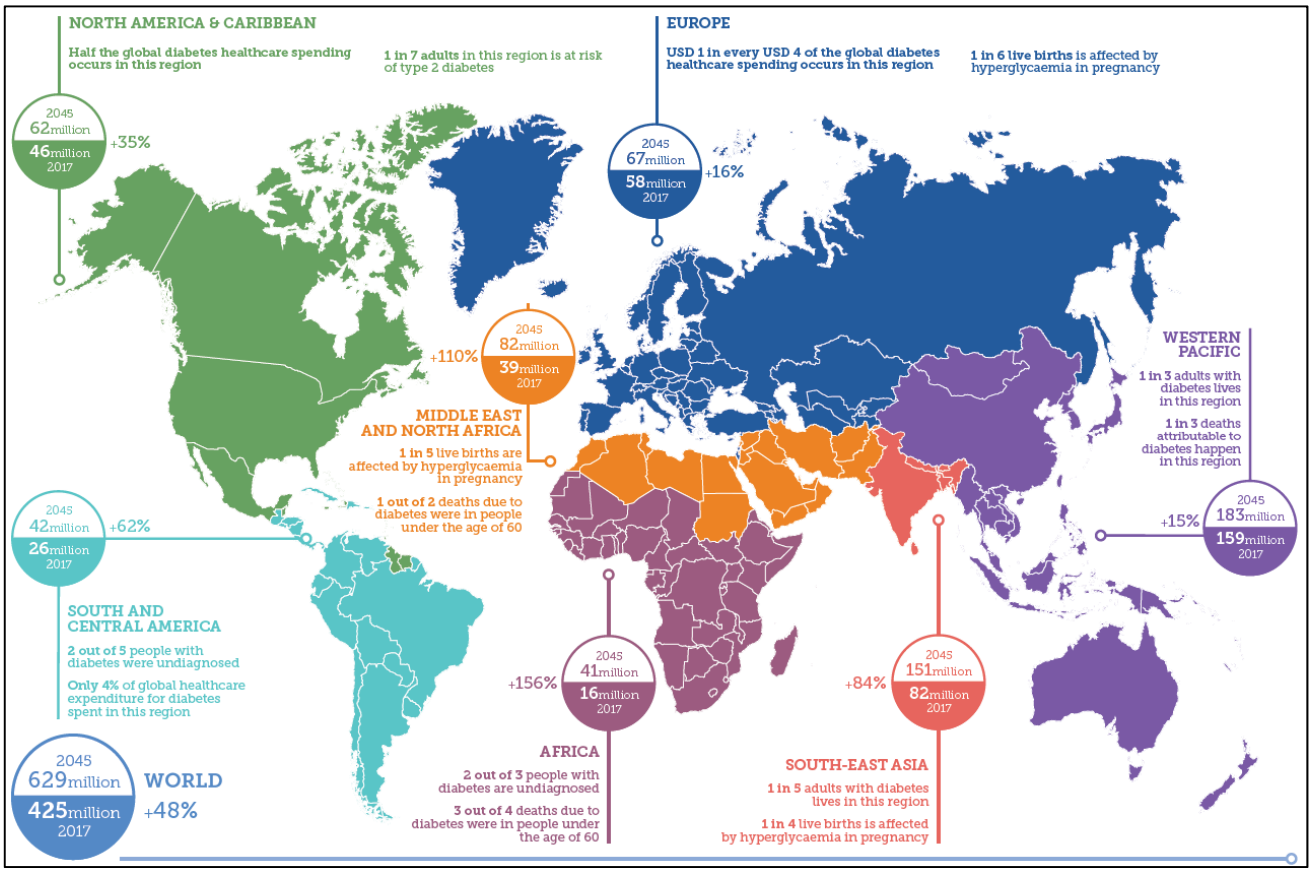

Figure 1-2: Estimated number of people with diabetes worldwide and per region in 2017 and 2045 (20–79 years) (13)

1.2 Role of Kidney and Homeostasis

1.2.1 Renal Physiology

The kidneys play a vital role in maintaining the homeostasis of extracellular fluid. They serve three main functions. Firstly, they act as a filter and remove metabolic wastes (including urea, uric acid and creatinine) and toxins from the circulating blood and excrete them through urine. Secondly, they maintain the volume and composition of the extracellular fluid with in normal range by regulating water and electrolyte balances, osmotic balance, acid base balance and by actively reabsorbing essential molecules such as amino acids, ions, glucose and water. Thirdly, they produce or activate hormones such as erythropoietin, 1-25- dihydroxy-vitamin D3, renin, angiotensin II, which are involved in erythrogenesis, Ca^{++} metabolism and the regulation of blood pressure and blood flow (26, 27).

1.2.2 Renal Histology

The kidney consists of three major parts – (a) **Renal cortex**, the outermost region of the kidney which lies immediately below the tough connective tissue capsule. (b) **Renal medulla,** situated below the cortex, comprises the inner part of the kidney. The cortex and medulla are mainly composed of nephrons, blood vessels, nerves and lymphatics. The medulla is divided into renal pyramids which are triangular structure containing densely packed nephrons. (c) **Renal pelvis,** it connects the kidney to the circulatory and nervous systems with rest of the body (28). Different parts of the kidney and nephron are shown in the figure 1-3.

1.2.2.1 The Nephron

The nephron is the main functional unit of the kidney. There are almost 1,200,000 nephrons in the human kidney (figure 1-3). They are responsible for producing urine by removing waste and excess substances from the blood. The nephron consists of a renal corpuscle, proximal tubule, loop of Henle and collecting duct system. The renal corpuscle also known as glomerulus, consists of glomerular capillaries and Bowman's capsule. Based upon the

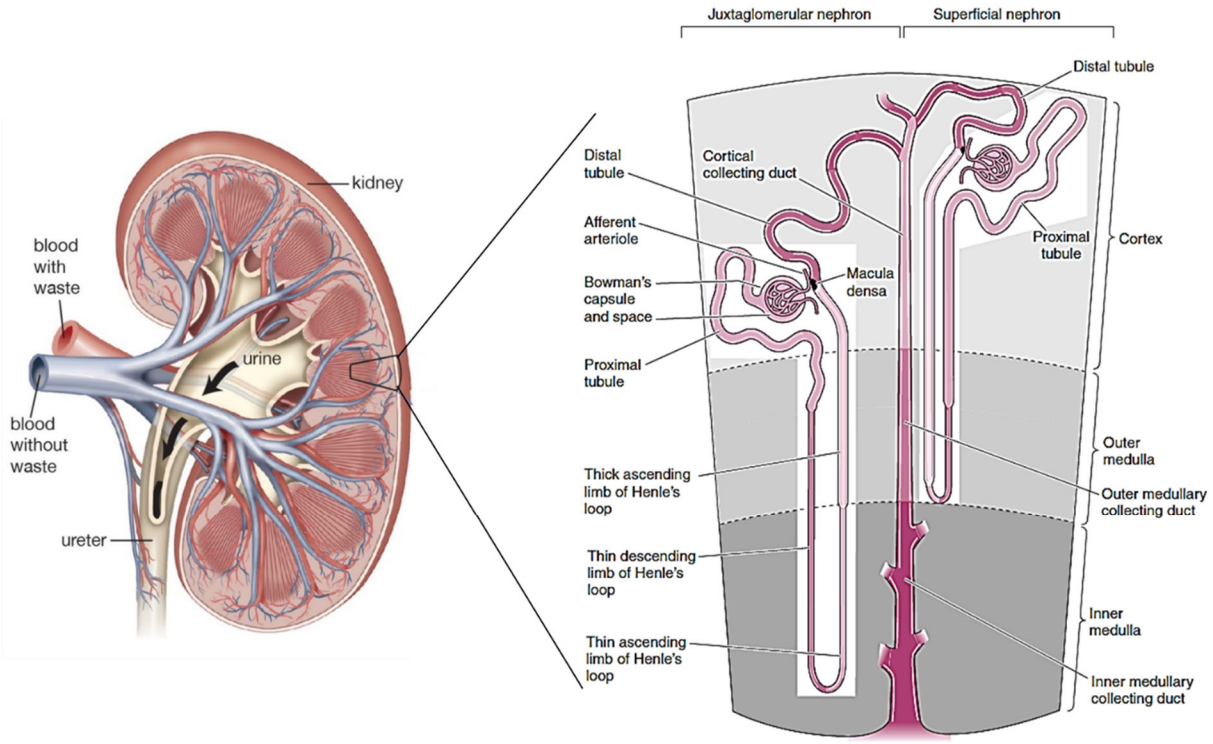

Figure 1-3: Diagram of a kidney, juxtaglomerular nephron and superficial nephron (28, 29).

A.

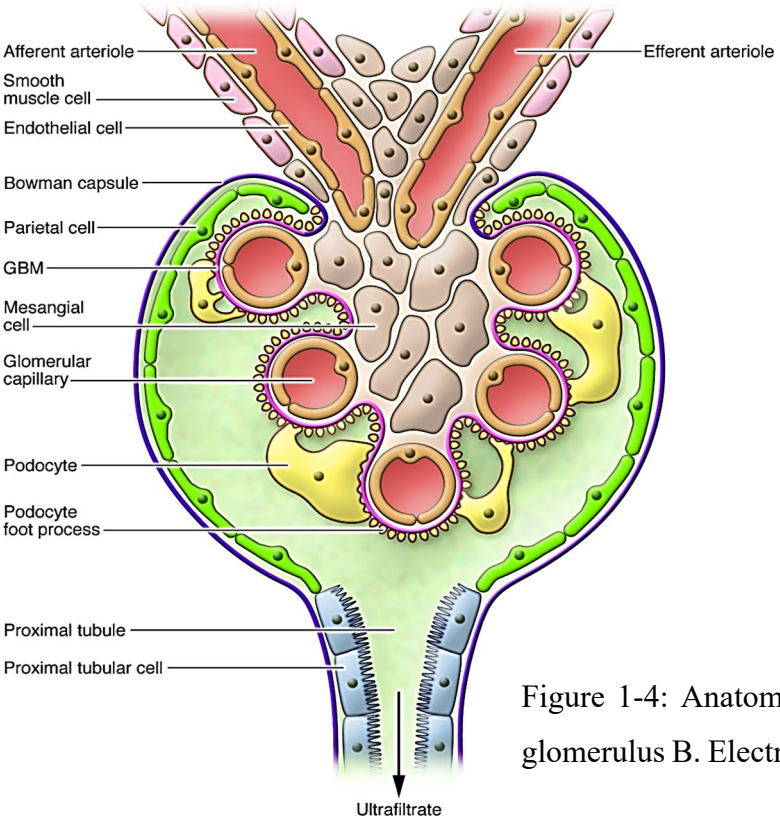

B.

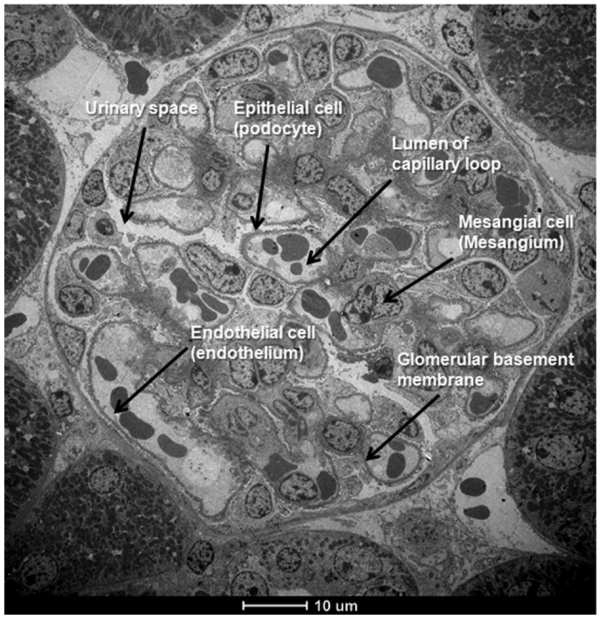

Figure 1-4: Anatomy of glomerulus. A. simplified diagram of the glomerulus B. Electron microscopy of a mouse glomerulus (30) (31).

location of the glomerulus, nephrons can be further divided in two types –. superficial or cortical nephron and juxtamedullary nephron (28). As shown in figure 1-3, glomeruli of superficial nephrons are located nearer to the outer parts of the cortex and their loops of Henle are short, whereas, juxtamedullary nephrons have a glomerulus near the junction of the cortex and medulla, with their loops of Henle penetrating deep into the medulla. In humans, about 85% of nephrons are superficial nephrons and only about 15% are juxtamedullary nephrons (32).

1.2.2.2 The Glomerulus

The glomerulus (or more precisely glomerular tuft) is a network of capillaries that receives its blood supply from an afferent arteriole of renal circulation that drains into the efferent arteriole. The glomerulus is surrounded by Bowman's capsule (BC), which transforms into the epithelium of proximal tubules at the urinary pole, while Bowman's space opens into the tubular lumen. The glomerular capillaries network is held together by the mesangium and covered by the glomerular basement membrane (GBM) (28).

Mesangial cells are specialized smooth muscle-like cells, which can contract and regulate blood flow to the glomerulus (31). The outer aspect of the GBM is surrounded by a layer of epithelial cells called podocytes (figure 1-4 and 1-5). The process of urine formation starts with the blood filtered through the glomerular capillaries into Bowman's capsule by passive movement. The plasma ultrafiltrate collected in the Bowman's capsule then flows into the proximal tubule, where smaller molecules, such as water, glucose and other minerals, ions get reabsorbed (28).

1.2.2.2 Glomerular Filtration Barrier

The glomerular filtration barrier (GFB) is a highly sophisticated blood filtration interface that allows the passage of small and midsize molecules, but it is impermeable to macromolecules, such as red blood cells and plasma albumin. The glomerular filter consists of three layers – glomerular endothelial cells, glomerular basement membrane and epithelial podocytes (figure 1-5). All three layers contribute greatly in the glomerular filtration barrier and damage to any layer might results in leakage of macromolecules passing through the GFB and ending up in the urine (33, 34).

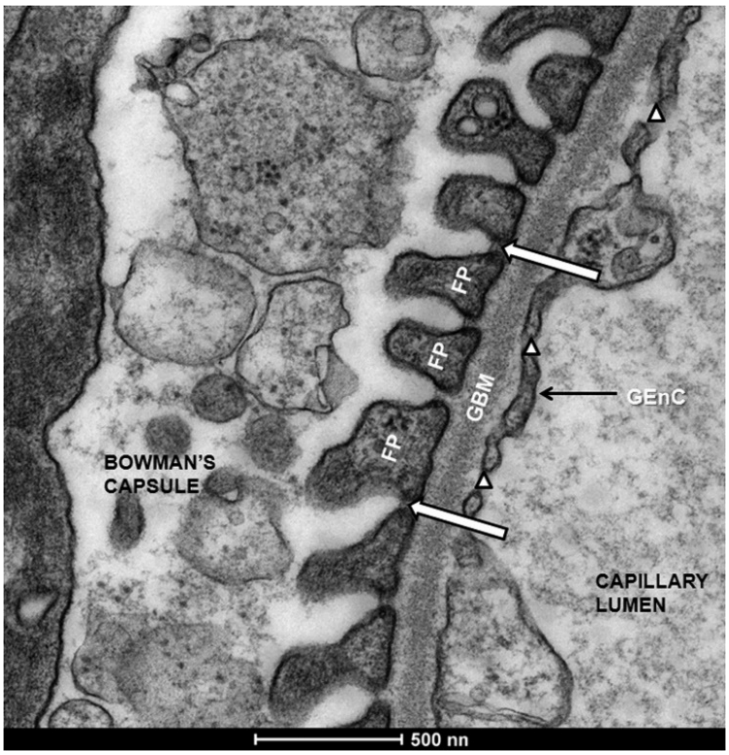

Figure 1-5: Transmission electron micrograph of the glomerular capillary cell wall. GEnCs, glomerular endothelial cells whose fenestrations are denoted by Δ, the GBM, and podocytes, whose tertiary foot processes are denoted by FP. Examples of a slit diaphragm between the foot processes are indicated by thick arrows (31).

Proteinuria and microalbuminuria are widely used as clinical urinary biomarkers of diabetic nephropathy. Some other biomarkers that can predict which component of GBM is affected are given below:

a. Podocyte level: - nephrin and podocalyxin

b. GBM level: collagen, laminin

c. Glomerular endothelial cells level: VEGF

d. Tubular cell level: NGAL, NAG, KIM, angiotensinogen (35)

1.2.2.3 Podocytes

Podocytes are highly specialized, terminally differentiated cells incapable of replication or proliferation. We are born with approximately 800 podocytes/glomerulus with roughly 2 million nephrons in two kidneys. The only way for the glomerulus to compensate the function of lost podocytes consists of cell hypertrophy which results in the glomerular tuft being covered by fewer podocytes, which eventually increases their vulnerability to further challenges (36).

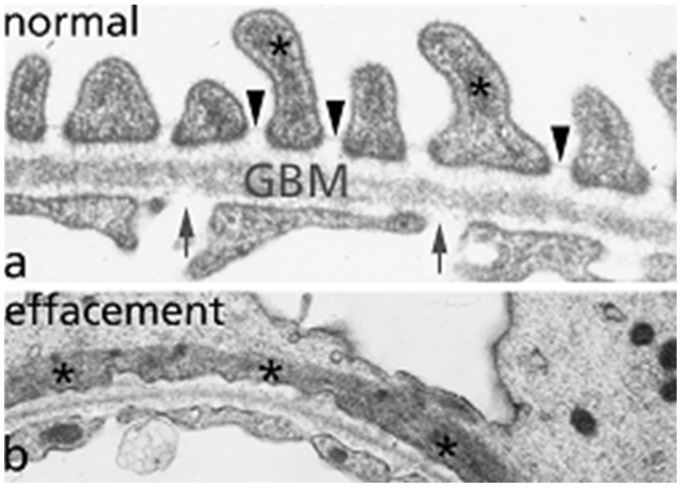

Figure 1-6: Podocyte foot process effacement. a. Normal condition, b. After podocyte effacement. Podocyte foot process is denoted by * (37).

Podocytes have long fingerlike, regularly spaced, interdigitated foot processes that completely encircle the outer surface of glomerular capillaries and form 40 nm wide filtration slits between adjacent processes. Each filtration slit is bridged by a thin diaphragm, the filtration slit diaphragm, which inserts laterally into the podocyte cell membrane and connects adjacent processes (figure 1-5). Podocyte integrity is essential for the maintenance of GFB. Under pathological conditions, when podocytes are injured or lost, they respond in a similar pattern. The intercellular junctions and the cytoskeletal structure of the foot processes are altered to a simplified effaced phenotype which is known as podocyte effacement (figure 1-6). This alteration leads to the disappearance of the slit diaphragm structure and results in the development of albuminuria. (36, 38).

1.2.2.4 Proximal Tubules

Proximal tubules receive the plasma filtrate from glomeruli and reabsorb the major fraction of water, sodium and other solutes from the tubular lumen back to the blood compartment (or peritubular capillaries), whereas other solutes such as uric acid, creatinine, organic anions, potassium and protons are secreted into the filtrate. The most distinctive feature of the proximal tubules is the presence of a "brush" border on the apical end (luminal surface) of the tubules due to the presence of microvilli. The basolateral plasma membrane of adjacent proximal tubule cells is extensively interdigitated. This provides an increased apical and basolateral plasma membrane surface area that corresponds to a higher transcellular solute transport rate. Proximal tubules have a higher content of mitochondria in their cytoplasm to provide the excess energy necessary for pumping ions and molecules against their concentration gradient (39). Substances reabsorbed and secreted by proximal tubules are shown in table 1-1.

Proximal tubules can be divided into two parts based on their location, morphology and function – proximal convoluted tubules (PCT) and proximal straight tubules (PST). It is called proximal tubule as it begins at the urinary pole of the renal corpuscle and convolutes, as it twists around. PCT is mainly situated at the renal cortex (cortical labyrinth), whereas PST is the straight segment of tubule situated in the medullary rays of the cortex and outer medulla (figure 1-7a) (39). Although the PST of the juxtamedullary nephrons are not straight, they are defined as "straight parts" by their location in the outer stripe (40). Proximal tubules can be further defined ultra-structurally into three segments: S1, S2, and S3 (figures 1-7b and 1-7c). The S1 comprises the first half of the convoluted tubule. S1 segment contains the largest basolateral plasma membrane surface area with the highest Na-K-ATPase activity per unit membrane area and the highest mitochondrial density, which decreases from S1 to S3. S1 transforms into S2 gradually within the second half of the convoluted portion and is evidenced by a reduction in structural complexity. S2 cells also form the first part of the proximal straight tubules in the medullary rays. The S2 segment contains prominent lysosomes and endocytic apparatus which is diminished in the S3 segment whereas the amount and size of peroxisomes increase from S2 to S3. In rats, the size of microvilli in S2 is markedly shorter than in S1 (rat S1: ~4.5 -4.0 μM, S2: ~4.0 -1.0 μM). In rabbits, dogs and humans, the size of microvilli further decreases in S3,

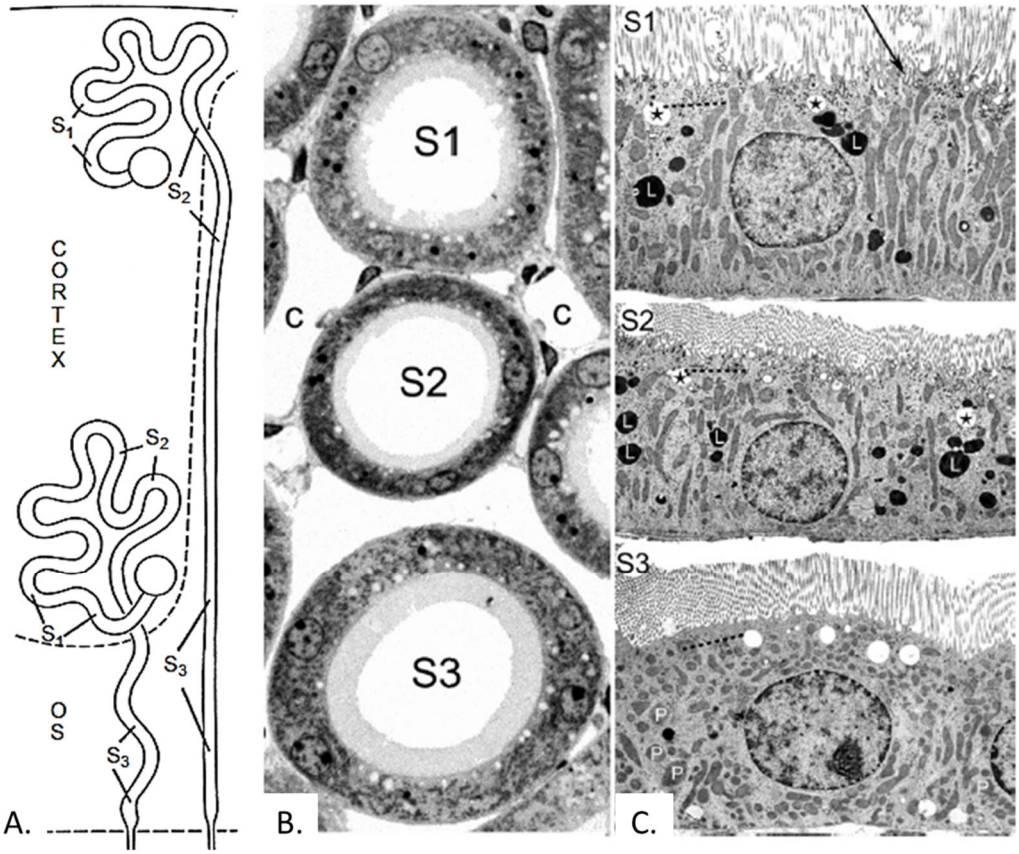

Figure 1-7: Schematic location and ultrastructure of proximal tubular S_1–S_3 segments in superficial and juxtamedullary nephrons. (A.) For superficial nephrons, S_1 segments begin at the urinary pole of the renal corpuscle in the superficial cortex, transform gradually into S_2 segments within the labyrinth, and S_2 are transformed at different levels within the medullary rays. S_3 segments terminate at the border of the outer stripe (OS) to the inner stripe. For juxtamedullary nephrons, S_1 and S_2 segments start at the urinary pole of the renal corpuscle in the inner cortex, and S3 segments also terminate at the border of the outer stripe (OS) to the inner stripe. (B) Profiles of S1, S2, and S3 segments of juxtamedullary proximal tubules; note the differences in brush border length, in cell height, cytoplasmic density, and outer diameter (c: Peritubular capillaries; Rat: 1mm Epon section; ×~1000). (C): Ultrastructures of S1, S2 and S3 proximal tubular cells in the rat kidney. Note that the mitochondria in S1 and S2 are in lateral cell processes, whereas in S3 they are mainly scattered throughout the cytoplasm. The endocytic apparatus is in the subapical cytoplasm which is most prominent in S1 and S2 segments (broken lines), whereas endosomes (stars) and lysosomes (L) are localized deeper in the cytoplasm. There are few vacuolar apparatus and lysosomes present in the S3 segment, but peroxisomes (P) are more frequent in this segment. C, capillaries. Magnification: X ~5400 from transmission electron microscopy (39).

whereas it is longest in S3 in rats (39). However, ultrastructural analyses reveal no obvious segmentation of the proximal tubule in C57/BL/6J mice, including the length of the brush border microvilli (41).

There are several well-known markers to identify proximal tubules (PT) such as aquaporin 1 (*AQP1*), sodium glucose cotransporter (*SGLT2* or *SLC5A2)*, megalin, prominin-1. With the advancement of technologies, it is now possible to separate the S1, S2, S3 sections of PT. Recently, studies with single cell transcriptomics identified several genes that are specifically expressed in different segments as shown below in figure 1-8 (42, 43),

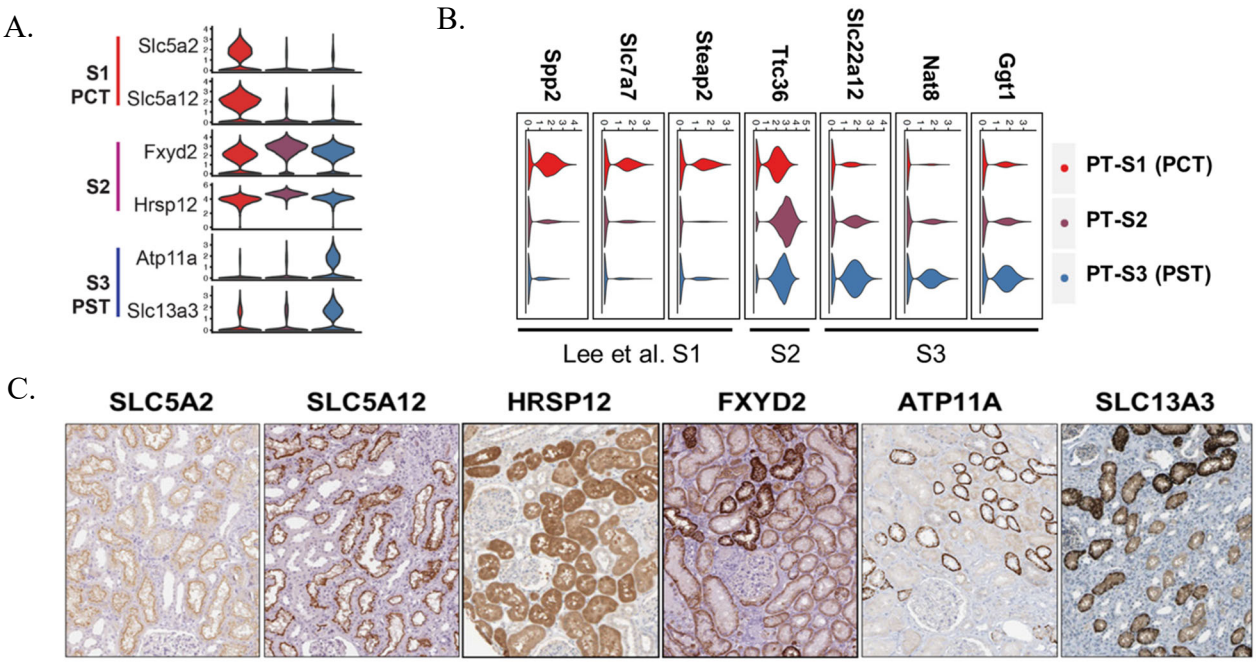

Figure 1-8: Proximal tubule markers of different segments. (A&B). Violin plot showing the expression level of different genes in S1, S2 and S3 segments of PT. PCT, proximal convoluted tubule, PST, proximal straight tubule. (C). The immunohistochemistry (IHC) data from The Human Protein Atlas showing marker expression patterns in proximal tubules (42, 43).

1.2.2.6 Loop of Henle

The loop of Henle carries filtrate from the proximal convoluted tubules to the distal convoluted tubules in the cortex. Functionally, it can be divided into three parts: A. The thin descending limb – where water is highly permeable, but ions are less permeable. B. The thin ascending limb that is impermeable to water but permeable to ions, C. The thick ascending limb (TAL), where almost 25% of the filtered sodium is reabsorbed by the $Na^+/K^+/2Cl^-$ co-transporter

(NKCC2). Its main function is to create a concentration gradient by the specific ionic and aqueous channel composition of each part to concentrate the urine. Major substances reabsorbed or secreted are shown in table 1-1

1.2.2.6 Distal Tubules

The distal tubules are a short segment of the nephron between the loop of Henle and the collecting duct. Only 5-10% of filtered sodium and chloride is reabsorbed by distal tubules under physiological conditions (44). Sodium reabsorption is mainly mediated by the aldosterone regulated thiazide sensitive Na-Cl cotransporter (NCC) (45), and to a lesser extent by sodium proton exchanger NHE2. It also plays a central role in maintaining calcium and magnesium homeostasis and participates in net K^+ and acid secretion (table1-1) (44). After distal tubules, connecting ducts then descend towards the renal pelvis and empty urine into the ureter.

1.2.2.5 Juxtaglomerular Apparatus

The juxtaglomerular apparatus (JGA) comprise a collection of specialised cells where thick ascending limb (TAL) contacts the afferent and efferent arterioles of the same nephron (figure 1-3 and 1-4A). It performs two major functions: (1) the high distal tubular NaCl induced afferent arteriolar vasoconstriction (tubuloglomerular feedback) and (2) low tubular NaCl induced renin release (46). The JGA includes (a) macula densa cells which represent specialized tubular cells at the end of the thick ascending limb of Henle's loop that are positioned adjacent to the glomerulus (figure 1-3). Their apical membrane is exposed to tubular fluid, whereas their basilar aspects are in contact with the cells of mesangium and the afferent arteriole, (b) the vascular smooth muscle cells (VSMC) and renin secreting granule cells in the afferent arteriole wall and (c) cells of extraglomerular mesangium, which fill the angle between the afferent and efferent glomerular arteriole, determine vasoconstriction or vasodilation via mesangial cell contraction (figure 1-4A) (47).

1.2.2.6 Tubuloglomerular Feedback

In the kidney, tubuloglomerular feedback (TGF) is the principal mechanism for autoregulation of GFR and renal blood flow (RBF). TGF acts as a negative feedback control mechanism which uses information from distal tubular fluid flow rate to control RBF. Because

GFR is affected by RBF, and thus distal fluid flow rate, TGF helps to maintains appropriate levels of GRF and RBF. TGF mechanism act by the coordinated interaction between cellular sensors – macula densa cells, mediators – juxtaglomerular cells and effectors – renal afferent and efferent arterioles. In response to increased flow of tubular fluid TGF decreases GFR by following a sequence of events (figure 1-9): (1) Changes in the Na^+, K^+, and Cl^- concentrations in the tubular fluid are sensed by the macular densa via the Na^+-K^+-$2Cl^-$ cotransporter (NKCC2) in its luminal membrane. The macula densa then send this information to the justaglomerular cells via a concentration-dependent uptake of Na^+, K^+, and Cl^- by NKCC2. (2) Cotransport dependent hydrolysis of ATP in macula densa cells would lead to enhanced generation of adenosine (ADO) by 5′-nucleotidase. (3) ADO is then transported to the interstitium and activates adenosine A_1 receptors, triggering an increase in cytosolic Ca^{2+} in extraglomerular mesangial cells (MC). (4) Gap junctions transmit the Ca^{2+} signaling to the target cells in the afferent arteriole, which results in the inhibition of renin secretion and afferent arteriolar vasoconstriction, thereby decreasing GFR. Local angiotensin II (Ang II) and neuronal nitric oxide synthase (NOS I) activity modulate this response (48). However, in response to decrease tubular fluid flow, TGF promotes renin secretion and RAS activation which leads to increased GFR.

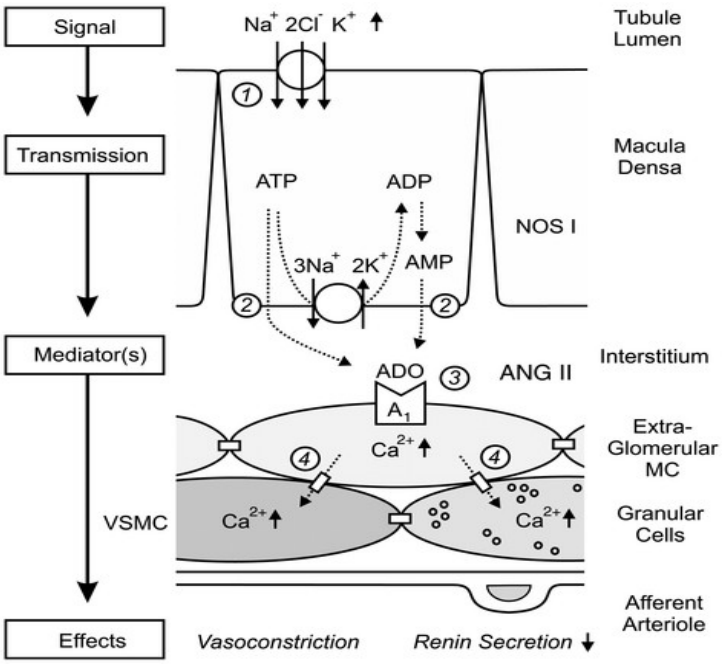

Figure 1-9: Proposed mechanism of tubuloglomerular feedback (TGF) (48).

Substance	Description	Proximal Tubule	Loop of Henle	Distal Tubule	Collecting Ducts
Glucose	Almost 100% reabsorbed by proximal tubule. When blood glucose level exceeds 160-180 mg/dl kidneys fail to reabsorb all glucose and secrete excess into urine developing glucosuria.	Almost 90% reabsorbed by SGLT2 (S1), and 10% by SGLT1 (S3) on the apical side; and secreted by GLUT2 (S1), GLUT 1 (S3), on the basolateral side	-	-	-
Oligopeptides, proteins, amino acids	Almost 100% reabsorbed by proximal tubules.	Reabsorbed by Na^+-co-transporter, B(0)AT3, B(0)AT1, PEPT1, PEPT2 etc.	-	-	-
Urea	Maintains osmolality. Transported by urea transporter UT-A (*SLC14a2*)	50% reabsorbed by diffusion; also secreted	Secretion, diffusion in descending limb	-	Reabsorption in medullary collecting ducts; diffusion
Sodium	Uses mainly NHE3, NHE2, NKCC2, Na^+-K-ATPase to transport transcellularly.	65% reabsorped. Mainly mediated by the Na^+/H^+ exchanger NHE3 at brush border and partly by Na^+ transporter coupled with substrates	25% reabsorbed, in thick ascending limb; mainly by NKCC2	5% reabsorbed, sodium-chloride symporter, NHE2	5% reabsorbed, stimulated by aldosterone, active
Chloride	Usually follows sodium. Active (transcellular) and passive (paracellular)	Reabsorbed, symport with Na^+ and K^+, diffusion	Reabsorbed at thick ascending limb, NKCC2	reabsorption by sodium-chloride cotransporter	reabsorbed symport, passive
Water	Reabsorbed by aquaporin water channels. Influenced by antidiuretic hormone (ADH).	Mainly reabsorbed by. AQP1(S1), also reported by AQP4 (mice, S3)	Reabsorbed only in descending limb, impermeable to ascending limb	Reabsorbed by AQP2	reabsorption increases by ADH, (via arginine vasopressin receptor 2)
Bicarbonate	Maintain acid-base balance.	80%-90% reabsorbed with sodium symport, (NHE3, S3)	reabsorption mainly by NHE3,NHE2	-	reabsorption intercalated cells, via band 3 and pendrin, Cl^-antiport
Protons	maintains electrochemical gradient across the cell to facilitate solute transport	Secrated, diffution	-	Secreted , active	Secreted, active (intercalated cells)
Calcium	Uses calcium ATPase, sodium-calcium exchanger	reabsorption	reabsorption (thick ascending) via passive transport	-	reabsorbed in the presence of parathyroid hormone
Phosphate		85% Reabsorption via Npt2a, NaPi-IIa, SLC34A1, Npt2c, NaPi-IIc, SLC34A3, Pit-2. Inhibited by parathyroid hormone.	-	reabsorbed, diffution	-
Potassium		65% reabsorbed	20% reabsorbed at thick ascending mainly by NKCC2	secreted, active	secretion via Na^+/K^+-ATPase, regulated by aldosterone
Magnesium		Reabsorption, TRPM6, TRPM7	Reabsorbed in thick ascendinglimb	reabsorption	-
Carboxylate		100% reabsorbed by carboxylate transporters.	-	-	-

Table 1-1: Substances secreted or reabsorbed in the nephron and their locations (39, 49)

1.3 Chronic Kidney Disease (CKD)

According to the international guidelines, CKD is defined as a decline in kidney function shown by a glomerular filtration rate (GFR) of less than 60 ml/min/1.73m^2, or markers of kidney damage or both, lasting more than 3 months regardless of the cause. The kidney function can no longer sustain life over time when GFR is decreased to less than 15 ml/min/1.73 m^2, a condition termed as End Stage Renal Disorder (ESRD) (50). When patients with CKD develop ESRD, they require kidney replacement therapy in the form of dialysis or kidney transplantation to survive. According to KDIGO recommendations CKD can be divided into different stages based on cause, GFR category (CKD Stage 1-5 as G 1-5), and by albuminuria category (A1, A2, A3) (measured by albumin: creatinine ratio or ACR) (Table-2) (51). For example, a patient with an estimated GFR of 40 ml/min/1.73 m^2 and an ACR of 30 mg/mmol has CKD G3bA2 (or simply CKD Stage 3b).

Prognosis of CKD by GFR and Albuminuria Categories: KDIGO 2012				Persistent albuminuria categories Description and range		
				A1	A2	A3
				Normal to mildly increased	Moderately increased	Severely increased
				<30 mg/g <3 mg/mmol	30-300 mg/g 3-30 mg/mmol	>300 mg/g >30 mg/mmol
GFR categories (ml/min/ 1.73 m^2) Description and range	G1	Normal or high	≥90			
	G2	Mildly decreased	60-89			
	G3a	Mildly to moderately decreased	45-59			
	G3b	Moderately to severely decreased	30-44			
	G4	Severely decreased	15-29			
	G5	Kidney failure	<15			

Table 1-2: Prognosis of CKD by GFR and albuminuria category. Green, low risk (if no other markers of kidney disease are present, no CKD); Yellow, moderately increased risk; Orange, high risk; Red, very high risk (51).

1.3.1 Prevalence of Chronic Kidney Disease

Patients with CKD have significantly higher rates of morbidity, mortality, hospitalization and healthcare utilization. Globally, diabetes and hypertension constitute the main causes of CKD. Worldwide, diabetes accounts for 30-50% of all causes of CKD, affecting 285 million (6.4%) adults, and this number is expected to reach by 69% in developed countries and 20% in developing low income countries (50). In 2000, hypertension accounted for 25% of all CKD patients and is estimated to increase 60% by 2025 (52). According to the latest report from United States Renal Data System (USRDS), overall prevalence of CKD in the US in 2011 to 2014 was 14.8% with stage 3 CKD (6.6%) among adults (53). In 2017, USRDS also reported, there were 741,037 prevalent cases of ESRD, with 285,614 of cases having diabetes. The prevalence of ESRD continues to rise by approximately 20000 cases per year (54). In 2015, the heath care associated cost for patients with CKD was $64 billion and another $34 billion for ESRD (55). The cost for ESRD is projected to rise by $54 billion by 2020 (56).

1.3.2. Laboratory Measurements for CKD

Clinically, CKD is defined by the persistent proteinuria and estimated GFR (eGFR) < 60 ml/min/1.73m^2 persisting for more than 3 months. Normal kidneys usually do not allow proteins to pass through the glomerular filter, but under pathological condition, they may allow large proteins such as albumin to leak from the blood to the urine. Proteinuria is easily measured by immunoassay, whereas GFR indicates the kidney function – it estimates how much blood passes through the glomeruli per minute. GFR is generally measured by an endogenous or exogenous filtration marker. KIDGO recommends to estimate GFR by using serum creatinine or serum Cystatin C ($eGFR_{creat}$ or $eGFR_{cys}$) (51). Inulin clearance is also used to precisely measure GFR, but due to its complexity, it is not preferred clinically (57). Inulin clearance is routinely used for mouse models because of its fast and accurate GFR estimation. Changes in kidney structure, including interstitial fibrosis, scarring and tubular atrophy, are closely related to GFR and proteinuria. Histologically, tubular cell area measurement is also associated with GFR (50). CKD biomarkers including cystatin C, blood urea nitrogen, B2-microglobulin, kidney injury molecule-1, neutrophil gelatinase-associated lipocalin (NGAL), fibroblast growth factor 23 and asymmetric dimethylarginine (ADMA) gives valuable early detection method for CKD (58).

1.4 Diabetic Nephropathy

Diabetic nephropathy (DN) also known as diabetic kidney disease (DKD) is a major microvascular complication of diabetes and is the principal cause of ESRD, leading to the need of dialysis, otherwise resuling in fetal consequences. The rising global prevalence in diabetes and CKD has encouraged research efforts to tackle the growing epidemic of DN.

1.4.1 The Pathogenesis and Progression of DN

DN is a progressive disease that takes many years to develop. It is classically characterised by the presence of microalbuminuria (defined as >30mg but <300mg urinary albumin excreted, UAE, per day) and reduced renal function reflected by an increase in plasma creatinine concentration and a decrease in GFR (59). Hyperglycemia and increased blood pressure levels are the major risk factors for DN. If untreated, ~80% of T1D patients will progress to overt nephropathy or clinical albuminuria (>300mg UAE per day) by 10-15 years. 50% of T1D patients with overt nephropathy will develop ESRD within 10 years and 75% within 20 years, whereas, 20% to 40% of T2D individuals with microalbuminuria will develop overt nephropathy by 15 years. Only ~20% of T2D individuals with overt nephropathy will progress to ESRD by 20 years (60, 61).

Different pathophysiological events leading to DN and progression to ESRD can be divided into early (haemodynamic and metabolic) and late (cellular and tissue remodelling) events (figure 1-11). In the early events, increased glucose filtration and glomerular hyperfiltration induce tubular hyper-reabsorption of glucose and sodium, which leads to glomerular and tubular hypertrophy and ultimately progresses to glomerulosclerosis and tubule atrophy. Injury and loss of glycocalyx and fenestration in endothelial cells leads to proteinuria and subsequently leads to microvascular rarefication promoting atrophy and scaring. Local expression of cytokines (angiotensin II etc.), chemokines, and immune cell recruitment (inflammation) also promotes tissue remodelling, contributing to atrophy and scarring (figure 1-10 and 1-11) (62).

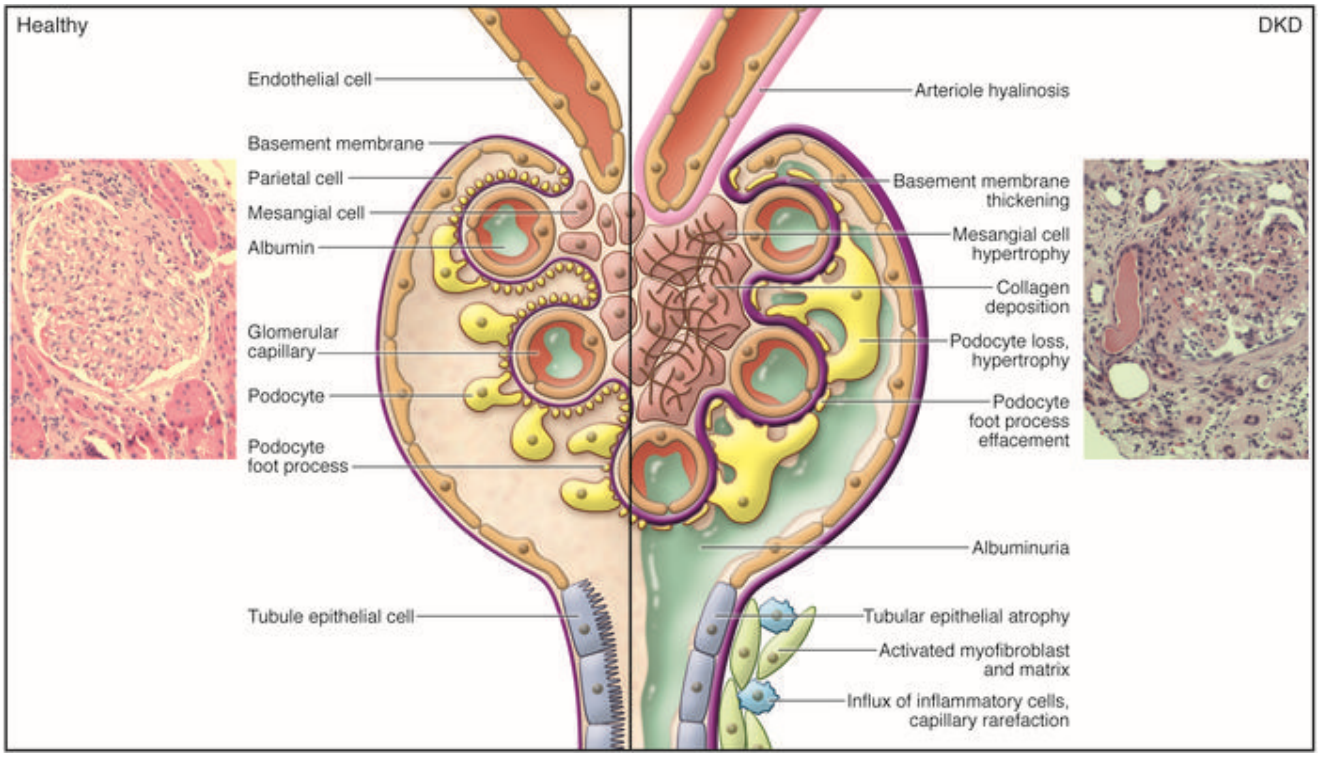

Figure 1-10: Pathological lesions of DKD. The normal healthy glomerulus is impermeable to albumin. In contrast, the diabetic glomerulus displays arterial hyalinosis, mesangial expansion, collagen deposition, basement membrane thickening, podocyte loss and hypertrophy, albuminuria, tubular epithelial atrophy, accumulation of activated myofibroblasts and matrix, influx of inflammatory cells, and capillary rarefaction. Moreover, PAS staining of normal healthy human glomerular section and a kidney section from a sample with DKD has been shown (63).

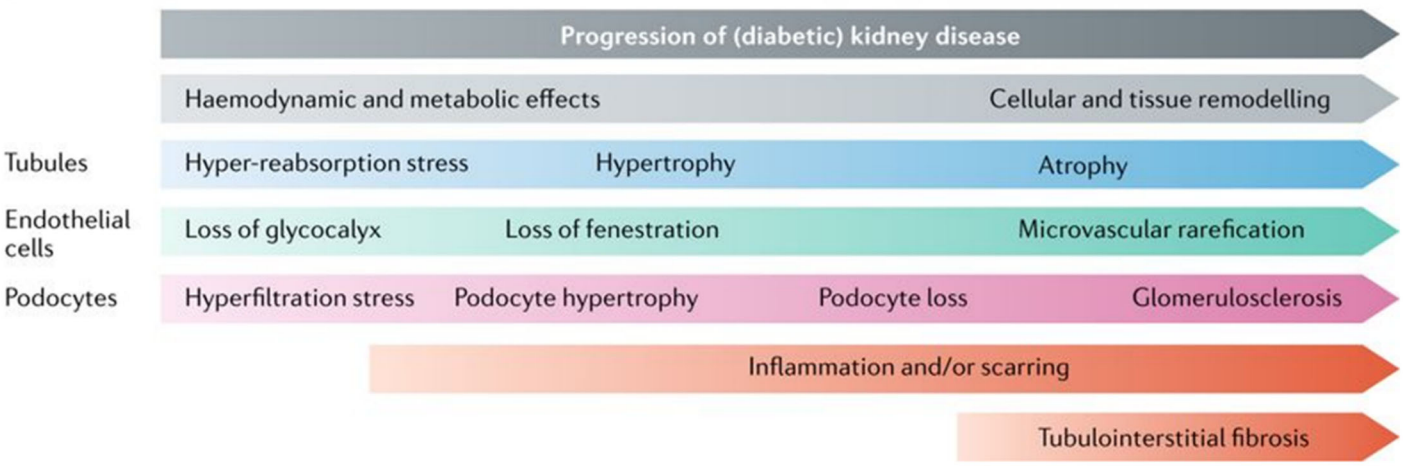

Figure 1-11: Pathophysiology and progression of DN (62).

Histopathologically DN can be distinguished in different phases of development. In the preliminary phase, glomerular hyperfiltration and hyperperfusion occur in the nephron at the glomerulus level, before the beginning of any measurable clinical changes. Afterwards, thickening of glomerular basement, glomerular hypertrophy and mesangial expansion, nodular glomerulosclerosis (Kimmelstiel-Wilson lesion) and arteriolar hyalinosis takes place (figures 1-10).

According to Tervaert *et al.*, pathological classification of DN includes four classes as described in table 1-3 below (64).

Class	Description and criteria
I	Mild or nonspecific light microscopy changes and GBM thickening proven by electronic microscopy. GBM > 395 nm in female and GBM >430 nm in male individuals
IIa	Mild mesangial expansion in >25% of the observed mesangium
IIb	Severe mesangial expansion in >25% of the observed mesangium
III	At least one convincing Kimmelstiel–Wilson lesion (nodular sclerosis)
IV	Advanced diabetic glomerulosclerosis. Global glomerular sclerosis in >50% of glomeruli

Table 1-3: Pathological classification of diabetic nephropathy (DN) (64).

1.4.2 Pathomechanisms of DN

Although the pathogenesis of DN is not fully understood, several factors play an important role in its progression such as hyperglycemia, hypertension, heamodynamic factors (*e.g.* renin-angiotensin-aldosterone system, endothelin systems), podocytes, reactive oxygen species, activation of protein kinase C, activation of the aldose reductase pathway, increased advanced glycation end products (AGEs), and cytokines like angiotensin II, TGF-β etc. Some of these factors are discussed below in detail.

1.4.2.1 Hyperglycemia and DN

Hyperglycemia leads to kidney damage directly or through hemodynamic modifications. In a normal glycemic adult human (plasma glucose concentration ~5.5 mmol/L; GFR 125ml/min/1.73m^2), kidneys can filter 160-180g of glucose per day. The proximal tubules reabsorbs 99% of glucose mainly by SGLT2 (~97%). This reabsorbed glucose is returned to circulation w hich contributes to maintain blood glucose level and overall metabolic balances.

Hyperglycemia increases the amount of glucose filtrated through the glomerular filtration barrier and induces hyper-reabsorption of glucose by proximal tubules (500-600g/24h), reaching plasma glucose concentration of approximately 10-12 mmol/L. This hyper-reabsorption of glucose induces glucose transporter expression (*e.g.* SGLT2) and increases energy consumption in the proximal tubules leading to an increase in oxygen demand in the cortex and outer medulla. This contributes to ischemia and expression of stress markers like NGAL and KIM1 in proximal tubules. Overwork by proximal tubules leads to proximal tubule hypertrophy and elongation, subsequently leading to kidney hypertrophy. Furthermore, SGLT2 increases sodium reabsorption in the proximal tubules, thereby decreasing sodium delivery to the distal tubules and macula densa. A low concentration of NaCl in the macula densa disables the tubuloglomerular feedback mechanism and leads to dilation of the afferent arteriole and persistent glomerular hyperfiltration. Concomitant activation of the renin angiotensin system (RAS) further increases single-nephron GFR (SNGFR) and glomerular hypertension (62, 65).

Along with tubular cells, as discussed above, persistent hyperglycaemia also exposes endothelial cells, mesangial cells, and podocytes to several stressors like hyperfiltration, hyper-reabsorption, advanced glycosylation end products, oxidative stress, and epigenetic changes, leading to further nephron loss over a period of time.

However, hyperglycemia alone does not account fully as the causative risk factor for DN in humans. Mauer *et al.* showed that, kidneys from nondiabetic human donors develop GBM and mesangial lesions when transplanted into patients with diabetes but the rate of development of these lesions differs widely in different kidneys irrespective of the blood glucose control (66, 67). This indicates that, in humans, hyperglycemia is necessary but not sufficient to cause renal damage and that other factors are needed for the clinical manifestation of DN.

Three major mechanisms have been proposed that might explain how hyperglycemia causes tissue damage – (a) Non-enzymatic glycosylation, (b) Activation of PKC and (c) Aldose reductase pathway (68). Hyperglycaemia induced ROS generation and oxidative stress is a common factor in all three pathways (Figure 1-16) (69).

1.4.2.2 Glycosylation and DN

Glycosylation of proteins contributes to the development and progression of DN and other microvascular complications. During persistent hyperglycemia, some of the excess glucose reacts non-enzymatically with the free amino groups in a variety of proteins, lipids and nucleic acids, and gives rise to two major classes of glycation products via the Maillard reaction. This glycosylation process affects the GBM and other matrix components in the glomerulus, by formation of reversible early glycosylation end products and later, irreversible advanced glycosylation end products (AGEs). Non-enzymatic glycosylation could be involved in the pathogenesis of DN by the following possible mechanisms (Figure 1-12):
(a) AGEs alter signal transduction pathways involving ligands on the extracellular matrix.
(b) AGEs alter signal transduction by alteration in the level of soluble signals such as cytokines, hormones and free radicals, *via* AGE specific cellular receptors.
(c) Intracellular glycation by glucose, fructose and metabolic pathway intermediates can directly change protein function, trafficking and breakdown in target tissues (70).

AGEs are involved in the accumulation of extracellular matrix (ECM) in glomerular mesangium and tubulointerstitium by creating an imbalance between synthesis and degradation of ECM components. This leads to the pathogenic accumulation of collagen, fibronectins and laminins. The formation of inter and intramolecular disulphide bridge crosslinking after glycation of collagen leads to structural alterations, including surface charge and packing density. This results in increased stiffness, reduced thermal stability, and resistance to proteolytic digestion of collagen (71).

Circulating AGEs are efficiently cleared by the normal kidney and excreted in the urine. However, with kidney dysfunction, AGEs start to accumulate in the serum, as seen in diabetic patients. Circulating AGEs with their biological activities, may contribute to further organ damage through re-deposition in the tissues (72). Several studies have implicated receptors for

AGEs (RAGE) in the development and progression of DN. Tanji et al. reported increased RAGE expression in the podocytes of DN patients by immunostaining. They also demonstrated that the severity of DN correlates with the AGE formation in the glomerular and tubulointerstitial compartments (73). In genetically diabetic db/db mouse models, administration of soluble RAGE reduces albuminuria and glomerulosclerosis and improve renal function. Streptozotocin (STZ) induced diabetic RAGE knockout mice were protected against renal injury and development of mesangial matrix expansion or thickening of the GBM was prevented (74). Similar renoprotective effects of the RAGE knockout mouse was also reported by Tan *et al.* (75). Conversely, diabetic transgenic mice overexpressing RAGE gene in vascular cells, develop more severe renal injury than non-transgenic mice (76).

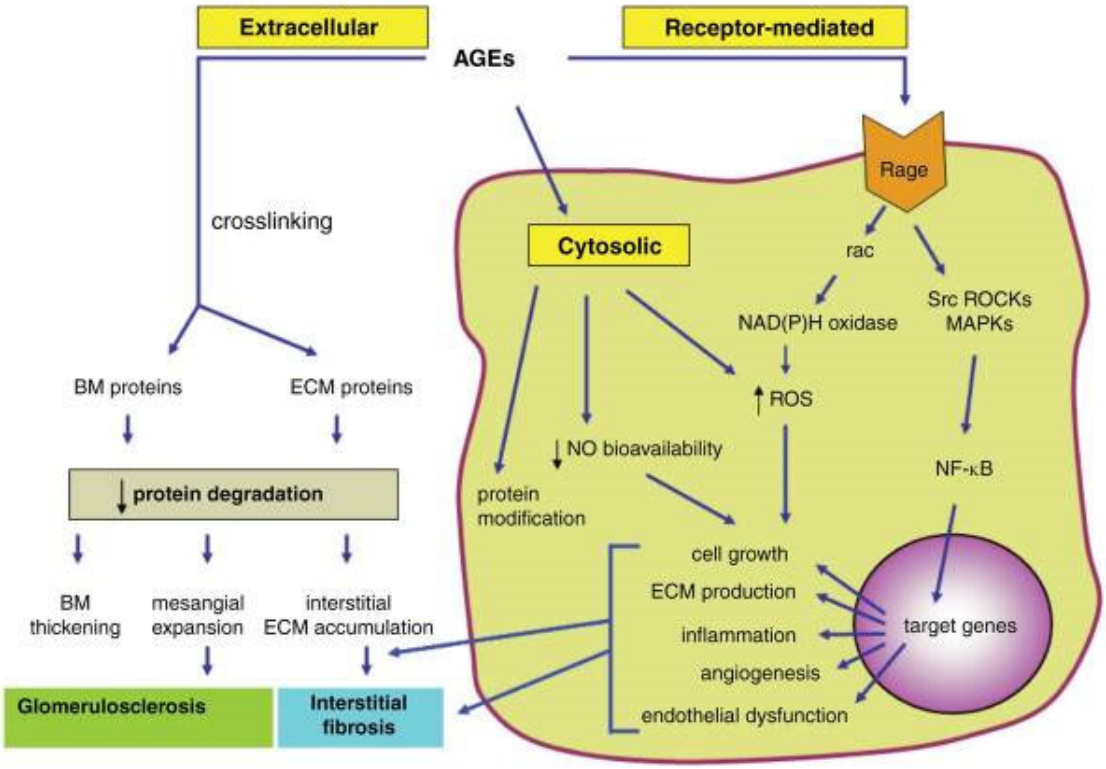

Figure 1-12: Consequences of AGEs formation in the diabetic kidney. The diagram shows the major mechanism of how AGEs exert their harmful effects in diabetic kidney. AGEs typically crosslink and alter protein structure and function in the extracellular compartment, modify cytosolic molecules and exert receptor-mediated effects that lead to activation of multiple signaling pathways and genes implicated in a variety of pathophysiological mechanisms in the diabetic kidney. ROCKs, Rho kinases; BM, basement membrane (77).

1.4.2.3 Protein Kinase C and DN

Activation of Protein Kinase C (PKC) is one of the mechanisms by which hyperglycemia promotes the development of DN. PKCs are a family of serine/threonine kinase that consists of 15 isoforms in humans. PKC isoforms are classified based on whether they have calcium and/or diacylglycerol (DAG) binding domains. Conventional or classical PKC isoforms (α, βI, βII and γ) bind to both calcium and DAG. Novel PKC isoforms (δ, ε, η, θ, and μ) are independent of calcium, but they require DAG and phosphatidyl serine (PS) for activation, whereas atypical PKC isoforms (ζ, *λ*) bind to neither calcium or DAG. The activation of these conventional or novel PKC isoforms require the phosphorylation of the isoforms and the presence of calcium or DAG as cofactors. Receptor-mediated activation of PKC occurs through the activation of phospholipase C, which leads to rapid and temporary increases of calcium and DAG levels. Chronic activation of PKC isoforms requires constant elevations of DAG, which involves the activation of phospholipase D/C or the *de novo* synthesis of DAG by glycerol-3-phosphate, which can be stimulated by high glucose levels. This chronic elevation of DAG levels then activates PKC. In addition, AGEs and ROS can also activate PKC indirectly (77, 78).

In diabetes, PKC can be activated via multiple mechanisms. In diabetic tissues, PKC activation is associated with increased DAG production. Figure 1-13 summarises various mechanisms by which activated PKC leads to diabetic complications. Several studies suggested the important role of specific PKC isoforms (mainly PKC α, βI, βII and δ) activation in the development of microvascular disease in diabetic animal models. Menne J. et al. showed that STZ-induced diabetic PKC-α knockout mice (PKCα)$^{-/-}$, were protected against albuminuria (79) and hyperglycemia-induced nephrin loss (80), indicating PKCα activation as an important intercellular signaling pathway to regulate nephrin expression and albuminuria in diabetic milieu (80). Selective inhibition of PKC-β has been reported to be nephroprotective in diabetic animal models. Administration of LY333531, a specific inhibitor of PKC-β1, can prevent TGF-β expression and ECM components such as fibronectin and collagen production in mesangial cells of diabetic rats (81).

Clinical trials with PKC-β inhibitor Ruboxistaurin in T2D patients reduced albuminuria and maintained estimated GFR (eGFR) over one year (82). Furthermore, genetic variant of PKC-β1 isoform is reported to be associated with ESRD in type 2 diabetic patients (83). Although

activation of PKC is associated with diabetic complications, some PKC isoforms like PKC-ε have protective effects in diabetic kidneys as suggested by the elevated fibrosis and TGF-β expression in the PKC-ε knockout mouse (84).

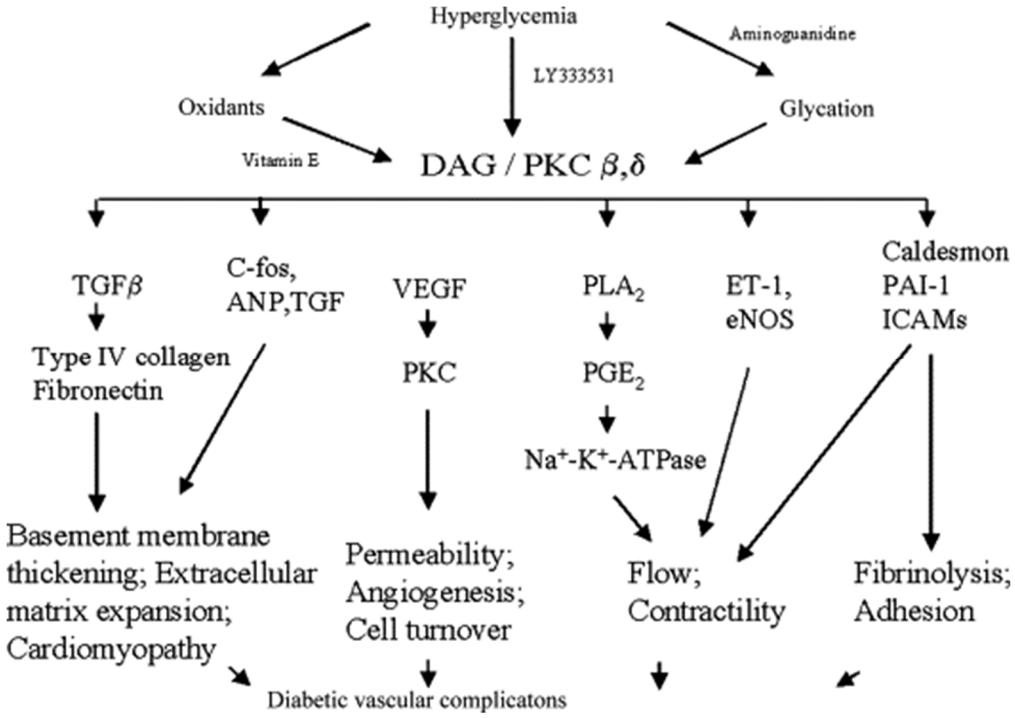

Figure 1-13: Physiological effects and cellular mechanisms of DAG–PKC activation induced by hyperglycemia (85).

1.4.2.4 Aldose Reductase Pathway and DN

Aldose reductase is the first enzyme of the polyol pathway and it catalyses the reduction of glucose into sorbitol. In non-diabetic normoglycemic individuals, the metabolism of glucose by the polyol pathway uses a very small percentage of total glucose in the cell. However, under hyperglycemic condition aldose reductase reduces glucose into sorbitol which is later oxidised into fructose. In this process aldose reductase uses NADPH as a cofactor which is critical for regeneration of the intracellular antioxidant reduced glutathione (figure 1-14). By reducing intracellular NADPH and reduced glutathione, the polyol pathway increase vulnerability to intracellular oxidative stress. Furthermore, by accumulating sorbitol in the cell, it increases intracellular osmotic stress (77).

The polyol pathway has been implicated in the pathogenesis of DN. Studies with aldolase reductase inhibitors showed a decrease in urinary albumin excretion in diabetic rats (86). It is

reported that inhibition of aldose reductase can attenuate glucose-induced PKC and TGF-β expression in mesangial cells (87). Moreover, the polyol pathway is also involved in glucose-mediated fibronectin accumulation in proximal tubular cells (88). However, more studies are required in humans to understand its role in DN progression.

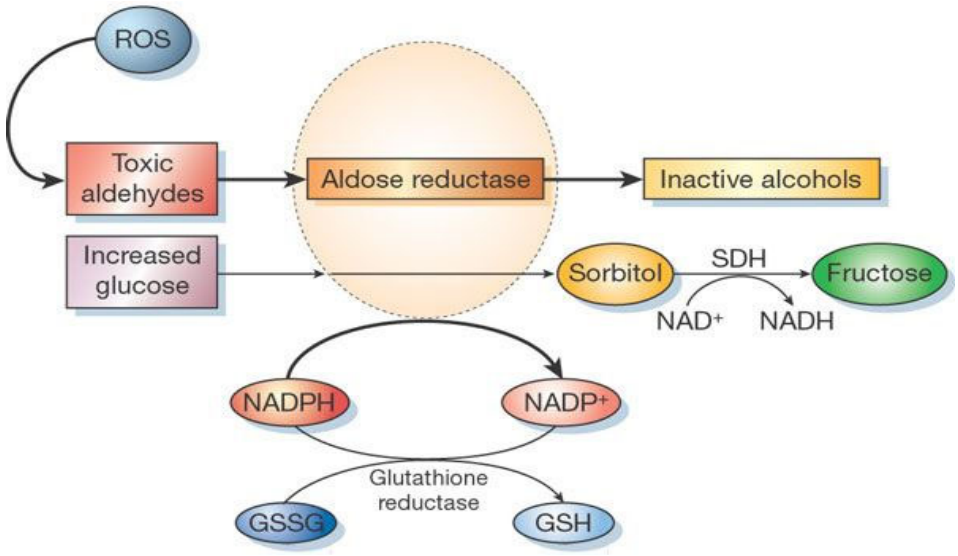

Figure 1-14: Polyol pathway and aldose reductase. The Aldose reductase reduces aldehydes generated by ROS into inactive alcohols and converts glucose to sorbitol, using NADPH as a co-factor. In high glucose conditions where aldose reductase activity is sufficient to deplete reduced glutathione (GSH), oxidative stress is increased. Sorbitol dehydrogenase (SDH) oxidizes sorbitol to fructose using NAD^+ as a co-factor (69).

1.4.2.5 Hypertension and DN

Hypertension is a common risk factor for patients with CKD and diabetes. Hypertension is highly prevalent in patients with DN and occurs twice more often in comparison to the general population. The prevalence of hypertension in DN increases in each CKD stages, from approximately 36% in stage 1 CKD to almost 84% in stage 4 and stage 5 CKD. The growing global epidemic of diabetes is driving the higher prevalence of hypertension and kidney disease that contribute to the progression of cardiovascular (CV) morbidity and mortality among diabetic population. In T1D, hypertension occurs in patients with microalbuminuria or overt nephropathy. However, in T2D hypertension exists before development of albuminuria and reductions in GFR (89, 90).

The mechanism of hypertension in DN is incompletely understood. Multiple factors are responsible for the development of blood pressure (BP) and hypertension in individuals with diabetes and DN. In both T1D and T2D, BP is maintained by the interplay between circulatory fluid volume and peripheral vascular resistance (Figure 1-15). The former is controlled by blood fluid volume and cardiac contractile force. Increased sodium reabsorption elevates blood fluid volume and increase extracellular volume, whereas peripheral vascular resistance is regulated by vascular tone due to vascular remodeling and dysregulation of multiple factors including renin-angiotensin system (RAS) (91). Activation of RAS, upregulation of ROS, endothelin1 (ET-1), downregulation of nitric oxide (NO), collaborate to cause hypertension (90).

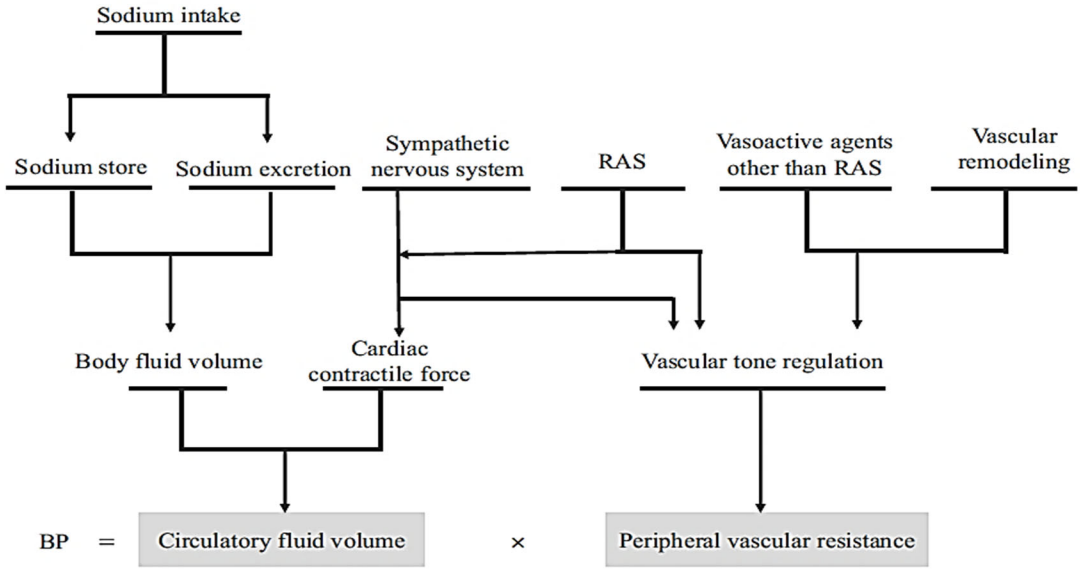

Figure 1-15: Pathophysiology of hypertension (91).

Sodium-glucose cotransporter 2 (SGLT2) inhibitors and hypertension: A new therapeutic approach to reduce hyperglycemia in diabetes is to enhance urinary glucose, sodium and fluid excretion by targeting sodium and glucose reabsorption via SGLT2 along the proximal convoluted tubule. Recent clinical studies suggested that in addition to reduceing hyperglycemia, the blood pressure lowering effects of SGLT2 inhibitors, such as canagliflozin and empagliflozin, protect from cardiovascular death even in diabetic patients with CKD and reduced GFR (92-94).

In diabetic patients, proximal tubular reabsorption of sodium and glucose via SGLTs increases and cause hypertrophy. This increased proximal tubular reabsorption reduces sodium

chloride and fluid delivery to the downstream macula densa, causing glomerular hyperfiltration due to the vasodilation of the afferent arteriole tone through a reduction in tubuloglomerular feedback (TGF). SGLT2 inhibition blocks sodium and glucose reabsorption in proximal tubules, thereby elevated sodium and fluid delivery to macula densa and increases TGF activity leasing to reduced GFR (95).

1.4.2.6 TGF-β and DN

Increasing number of evidences from the last two decades established transforming growth factor-β (TGF-β) as an important growth factor involved in the pathogenesis of DN and ESRD. In DN, as discussed above, elevated hyperglycemia and oxidative stress induced the expression and activation of TGF-β1 and its receptors via multiple pathways, including increased oxidative stress, formation of AGEs, polyol pathway, PKC pathway, hexosamine pathway. Hyperglycemia can further activate TGF-β1 via activation of angiotensin II, platelet derived growth factor (PDGF) and glucose transporters (GLUT) (96). Activated TGF-β1 further promotes cell hypertrophy, extracellular matrix accumulation, which leads to glomerulosclerosis, tubulointerstitial fibrosis and tubular atrophy. Several studies including transgenic animal model overexpressing TGF-β1 demonstrated that TGF-β 1 also promotes development of albuminuria by increasing glomerular permeability and decreasing reabsorption in the proximal tubules (97).

TGF-β1 induced ECM accumulation in DN: Several studies with neutralizing anti-TGF-β antibodies prevented renal fibrosis, and reduced expression of ECM genes including fibronectin, type IV collagen (ColIV), Col1a1 in unilateral ureteral obstruction (UUO) or diabetic mouse models (98, 99), suggesting that TGF-β signaling plays a critical role in ECM accumulation in DN. The role of TGF-β in renal fibrosis was further demonstrated by the finding that proximal tubule specific tetracycline-inducible overexpression of TGF-β1 increased collagen1 expression and develop peritubular fibrosis spontaneously (100). Previous studies demonstrated that TGF-β1 can stimulate the transcription of ECM components, such as collagen, fibronectin and laminin. In addition, TGF-β1 increases the expression of plasminogen activator inhibitor-1 (PAI-1) and tissue inhibitor of metalloproteinases-1 (TIMP1), which inhibits ECM-degrading matrix metalloproteinases (MMP) activity (97). Overexpression of MMP-2 in mouse tubular epithelial cells is reported to be adequate to induce tubulointerstitial

fibrosis (101). Thus, in one hand, TGF-β1 stimulates ECM production, accumulation and stabilization, while suppressing its degradation. This contributes to the development of glomerulosclerosis and interstitial fibrosis in DN.

TGF-β1 Facilitates Dedifferentiation of Renal Cells: Emerging evidence suggests that the accumulation of myofibroblasts (a type of mesenchymal stem cell), a predominant source for ECM production, is a critical step in the progression of renal fibrosis. TGF-β1 reported to induce epithelial-mesenchymal transition (EMT), a dedifferentiation process through which an epithelial cell is transformed into a myofibroblast. Although proximal tubular cells are highly polarized cells, through the process of EMT, they can lose cell polarity and gain migratory and fibrogenic properties of myofibroblasts. Hypoxia-inducible factor-1α (HIF-1α) has been demonstrated to enhance TGF-β1 induced EMT process in mouse proximal tubular cells (97). Zeisberg *et al.* demonstrated using three mouse models of CKD that during injury, endothelial cells can also contribute to the fibrosis via the process of endothelial-to-mesenchymal transition (EndMT) (102). They also reported that TGF- β1 as the main mediator of EndMT process (103). LeBleu *et al.* generated α-SMA-RFP (myofibroblast specific marker) reporter mice and using fate mapping experiments they reported that α-SMA$^+$ interstitial myofibroblasts is probably derived from the resident fibroblasts through proliferation (50%), bone marrow-derived cells (35%), epithelial cells (EMT, 5%), and endothelial cells (EndMT, 10%). Specific deletion of TβRII in αSMA$^+$ cells further reveals that both EMT and EndMT likely involve TGFβ1 dependent-differentiation (104). Therefore, TGF-β1 induced EMT and EndMT decreases functional renal cells and increases the accumulation of ECM, leading to kidney fibrosis and DN progression.

Several studies have established that TGF-β1 activity contributes to the major pathological changes in DN, such as mesangial cell hypertrophy with mesangial matrix expansion and thickening of the GBM, podocyte foot process effacement and albuminuria. Surprisingly, treatment with anti-TGF-β neutralizing antibody or interfering with Smad3 signaling using Smad3 KO mice markedly attenuate ECM deposition, GBM thickening and fibrosis without affecting albuminuria (98, 99, 105).

1.5 ROS and Oxidative Stress

In physiological system, molecular oxygen undergoes a series of reductive biosynthetic stages forming several unstable, highly reactive and energized oxygen intermediates including superoxide ($O_2^{\bullet-}$), hydroxyl ($^{\bullet}OH$) and nonradicals, such as hypochlorous acid (HOCl), ozone (O_3), singlet oxygen ($^1O_2$), peroxynitrite ($ONOO^-$), hydrogen peroxide (H_2O_2), commonly known as reactive oxidative species (ROS). Numerous studies over the last decades have established that ROS are important secondary messenger for various intra and intercellular signaling pathways connected with cellular proliferation, apoptosis, damage and inflammation. However, overproduction and impaired removal of ROS leads to the development of oxidative stress and many adverse effects including T1D and T2D complications and DKD. Prolonged hyperglycaemia in diabetes has been linked to generation and accumulation of ROS via various pathways (AGEs, PKC, TGF-β, etc.) that leads to these complications.

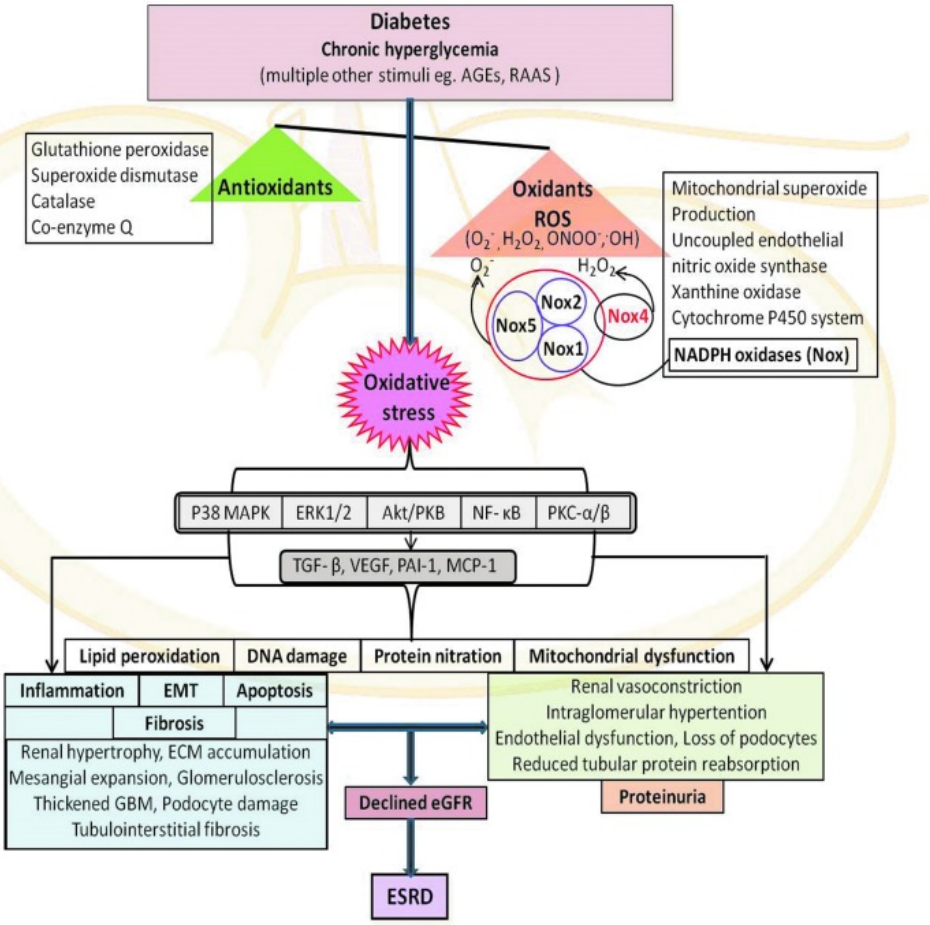

Figure 1-16: Overview of oxidative stress mediators involved in the pathogenesis of DKD (106).

1.5.1 ROS Generation and ROS Sources in the Kidney

Within the kidney there are several intracellular sources involved in ROS production, including cellular organelles, such as mitochondria (electron transport chain, ETC), endoplasmic reticulum (ER; during ER stress), peroxisomes (metabolizing long chain fatty acids, LCFA) and various enzymes including NADPH oxidases (NOXs), uncoupled NO synthase (NOS), xanthine oxidase, cytochrome P450 systems etc. (figure 1-17) (107).

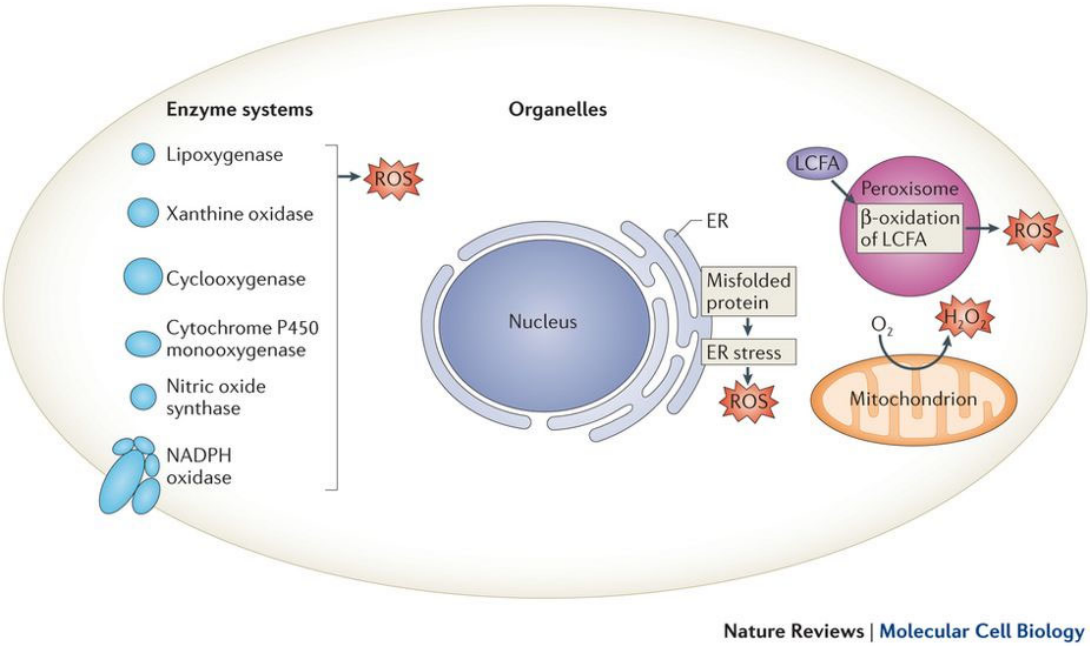

Figure 1-17: Various intracellular sources of ROS(107).

ROS produced by uncoupled NOS leads to lower endothelial NO bioavailability, resulting in vascular endothelial dysfunction in DN (108). However, mitochondrial superoxide and NOX derived ROS are the major contributors of DN which are discussed in detail below.

1.5.1.1 Mitochondrial ROS and DN

Under normal physiological conditions, mitochondria produce significant amounts of superoxide due to electron leakage from the oxidative phosphorylation pathway. The major locations of superoxide production are usually believed to be within complex I (NADH:ubiquinone oxidoreductase) and complex III (ubiquionol:cytochrome c oxidoreductase) of the ETC. According to the Brownlee theory, under diabetic conditions, excess glucose uptake by susceptible cells would lead to an increase in glucose derived pyruvate production, which is oxidized in the citric acid cycle in mitochondria that pushes more electron

donors (NADH and $FADH_2$) into the ETC, resulting in electron leakage and overproduction of superoxide (109). Moreover, chronic hyperglycemia impairs the activity of mitochondrial ETC causing a positive feedback loop of persistent oxidative stress, leading to mitochondrial dysfunction, cellular damage and apoptosis. Indeed, in the kidneys of type 1 (Akita) and type 2 (db/db) diabetic mouse models, increased mitochondrial ROS (mtROS) generation was observed and was associated with albuminuria podocyte loss and apoptosis (110). Reduced mitochondrial ATP production is also associated with mitochondrial dysfunction. Kidney proximal tubular cells contain abundant mitochondria and require ATP, considering their several functional roles, including energetically active reabsorption of glucose, sodium and electrolytes from the urinary filtrate. In diabetic condition, higher amount of ATP is required to maintain the glucose gradient. ATP depletion in proximal tubular cells causes impaired solute and ion transport, disruption in the apical basolateral protein polarization and apoptosis. Different factors involved in DN are illustrated in the figure 1-18 below (106).

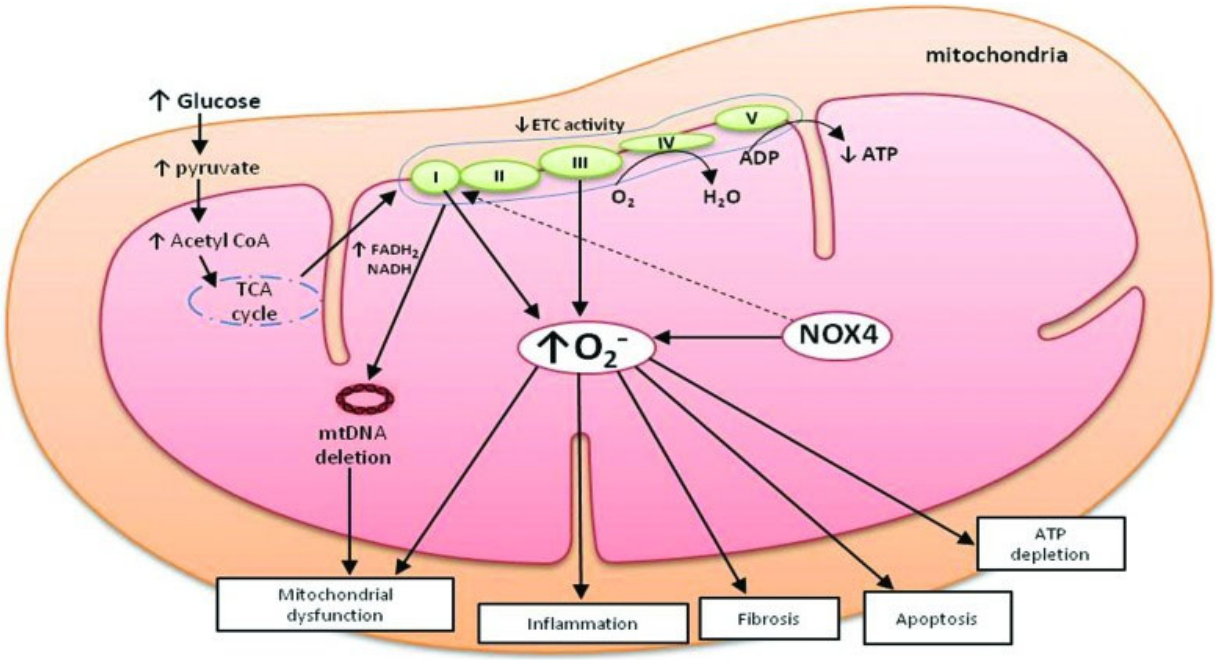

Figure 1-18: Factors associated with mitochondrial dysfunction and ROS generation in DN (106).

It is still unclear whether reduced mitochondrial content and function contribute to increased mitochondrial ROS production and renal dysfunction in diabetes. AMP-activated protein kinase (AMPK) is a serine/threonine kinase that plays major role in maintaining cellular energy homeostasis. AMPK is activated under low energy or ATP levels and regulated by the

AMP/ATP ratio. Activation of AMPK has been reported to improve energy efficiency by reducing protein synthesis and enhancing glucose entry into cells and stimulation of PGC1α (a master regulator of mitochondrial biogenesis) and mitochondrial biogenesis. Several studies have reported that the activity of AMPK is reduced in type 1 and type 2 diabetic kidney disease including high fat diet induced obesity model of kidney disease (111, 112). However, there are two conflicting models that have been proposed to explain the role of mtROS in the attenuation of AMPK activity. One model upholds the widely believed theory that overproduction of superoxide from mitochondria reduces the AMPK activity, leading to mitochondrial dysfunction and causing diabetic complications and diabetic kidney disease (106).

In contrarst, Dr. Sharma's group developed a DHE-based in vivo assessment of superoxide in mice and reported reduced superoxide production in STZ-induced diabetes mice in comparison to normal mice, suggesting reduced mitochondrial activity. This observation was further confirmed using confocal microscopy and electron paramagnetic resonance analysis. Furthermore, they demonstrated that the reduced mitochondrial function in diabetes was due to reduced AMPK along with a decrease in pyruvate dehydrogenase activity and PGC1-α expression. Reduced mitochondrial superoxide dismutase (SOD) was associated with higher superoxide production. However, they speculated that the source of ROS in the diabetic kidney possibly arised from NADPH oxidases. In diabetic heterozygous *Sod2*$^{+/-}$ mice, they did not find any evidence of increased kidney disease, indicating mitochondrial superoxide might not prove essential or sufficient for development of diabetic kidney disease. Their study further revealed that activation of AMPK would increase superoxide production and mitochondrial function while reducing fibrosis and TGF-β1 (113). In another study with human diabetic kidneys they found less mitochondrial proteins and PGC1α expression in the kidney and less mtDNA in the urinary exosomes (derived from podocytes and tubular cells) indicating a reduction in renal epithelial mitochondrial content and mitochondrial dysfunction in DKD (114). Therefore, improving mitochondrial function or biogenesis rather than reducing mitochondrial ROS may provide novel therapeutics to improve DN complication.

1.5.1.2 NADPH Oxidases and DN:

NADPH oxidases are a group of transmembrane enzymes that catalyzes the generation of superoxide (O_2^-) through the reduction of molecular oxygen by transferring electrons from NADPH. The existence of this group of enzymes ($gp91^{phox}$ or NOX2) was first reported in neutrophils and phagocytes as a defensive mechanism to protect against invading microorganisms. Since then, seven isoforms of NOX have been identified in different tissues. These are NOX2, NOX1, NOX3, NOX4, NOX5 and dual oxidases (DUOX1 and DUOX2). Among them, Nox1, Nox2 and Nox4 are the main NOX isoform expresses in human and rodent

$$2\,O_2 + \mathrm{NADPH} \xrightarrow{\mathrm{NOX}} 2\,O_2^- + \mathrm{NADP^+} + H^+$$

kidneys. Nox4 is also called Renox (renal oxidase) as it is expressed abundantly in kidney, specifically in the kidney cortex. More importantly, calcium-dependent Nox5 isoform is only found in human vasculature and kidney but not in rodents. Currently, there is no evidence of Nox3 or Duox1/2 expressions in the kidney or its contribution in diabetes (106). The membrane bound catalytic isoforms of NOX require to assemble with their cytoplasmic regulatory subunits $p47^{phox}$, $p67^{phox}$, $p40^{phox}$, the small GTPase Rac and Rap 1A for activation and superoxide production. The catalytic subunits of Nox1, Nox2, Nox3, and Nox4 isoforms require $p22^{phox}$, a common subunit required for the activity of the enzyme, whereas, Nox5, Duox1, and Duox2 are $p22^{phox}$-independent isoform, and are calcium dependent (figure 1-19) (115).

Nox2 in DN: Dr. Sharma's group generated $Nox2^{-/-}$ mouse to investigate its role in type 1 diabetic kidney. When $Nox2^{-/-}$ mouse was injected with STZ to induce diabetes, there was no reduction in albuminuria, H_2O_2 production, renal and glomerular hypertrophy, activation of TGF-β1, p38MAPK, and ECM production in glomeruli as compare to WT-STZ mice. Deletion of Nox2 did not affect diabetic glomerular and tubulointerstitial injury either. Interestingly, diabetic Nox2 KO mice had marked upregulation of renal Nox4 at both the glomerular (podocytes) and kidney cortex, probably as a compensation for Nox2 (116). This study indicated that Nox2 is not the major regulator of ROS production in kidney and progression of DN.

Nox4 in DN: Nox4 has been extensively studied in DN, and it is upregulated in the kidney of type 1 and type 2 diabetic mouse model. Several studies have shown high glucose

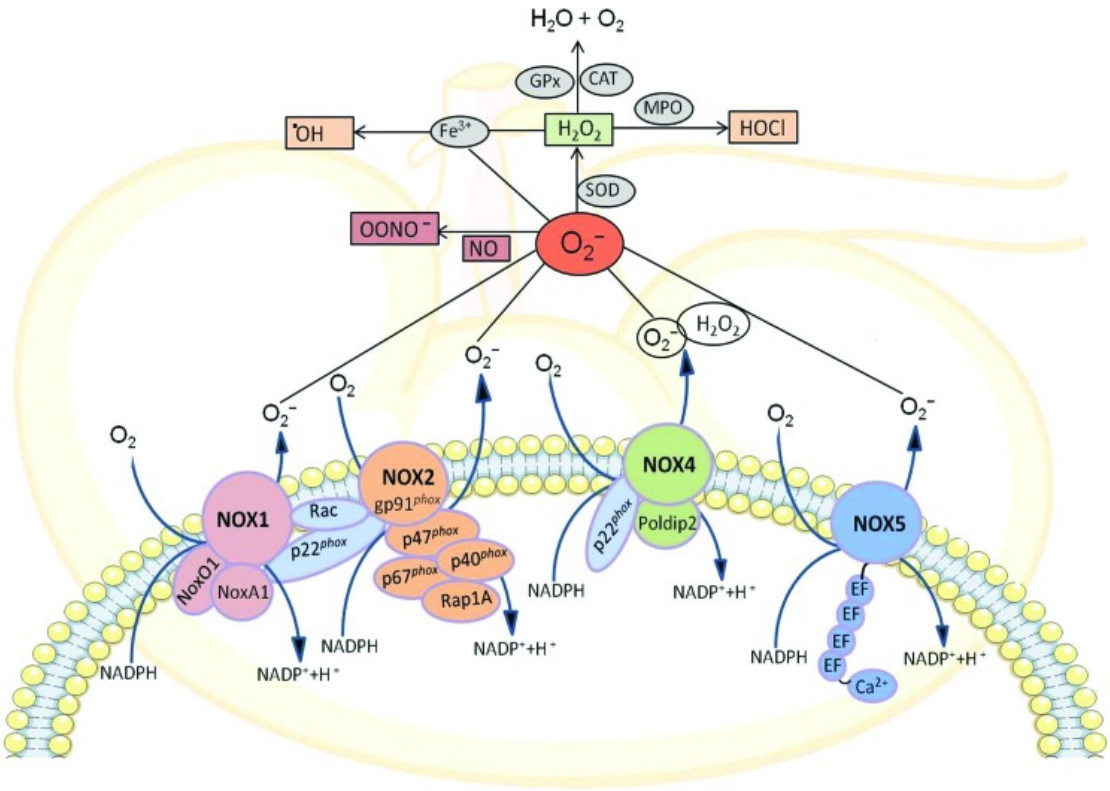

Figure 1-19: Classical components of NOX catalytic subunits NOX1, NOX2 (gp91phox), NOX4, and NOX5, and their regulatory subunits (p47phox, p67phox, p40phlox, NoxO1, NoxA1, Rac1/2, and Rap 1A) along with sources of ROS generated endogenously by renal cells and key metabolic pathways for these NOX family enzymes. CAT, catalase; Gpx, glutathione peroxidase; HOCl, hypochlorous acid; MPO, myeloperoxidase; NO, nitric oxide; NOXA1, NOX activator 1; NOXO1, Nox organizer 1; Poldip2, polymerase delta interacting protein 2; Rac, Ras-related C3 botulinum toxin substrate; SOD, superoxide dismutase (106).

elevated Nox 4 expression in tubular epithelial cells, mesangial cells, and podocytes in culture medium, as well as in kidney tissue from different diabetic rodent models (117). Several signaling pathways have been implicated in Nox4 expression including TGF-β1/Smad2/3 in podocytes, PI3 kinase/Akt/PKC, AMPK in mesangial cells, Angiotensin II in mitochondrial ROS production and fibrosis, Nrf2-keap1, p53, HIF-1α, in apoptosis, NF-κB in inflammation etc. (118). Following figure summarises function of Nox4 in different kidney cells (figure 1-20).

Studies by Gorin Y *et al.* showed STZ-induced diabetic rats develop increased Nox4 mediated ROS production in the glomeruli, leading to glomerular hypertrophy and increased fibronectin expression which is attenuated by the administration of antisense oligonucleotides

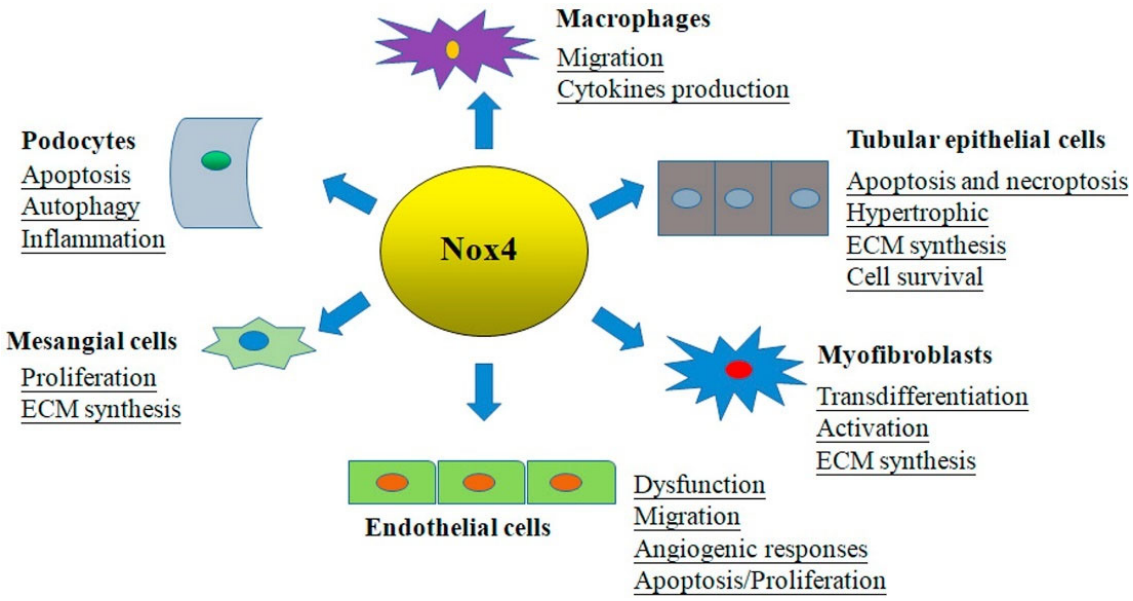

Figure 1-20: Function of Nox4 in different renal cells (118).

to Nox4 *in vivo* (119). Jandeleit-Dahm's group used global genetic deletion of Nox4 and showed that it mediated kidney injury via PKC dependent pathway in diabetic mice (120). Deletion of Nox4, but not Nox1, resulted in renal protection from diabetes-induced increased mesangial expansion, glomerulosclerosis, accumulation of ECM proteins (collagen IV, fibronectin) via a reduced ROS generation in STZ-induced diabetic $ApoE^{-/-}$ mice. Pharmacological inhibition of NOX1/4 with GKT137831 in diabetic mice can provided similar renoprotection as observed in Nox4 knockout mice (121). Podocyte-specific NOX4 deletion in diabetic mice provided protection against glomerular injury including attenuated albuminuria glomerulosclerosis, mesangial expansion and accumulation of ECM proteins by reducing the production of VEGF and deactivating PKC signaling (122). However, Babelova *et al.* found conflicting data with Nox4 KO mice in B6 background. Although they found that Nox4 was mainly responsible for majority of H_2O_2 production in kidney, Nox4 deletion in diabetic condition did not improve albuminuria or ECM accumulation (123).

To clarify the role of Nox4 in DKD, Dr. Sharma's group generated podocyte specific inducible Nox4 transgenic (Tg) mice and showed that overexpression of Nox4 in podocytes was sufficient to develop many classical features of diabetic kidney disease, including glomerular hypertrophy, mesangial ECM accumulation, GBM thickening, albuminuria, and podocyte loss. Administration of Nox1/Nox4 blocker GKT137831 in F1 Akita model of DKD was able to

reduce albuminuria, glomerular hypertrophy and mesangial matrix accumulation. Furthermore, with urine metabolomics studies, they showed Nox4 modulate TCA cycle intermediate fumarate through its effect on fumarate hydratase, a regulator of urine fumarate accumulation, which regulates metabolic pathways and DKD pathogenesis by inducing ER stress, matrix production, and HIF-1α and TGF-β production (124). All these studies indicate the major contribution of Nox4 mediated ROS in DKD.

Recently completed phase 2 clinical trial with GKT137831 in patients with diabetic kidney disease have demonstrated excellent safety profile and reduction of various markers of chronic inflammation and ROS, but not albuminuria after 12 weeks of treatment (125, 126).

Nox5 in DN: Nox5 is absent in mouse and rat genome but expresses in human kidney. In cultured human endothelial cells and podocytes, AngII induces renal Nox5-dependent ROS generation probably via increasing intracellular calcium concentrations (127, 128). Holterman *et al.* reported that Nox5 expression is increases in the podocytes of patients with DN. They generated podocyte-specific Tg mice over-expressing human Nox5 and showed increased albuminuria, podocyte foot process effacement, tubulointerstitial fibrosis and elevated blood pressure. STZ-induced diabetes in these Tg mice further develop more severe damage (128). Recently, Jha *et al*. reported increased Nox5 expression in mesangial cells in the biopsies of human diabetic kidney. STZ-induced diabetic Tg mice overexpressing Nox5 in mesangial cells enhances glomerular ROS production, glomerular injury, ECM proteins accumulation, macrophage infiltration and PKC-α/β expression. *In vitro*, silencing of Nox5 in human mesangial cells using shRNA attenuates high glucose and TGF-β1–mediated ROS formation and decreases fibrosis and inflammation markers expression (129). Yu *et al.* demonstrated that Nox5 expression and ROS production increased in human proximal tubules obtained from hypertensive individuals in comparison with normotensive individuals. In addition, silencing with Nox5 siRNA in proximal tubule cells from hypertensive individuals reduces ROS production and fibrosis (130). These studies indicate the important role played by Nox5 and its derived ROS in the development of human DN.

1.5.2 Antioxidants

To combat various enzymes that over produce ROS, cells are equipped with several potent antioxidant defences to maintain redox homeostasis. Each intracellular antioxidant enzyme has a different function. The superoxide dismutase (SODs) acts on superoxide whereas catalase, peroxiredoxin (PRDX) and glutathione peroxidase (GPx) enzymatically reduces hydrogen peroxide to water to limit its harmful effects. Non-enzymatic ROS regulation is accomplished by scavengers such as glutathione, α-lipoic acid, vitamin C, α-tocopherol, etc. In DN, hyperglycemia induces increased ROS production while reducing normal antioxidant defence system. Several strategies have been employed to boost antioxidant defence system either by direct ROS scavenging or inhibiting the source of ROS generation to ameliorate this excess in oxidative stress

1.5.2.1 Dietary antioxidant supplement:

Several dietary antioxidant supplements containing vitamins have been demonstrated to reduce kidney damage in animal models by normalizing superoxide dismutase, inducing hemoxygenase, or inhibiting NADPH oxidase (131). However, clinical trials with dietary antioxidant supplements, such as vitamin A, C and E, have been mostly controversial and disappointing (132-135).

1.5.2.2 Superoxide dismutase

Superoxide dismutase convert $O_2^{\bullet-}$ into H_2O_2 and O_2. There are three SOD isoforms in mammals: cytoplasmic CuZnSOD (SOD1), mitochondrial MnSOD (SOD2), and extracellular CuZnSOD (SOD3, ecSOD), all of which require catalytic metal (Cu or Mn) for their activity. SODs also play a crucial role in inhibiting oxidative inactivation of nitric oxide (NO) and prevent peroxynitrite ($ONOO^-$) formation, hence protecting against endothelial and mitochondrial dysfunction (136). Several studies reported reduced SOD activity in peripheral blood cells in DN. In addition polymorphism in SOD1 and SOD2 have been implicated as a risk factor in DN (137). SOD1 is the predominant isoform in the renal cortex and glomeruli accounting for more than 90% of total SOD activity in these tissues. Knocking out SOD1 in STZ-induced diabetic mice accelerated renal injury, while treatment of these mice with the SOD mimetic tempol for 4 weeks suppressed albuminuria, glomerular TGF- β, collagen α1(IV),

nitrotyrosine, and glomerular superoxide (138). Overexpressing SOD1 in both STZ-induced T1D and type 2 diabetic db/db mice showed renoprotective effects to diabetic injuries, including attenuated albuminuria, ECM proteins expression and TGF-β expression production (139, 140). In heterozygous *Sod2*$^{+/-}$ mice, though there was an increase in superoxide production, there was no evidence of an increase in albuminuria or mesangial matrix expansion in the *Sod2*$^{+/-}$ mice with or without diabetes, indicating SOD2 is not sufficient for development of diabetic kidney disease (113).

1.5.2.3 Catalase

Intracellular accumulation of $O_2^{\bullet-}$ and H_2O_2 can activate several signaling pathways that leads to diabetic complications. After SODs convert highly reactive superoxide ($O_2^{\bullet-}$) into less reactive H_2O_2, catalase catalyses conversion of H_2O_2 into H_2O and O_2 takes place, thereby maintaining redox homeostasis. Catalase is a 240 kDa homo-tetrameric enzyme and it contains four porphyrin heme (iron) groups that enable it to react with hydrogen peroxide (141). It is mainly expressed in peroxisomes but also in cytosol. In the kidney, catalase is localized predominantly in the cytoplasm of proximal tubules of the superficial cortex but has not been detected in the glomeruli, or distal tubules (142).

In STZ-induced diabetic rat kidneys, catalase and glutathione peroxidase activity are significantly reduced compared to non-diabetic rat kidneys (143). Knocking out catalase in STZ-induced diabetic mice increased mitochondrial ROS and fibronectin expression in response to free fatty acids. Furthermore, catalase deficiency disrupts peroxisomal and mitochondrial biogenesis under diabetic stress, suggesting important protective role played by endogenous catalase during diabetes (144). Studies by Chan's group using double transgenic mice showed that proximal tubule specific overexpression of catalase can prevent angiotensinogen induced hypertension, albuminuria, tubular fibrosis and apoptosis (145). They further reported that proximal tubule specific overexpression of catalase in type I diabetic Akita mice prevent hypertension, renal fibrosis and normalise angiotensin-converting enzyme-2 (ACE2) expression, suggesting protective role of catalase in the progression of DN (146).

1.5.3 Nrf2-Keap1 system

The transcription factor nuclear factor erythroid 2 related factor 2 (Nrf2), is a master regulator of cellular antioxidant responses and phase 2 detoxifying enzymes. It is negatively regulated by actin binding cytosolic protein Kelch-like ECH-associated protein1 (keap1).

1.5.3.1 Structure and Function of Nrf2

Nrf2 belongs to the CNC (cap 'n' collar) family of basic leucine zipper (bZIP) transcription factors and is encoded by the nuclear factor, erythroid-derived 2-like 2 (*NFE2L2*) gene. Besides Nrf2, other CNC-bZIP family members including p45-NF-E2, Nrf1 and Nrf3,

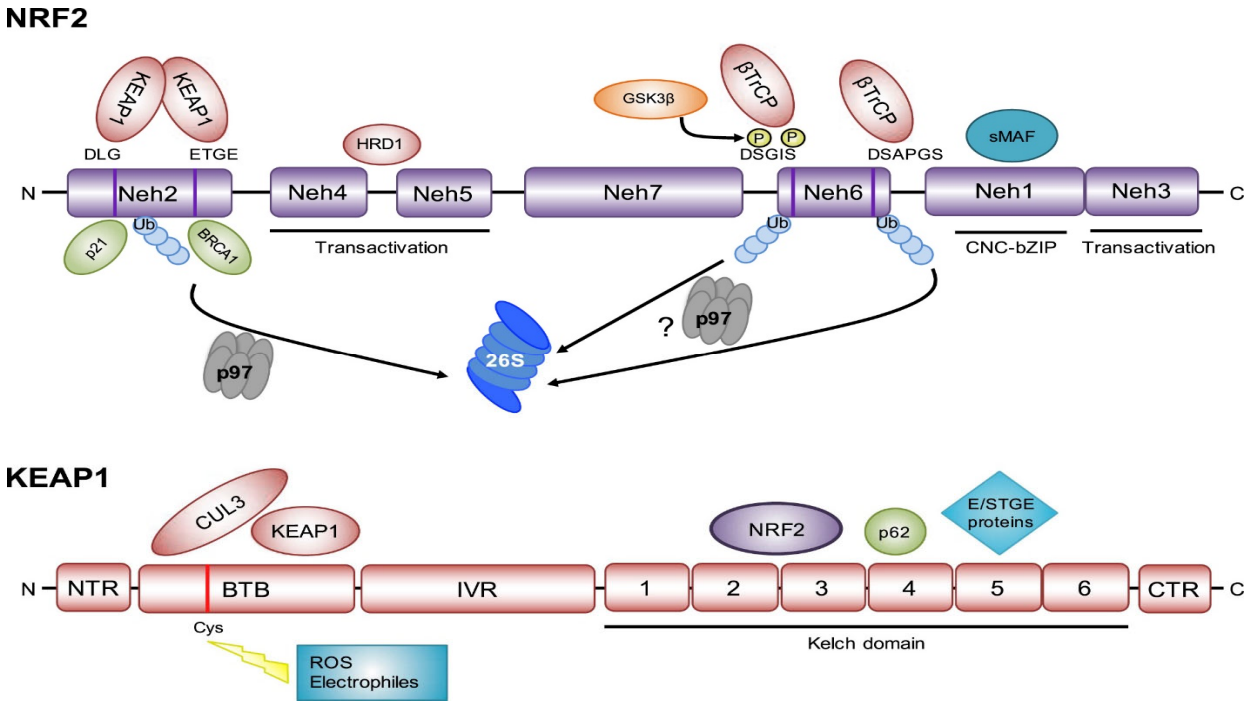

Figure 1-21: Domain structures of Nrf2 and repressor Keap1 (147).

act through the formation of a heterodimer with one of the small Maf proteins (148). Nrf2 consist of seven highly conserved Neh (NRF2-ECH homology) domains Neh1 to Neh7 (figure 1-21.). Neh1 includes a bZIP structure for dimerization with small Maf proteins and binds to DNA (148). Neh2 and Neh6 domains allow Nrf2 targeting to proteasomal degradation by Keap1 and β-TrCP (β-transducin repeats-containing proteins) (149). The Neh4 and Neh5 are Nrf2-dependent transactivation domains that bind to CBP. Neh7 domain has been reported to bind with retinoic X receptor alpha (RXRα) and repress Nrf2 (150). Together, Maf and Nrf2

heterodimer can recognize more than 200 genes, which contains antioxidant-response elements (ARE) in their regulatory regions, including many antioxidant and phase II detoxification enzymes such as catalase, SOD, glutathione S-transferases, NADP(H), quinone oxidoreductase 1 (*NQO1*), heme oxygenase-1 (*HO1*) and UDP-glucuronyl transferase 1a6, ABC transporters, etc (147, 151).

1.5.3.2 Regulation of Nrf2

1. Keap1-dependent regulation: Under physiological conditions, Nrf2 mRNA is constitutively expressed and the level of Nrf2 protein is maintained in the cytoplasm by its interaction with cytosolic repressor protein Keap1. Homodimer of Keap1 binds to Nrf2 through its C- terminal Kelch domain via interacting with amino acid motifs DLG and ETGE located in the Neh2 domain of Nrf2 (figure 1-21). With their N terminal BTB domain, Keap1 interacts with cullin3 (Cul3)/RING box protein1 (Rbx1) based E3 ubiquitin ligase complex, which leads to ubiquitination of Nrf2 (147). Ubiquitinylated Nrf2 is then extracted from Keap1/Cul3/Rbx1/E3 ligase complex by p97 chaperone and sent to 26S proteasome for degradation (figure 1-21) (152). This regulatory mechanism ensures the lower expression of Nrf2 in the cells. However, during oxidative stress, electrophiles and ROS reacts with the sensitive cysteines (especially Cys 151, but also Cys-273/Cys-288; Cys-226/Cys-613 and Cys-434 for sensing specific toxins) in Keap1 and cause a conformational change that prevents Nrf2 ubiquitylation (153, 154). As a result, Nrf2/Keap1/Cul3 complex is stabilised and newly synthesised Nrf2 accumulates in the cytosol which afterward translocates into the nucleus and activates transcription of ARE containing genes (154). After Nrf2 induced newly synthesised proteins remove cellular stress, Keap1 facilitates escorting nuclear export of Nrf2 in the cytosol for ubiquitination and degradation (155, 156). This model of Nrf2 regulation is called the canonical pathway.

The noncanonical pathway of Nrf2 regulation is also Keap1-dependent but cysteine independent involving autophagy related protein p62 (SQSTM1). p62 interact with Nrf2 binding site on Keap1 and competes with Nrf2. Phosphorylation of p62 on serine residue of STGE motif markedly increases binding affinity of p62 for Keap1 (157). A deficiency in autophagy facilitates p62 accumulation, which sequesters Keap1 into the autophagosomes, thereby reliving Nrf2 from Keap1 dependent degradation. This results in increased levels of Nrf2 and

transcriptional activation of Nrf2 target genes (158). However, noncanonical pathway does not have any mechanism to stop Nrf2 signaling after redox homeostasis is achieved which leads to prolonged Nrf2 activation causing tissue damage and cancer (159) .

Nrf2 activity can also be regulated by post-translational modification. Activation of several protein kinases such as P13K, p38, ERK, PKC, JNK causes Nrf2 phosphorylation and dissociation from Keap1 and subsequent translocation to nucleus (160). PKC catalyzes phosphorylation of Nrf2 at serine 40 which leads to Nrf2 dissociation from Keap1 and trigger Nrf2 nuclear translocation to activate ARE containing genes (figure 1-22 (ii)) (161). In the nucleus after gene activation, Nrf2 activity is regulated by phosphorylation within the nucleus by the SRC family tyrosine kinase Fyn. In the cytosol, glycogen synthase kinase 3β (GSK-3β) phosphorylates the Fyn at threonine residues. This leads to Fyn nuclear translocation where it phosphorylates Nrf2 tyrosine 568, resulting in Nrf2 nuclear export, and subsequent cytosolic Nrf2 degradation by Nrf2/Keap1/Cul3/E3 ubiquitin ligase complex (figure 1-22 (iv)) (151) .

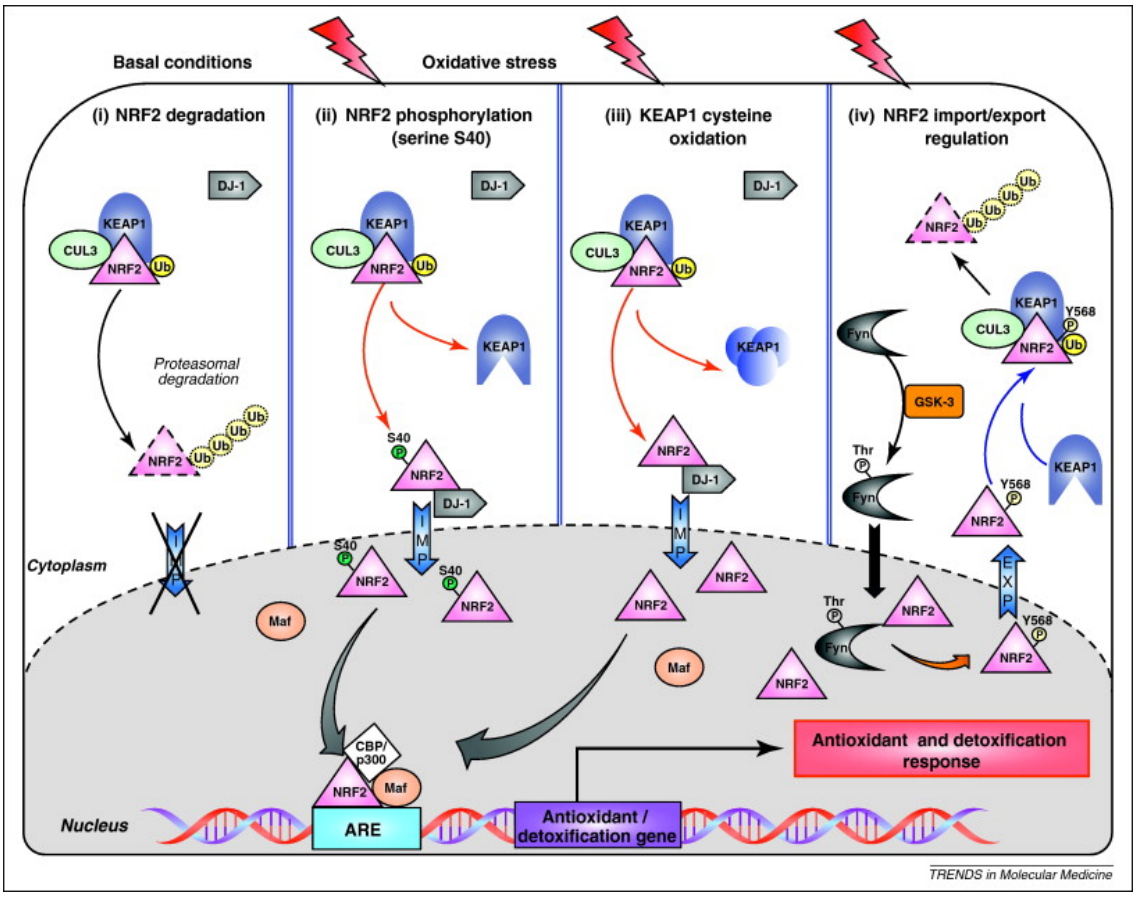

Figure 1- 22: Regulation of Nrf2 by different pathways (151).

2. β-TrCP-Dependent Regulation of Nrf2: Neh 6 domain of Nrf2 contains DSGIS and DSAPGS motifs, which are the binding site for adaptor protein β-TrCP (figure 1-21). GSK3β enhances binding affinity of β-TrCP for Nrf2 phosphorylation of serine residues in the DSGIS motif, but not DSAPGS motif. β-TrCP binds through to SKP1-CUL1-RBX1 E3 ubiquitin ligase complex and facilitates nuclear ubiquitylation and degradation of Nrf2 in a Keap1 independent manner (147, 162). Moreover, the BTB and CNC homology 1 (Bach1) transcription factor represses ARE activity by competing with Nrf2 for its ARE binding sites on DNA, consequently suppressing Nrf2-mediated gene induction (163).

1.5.3.3 Nrf2 activator Oltipraz

Oltipraz [5-(2-pyrazinyl)-4-methyl-1,2-dithiol-3-thione] has been extensively studied as a cancer chemopreventive agent. Comprehensive mechanistic studies suggested that oltipraz is a potent inducer of many ARE-regulated genes, including glutathione-*S*-transferases (GSTs), glutathione reductase, NAD(P)H:quinone oxidoreductase (NQO1), glutamate cysteine ligase, microsomal epoxide hydrolase, aflatoxin B1 aldehyde reductase, and ferritin in both cultured cells and rodent organs (164, 165). Induction of these enzymes by oltipraz has been linked to the transcription factor Nrf2. Several studies demonstrated using rodents treated with oltipraz triggers nuclear accumulation of Nrf2 and enhances its ARE binding activity (166-168). Treatment with oltipraz in the $Nrf2^{-/-}$ mice diminished the expression of ARE containing phase II enzymes, further supports the role of Nrf2 in oltipraz induced ARE containing gene activations (166, 169).

It has been suggested that oltipraz induced production of ROS may be a critical mechanism by which it exerts chemoprevention (170). Velayutham *et al.* using electron paramagnetic resonance (EPR) spin trapping demonstrated that oltipraz slowly reacts in the presence of oxygen to generate the superoxide anion radical in a concentration- and time-dependent manner sensory cysteines (Cys-151) in Keap1 causing a conformational change and subsequent release of Nrf2. Nrf2, then translocate to nucleus and activate transcription of ARE containing genes.

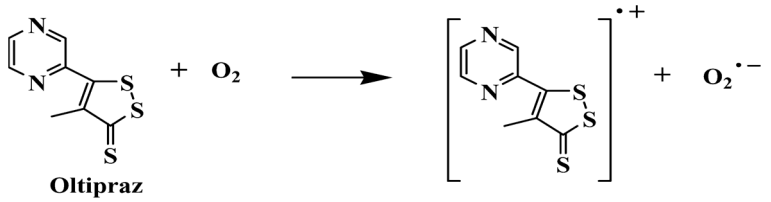

Oltipraz

Although some pre-clinical and clinical trials with cancer and liver disease suggested that oltipraz may be beneficial with mild toxicity, Kelley *et al.* in a clinical trial with oltipraz in chronic smokers report that weekly oral oltipraz administration did not show any benefit nor showed increase mRNA or enzymatic activity of phase II enzymes with unchanged glutathione levels (171). However, it should be noted that oltipraz is not a typical Nrf2 activator, so its effects may not be solely due to Nrf2 activation. In addition to activating Nrf2, oltipraz is also reported to activate other transcription factors such as aryl hydrocarbon receptor (AHR) and constitutive androstane receptor (CAR) that regulate cytochrome P450 enzymes (*e.g.,* CYP1A1) in a Nrf2 independent manner (164, 172). The researcher here has used oltipraz for the current study as it can induce Nrf2 activation in a dose dependent manner both *in vivo* and *in vitro* effectively.

1.5.4.5 Nrf2 inhibitor Trigonelline

Trigonelline (trig), a coffee alkaloid found in green coffee beans, has been demonstrated in several studies to inhibit Nrf2. Artl *et al.* demonstrated that trig efficiently decreased basal and tertiary butylhydroquinone (tBHQ)-induced Nrf2 activity in chemoresistant pancreatic carcinoma cell lines (Panc1, Colo357, and MiaPaca2) which have high Nrf2 activity. They further showed that trig decreased the nuclear level of Nrf2 protein by impairing Nrf2 nuclear import, but not its export or intranuclear stability (173). Boettler *et al.* also reported trig modulate Nrf2 nuclear translocation thereby reducing nrf2 activity (174). Moreover, the researcher's group has recently demonstrated that trig possess an intrinsic antioxidant property to lower ROS generation. Trig can markedly decrease ROS generation and oxidative stress in kidneys of T1D Akita mice and inhibit Nrf2 transcription and nuclear translocation. The group has further demonstrated that trig can prevent high glucose induced ROS generation in a concentration-dependent manner in rat immortalised renal proximal tubular cells (IRPTC) (175, 176).

Trig is reported to have antioxidant, hypoglycemic, hypolipidemic, neuroprotective, antimigraine, and antitumor activities. Trigonelline alkaloid acts by affecting β cell regeneration, insulin secretion and activities of enzymes related to glucose metabolism and ROS generation in the system (177). Indeed, in a small randomised human clinical trial with trig, it reduced early glucose and insulin responses during a 2h oral glucose tolerance test (OGTT) (178).

1.6 Renin-Angiotensin System (RAS)

Renin Angiotensin system is a complex system of enzymes, receptors and peptides that act as the major regulator of arterial blood pressure, sodium homeostasis, cardiovascular and renal function. In 1898, Tigerstedt and Bergmann first identified the enzyme renin in the kidney. Since then new functional component and different pathways of RAS has been discovered.

1.6.1 Classical RAS

The classical or circulatory RAS is a peptidergic system with endocrine characteristics. The major biologically active peptide of this system is angiotensin II (AngII) which is derived from the substrate molecule angiotensinogen (Agt, released from liver) in two proteolytic steps. First, renin, secreted from the juxtaglomerular apparatus of the kidney cleaves the Agt in the circulation to form a decapeptide angiotensin I (AngI). Circulating AngI is then cleaved by lung-derived membrane bound metalloproteinase angiotensin converting enzyme (ACE) to produce activated octapeptide AngII. AngII then act on specific receptors (AT_1R and AT_2R) triggering

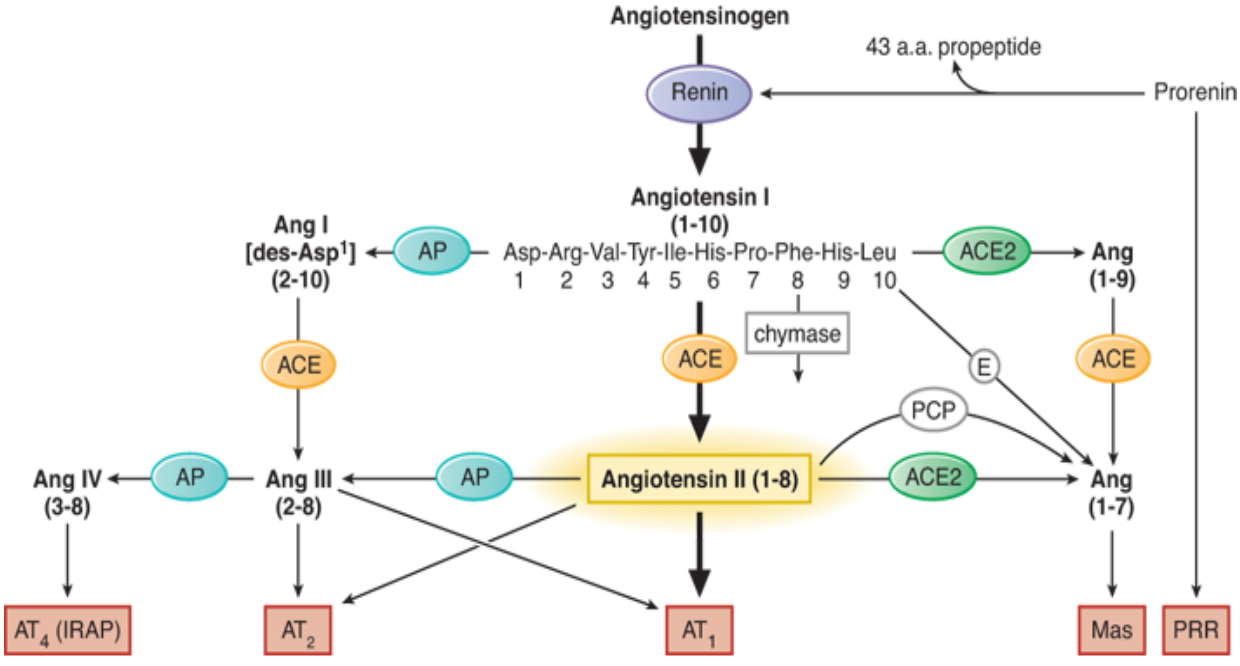

Source: L. L. Brunton, B. A. Chabner, B. C. Knollmann: Goodman & Gilman's: The Pharmacological Basis of Therapeutics, 12ed.

Figure 1-23: Components of RAS. Heavy arrows show classical renin/ACE/AngII/AT_1 and AT_2 axis and light arrows indicates other alternative pathways. AP, aminopeptidase; E, endopeptidases (neprilysin); IRAP, insulin-regulated amino peptidases; PCP, prolylcarboxylpeptidase; PRR, (pro)renin receptor. Receptors involved: AT_1, AT_2, Mas, AT_4, and PRR (179).

various responses including vasoconstriction, cell hypertrophy, aldosterone secretion from adrenal cortex and NOX activation (180). This mode of RAS activation is known as renin/ACE/AngII/AT_1 and AT_2 axis. However, recent progresses in RAS research has demonstrated that AngII is not the only active peptide of RAS, since AngII can be hydrolyzed by various protease, aminopeptidases, ACE2 and neprilysin to generate Ang(1-7), AngIII, AngIV and AngA. Prorenin and smaller Ang fragments can bind to their respective receptors triggering physiological effects. Recently three other axis has been described for RAS system including ACE2/Ang (1-7)/Mas receptor axis, the prorenin/PRR/MAP kinases ERK1/2 axis and AngIV/AT4/IRAP (insulin regulated aminopeptidase) axis (181). These are summarised in the figure 1-23.

1.6.2 Local RAS

As our knowledge expanded in recent years, the existence of local (tissue) RAS which operates independently of the circulating RAS has been recognised. Emerging evidence has demonstrated that besides circulating RAS, AngII is also produced locally by various organs including the kidneys, brain, heart, vasculature, adrenal glands and eyes, and it has paracrine and autocrine activities. In addition, locally produced AngII induces inflammation, proliferation, mitogenesis, apoptosis, activates multiple intracellular signaling pathways, as well as regulates gene expression of various substances. All of these can contribute to tissue injury (180, 182). Among others, the intrarenal RAS is unique as the kidney contains all the components of RAS.

1.6.2.1 Intrarenal RAS

In past years, the intrarenal RAS has been studied extensively. Both in fetal and adult kidneys, proximal tubules are reported to express mRNA and protein for all the necessary components of RAS to produce AngII (183-185). The level of AngII is much higher in the lumen of proximal tubules than plasma, almost 1000-fold. In addition, components RAS have been detected in the glomeruli of both animals and humans. AngII concentration in glomeruli is also higher than in plasma (186-188). AngII produced in the kidney plays significant role to regulate renal homodynamics and functions. Navar *et al.* reported that elevation in intrarenal AngII causes attenuated renal function and structural changes and contributes to the development of hypertension and renal injury via AT_1 receptor (189, 190).

1.6.3 Components of intrarenal RAS

1.6.3.1 Prorenin and Renin

Renin is an aspartyl protease, synthesized by the granular juxtaglomerular cells (JC) located in the walls of the afferent arterioles that enters glomeruli (figure 1-4A), which is the primary source of both circulating and intrarenal renin levels. It is initially secreted as preprorenin protein of 406 amino acid residues which is cleaved and processed to prorenin and transferred to golgi. Prorenin is further cleaved by cathepsin B enzymes that remove 43 amino acids from N terminal to uncover the active form of 340 amino acids long renin. Both renin and prorenin are stored in the JC and released in the circulation. Renin expression and release is controlled by mainly cAMP, cGMP and calcium signaling and can be influenced by blood pressure, salt intake and various drugs (179, 191).

As discussed above, the major function of renin is to act on angiotensinogen to produce decapeptide AngI. Furthermore, the binding of prorenin and renin to the cell surface of renal cells plays a major role as it provides a mechanism to produce AngII locally in excess of the circulatory AngII. Nguyen *et al.* cloned human renin receptor that binds to both prorenin and renin, which shows dual function (figure 1-23). Firstly, binding of renin and prorenin to this receptor acts as a cofactor by enhancing the efficiency of Agt cleavage to generate Ang1 by four-fold. Secondly, binding of prorenin to the receptor activates cellular responses that are independent of AngII production by activating MAP kinase, ERK1 and ERK2 signaling pathways. Furthermore, they showed that the receptor is localised in the kidney mesangium, vascular smooth muscle cells and in the subendothelium of kidney and coronary artery (192, 193). Ichihara *et al.* reported that nonproteolytic activation of prorenin significantly contributed to the activation of kidney RAS and subsequently in the development of DN (194).

1.6.3.2 Angiotensinogen (Agt)

Although liver is the major source of circulating Agt, the kidneys have also been demonstrated to produce Agt. The presence of intrarenal Agt mRNA and protein localized in the proximal tubules indicated that the intratubular Agt might be derived from Agt which is produced and secreted locally (182, 195). Because of the lower molecular weight of Agt as compared to albumin, it is believed that circulatory Agt does not get filtered by the glomerular

membrane. This further supports the theory that proximal tubules locally produce Agt and secrete directly into tubular lumen (182). Kobori *et al.* demonstrated by infusing human Agt into rats that proximal tubule produced intrarenal Agt, but not circulatory Agt and intrarenal Agt is the major source of urinary Agt (196).

AngI is cleaved from amino terminal end of Agt by renin which is subsequently converted into AngII, AngIII and AngIV by different enzyme system as described in figure 1-23. Chan's group using Tg mice demonstrated that mice overexpressing rat Agt in renal proximal tubules develop hypertension, albuminuria, renal injury and tubular apoptosis leading to nephropathy (197, 198). Human Agt is not cleaved by murine renin.

1.6.3.3 Angiotensin II (AngII)

A. Role of AngII in the regulation of renal hemodynamics: Administration of exogenous AngII induces dose dependent constriction of afferent and efferent arterioles, thereby decreasing renal blood flow and GFR (182, 199). In both animals and humans, acute AngII infusion was sufficient to elicit glomerular hemodynamic changes but not proteinuria (200, 201). However, chronic infusion of AngII induces proteinuria and causes injury to glomerular filtration barrier (202, 203). In addition, AngII regulates renal hemodynamics by modulating tubuloglomerular feedback mechanism. Blocking of AngII in animal models using ACE inhibitors (ACEi) and AngII receptor blockers (ARB) reduced proteinuria, tubuloglomerular feedback, while increasing renal blood flow and GFR, suggesting that the hemodynamic effects of AngII are critical in the pathogenesis of DN (180, 182). In hypertensive and diabetic patients, blockage of AngII by using of ACEi and ARBs was found to be beneficial beyond blood pressure control including normalised GFR, and reduced proteinuria (204).

B. Non-hemodynamics effects of AngII: In addition to its hemodynamic effects, AngII has other functions in the kidney such as inducing cell hypertrophy, increasing tubular reabsorption, promoting proliferation, fibrosis and apoptosis. Several studies have shown that AngII can act as a growth factor for kidney cells, causing both hypertrophy and proliferation (205). Thus, the proliferation of mesangial cells results in an increase in extracellular matrix synthesis, which contributes to the characteristic glomerulosclerosis of DN. Moreover, AngII increases the expression of TGF-ß1, probably through the activation of PKC and the p38 MAPK

pathway and the JAK/STAT pathway (206, 207). In human mesangial cells, AngII stimulated vascular endothelial growth factor (VEGF) expression contributes to increased permeability and proteinuria in glomerular disease (208). VEGF also induces angiogenesis and significantly increases microvascular permeability, indicating a key role in the development of pathogenesis related to renal microvascular complications (209).

AngII has been reported to increase *PAI-1* gene expression in mesangial cell cultures, which controls plasminogen activators and has the effect of increasing extracellular matrix accumulation. In the researcher's laboratory, Tg mouse models overexpressing Agt in the proximal tubules were used as a model for intrarenal RAS activation. These mice were characterized as having a higher level of TGF-ß1 and PAI-1 expression as well as increased interstitial fibrosis than control mice, supporting the role of AngII and its non-hemodynamic effects (197, 198).

1.6.3.4 ACE

Membrane bound angiotensin converting enzymes (ACE) hydrolyzes circulating peptides and catalyzes the extracellular conversion of decapeptide Ang1 to octapeptide AngII. Human ACE contains 1277 amino acid and has two domains each with a zinc binding site and a catalytic site. ACE is located on the luminal surface of endothelial cells throughout the vascular system including brush border membranes of proximal tubules. (179). It has also been reported that ACE inactivates the vasodilator peptides bradykinin and kallidin which are derived from kininogen by the action of kallikrein (210). ACE inhibitors such as Captopril and Lisinopril are used as antihypertensive agent because they decrease AngII activation and increase vasodilator bradykinin level, thereby reduceing blood pressure (211).

1.6.3.5 ACE2

Two groups independently identified a novel zinc metalloprotease that shares 42% homology with the catalytic domain of ACE and termed ACE2. It is highly expressed in vascular endothelial cells of heart, kidney and testis (212, 213). In contrast to ACE, ACE2 cleaves single amino acid from the carboxyl terminal to convert AngII into Ang-(1-7) and AngI into Ang-(1-9). The affinity of ACE2 for its substrate AngII is 400-fold higher than AngI as a substrate. Ang-(1-9) can be further converted to Ang-(1-7) by ACE. Ang-(1-7) binds to MAS receptor and

induces vasodilator and anti-proliferative responses (214). ACE2 can also cleave des-Arg9-bradykinin but it does not cleave bradykinin and is not inhibited by ACE inhibitors (212, 213).

Although ACE2 exhibits protective effect by acting as vasodilator, in diabetes the role of ACE2 still remains undefined. In young T2D, ACE2 expression is reported to be increased and was thought to be renoprotective (215). However, STZ-induced diabetic rats showed reduced level of tubular ACE2 protein compared with the control group (216). Further studies are required to eliminate these discrepancies in T2D and T1D.

1.6.3.6 Angiotensin Receptors

The physiological actions of AngII are mediated through two G protein coupled receptors termed AT_1 and AT_2 receptor, as discussed below.

AT_1 Receptor: The angiotensin AT_1 receptor mediates virtually all major physiological effects of AngII on renal and cardiovascular cells. Chronic activation of the AT_1 receptor can lead to the development of hypertension, cardiac arrhythmia, stroke, DN, and metabolic disorders, which can be effectively treated by ARBs. AT_1 receptor mRNAs can be found localised in proximal tubules, glomeruli, thick ascending limb of loop of Henle, arterial vasculature, vasa recta, arcuate arteries and juxtaglomerular cells (182, 217).

Two subtypes of AT_1 have been identified as AT_{1A} and AT_{1B} in rat and mouse. Even though they share 95% amino acid sequence homology, the noncoding regions of their genes are very different. This difference suggests the possible differences in tissue-specific expression and regulation of AT_{1A} and AT_{1B} receptor. Indeed, different studies confirms that both receptor subtypes are pharmacologically and functionally similar, but they differ in tissue distribution and transcriptional regulation. In the kidney, AT_{1A} mRNA has been reported to be present in mesangial and juxtaglomerular cells, proximal tubules, vasa recta, and interstitial cells, whereas AT_{1B} mRNA is found in podocytes, mesangial and juxtaglomerular cells, and in the renal pelvis. AT_{1A} in the murines considered as the closest homologue of human AT_1 receptor (191, 218).

All classic effects of AngII, such as vasoconstriction, aldosterone and vasopressin release, sodium and water retention, and sympathetic facilitation are mediated through AT_1 receptor induced cellular response via signal transduction. AngII acting through AT_1 receptor is also involved in cell proliferation, left ventricular hypertrophy, nephrosclerosis, vascular media

hypertrophy and endothelial dysfunction (219). AT_1 receptor blockers (ARB) are selective non-peptide antagonists which are currently in clinical use for the treatment of high blood pressure, diabetes, and various human cardiovascular disorders (217). Currently, eight ARBs –azilsartan, eprosartan, candesartan, irbesartan, losartan, telmisartan, olmesartan and valsartan are available for clinical use. Table 1-4 summarises the action of AT_1 receptor.

AT_2 Receptor: The AT_2 receptor shares approximately 34% amino acid sequence homology with AT_1 receptor. AT_2 receptors are reported to be localized in the glomerular epithelial cells, proximal tubules, collecting ducts, and parts of the renal vasculature of the adult rat. AT_2 receptor signaling is mediated by both G protein-dependent and independent pathways (217). AT_2 receptor activation counteracts the effects of AT_1 receptors by stimulating activation of phosphoprotein phosphatases, K^+ channels, synthesis of NO and cGMP, bradykinin production, and inhibition of Ca^{2+} channel functions (220). Homo-oligomerization of AT_2 receptors also has been reported to induce apoptosis independent of its ligand (221). AbdAlla *et al.* reported that the AT_2 receptor may directly bind to the AT_1 receptor, thereby antagonize the function of AT_1, which was independent of AT_2 receptor activation and signaling (222). AT_2 receptor activation has also been reported to influence proximal tubule sodium reabsorption, either by a cell membrane receptor-mediated mechanism or by an interstitial NO-cGMP pathway (223). AT_2 receptor knockout mice develop mild hypertension. Infusion of Ang II to the AT_2 knockout mice leads to exaggerated hypertension and reductions in renal function, probably due to decreased renal interstitial fluid levels of bradykinin and cGMP available that counteract the direct effect of Ang II (224). Table 1-4 summarises the action of AT_2 receptor.

MAS Receptor: The Mas receptor mediates the effects of Ang (1-7). Activation of Mas receptor by Ang-(1-7) elicits vasodilation, and anti-proliferation effect. In Mas knockout mice, cardiac dysfunction, endothelial dysfunction and increased BP was observed which might be due to imbalance in the NO and ROS. ACEi and ARB evokes increased ACE2 expression and plasma Ang-(1-7). Therefore, the ACE2/Ang-(1-7)/Mas axis could be a potential target for blood pressure control (217, 225, 226).

Angiotensin II (AngII)		
AT_1 Receptor	**AT_2 Receptor**	**MAS Receptor**
• Reduce renal blood flow • Increase glomerular pressure and enhanced glomerular damage • Sodium and fluid retention • Aldosteron production • Urinary concentration • Inhibit renin secretion • Collagen synthesis and deposition, Fibrosis • Increase intracellular calcium • Vasoconstriction, increase vascular resistance • NOX activation and ROS generation • Vascular smooth muscle hypertrophy and vascular remodeling • Activation of protein kinase (PKC, PTC, MAPK, JAK, JUN) • Activation of transcription factor (AP-1, STAT, CERB, NF-kB) • Decrease insulin sensitivity • Negative modulation of insulin signaling	• Natriuresis • Inhibit NF-kB activation and limit renal inflammation • Anti-proliferation/fibrosis/ apoptosis • Anti-oxidative stress • Inhibit prorenin bioprocessing • eNOS phosphorylation and NO generation • NO/cGMP activation • Vasodilation • Angiogenesis • Inhibition of vascular damage • Production of prostaglandins and ceramides.	• Vasodilation (BK and NO release) • Diuresis/Natriuresis • Anti-hypertrophy • Anti-proliferation • Anti-inflammation • Facilitation of insulin action • Improvement of lipid metabolism

Table 1-4: Action of angiotensin receptors in kidney and vasculature.

1.6.4 Clinical trials with RAS blockers

Treatment of diabetic nephropathy patients can be divided into four categories: cardiovascular risk reduction, glycemic control, blood pressure control and inhibition of RAS. Inhibition of RAS with AT_1 receptor blockers (ARB) and ACE inhibitors (ACEi) are best evidence-based therapy for DN (227, 228). Some of the landmark trials are listed in the following table 1-5.

Trial	Patients	Drug	Description and Outcome
ROADMAP, 2011 NCT00185159	T2D without microalbuminuria;	ARB-Olmesartan	Olmesartan vs placebo; n=4449; it delayed the onset of microalbuminuria, lower BP and more CV deaths
IRMA-2, 2001 NTC00317915	T2D and microalbuminuria	ARB-Irbesartan	Irbesartan 150mg vs 300mg vs placebo; n=590; it reduced overt proteinuria with dose dependent effect.
IDNT, 2000	T2D with proteinuria and nephropathy	ARB-Irbesartan	Irbesartan vs amlodipine vs placebo; n=1715; Irbesartan reduces the risk of doubling SCr, ESRD or death
RENAAL, 2001	T2D with proteinuria and nephropathy	ARB-Losartan	Losartan vs placebo; n=1513; it was well tolerated and reduces the risk of doubling SCr, ESRD.
CSG Captopril trial, 1993	T1D with proteinuria	ACEi Captopril	Captopril 25mg vs placebo; n=409; it reduces doubling of SCr, death, dialysis and transplantation
MICRO-HOPE, 2000	Diabetic patients without clinical proteinuria	ACEi-Ramipril	Ramipril vs placebo; n=3577; it was beneficial for CV events and overt nephropathy in diabetic patients.
ADVANCE, 2006 NCT00145925	T2D	ACEi-Perindopril	Perindopril and indapamide vs placebo; n=11,140; intensive glucose control in T2D reduces risk of vascular events, death
BENEDICT, 2006 NCT00235014	T2D with hypertension	Trandolapril (ACEi) & verapamil;	Trandolapril alone or with calcium channel blocker verapamil vs placebo; n=1204; both arms decrease microalbuminuria and CV events
ONTARGET, 2008, NCT00153101	Patients with CV risk	ACEi-Ramipril; ARB-Telmisartan	Ramipril vs telmisartan vs combined; =25,620; No CV benefit among 3 arms, doubling of SCr and reduction in proteinuria in combination therapy
ALTITUDE, 2012, NCT00549757	T2D, proteinuria and CV risk.	Renin inhibitor Aliskiren	ACEi or ARB and aliskiren vs ACEi or ARB and placebo; n=8561; early trial termination due to adverse events
NEPHRON-D, 2013, NCT00555217	T2D and proteinuria and nephropathy	ARB-Losartan & ACEi-lisinopril	Losartan and lisinopril vs losartan and placebo; n=1448; early termination due to adverse events

Table 1-5: Summary of major trials with RAS blockers. SCr, serum creatinine ratio.

1.7 Apoptosis

Apoptosis is a mechanism of programmed cell death, which is essential for development and homeostasis.

1.7.1 Mechanism involved in apoptotic cell death

The nomenclature committee on cell death 2018, has described 12 modalities of regulated cell death based on molecular and essential aspects of the process. These are: (1) intrinsic apoptosis, (2) extrinsic apoptosis, (3) mitochondrial permeability transition (MPT)-driven necrosis, (4) necroptosis, (5) ferroptosis, (6) pyroptosis, (7) parthanatos, (8) entotic cell death, (9) NTPotic cell death, (NTP, neutrophil extracellular trap), (10) lysosome -dependent cell death, (11) autophagy dependent cell death, and (12) immunogenic cell death. These modalities of cell death were described in detail by Galluzzi *et al*. (229). They are all forms of programmed or regulated cell death (RCD) because they are regulated at the genetic and cellular level. Each RCD mode shows a substantial degree of interconnectivity. Moreover, each type of RCD can show the entire range of morphological features ranging from fully necrotic to fully apoptotic (229).

1.7.1.1 Extrinsic apoptosis

Extrinsic apoptosis is an regulatory cell death (RCD) modality, also known as the death receptor pathway, and is initiated by any of two types of plasma membrane receptor: (a) ligand binding death receptors, and (b) dependent receptors, whose activation occurs when level of their specific ligand drops below threshold (229, 230). Major death receptors belong to the tumor necrosis factor (TNF) family and includes Fas cell surface death receptor (FAS), TNF receptor 1 (TNFR-1), TNFR10A (TRAILR1 or DR4) and TNFR10B (TRAILR2 or DR5). Ligation of death receptors with proper ligand allows the assembly of multiprotein complex known as death inducing signaling complex (DISC) at the intracellular tail of the receptor. Adaptor molecules, such as FADD (Fas associated via death domain), TRADD (TNFR-1 associated death domain) or Daxx (Death-associated protein 6), contains death domains so that they can interact with death receptors and assemble into DISC. These adaptor proteins then recruit caspase 8 (or

caspase 10) to complete DISC assembly which ultimately activates executioner caspase 3 leading to cellular apoptosis (229, 231).

For example, Fas ligand (FasL) binds to FAS and causes oligomerization of its receptor. This results in clustering of death domain and binding of adaptor protein FADD with receptor. FADD then recruits procaspase 8 via its death effector domain (DED) motif and complete formation of DISC assembly. Procaspase 8 is activated through self-cleavage to caspase 8 which then activates caspase 3 and commits the cell to apoptosis. (Figure 1-24) (231, 232).

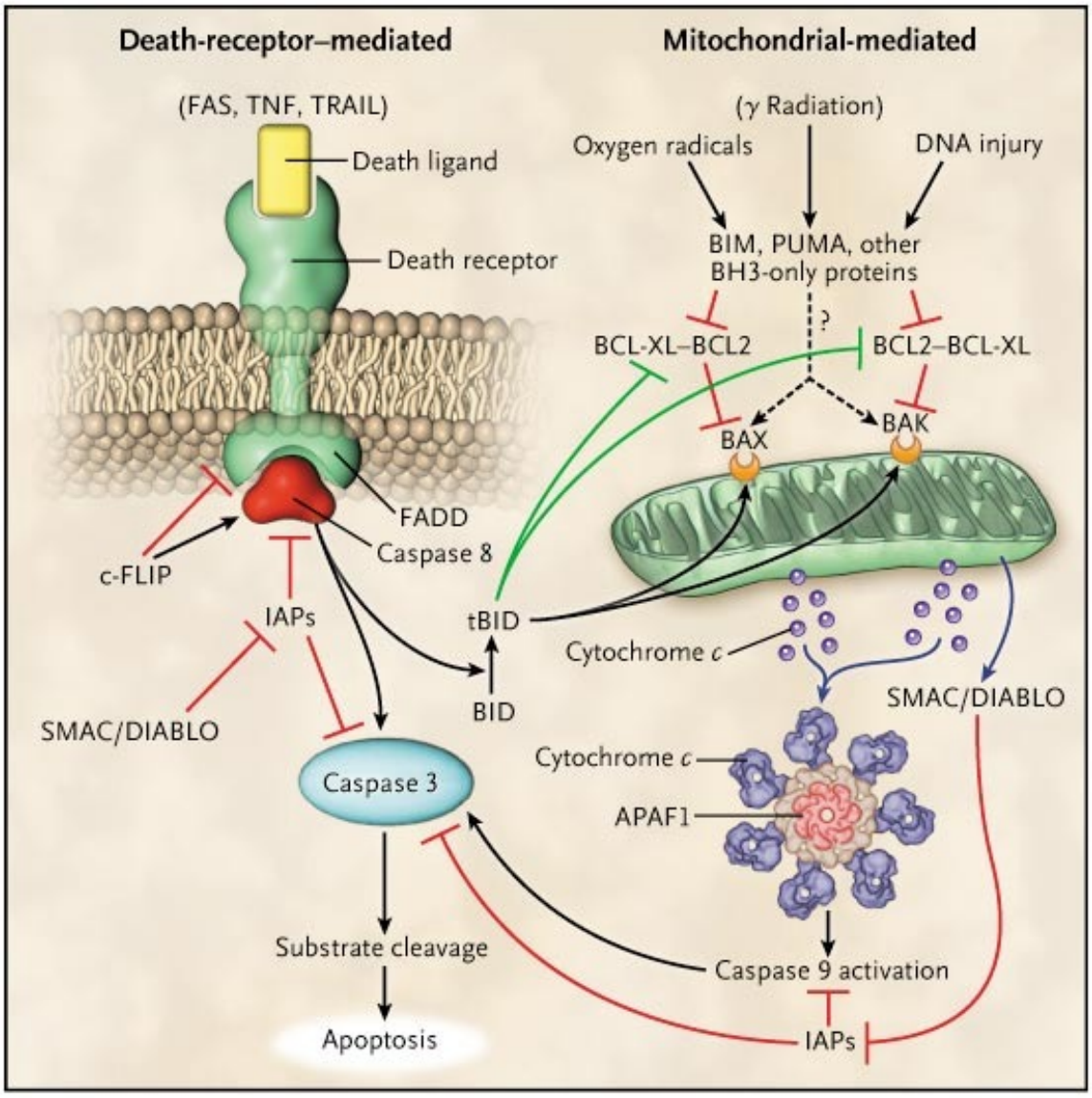

Figure 1-24: Pathways of cellular apoptosis (231).

1.7.1.2 Intrinsic apoptosis

Intrinsic apoptosis is another form of RCD, also known as mitochondrial death pathway, which is initiated by various cellular stressors such as growth factor removal, ER stress, ROS, cytoskeletal damage, loss of integrin dependent anchorage (anoikis), DNA damage and replication stress. Complex interactions between anti-apoptotic and the proapoptotic members of Bcl-2 family of proteins regulate the integrity of the outer mitochondrial membrane (OMM). The intrinsic apoptosis pathway involves in irreversible mitochondrial outer membrane permeabilization (MOMP) as the initial step of this pathway. MOMP directly promotes the release of several proapoptotic proteins from the mitochondrial intermembrane space into the cytoplasm such as cytochrome c, second mitochondria-derived activator of caspases (Smac/Diablo), apoptosis inducing factor (AIF) and endonuclease G. Once in cytoplasm, cytochrome c oligomerizes with an adaptor protein Apaf-1 (apoptotic protease-activating factor 1) and cofactor dATP, and it forms a scaffold called apoptosome complex. The apoptosome then binds and activates pro-caspase 9 by facilitating its dimerization. Caspase 9 later activates caspases 3 and 7 thereby killing the cell. Smac/Diablo is also released after MOMP and act to block the inhibitory action of IAPs (inhibitors of apoptosis proteins, which inhibits caspase activation), thus allowing the activation of caspase and progression to apoptosis (figure 1-24) (231, 233).

There is potential cross-talk between the intrinsic and extrinsic pathway, which is mediated by the truncated form of BID (tBID) (figure 1-24). tBID is produced during caspase 8–mediated BID cleavage and translocate to mitochondria where it inhibits the Bcl2–Bcl-X_L pathway to activate Bax and Bak and thereby triggering intrinsic apoptotic pathway (231).

1.7.2 Regulation of Apoptosis by Bcl-2 Family Proteins: The Sentinels of Life and Death

Members of Bcl-2 family are crucial regulator of the mitochondrial apoptotic pathway. These proteins share one or more conserved α-helical regions called Bcl2 homology (BH) domain. The Bcl-2 family members can be categorized according to their function into three groups (a) anti-apoptotic or pro-survival Bcl-2 family members, (b) the multi BH domain pro-apoptotic members and (c) pro-apoptotic BH3-only proteins (figure 1-25) (234)

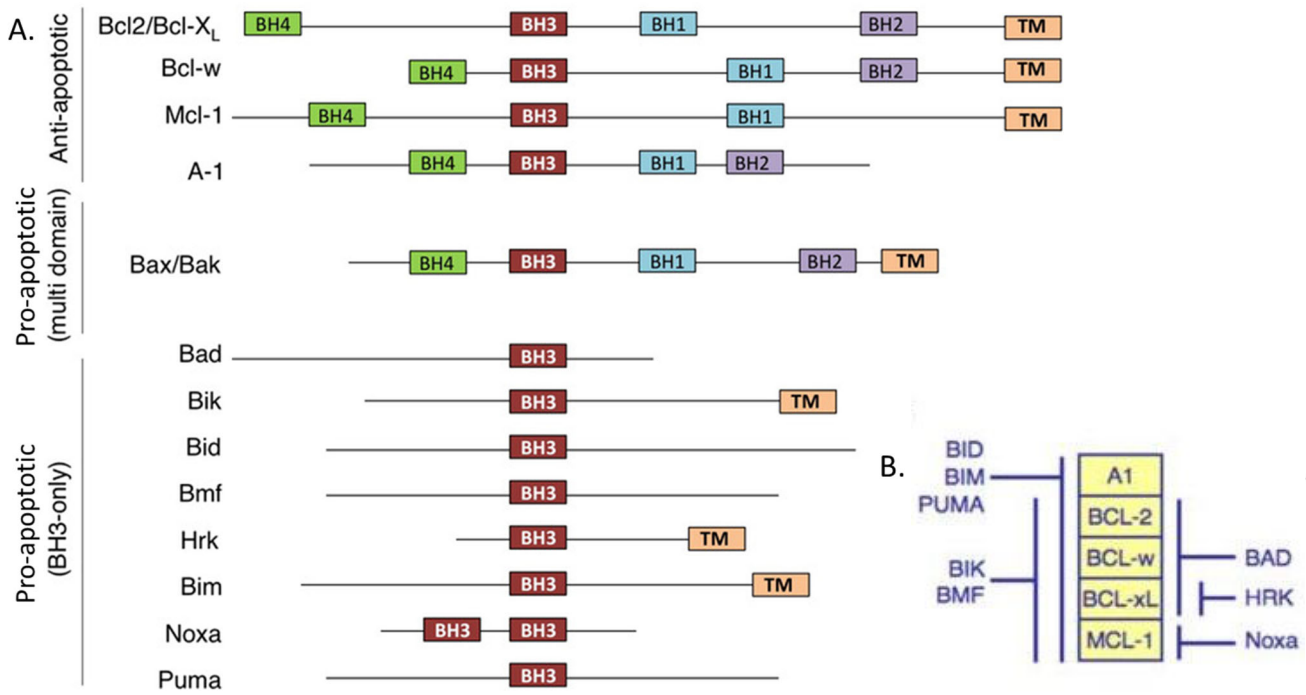

Figure 1- 25: A. Domain organization of various Bcl2 family members. BH, Bcl2 homology domain; TM, transmembrane domain. B. Binding affinity of different BH3-only proteins towards anti-apoptotic Bcl-2 members (235) .

Pro-survival Bcl-2 family proteins: This group consist of five anti apoptotic proteins including Bcl-2 itself, Bcl-2 like 1 (BCL2L1; best known as BCL-X_L), Mcl-1, BCL2 like 2 (BCL2L2; best known as Bcl-w), and Bcl-2 related protein A1 (BCL2A1; best known—in human—as BFL-1). All these anti-apoptotic proteins contain all four distinct BH domains which are anchored into the OMM or in the ER membrane through their transmembrane α9 helix. They directly bind to `the pro-apoptotic members of Bcl2 family and exhibit anti-apoptotic function (235, 236). Besides binding to pro-apoptotic members, some anti-apoptotic Bcl-2 family proteins contributed to cell survival by (a) regulating Ca^{++} homeostasis at the ER, (b) promoting bioenergetic metabolism upon interaction with the mitochondrial F_1F_O ATP synthase and (c) contributing to the regulation of redox homeostasis (229, 237, 238).

Multi BH-Domain Pro-Apoptotic Proteins: Bcl-2 associated x protein (Bax) and Bcl-2 antagonist killer (Bak) are the effector proteins that contains four BH domains (figure 1-25). Under physiological conditions, Bak resides on the mitochondria, while Bax resides is in the

cytosol. When activated, Bax and Bak are translocated to the outer mitochondrial membrane and homo-oligomerize causing pore formation leading to MOMP, freeing apoptogenic factors, such as cytochrome c, into the cytoplasm where they promote caspase activation, which mediates cell demolition (234). Mice lacking only Bax or Bad have no effect in program cell death but Bax and Bad double knockout mice exhibited developmental abnormalities and died soon after birth. Cells isolated from this double knockout mouse are resistant to many apoptotic stimuli, indicating that Bax and Bad are essential for mitochondrial intrinsic apoptosis pathway (239, 240).

Pro-Apoptotic BH3-Only Proteins: Members of BH3-only proteins are pro-apoptotic and contains only one homology domain, BH3, which is required to bind with Bcl-2 like pro survival members. They act as sentinels of cellular stress, and their activation commits cells towards apoptosis. First, BH3-only protein Bad (Bcl-2 associated death promoter) was discovered two decades ago and since then, seven more BH3-only protein have been identified in mammals. These are BH3-interacting domain death agonist (Bid), Bcl-2 interacting killer (Bik), Bcl-2 modifying factor (Bmf), Harakari (Hkr), Bcl-2 interacting mediator of death (Bim), p53-upregulted modulator of apoptosis (Puma) and Noxa (figure 1-25A). Individual BH3-only proteins have varying affinity for binding with different pro-survival proteins as shown in figure 1-25B. Among them Bim has highest affinity to bind with all pro-survival proteins, making it most potent killer. BH3-only protein can be further subdivided into 2 groups according to their function: direct activators BH3 only proteins (Bim and Bid) and sensitizer/de-repressors BH3 only proteins (Bad, Bik, Bmf, Hrk, Noxa and Puma) (241, 242).

Presently, two models have been proposed to categorize the function of Bcl-2 family proteins (for Bax/Bak activation): (a) the indirect activation model or the antipodean view (figure 1-26B) and (b) the direct activation model or hit and run model (figure 1-26A). Under physiological conditions, Bax/Bak molecules are sequestered by anti-apoptotic Bcl-2 family proteins to block their activation and pro-apoptotic effects. According to the indirect activation model, the primary role of BH3-only proteins is to bind with the pro-survival Bcl-2 family members, thereby displacing Bax/Bak from Bcl-2 complex. This also prevents pro-survival Bcl-2 family members to bind and neutralise any activated Bax or Bak. Displaced free activated Bax/Bak then oligomerized in OMM causing MOMP and release of cytochrome c and

eventually killing the cells (figure 1-26B) (241-243). The direct activation model proposed that certain direct activator BH3-only proteins (Bid and Bim) binds transiently with Bak/Bak (hit and run), hence triggering their conformational changes and subsequent oligomerization on the mitochondrial membrane. According to this model, apoptotic stimuli cause sensitizer/de-repressor BH3-only proteins bind only to pro-survival Bcl-2 family members and unleash the direct activator Bid and Bim to activate Bax or Bak directly (figure 1-26A) (235, 244, 245).

In addition to apoptotic signals, different cell types can regulate the function of other various BH3-only proteins. For example, Bik is not only important for cell death in hematopoietic cells but also crucial for IFN-gamma induced cell death in human airway epithelial cells (246, 247). Similarly, Bmf upregulation protects seizure-induced neuronal death in brain regions (248). However, Bmf upregulation causes apoptosis in the renal proximal tubules of diabetic mice (249).

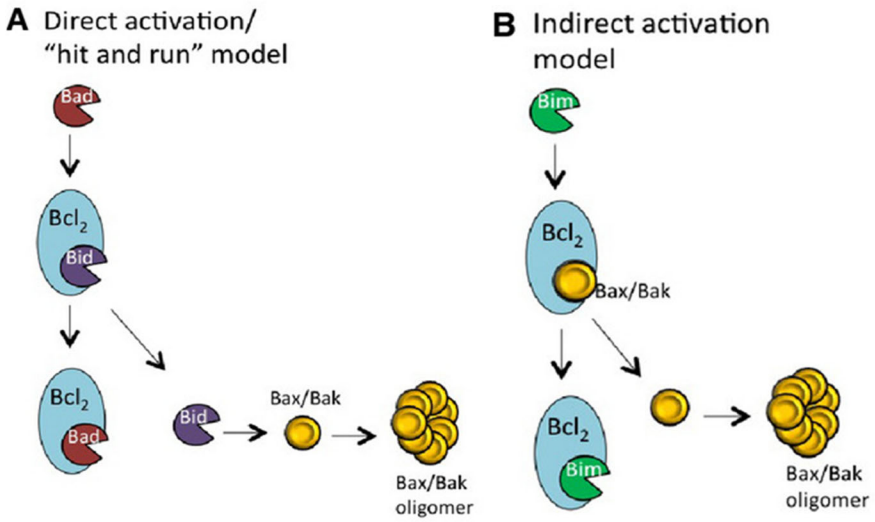

Figure 1-26: The two alternative models for Bax/Bak activation (235).

1.7.2.1 The BH3-only protein Bmf

Bmf is a member of pro-apoptotic BH3 only protein and was discovered by Puthalakath *et al.* in a yeast two-hybrid assay of a mouse embryonic cDNA library using Mcl-1 as bait. It is found to be expressed in the pancreas, liver, kidney, neurones, and hematopoietic tissues with the highest levels found in immature B and T cells. In healthy cells, Bmf interacts with the actin-based myosin V motor complex by association with dynein light chain2 (DLC2), which

sequesters Bmf to cytoskeleton. In response to certain stress, such as UV irradiation, oxidative stress, loss of extracellular matrix adhesion, Bmf detaches from cytoskeleton and translocate to the mitochondria where it interacts with pro-survival Bcl-2 family members to elicit pro apoptotic activity. *In vitro,* mutation in the light chain-binding domain of Bmf increases its apoptotic activity Bmf (250, 251).

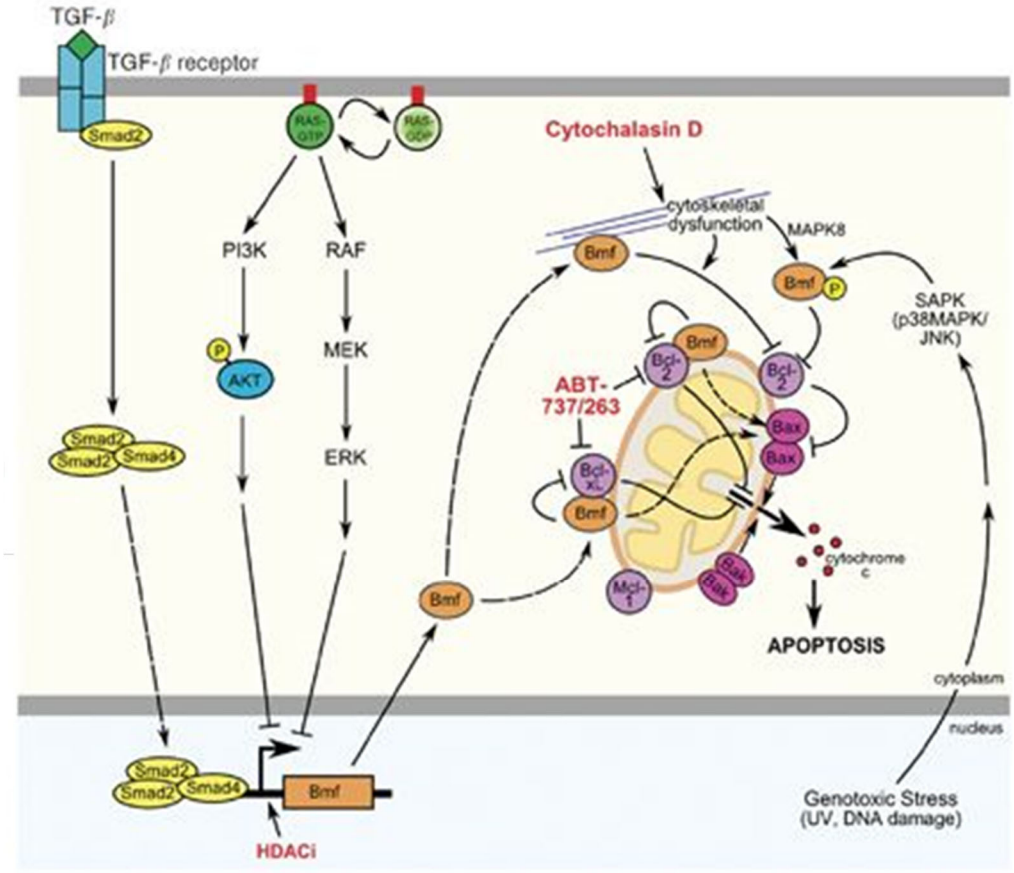

Figure 1-27: Function and regulation of Bmf (252).

Regulation of Bmf: At post transcriptional level, Bmf can be rendered inactive by binding to actin filament through DLC2. JNK phosphorylation was shown to phosphorylate Bmf on serine 74 in HEK293 cells (253, 254). Shao *et al.* demonstrated that ERK2 can directly phosphorylate Bmf on serine 74 and serine 77 with serine 77 being the major phosphorylation site. Serine 77 phosphorylation of Bmf was shown to downregulate its pro-apoptotic function independent of its mitochondrial translocation or interaction with DLC2 (255). Later studies on mice with knock-in mutation disrupting Serine 74 site has suggested that Bmf phosphorylation on Serine 74 is not essential for Bmf function (256).

Several studies have reported that Bmf can also be regulated at transcriptional level in various cell types (257-259), as well as post-transcriptionally by microRNAs and competing endogenous RNA (ceRNA) network such as miR221, miR-125b, STARD13 3'UTR and other post-transcription modification (250, 260-262). Morales *et al.*, using B-chronic lymphocytic leukemia cells demonstrated that human Bmf gene is alternatively spliced to generate three isoforms: Bmf or Bmf I, Bmf II and Bmf III. However, only Bmf or Bmf-I isoform has BH3 domain, but not Bmf II and Bmf III, making them unable to bind pro-survival Bcl-2 family proteins, thereby having no effect apoptotic process (263). Acetylation and deacetylation of Bmf promoter regions by chromatin remodeling enzymes by histone acetyltransferase (HATs) and histone deacetylases (HDACs) regulates Bmf transcription. HDAC inhibitors such as FK228, CBHA, SAHA (suberoylanilidehydroximic acid) has been reported to upregulate Bmf and induce apoptosis in cancer cells (257). However, Bmf does not mediate Trichostatin A (TSA) or CBHA induced cell death in thymocytes and pre-B cells (259). Amelia *et al.* demonstrated that interferon-γ induced deacetylation and nuclear accumulation of p53 can supress Bmf promoter activity and expression and thereby induce autophagy in airway epithelial cells.

TGF-β signaling, one of the major pathogenic contributors in diabetic nephropathy, has also been demonstrated to promote Bmf transcription and induce apoptosis (figure 1-27) (264). The researcher's group, using renal proximal tubular cells, demonstrated that high glucose-stimulated ROS can induce Bmf transcription. Furthermore, dose dependant increase in Bmf expression in response to human TGF-β was also observed (249).

1.8 The Heterogenous Ribonucleoproteins

The heterogeneous nuclear ribonucleoproteins (hnRNPs) are comprised of a diverse family of RNA binding proteins that contribute to multiple aspects of nucleic acid metabolism, including packaging of nascent transcripts, alternative splicing and transcriptional and translational regulation. Many hnRNPs share functional similarities among themselves, but they differ mainly in domain composition and functional properties.

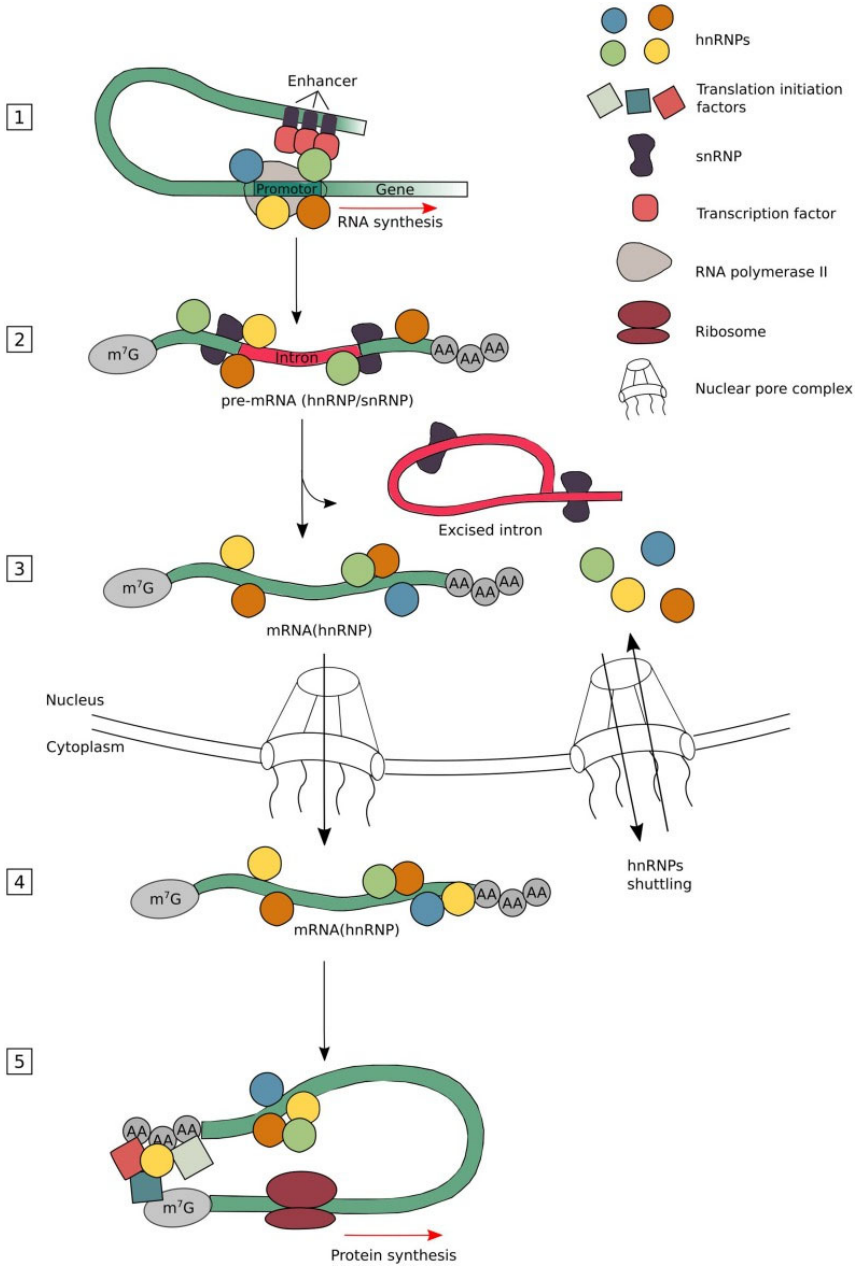

Figure 1-28: Different cytoplasmic and nuclear function of hnRNPs (265).

Figure 1-28 describes five major functions of hnRNPs involved in different stages of mRNA metabolism. In first stage, the hnRNPs bind with several transcription factors and other RNA binding proteins (RBPs) at promoter and enhancer sequence, to direct transcription. In the second stage, as soon as newly formed transcript is released by the RNA polymerase II, the hnRNPs and snRNPs bind rapidly with their nascent transcript to stabilize it. In the third stage, after the correct RBP complexes are formed, intronic sequences are removed by the spliceosome. Many hnRNPs including hnRNP F is known to regulate alternative splicing leading to exon skipping or intron retention. In the fourth step, these processed mature mRNAs are stabilised and transported by RBPs including hnRNPs through nuclear pore complex to cytoplasm for translation initiation. In the final step, or during translation, hnRNPs can bind at the 3'- and 5'- UTR of mRNA to control the translational enhancement or repression (265). Furthermore, many hnRNPs are found to be present in the same complexes, indicating multiple hnRNPs share a common structure and function. Indeed, as shown in the figure 1-29, several shared structural domains are found in different family members, which partly explains some of their shared functional properties.

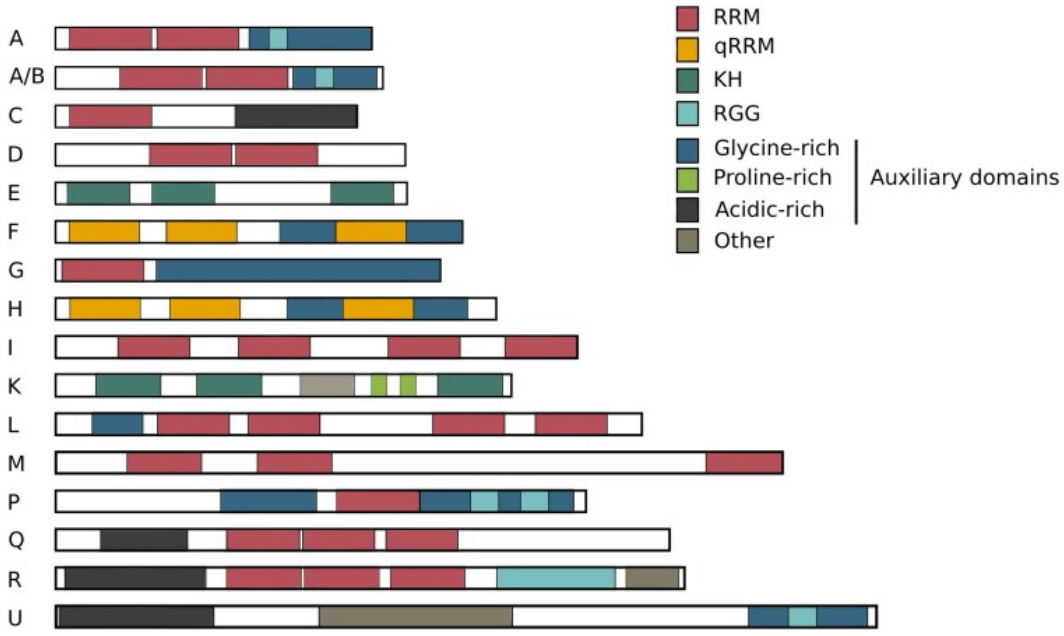

Figure 1-29: Domain structure of the hnRNP family members. *RRM,* RNA recognition motif; *qRRM,* quasi-RNA recognition motif and *KH,* K-homology domain, *RGG,* Arg-Gly-Gly repeat containing RNA-binding domain (265).

Emerging studies suggesting the role of hnRNPs in gene regulation during various diseases such as cancer, Alzheimer's, dementia, muscular atrophy, as the level of hnRNPs altered. Our group demonstrated that hnRNP F and hnRNP K level in the kidney of diabetic mice altered, suggesting also involved in the metabolic disorder like diabetes and nephropathy. We further showed that hnRNP F and K can directly regulate the gene expression of some genes implicated in DN including, major RAS components angiotensinogen, ACE2 and others such as Sirtuin1, Nrf2 etc. (266-272).

1.8.1 hnRNP K

Several studies, including the present one, have established that hnRNP K has multiple nuclear and cytosolic functions, including the regulation of transcription, mRNA silencing, mRNA stability, translation and signal transduction (265-267, 272-274). Dreyfuss *et al.* first characterized poly C binding hnRNP K protein as a member of hnRNP family (275). HnRNP K is very similar to hnRNP E_1/E_2, but markedly different from other members of hnRNP family due to the presence of KH (KH; K-Homology) domain. This evolutionary conserved KH domain containing a triple β-sheet platform supporting three α-helics (βααββα fold) has originally been found as triple repeats in hnRNP K by Dreyfuss *et al*. (figure 1-29) (276). Functionally, KH domains bind to RNA or ssDNA, which are also found in proteins associated with transcriptional and translational regulation.

The hnRNP K protein contains multiple K interactive regions, which act as a docking site for multiple kinases and proteins including chromatin, transcription, splicing and translation factors. Thus, hnRNP K is at the center of a vast interaction network, which enable it to play different roles in the cells (274). the researcher's group has identified that hnRNP K can interact with hnRNP F using co-immunoprecipitation (272).

1.8.2 hnRNP F

Matunis *et al*. isolated and cloned hnRNP F in 1994 (277). The open reading frame of rat and human hnRNP F cDNA has 98% similarity. hnRNP F is highly similar in sequence, structure and binding preferences to hnRNP H (figure 1-29), but they are functionally different. They are also regulated differently and have different binding specificities for gene regulatory elements (273). Unlike other hnRNPs which do not need a specific sequence to bind to RNA or

ssDNA, hnRNP F and H only bind to three consecutive guanines (G-tracts). The RNA-recognition motif (RRM) of hnRNP F and H is also different than others. The residues that contact RNA in the RRM are not conserved and this class of RRM was named quasi RRM (qRRM). These qRRMs interact with RNA by 'encaging' the G-tract RNA sequence (278). Several studies have described the major role of the hnRNP F in the regulation of alternative splicing by remodeling RNA structure (figure 1-28) (278, 279). The researcerh's group demonstrated that hnRNP F regulate transcription of various genes by binding to G rich promoter sequences and prevent DN in diabetic milieu (268-271).

1.9 Insulin Signaling in the Kidney

Insulin is secreted by the pancreatic β-cells in response to high glucose level. Insulin signaling is initiated when secreted insulin or insulin like growth factor (IGF) binds to the insulin receptor. When bound to its receptor, insulin activates a signaling cascade that promotes glucose uptake. Besides glucose uptake, insulin signaling affects multiple physiological processes by altering various intracellular metabolic pathways. Moreover, insulin signaling regulates the transcription of several genes and modulates cellular growth and differentiation. Abnormality in insulin production or signaling leads to disease condition. T1D is characterized by the inability to synthesize insulin, whereas in T2D, due to insulin signaling abnormalities the body becomes resistant to the effects of insulin.

1.9.1 Insulin Receptors

Insulin exerts its effect by binding to specific transmembrane receptors that belongs to tyrosine protein kinase family. These receptors include insulin receptor (IR), IGF receptor-I (IGF-IR) and insulin receptor related receptors (IRR), all of which are structurally related and mediate the actions of IGF-I, IGF-II and insulin, though with different affinities. The IR in humans is located on chromosome 19 and is encoded by a single gene *INRS* containing 22 exons and 21 introns spanning 120 kb. IR is a heterotetrameric receptor and consists of two extracellular insulin binding α-subunit and two intracellular tyrosine kinase β-subunits, which are linked by disulfide bonds in a β-α-α-β configuration (280). Alternate splicing of IR gene results in two isoforms, A and B, that either include or exclude exon 11 in the *α* subunit. IR-A lacks exon 11 and has a lower insulin affinity, whereas IR-B includes it and has highest insulin binding affinity. Insulin mediated receptor activation leads to auto-phosphorylation of tyrosine residues in the cytosolic domain of β subunits and initiates various cascades of phosphorylation (31, 281).

In the kidney, the high-affinity IR receptor is reported to present abundantly in all of the cells of the glomerulus and renal tubule, including the podocytes, proximal tubule, collecting ducts etc. IR-B isoform was shown to be present in the kidney abundantly (281). Due to the small size of active insulin molecule (6kDa), it can freely cross the glomerular filtration barrier and pass into the tubular lumen thereby affecting all renal cells of the kidney (31). Insulin

mediates different functions in the kidney ranging from glucose uptake to regulation of glomerular function, gluconeogenesis and tubular transport.

1.9.2 Insulin Signaling Pathways

Activated IR first recruit and phosphorylates intracellular adaptor proteins including insulin receptor substrate (IRS) isoforms IRS1 or IRS2 or other adaptor proteins including IRS3, IRS4, SHC, CBL, APS and SH2B, GAB1, GAB2, DOCK1, and DOCK2. Phosphorylation of these scaffold proteins on tyrosine residues by the IR is responsible for further recruiting and activation of various downstream effector proteins (282). The two major pathways of IR signal transduction are (1) IRS–phosphatidylinositol 3-kinase (PI3K)–Akt (also known as PKB) pathway and (2) the growth factor receptor-bound protein 2 (Grb2)–son of sevenless homologue 1 (SOS)–Ras–mitogen-activated protein kinase (MAPK, also known as ERK) pathway (figure 1-30) Besides this two major pathways, insulin signaling is also involved in IR-mediated phosphorylation of Cbl-associated protein (CAP), and formation of the CAP/CBL/CRKII complex to facilitate translocation of GLUT4 vesicles for glucose uptake (31, 282).

(1) **IRS/PI3K/Akt Pathway:** In response to insulin, activated IRS recruit and phosphorylates PI3K enzyme. Activated PI3K then phosphorylates phosphatidylinositol 4,5-bisphosphate (PIP2) to phosphatidylinositol 3,4,5-triphosphate (PIP3), a membrane bound lipid enzyme which then recruits the serine/threonine kinase Akt and 3-phosphoinositide-dependent protein kinase–1 (PDK1) to the plasma membrane where PDK1 activates Akt. Akt phosphorylates and activates many substrates such as (a) glycogen synthase kinase 3 (GSK3) for cell growth and glycogen synthesis; (b) mTOR complex 1 (mTORC1) and ribosomal protein S6 kinase (S6K) for protein and lipid synthesis as well as to regulate autophagy; (c) transcriptional regulators such as forkhead box O family members (FoxO) to regulate gluconeogenesis and lipid biosynthesis; (d) sterol regulatory element binding protein (SREBP) to maintain lipid homeostatic; (e) peroxisome proliferator-activated receptor γ co-activator 1 (PGC1α) for mitochondrial biogenesis; and (f) the GTPase-activating protein Akt substrate 160 kDa (AS160) for GLUT 4 mediated glucose uptake. PDK1 also phosphorylates the atypical protein kinases (aPKC), PKCζ and PKCλ/ί, which further facilitates insulin-stimulated glucose uptake and lipid synthesis (283).

(2) Grb2/SOS/Ras/MAPK pathway: SHC is another immediate downstream substrate for the IR. Upon activation SHC and IRS both can associates with growth factor receptor binder-2 (Grb2), an adaptor protein containing SH3 domains, which in turn associates with SOS and activates the cascade of serine/threonine kinases Ras/Raf/MEK/ERK1/2. Activated ERKs then translocate to the nucleus and phosphorylate different transcription factors, changing gene expression to promote growth, differentiation or mitosis (284).

Insulin resistance state: Insulin signal transduction also activates negative regulators, which tightly controls insulin signaling in the cells to avoid severe metabolic and proliferative dysfunction. These negative regulators are mainly phosphotyrosine/serine/threonine protein phosphatases (PTP1B, PP2A, PTP2B and PTB2C), lipid phosphatases PTEN, and SHIP, and adaptor proteins of the insulin receptor and IRS (Grb and SOCS) (figure 1-30). Hyperglycaemia, hyperinsulinaemia, high plasma free fatty acid (FFA) levels, inflammation etc. leads to dysregulation of these negative regulators which results in a chronically reduced cellular response to insulin or development of insulin resistence (283).

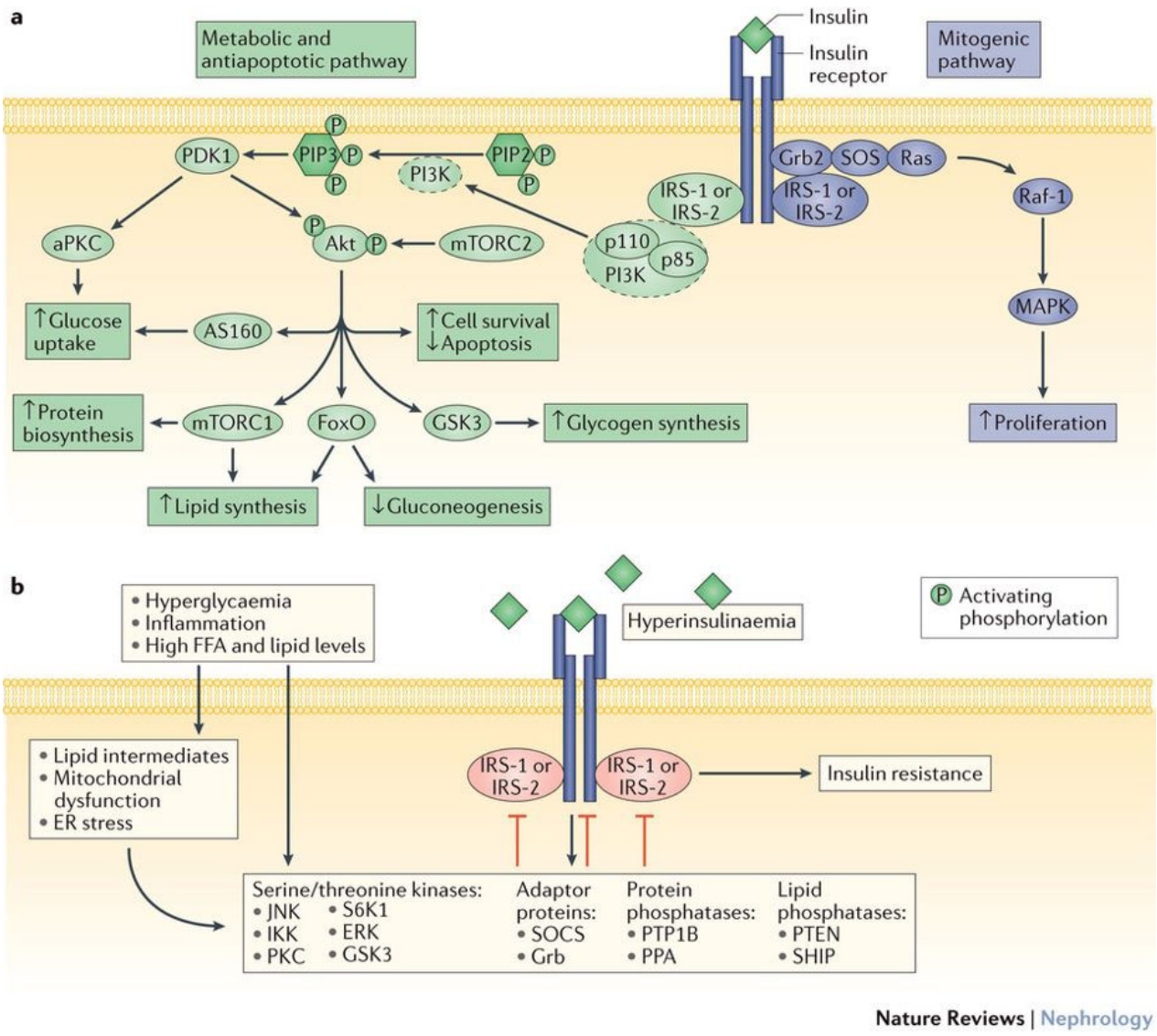

Figure 1-30 Insulin signaling pathways. **(a) Activation of two major insulin signalling pathways.** Insulin binding activates the IR and leads to the recruitment of IRS isoforms and subsequent activation of the PI3K/Akt pathway, which regulates glucose and lipid metabolism, protein biosynthesis, cell survival and apoptosis. Insulin-induced activation of the Ras/MAPK pathway increases transcription and cell proliferation. **(b) Negative regulation of insulin signalling pathways.** Hyperglycaemia, hyperinsulinaemia, high plasma FFA levels and inflammation activate serine/threonine kinases, adaptor proteins and phosphatases either directly or via lipid intermediates, mitochondrial dysfunction or the induction of endoplasmic reticulum (ER) stress. Activation of these negative regulators results in a chronically reduced cellular response to insulin. IKK, IκB kinase; JNK, c-Jun N-terminal kinase; PPA, protein phosphatase A; PTEN, phosphatase and tensin homologue; PTP1B, protein-tyrosine phosphatase 1B; p85, PI3K 85 kDa regulatory subunit α; p110, PI3K 110 kDa catalytic subunit α; Raf-1, RAF proto-oncogene serine/threonine-protein kinase; SHIP, SH2 domain-containing inositol phosphatase; SOCS, suppressor of cytokine signalling; S6K1, ribosomal protein S6 kinase β1 (283).

1.10 Animal model of Diabetic Nephropathy

Animals, specifically rodents offer an experimental model of unparalleled flexibility for studying diabetic nephropathy, including genetic modifications which can not be performed in humans. Although the major deficiency of studying animal models of DN is the absence of renal failure, several other short-term consequences, such as development of glomerular hyperfiltration, increased albuminuria, GFR and histopathologic changes can be detected in animal models that mimics pathophysiological characteristics of human DN. The Animal Models of Diabetic Complications Consortium (AMDCC) proposed following three criteria for an ideal progressive mouse model of DN: **(A)** Greater than 50% decline in GFR over the life time of the mice. **(B)** Greater than 10-fold increase in albuminuria than control mice. **(C)** Pathologic changes in kidneys, including advanced mesangial matrix expansion +/− nodular sclerosis and mesangiolysis, any degree of arteriolar hyalinosis, glomerular basement membrane thickening by >50% over baseline, and tubulointerstitial fibrosis (285). While some mouse strains are more susceptible to nephropathy than others, currently there is no mouse model of T1D or T2D that replicates all features of human DN mentioned above. Some of the widely used mouse models are discussed in detail below.

1.10.1 Mouse Model of Type 1 Diabetes

1.10.1.1 Streptozotocin (STZ)-Induced Diabetes

STZ induced T1D has be widely used as a model for DN. STZ is an antibiotic composed of glucosamine-nitrosourea. STZ is toxic as its glucose moiety gets transported into β-cells by GLUT2 causing pancreatic beta cell failure. This leads to hypoinsulinemia and hyperglycemia, leading to subsequent development of diabetes in animal. STZ treated animals develop proteinuria, increased albumin to creatinine ratio (ACR) as well as mesangial matrix expansion, depending on the genetic background of the animals. A major advantage of STZ model is the rapid development of diabetes and this can be induced in both resistant and susceptible strains of DN. One major disadvantage of STZ model is non-specific toxicity which can complicate the interpretation of results. Besides different strains might need different dose of STZ to minimise its toxicity (286). Low dose STZ method requirs daily intraperitoneal injections of 40–50 mg/kg of STZ for 5 consecutive days as recommended by AMDCC.

1.10.1.2 Akita *Ins2*$^{+/C96Y}$ mutant mice

The toxicity of STZ can be avoided by using genetically modified Akita strains of mice to develop T1D. Akita mice have an autosomal dominant mutation, a single nucleotide substitution (cysteine, T**G**C to tyrosine, T**A**C) in the *Ins2* gene. This mutation disrupts a disulfide bond between A and B chains of insulin, causing abnormal folding of the insulin protein, toxic injury to pancreatic β cells and diminished capacity to secrete insulin, resulting in T1D (287). Several group, including the researcher's, reported that in C57BL/6 strain, Akita mice develop hyperglycemia, hypertension, modest levels of albuminuria, increased mesangial matrix and basement membrane thickening, depletion of podocytes, increased apoptosis and thereby manifests early in development of DN (266, 288). Akita mice are available commercially from Jackson Laboratories. One disadvantage of Akita mice is lack of genetic background other than C57BL/6, which is relatively resistant to nephropathy. Moreover, hyperglycemia in females is relatively mild as compared to males (286).

1.10.2 Mouse models of type 2 diabetes

1.10.2.1 db/db mouse model

The db/db mouse model of leptin deficiency is currently the most widely used mouse for DN in settings of T2D and exhibits many features similar to human DN. Db/db mice have a deletion mutation in the leptin (adipocyte-derived hormone) receptor (*LepR db/db*) which results in abnormal splicing and defective leptin signaling (289). Leptin deficiency results in susceptibility to obesity, insulin resistance, and T2D. DN in these mice is characterized by albuminuria, podocyte loss, and mesangial matrix expansion. The mice become obese around 3 to 4 weeks of age, while increase in plasma insulin begins at 10 to 14 days and blood sugar at 4 to 8 weeks (286, 290, 291). Db/db mice are commercially available but their major disadvantage is being infertile and autosomal recessive. Furthermore, db/db mice in C57BL/6 background does not result in significant DN.

1.10.2.2 High fat diet model

High-fat diet (HFD) feeding in C57BL/6 mice causes various systemic metabolic abnormalities, including obesity, insulin resistance, hyperglycemia, and abnormal lipid profiles

and subsequent renal injuries, such as albuminuria, which are similar to human metabolic syndrome including T2D. After 12 weeks of HFD feeding, C57BL/6 mice exhibited a mild increase in urinary ACR and renal pathophysiological alterations including the accumulation of collagen IV, glomerular basement thickening, oxidative stress, inflammation and impaired sodium handling (292). However, attention must be given to the fact that systemic lipid overload (lipotoxicity), rather than hyperglycemia, may be related to the pathological changes.

Some other currently recommended models used in DN are described below (293, 294)

Mouse Model	Description
ApoE$^{-/-}$ on C57BL6 mice	T1DM, Specific genetic modifications to accelerate nephropathy. STZ-induced diabetes combined with hyperlipidemia due to lack of apolipoprotein E.
eNOS$^{-/-}$ on C57BL6 or db/db mice	Vascular dysfunction and hypertension induced by eNOS deficiency accelerate renal injury in either STZ-induced diabetes (T1DM) or when backcrossed to db/db mice (T2DM). Currently, *eNOS*$^{-/-}$ mice are available on B6, BKS-db/db and BALB/cBy backgrounds from Jackson Laboratory.
Zucker rat	T2DM, hyperphagic and obese, due to missense mutation in the gene coding the leptin receptor
OVE26 mice on FVB background	T1DM, mutation in the calmodulin gene results in toxic accumulation of defective proteins in beta-cells (nephropathy can be further exacerbated by uninephrectomy)
NOD	Spontaneous development of β-cell failure may mimic pathophysiology of disease in humans, commercially available. Major disadvantages including npredictable timing of development of diabetes; absence of control strain; needs insulin therapy to survive long periods;
DBA/2J mice	T1DM, STZ injection induces diabetes on a strain susceptible for nephropathy
Bradykinin B2 receptor (B2R) deficiency	B2R (*Bdkrb*2) deletion in *Ins2*$^{Akita/+}$ mice on a B6 background develop a 4-fold increase in albuminuria and profound mesangial expansion that resembles human diabetic glomerulosclerosis (295).
Renin-overexpression TTRhRen on FVB mice	T1DM, hypertension induced by human renin overproduction combined with diabetes induced by STZ injection or OVE26 mutation (296).

Table 1- 6: Animal models of DN.

1.11 Objective and hypothesis of the present study

Rational: Patients with diabetes have a higher risk of developing DN, which is the leading cause of ESRD in North America (13). Although glomerular dysfunction is associated with early events of DN, tubulopathy, including tubular atrophy and tubule-interstitial fibrosis is invariably associated with gradual loss of renal function in later stages of DN. Tubulopathy is now considered a better predictor of renal disease progression than glomerular pathology (297-300).

Hyperglycemia, hyperlipidemia, oxidative stress and dysregulation of RAS has been implicated in the progression of DN. Intensive insulin therapy and chronic RAS blockers to maintain respective normal blood glucose and blood pressure are the most effective treatment in retarding DN progression (18, 301, 302). Furthermore, their underlying molecular mechanisms of action remains incompletely understood. The main objective of this thesis is to understand how hyperglycemia-induced oxidative stress and RAS activation leads to systemic hypertension and kidney injury and to elucidate underlying molecular mechanisms regarding how insulin prevents hypertension and kidney injury in diabetic mice.

Dr. Chan's laboratory previously established that high glucose enhances Agt gene expression via ROS generation in rat RPTCs in vitro (303-306). Transgenic mice overexpressing Agt in RPTC develop hypertension, tubular apoptosis, albuminuria and kidney injury (197). Moreover, hyperglycemia and renal Agt overexpression act in concert to enhance hypertension, albuminuria and RPTC apoptosis (307, 308). In contrast, catalase (Cat) overexpression in RPTC attenuated Agt expression, ROS generation, hypertension, RPTC apoptosis in nondiabetic Agt/Cat-Tg mice as well as in diabetic mice (146, 309, 310). All these demonstrated the crucial role played by oxidative stress and RAS dysregulation in DN progression.

Enhanced oxidative stress triggers upregulation of antioxidants and phase II detoxifying enzymes via upregulating Nrf2, a transcription factor, which binds to the anti-oxidant responsive element (ARE) sequence of the genes and promote their transcription. In murine models of diabetes, Nrf2 activation remains controversial because of conflicting results (159, 311-315). A recent phase 3 clinical trial (BEACON) with chronic Nrf2 activation in T2D patients was prematurely terminated because of insufficient improvement in renal function and higher cardiovascular mortality (316). The reasons for this disappointing outcome remain unknown.

As Nrf2 activation seems to be associated with higher rate of heart failure, and increased blood pressure and albuminuria, this encouraged investigation into whether Nrf2 is involved in RAS activation as one possible cause of increased blood pressure and albuminuria. Dr. Chan's group previously demonstrated that in diabetic condition, hyperglycemia and lower catalase activity induces ROS generation which in turns activate Nrf2. Nrf2 activation in turn increases Agt transcription via binding to ARE sequence in Agt gene which leads to development of hypertension and kidney injury. Moreover, overexpression of catalase in RPTC of diabetic Akita mice could attenuate Agt activation by lowering ROS generation and Nrf2 expression, thereby prevents hypertension and kidney injury.

Dr. Chan's group has previously established that insulin can also inhibit high glucose and ROS stimulation of renal Agt expression via a putative insulin response element (IRE) present in the rat Agt promoter that binds to two nuclear proteins, hnRNP F and hnRNP K, *in vitro* (271, 272, 317). This observation has been further confirmed by overexpressing hnRNP F in the RPTC of Akita mice which exhibit lower Agt expression and hypertension (268). Recently, Dr. Chan's group has shown that hnRNP F and K mediates, at least in part, insulin inhibition of renal Agt gene expression in Akita mice (266). These observations prompted us to investigate if insulin can directly regulate Nrf2 expression beyond its glucose-lowering effects. We hypothesised that insulin can downregulate Nrf2 gene transcription via hnRNP F/K and prevent Nrf2 stimulation of Agt gene expression, thereby attenuating hypertension and renal injury in Akita mice.

To understand how ROS mediates RPTC apoptosis, Dr. Chan's group used microarray analysis and discovered that a pro-apoptotic gene Bmf expression was up-regulated in RPTCs of db/db mice, compared to db/m+ mice and normalized in db/db Cat-Tg mice. STZ treated diabetic mice also upregulated Bmf expression which was normalised by insulin treatment. Furthermore, Bmf expression was markedly increased and localised to apoptotic RPTCs in human diabetic kidneys (249). In response to cellular stress, Bmf was reported to induce apoptosis and anoikis (250, 318). However, whether enhanced Bmf expression would induce RPTC apoptosis *in vivo*, required further investigation. In addition, the molecular regulation of Bmf expression in RPTCs remains unknown. This leads us to hypothesize that (a) Bmf overexpression in RPTC causes tubular apoptosis, anoikis and renal injury; and (b) insulin

supresses Bmf gene transcription via putative IRE in the Bmf promoter region that binds to hnRNP F. Therefore, the major aims of this thesis are:

1. To investigate whether insulin could inhibit Nrf2 gene transcription and Nrf2-stimulation of Agt gene expression via hnRNP F/K and subsequently inhibit the development of hypertension and renal injury in Akita mice.

2. To investigate if overexpression of human Bmf in mouse RPTC could induce RPTC apoptosis and tubulopathy and whether insulin could inhibit Bmf gene transcription via hnRNP F that binds to the insulin (or hnRNP F) responsive element in the Bmf gene promoter and subsequently attenuating RPTC apoptosis and tubulopathy in Akita mice.

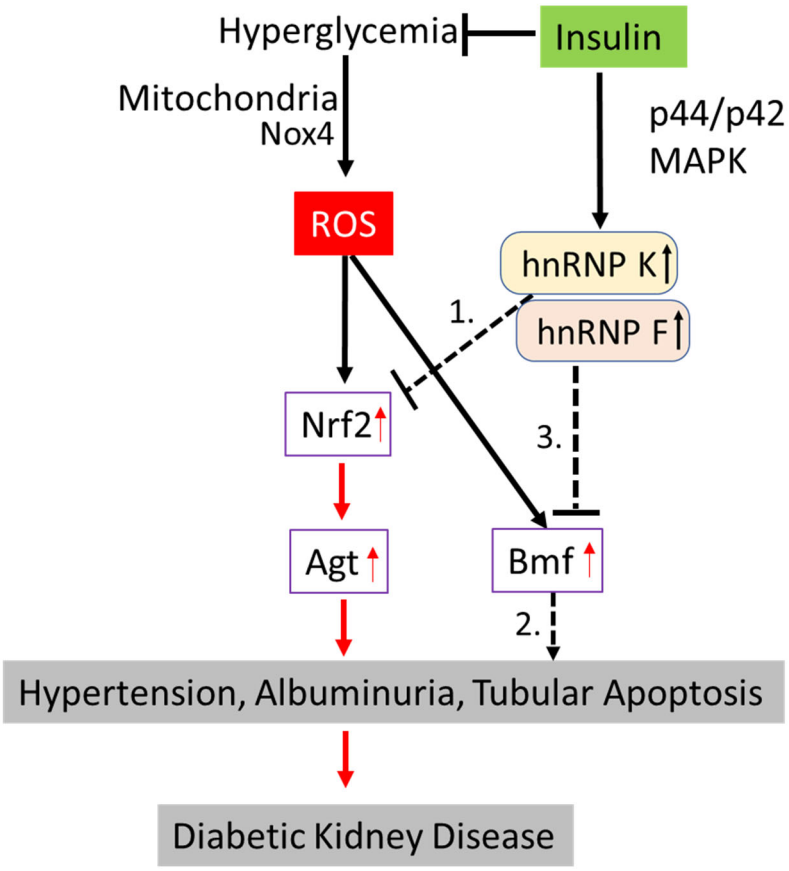

Figure 1-31: Proposed hypothesis for the current study. Aims of the study were shown as numbered. **1.** Whether insulin down-regulate Nrf2 expression via hnRNP F/K mediated IRE binding in the Nrf2 promoter? **2.** Whether overexpression of Bmf can cause RPTC apoptosis and renal dysfunction? **3.** Whether insulin can down regulate Bmf expression via hnRNP mediated IRE binding in the Bmf promoter?

Chapter 2: Article 1

Published in Endocrinology (2017) 158 (4): 903-919

Insulin Inhibits Nrf2 Gene Expression via Heterogeneous Nuclear Ribonucleoprotein F/K in Diabetic Mice

Anindya Ghosh[1,4], Shaaban Abdo[1,4], Shuiling Zhao[1], Chin-Han Wu[1], Yixuan Shi[1], Chao-Sheng Lo[1], Isabelle Chenier[1], Thierry Alquier[1], Janos G. Filep[2], Julie R. Ingelfinger[3], Shao-Ling Zhang[1*], John S. D. Chan[1*]

[1]Department of Medicine, Université de Montréal and Centre de recherche du Centre hospitalier de l'Université de Montréal (CRCHUM), 900 Saint-Denis St., Montreal, QC, Canada H2X 0A9

[2]Department of Pathology and Cell Biology, Université de Montréal and Centre de recherche, Hôpital Maisonneuve-Rosemont, 5415 boul. de l'Assomption, Montreal, QC, Canada H1T 2M4

[3]Pediatric Nephrology Unit, Massachusetts General Hospital, Harvard Medical School, 15 Parkman Street, WAC 709, Boston, MA 02114-3117, USA

[4]These authors contributed equally to this work
[1*]John S.D. Chan and Shao-Ling Zhang are joint senior authors

Abbreviated Title: Insulin and Nrf2 in diabetic kidney
***Key terms*:** Insulin, Nuclear factor erythroid 2-related factor 2, hypertension, diabetic kidney, Akita mice

Abstract: 203 words; Main text: 4,007 words

Number of figures and tables: 10

Corresponding authors and persons to whom reprint requested should be addressed:

John S.D. Chan, Ph.D. and/or Shao-Ling Zhang
Centre de recherche du Centre hospitalier de l'Université de Montréal (CRCHUM)
900 Saint-Denis St., Montreal, QC, Canada H2X 0A9
Telephone: (514) 890-8000 Extension 15080 or 15633; Fax: (514) 412-7655
E-mail: john.chan@umontreal.ca; shao.ling.zhang@umontreal.ca

Disclosure Statement: The authors have nothing to disclose

Abstract

Oxidative stress induces endogenous antioxidants via nuclear factor erythroid 2-related factor 2 (Nrf2), potentially preventing tissue injury. We investigated whether insulin affects renal Nrf2 expression in type 1 diabetes (T1D) and studied its underlying mechanism. Insulin normalized hyperglycemia, hypertension, oxidative stress and renal injury, inhibited renal *Nrf2* and angiotensinogen (*Agt*) gene expression and up-regulated heterogeneous nuclear ribonucleoprotein F (*hnRNP F*) and *hnRNP K* expression in Akita mice with T1D. In immortalized rat renal proximal tubular cells, insulin suppressed *Nrf2* and *Agt* but stimulated *hnRNP F* and *hnRNP K* gene transcription in high glucose via p44/42 mitogen-activated protein kinase signalling. Transfection with small interfering RNAs of *p44/42 MAPK, hnRNP F* or *hnRNP K* blocked insulin inhibition of *Nrf2* gene transcription. Insulin curbed *Nrf2* promoter activity via a specific DNA-responsive element that binds hnRNP F/K, and hnRNP F/K overexpression curtailed *Nrf2* promoter activity. In hyperinsulinemic-euglycemic mice, renal *Nrf2* and *Agt* expression was down-regulated, whereas *hnRNP F/K* expression was up-regulated. Thus, the beneficial actions of insulin in diabetic nephropathy appear to be mediated, in part, by suppressing renal *Nrf2* and *Agt* gene transcription and preventing Nrf2 stimulation of *Agt* expression via hnRNP F/K. These findings identify hnRNP F/K and Nrf2 as potential therapeutic targets in diabetes.

Introduction

Under physiological conditions, oxidative stress triggers up-regulation of endogenous antioxidants via nuclear factor erythroid 2-related factor 2 (Nrf2), which may prevent tissue injury by the induction of genes encoding various antioxidant and phase 2-detoxifying enzymes (319-321). Pre-clinical studies have postulated a renoprotective role for Nrf2 activation in diabetes (312, 322, 323) . Clinical trials with bardoxolone methyl (an Nrf2 activator that activates Nrf2 signaling and also inhibits NF-κB and STAT signaling in human cell lines) (324, 325), however, have yielded conflicting results. The phase 2 BEAM study targeted renoprotective actions of bardoxolone methyl in patients with type 2 diabetes (T2D) with stage 3b or 4 chronic kidney disease (CKD) (326). In contrast, the phase 3 BEACON trial in T2D patients with stage 4 CKD was discontinued after 9 months owing to insufficient improvement in renal function and unchanged risk of end-stage renal disease (327). Bardoxolone methyl actually increased the risk of heart failure and cardiovascular death in the BEACON trial (327). The reasons for these disparate outcomes remain unknown.

We reported previously that catalase (Cat) overexpression in renal proximal tubular cells (RPTCs) prevents hypertension and nephropathy, attenuates renal angiotensinogen (Agt) and Nrf2 gene expression, and blocks Nrf2 stimulation of Agt gene transcription, in type 1 diabetes (T1D) Akita Cat-Tg (transgenic) mice (146, 176, 310). Our data suggested that chronic Nrf2 activation by hyperglycemia might aggravate renal dysfunction via enhanced intrarenal renin-angiotensin system (RAS) in diabetes.

Beyond its hypoglycemic effect, insulin has been shown to regulate the expression of transcription factor genes and genes involved in inflammation and insulin signaling (328, 329). We previously established that insulin inhibits high-glucose (HG) and reactive oxygen species

(ROS) stimulation of renal *Agt* expression via 2 nuclear proteins, heterogeneous nuclear ribonucleoprotein F and K (hnRNP F and hnRNP K) that bind to a putative insulin-responsive element (*IRE*) in the rat *Agt* gene promoter (271, 272, 305, 306, 317, 330). We further established that hnRNP F normalizes systemic hypertension via suppression of renal Agt production in Tg mice specifically overexpressing hnRNP F in their RPTCs (268). Recently, we showed that hnRNP F and hnRNP K mediate, at least in part, insulin suppression of renal *Agt* gene expression (266).

Here we investigated whether insulin could inhibit *Nrf2* gene transcription, avert Nrf2-stimulation of *Agt* gene expression via hnRNP F/K and, subsequently, prevent systemic hypertension and renal injury in T1D mice.

Materials and Methods

Chemicals and Constructs

D-glucose, D-mannitol, human insulin, PD98059 (a p44/42 mitogen-activated protein kinase (p44/42 MAPK) inhibitor), wortmannin and Ly-294,002 (specific inhibitors of phosphatidylinositol 3-kinase: PI3-K), and oltipraz (an Nrf2 activator) were purchased from Sigma-Aldrich Canada Ltd. (Oakville, ON, Canada). U0126 (a p44/42 MAPK inhibitor) was obtained from Cell Signaling Technology (New England Biolabs Ltd., Whitby, ON, Canada). Dulbecco's Modified Eagle's Medium (DMEM, 5 mmol/l D-glucose, catalogue no. 12320), penicillin/streptomycin and fetal bovine serum (FBS) were procured from Invitrogen, Inc. (Burlington, ON, Canada). Insulin implants (Linβit, with a release rate of approximately 0.1 unit/implant/day for >30 days) were sourced from Linshin (Scarborough, ON, Canada). pGL4.20 {Luc/Puro] vector containing luciferase reporter came from Promega Corporation

(Sunnyvale, CA, USA). The pGL4.20 construct, containing the rat *Agt* gene promoter N-1495 to N+18 or the rat *Nrf2* gene promoter N-1960 to N+111, has been described previously (176, 331). The *hnRNP F* gene promoter N-1,500 to N+99 and the *hnRNP K* gene promoter N-1,516 to N+16 were cloned from rat genomic DNA by conventional polymerase chain reaction (PCR) with specific primers (**Table 1**), confirmed by DNA sequencing and then inserted into pGL4.20 vector via Kpn I and Hind III restriction sites. Rabbit polyclonal antibodies specific to rat hnRNP F and polyclonal antibodies against rat Agt were generated in our laboratory (JSDC) (271, 332). The other antibodies used are listed in **Table 2**. Scrambled Silencer Negative Control #1 and *p44/42 MAPK*, *Nrf2*, *hnRNP F* and *hnRNP K* small interfering RNAs (siRNAs) were provided by Ambion, Inc. (Austin, TX, USA). Restriction and modifying enzymes were supplied by Invitrogen, Inc. and New England Biolabs. Oligonucleotides were synthesized by Integrated DNA Technologies (Coralville, IA, USA). QuickChange II Site-Directed Mutagenesis Kit and LightShift Chemiluminescent EMSA (electrophoretic mobility shift assay) Kit were procured from Agilent Technologies (Santa Clara, CA, USA) and Thermo Scientific (Life Technologies Inc., Burlington, ON, Canada), respectively. Primer biotin-labeling kit was purchased from Integrated DNA Technologies.

Physiological Studies

Adult male wild type (WT) and heterozygous Akita mice with mutated *insulin2* gene (C57BL/6-Ins2^{Akita}/J) were purchased from Jackson Laboratories (Bar Harbor, ME, USA: http://jaxmice-jax.org).

Male Akita mice (age 10 weeks) were divided into 2 groups with and without insulin implants at week 12 until week 16 (266). Non-Akita littermates served as controls. All animals

had access to standard mouse chow and water *ad libitum*. Animal care and procedures were approved by the CRCHUM Animal Care Committee and followed the Principles of Laboratory Animal Care (NIH publication no. 85-23, revised 1985: http://grants1.nih.gov/grants/olaw/references/phspol.htm).

Blood glucose levels and systolic blood pressure (SBP) were measured with an Accu-Chek Performa System (Roche Diagnostics) and BP-2000 tail-cuff pressure monitor (Visitech Systems, Apex, NC, USA), respectively (146, 176, 266, 268, 308, 310). The mice were housed individually in metabolic cages 24 h prior to euthanasia. Blood was collected by cardiac puncture before sacrifice and centrifuged for serum. Urine was sampled and assayed for albumin/creatinine ratio (ACR) by enzyme-linked immunosorbent assay (ELISA) with Albuwell and Creatinine Companion (Exocell, Inc., Philadelphia, PA, USA) (146, 176, 266, 268, 308, 310).

Glomerular filtration rate (GFR) was estimated with fluorescein isothiocyanate inulin (176, 266, 268, 308). Kidneys were removed immediately after GFR measurement, decapsulated and weighed before Percoll gradient isolation of renal proximal tubules (RPTs) (176, 266, 268, 308). Aliquots of freshly-isolated RPTs from individual mice were immediately processed for total RNA and protein isolation.

Separate hyperinsulinemic-euglycemic clamp experiments were performed on conscious male C57Bl/6 mice (age 12-14 weeks) after 4-h food restriction (333).

Serum and Urinary Agt and Angiotensin II (Ang II)

Serum and urinary Agt and Ang II levels were quantified by ELISA (Immuno-Biological Laboratories, Inc., Minneapolis, MN, USA) (146, 176, 266, 268, 308).

Morphologic Studies

Kidney sections (3-4 μm thick, 4-5 sections per kidney, 5-6 kidneys per group) were stained with standard periodic acid Schiff (PAS) or Masson's trichrome or processed for immunohistochemistry (ABC Staining, Santa Cruz Biotechnology, Santa Cruz, CA, USA) (146, 176, 266, 268, 308, 310). Tubular luminal areas, mean glomerular tuft and RPTC volumes were assessed on PAS-stained sections (146, 176, 266, 268, 308, 310). Immunostained images were quantified by NIH ImageJ software (http://rsb.info.nih.gov/ij/).

ROS generation as an index of oxidative stress was assessed by dihydroethidium (DHE; Sigma-Aldrich Canada Ltd.) staining of frozen kidney sections (146, 176, 266, 268, 308, 310) and by lucigenin in freshly-isolated RPTs (146, 176, 266, 268, 305, 306, 308, 310, 330). The results were confirmed by standard Cat and nicotinamide adenine dinucleotide phosphate (NADPH) oxidase activity assays (266, 268, 308, 334).

Effect of Insulin on Gene Expression in Immortalized Rat Renal Proximal Tubular Cells (IRPTCs)

Rat IRPTCs (335) (passages 12 to 18) were studied. Plasmids pGL4.20-*Agt*, pGL4.20-*Nrf2*, pGL4.20-*hnRNP F* and pGL4.20-*hnRNP K,* respectively containing *Agt, Nrf2, hnRNP F* and *hnRNP K* gene promoters, were transfected into IRPTCs. Stable transformants were selected in the presence of 0.6 mg/l of puromycin (176).

To study the effects of insulin, stable transformants (75-85% confluence) were synchronized overnight in serum-free DMEM containing 5 mmol/l D-glucose, then incubated in normal glucose (NG, 5 mmol/l D-glucose plus 20 mmol/l D-mannitol) or HG (25 mmol/l D-

glucose) DMEM containing 1% depleted FBS and insulin (10^{-7} mol/l) for up to 24 h ± p44/42 MAPK inhibitors (PD98059 or U0126), PI3-K inhibitors (Ly-294,002 or wortmannin) or the Nrf2 activator oltipraz. The cells were then harvested, and promoter activity was measured by luciferase assay (176, 266, 269). IRPTCs stably transfected with pGL4.20 served as controls.

In additional studies, stable IRPTC transformants were transfected with scrambled siRNA, *p44/42 MAPK, Nrf2, hnRNP F* or *hnRNP K* siRNAs (176, 266, 269), and their effects on gene promoter activity, mRNA and protein expression were analyzed after 24 h of culture.

Real Time-Quantitative PCR (RT-qPCR) Assays and Western Blotting (WB)

Cat, Agt, hnRNP F, hnRNP K, Nrf2, heme oxygenase-1 (*HO-1),* Kelch-like ECH-associated protein 1 (*Keap1), Nox1, Nox2, Nox4* and β-*actin* mRNA levels in RPTs and IRPTCs were quantified by RT-qPCR with specific primers (**Table 1**).

WB was undertaken (146, 176, 266, 268, 269, 308, 310, 334). The relative densities of Cat, Agt, hnRNP F, hnRNP K, Nrf2, HO-1, Keap1 and β-actin bands were quantified by computerized laser densitometry (ImageQuant software, version 5.1, Molecular Dynamics, Sunnyvale, CA, USA).

Statistical Analysis

Values were expressed as mean ± SEM. Data were analyzed using 1-way or 2-way analysis of variance, as appropriate, followed by a Bonferroni multiple comparison testing. $p<0.05$ values were considered statistically significant.

Results

Physiological Studies

Table 3 reports the results of physiological measurements in non-Akita WT, Akita and Akita mice treated with insulin at the age of 16 weeks. Insulin normalized blood glucose, SBP, kidney weight/tibia length and heart weight/tibia length ratios, ACR, GFR, urinary Agt and Ang II levels in Akita mice compared to untreated Akita controls. No changes in serum Agt levels were detected among the different groups.

Histological Studies

Consistent with earlier observations (146, 176, 266, 268, 269, 308, 334), Akita mice developed renal damage, including proximal tubule cell atrophy, tubule lumen dilation, accumulation of cell debris (Online Supplemental Figure 1A), as well as increased extracellular matrix proteins in glomeruli and tubules (Online Supplemental Figure 1B). Glomerular tufts, RPTC volume and renal tubule lumen areas were augmented significantly in Akita mice compared to WT controls. Insulin treatment normalized these changes (**Table 3**).

Average SBP was 20-25 mmHg higher in Akita mice at age 11 weeks than in WT mice ($p<0.005$) and remained significantly elevated for the study's duration (**Fig. 1A** and **Table 3**). Insulin treatment completely normalized SBP in Akita mice.

Cat immunostaining (**Fig. 1B)** and semi-quantitation of Cat-immunostained areas (**Fig. 1C**), Cat activity (**Fig. 1D**), but not *Cat* mRNA expression (**Fig. 1E**), were significantly lower in RPTs from Akita versus WT mice. Insulin treatment reversed these changes in Akita mice. In contrast, Akita mice exhibited significantly greater DHE staining (**Fig. 1F**), ROS levels (**Fig.**

1G), NADPH oxidase activity (**Fig. 1H**), and *Nox4* mRNA expression (**Fig. 1I**) than WT controls. Insulin normalized these changes. No differences in *Nox1* and *Nox2* mRNA expression were detected (**Fig. 1J** and **Fig. 1K**).

Renal Agt, HO-1, Nrf2, Keap1 and HnRNP F/K expression

Agt, HO-1 and Nrf2 immunostaining increased in RPTCs of Akita mice compared to WT controls. Treatment with insulin normalized these changes (**Fig. 2A**). Keap1 immunostaining did not differ between groups (**Fig. 2A**). WB of Agt and HO-1 (**Fig. 2B**), Nrf2 and Keap1 (**Fig. 2C**), and RT-qPCR of *Agt*, *HO-1, Nrf2* and *Keap1* mRNA expression (**Fig. 2E**, i-iv, respectively) from isolated RPTs confirmed these findings. Furthermore, insulin treatment decreased nuclear Nrf2 and phosphorylated (p)-Nrf2 (s-40) expression without significantly affecting cytosolic Nrf2 and p-Nrf2 expression in RPTs of Akita mice (**Fig. 2D**). Consistent with previous observations (266), immunostaining of hnRNP F/K (Online Supplemental Figure 1C (i)) and WB of hnRNP F/K showed decreases in Akita compared to WT mice, with normalization by insulin (Online Supplemental Figure 1C (ii)).

Effect of Insulin on Agt, HnRNP F/K and Nrf2 Gene Expression in IRPTCs

Insulin attenuated *Nrf2* and *Agt* gene promoter activity in NG and prevented HG stimulation of *Nrf2* and *Agt* gene promoter activity in IRPTCs in a time-dependent manner (Online Supplemental Figure 1D and Figure 1E, respectively). In contrast, insulin stimulated *hnRNP F* and *hnRNP K* gene promoter activity in NG and HG in IRPTCs in a time-dependent manner (Online Supplemental Figure 1F and 1G, respectively). PD98059 and U0126, but not wortmannin or Ly-294,002, prevented insulin inhibition of *Nrf2* gene promoter activity (**Fig.**

3A), *Agt* gene promoter activity (**Fig. 3B**) and insulin stimulation of *hnRNP F* (**Fig. 3C**) as well as *hnRNP K* promoter activity (**Fig. 3D**) in IRPTCs.

Insulin stimulated p44/p42 MAPK phosphorylation in a time-dependent manner in NG and HG in IRPTCs (Online Supplemental Figure 2A (i) and (ii)). Transient transfection of *p44 MAPK* and *p42 MAPK* siRNAs attenuated the expression of respective p44 MAPK and p42 MAPK in IRPTCs, whereas scrambled siRNA had no effect (Online Supplemental Figure 2B). Transfection with *p44 MAPK* or *p42 MAPK* siRNAs or both reversed insulin inhibition of *Nrf2* and *Agt* gene promoter activity (**Fig. 3E** and **Fig. 3F,** respectively) and insulin stimulation of *hnRNP F* and *hnRNP K* gene promoter activity (**Fig. 3G** and **Fig. 3H**, respectively). Quantitation of *Nrf2*, *Agt*, *hnRNP F* and *hnRNP K* mRNA expression (Online Supplemental Figures 2C to 2F, respectively) confirmed these observations. Our findings lend additional support to the concept that insulin inhibition of *Agt* and *Nrf2* and stimulation of *hnRNP F* and *hnRNP K* transcription requires p44 MAPK or p42 MAPK alone or both signaling in RPTCs *in vivo*.

Insulin Prevents Nrf2 Stimulation of *Nrf2* and *Agt* Gene Expression via HnRNP F/K Expression in IRPTCs

We next explored whether insulin inhibits *Nrf2* gene expression via hnRNP F/K and whether hnRNP F/K could prevent Nrf2 stimulation of *Agt* and *Nrf2* gene transcription in IRPTCs. As anticipated, oltipraz (an Nrf2 activator) stimulated both *Nrf2* and *Agt* gene promoter activity in IRPTCs (176), which was tempered by insulin (**Fig. 4A** and **Fig. 4B,** respectively). In contrast, oltipraz diminished *hnRNP F* and *hnRNP K* gene promoter activity which was reversed by insulin (**Fig. 4C** and **Fig. 4D**, respectively). Once again, PD98059 reversed these

actions of insulin (**Figs. 4A-D**). Our observations were confirmed by RT-qPCR and WB of their respective mRNA (**Figs 4E-H**) and protein (**Figs. 4I** and 4**J**) expression.

Transfection of *hnRNP F* or *hnRNP K* siRNA or both reversed the inhibitory effect of insulin on *Nrf2* promoter activity and Nrf2 mRNA expression in IRPTCs in HG (**Fig. 5A** and **Fig. 5B**, respectively), whereas transfection of *Nrf2* cDNA attenuated insulin's inhibitory impact on both *Nrf2* and *Agt* promoter activity in a concentration-dependent manner (**Fig. 5C** and **Fig. 5D**, respectively). In contrast, *Nrf2* siRNA transfection further enhanced the suppressive action of insulin on both *Nrf2* and *Agt* gene promoter activity (**Fig. 5E** and **Fig. 5F**, respectively). Interestingly, co-transfection with *hnRNP F* and/or *hnRNPK* cDNA tempered the stimulatory effect of *Nrf2* cDNA on *Nrf2* and *Agt* gene promoter activity (**Fig. 5G** and **Fig. 5H**, respectively) and their mRNA levels (**Fig. 5I** and **Fig. 5J,** respectively), indicating that hnRNP F and hnRNP K compete with Nrf2 on *Nrf2* and *Agt* gene transcription in RPTCs *in vivo*.

Localization of *HRNP F-RE* in Rat Nrf2 Gene Promoter

To localize putative DNA-responsive elements (REs) that mediate insulin's inhibitory action, plasmids containing various lengths of the rat *Nrf2* gene promoter were transiently transfected into IRPTCs. pGL4.20-*Nrf2* promoter N-1960/N+111 exhibited 10-fold increases compared to control plasmid promoterless pGL4.20 in IRPTCs (**Figure 6A**). Deletion of nucleotides to N-820, N-537 and N-400 augmented the activity of pGL4.20-*Nrf2* promoter N-820/N+111, pGL4.20-*Nrf2* promoter N-537/N+111 and pGL4.20-*Nrf2* promoter N-400/N+111 to 22-, 18- and 10-fold compared to control plasmid pGL4.20, respectively. Furthermore, deletion of nucleotides to N-150 lowered the promoter activity of pGL4.20-*Nrf2* promoter N-150/+111 to 2.5-fold higher than the control (**Figure 6A**). Insulin averted the stimulatory effect

of HG on pGL4.20-*Nrf2* promoters N-1960/N+111, N-820/N+111 and N-537/N+111, whereas HG and insulin had no impact on the activity of the pGL4.20-*Nrf2* promoters N-400/N+111 and N-150/N+111 (**Fig. 6B**). Interestingly, deletion of nucleotides N-463 to N-444 (5'-cgcgccccgcccccgcggga-3') in the *Nrf2* gene promoter completely abolished the inhibitory action of insulin on pGL4.20-*Nrf2* promoter N-1960/N+111 activity in HG, whereas deletion of N-607 to N-592 (5'-ggggcccgggctccc-3') in the *Nrf2* gene promoter had no effect (**Fig. 6C**). Furthermore, transfection of the plasmid pCMV-Myc containing *hnRNP F* or *hnRNP K* cDNA or both plasmids inhibited pGL4.20 *Nrf2* promoter N-1960/N+111 activity with or without N-607 to N-592 deletion but had no impact on *Nrf2* gene promoter activity with N-463 to N-444 deletion (**Fig. 6D**). These data would point towards nucleotides N-463 to N-444 as a putative *IRE* that binds hnRNP F/K.

The EMSA showed that the double-strand DNA fragment, N-465 to N-443 (WT), binds to nuclear proteins from IRPTCs and could be displaced by the respective WT DNA fragment, but not by mutated DNA fragments (**Fig. 6E**). Furthermore, addition of anti-hnRNP F or anti-hnRNP K antibody induced a supershift of the *hnRNP F-RE* with nuclear proteins (**Fig. 6F,** i and ii, respectively).

Oxidative Stress and Gene Expression in Hyperinsulinemic-Euglycemic Mouse Kidneys

To investigate whether insulin could influence renal *Agt*, *Nrf2*, *hnRNP F* and *hnRNP K* expression independently of its glucose-lowering effect *in vivo*, we performed hyperinsulinemic-euglycemic clamp experiments on WT mice (Online Supplemental Figures 3A-C). DHE staining, ROS generation, *Cat, Nox1, Nox2* and *Nox4* mRNA expression (Online Supplemental Figures 3D-I) did not differ from RPTs of saline-infused and hyperinsulinemic

mice. In contrast, hyperinsulinemia decreased Agt and increased hnRNP F and hnRNP K immunostaining (**Fig. 7A**). It also reduced Nrf2 and HO-1 immunostaining without affecting Keap1 compared to saline infusion (**Fig. 7B**). WB (**Fig. 7C** and **Fig. 7D**) and RT-qPCR (**Fig. 7E** i-iv) of their respective protein and mRNA expressions confirmed these findings.

Discussion

Our present study identifies a novel inhibitory action of insulin on renal *Nrf2* gene transcription via a novel putative *IRE* in the *Nrf2* gene promoter that binds hnRNP F/K. Insulin also prevents *Nrf2* stimulation of *Agt* expression via hnRNP F/K expression in diabetes. These insulin-mediated effects largely occur independently of its glucose-lowering effect.

Intensive insulin therapy is critical for preventing the progression of nephropathy in T1D, although the underlying mechanisms remain incompletely understood (336-338). The existence of a local renin-angiotensin system (RAS) in the kidney is well-established (339, 340). RPTCs express all components of the RAS (335, 341, 342). We demonstrated previously that insulin prevents hypertension and attenuates kidney injury by suppressing renal *Agt* gene transcription via hnRNP F/K up-regulation in Akita mice (266). The present study provides *in vivo* and *in vitro* evidence that insulin modulates *Agt* expression more proximally-- it curtails renal *Nrf2* gene transcription and prevents Nrf2 stimulation of *Agt* expression by increasing hnRNP F/K expression, which may be critical for its anti-hypertensive and renoprotective actions in diabetes.

The Akita mouse, an autosomal dominant model of spontaneous T1D (*insulin2* mutation), develops hypoinsulinemia (60-70% lower circulating immunoreactive insulin levels), hyperglycemia, hypertension and cardiac as well as renal dysfunction (287, 343) closely

resembling changes in T1D patients. We detected markedly increased oxidative stress in RPTCs from Akita compared to non-Akita mice, and insulin normalized these changes. Consistently, insulin treatment lowered RPT *Nrf2* and *Agt* expression as well as urinary Agt and Ang II levels in Akita mice versus WT controls. Thus, the Akita mouse is an excellent model of T1D with insulin repletion.

Cat expression and activity, but not *Cat* mRNA expression, were significantly lower in RPTs from Akita versus WT mice at 16 weeks of age. In contrast, no significant change of Cat expression and activity was observed in RPTs of Akita mice at 4 weeks of age, compared to WT mice (Online supplemental Figures 4A-D), indicating that the lower Cat expression and activity observed in Akita mice at 16 weeks of age might be due to exhaustion of the scavenging system.

Interestingly, treatment of Akita mice with insulin implants at 20 weeks of age markedly attenuated SBP, fasting blood glucose, KW–body weight ratio and KW/TL, (with the exception of urinary ACR), normalized *Nrf2*, and *Agt* mRNA expression and stimulated p44/42 MAPK phosphorylation in RPTs of Akita mice at 24 weeks [Supplemental Table 1 and Supplemental Fig. 5(a–c)]. These findings are consistent with those of Lizotte *et al.*(344), who reported that insulin treatment was effective in lowering fasting blood glucose, but not urinary ACR in Akita mice when begun at the age of 20 weeks. However, whether insulin is effective in even older Akita mice remains to be investigated.

The insulin level used *in vitro* (10^{-7} M or 573 ng/mL) was at least 200-fold higher than the mean circulating insulin level in Akita mice bearing insulin implants (2.3 ± 1.1 ng/mL), similar to those reported (3.4 ± 0.4 ng/mL) by others (345). However, we routinely used insulin at 10^{-7} M for our *in vitro* studies because we found that insulin at 10^{-7} M completely normalized

Nrf2 and *Agt* promoter activity and enhanced *hnRNP F/K* promoter activity 1.5-fold compared with insulin at 10^{-9} M in HG [Supplemental Fig. 6(a–d)].

Combining pharmacological inhibitors and gene knockdown with siRNAs, we identified a key role of the p44/42 MAPK pathway mediating insulin suppression of renal *Nrf2* and *Agt* as well as stimulation of *hnRNP F/K* gene transcription. At present, we do not understand the exact mechanism by which insulin decreases nuclear Nrf2 accumulation in Akita mice. Studies of Zheng *et al.* (346), which reported that mutation of consensus sites (s215, s408, and s577) for MAPK phosphorylation in Nrf2 by MAPKs had a limited impact in mediating Nrf2 nuclear translocation and activity in HEK293T cells. One possibility is that insulin activates p44/42 MAPK following binding to insulin receptors (266, 347, 348), then phosphorylates Nrf2, thereby modulating or hindering their nuclear translocation and activity. This possibility is supported by our data, which show that insulin treatment attenuates nuclear accumulation of Nrf2 and *p*-Nrf2 (s-40) without apparent effect on cytoplasmic Nrf2 and *p*-Nrf2 (s-40) in Akita mice and increases p44/42 MAPK phosphorylation [Supplemental Fig. 4(a) and 4(b), respectively]. During oxidative stress, PKC-δ phosphorylates Nrf2 at serine 40 to enhance its nuclear translocation (349, 350). Another possibility is that p44/42 could directly affect *Agt, Nrf2*, and *hnRNP F/K* transcription via binding to the putative MAPK-responsive element(s) in the respective promoters. Hu *et al.* (351) reported that MAPK1 could act as a transcriptional repressor for interferon gamma-induced genes via binding to a G/C AAA G/C consensus sequence. Clearly, additional studies along these lines are required to elucidate the mechanisms underlying the effects of p44/42 MAPK on *Agt, Nrf2*, and *hnRNP F/K* transcription.

Interestingly, Nrf2 overexpression prevented—whereas Nrf2 siRNA enhanced—insulin inhibition of *Nrf2* and *Agt* gene transcription in IRPTCs. These effects could be explained by

the presence of *Nrf2-RE* in both *Nrf2* (352) and *Agt* (176) promoters. Nrf2 may exert a positive auto-feedback on *Nrf2* transcription (352).

The precise mechanism by which hnRNP F/K mediate insulin downregulation of renal *Nrf2* gene expression in diabetes remains unclear. One possibility is that hnRNP F/K bind to putative *DNA-RE* (tentatively designated as "*IRE*") in *Nrf2* gene promoter, subsequently suppressing *Nrf2* gene transcription. This possibility is supported by our finding that hnRNP F/K overexpression considerably decreases *Nrf2* gene promoter activity, and *hnRNP F/K* siRNA reverse insulin downregulation of *Nrf2* gene transcription. DNA sequence analysis discerned 2 GC-rich regions, nucleotides *N*-463 to *N*-444 (5′-cgcgccccgcccccgcggga-3′) and *N*-607 to *N*-592 (5′-ggggcccgggctccc-3′), in the *Nrf2* gene promoter. Nucleotides *N*-463 to *N*-444 contain the core sequence 5′-**ccccgcccc**-3′, which is homologous to the core sequence of *IRE* (*N*-882 to *N*-855; 5′-cctccct**tcccgccct**tcactttctagt-3′) of the rat *Agt* gene promoter (271, 272). Deletion of *N*-463 to *N*-444, but not *N*-607 to *N*-592, in the *Nrf2* gene promoter markedly reduces insulin- and hnRNP F/K-downregulation of *Nrf2* gene promoter activity in IRPTCs. Moreover, biotinylated-labeled *IRE* (*N*-463 to *N*-444) specifically binds to RPTC nuclear proteins, and the addition of antihnRNP F or antihnRNP K antibody yields a supershift of biotinylated-labeled *IRE* binding with nuclear proteins on EMSA. These data demonstrate that hnRNP F/K bind to a putative *IRE* (*N*-463 to *N*-444) and inhibit *Nrf2* gene transcription. It is noteworthy that hnRNP F/K are not restricted to *Nrf2* gene expression but also affect the expression of *Agt* (271, 272), *Ace2* (269) and other genes (353, 354)

In RPTCs of hyperinsulinemic-euglycemic mice, insulin suppressed *Agt*, *Nrf2*, and *HO-1* expression and stimulated *hnRNP F/K* expression. Its effect was rapid (3 hours after hyperinsulinemia) compared with insulin implants in Akita mice (after 4 weeks of insulin

implantation). Such rapid transcription is consistent with other studies of upregulated and downregulated genes in muscles and liver within 2 to 4 hours under euglycemic-hyperinsulinemic conditions (328, 329). This would indicate that insulin could directly impact renal *Nrf2* and *Agt* gene expression, in addition to its glucose-lowering action.

Finally, *post hoc* analysis of bardoxolone methyl failure in the BEACON trial suggests that the adverse effects in treated patients might be mediated through the endothelin 1 pathway (355, 356). It has been noted (357), however, that bardoxolone methyl heightened SBP and worsened albuminuria, whereas selective ET-A antagonists lessened them in the Efficacy and Safety of Pirfenidone in Patients With Idiopathic Pulmonary Fibrosis trial (358). Our study demonstrates that insulin treatment prevents oltipraz and Nrf2 stimulation of *Agt* gene expression, suggesting that chronic Nrf2 activation by hyperglycemia and/or Nrf2 activator(s) may exaggerate renal dysfunction via activation of the intrarenal RAS, thereby enhancing renal fluid and salt reabsorption.

In summary, our data demonstrate that insulin inhibits *Nrf2* gene transcription and prevents Nrf2 stimulation of intrarenal *Agt* gene expression via hnRNP F/K, indicating that Nrf2 activation may amplify renal dysfunction via intrarenal RAS activation in diabetes. Our study identifies renal hnRNP F/K and Nrf2 as potential targets for the treatment of hypertension and kidney injury in diabetes.

Acknowledgements

This manuscript or any significant part of it is not under consideration for publication elsewhere. The data, however, were presented, in part, as poster communications at the Annual Meeting of

the American Society of Nephrology, Philadelphia, PA, USA, November 12-16, 2014 and Chicago, IL, USA, November 15-20, 2016.

Funding

This work was supported by grants from the Canadian Institutes of Health Research (MOP-84363 and MOP-106688 to JSDC, MOP-86450 to SLZ, and MOP-97742 to JGF), the Canadian Diabetes Association (NOD_OG-3-14-4472-JC to JSDC), and the National Institutes of Health (NIH) of USA (HL-48455 to JRI). TA was supported by a salary award from Fonds de recherche du Québec - Santé (FRQS). CSL was the recipient of a fellowship from the Montreal Diabetes Research Centre of the CRCHUM. Editorial assistance was provided by the CRCHUM Research Support Office and Ovid Da Silva.

Disclosure

None reported.

Contribution statement

JSDC is the guarantor of this work, has full access to all study data, takes responsibility for data integrity and the accuracy of data analysis. JSDC contributed to study conception and design, drafted and reviewed/edited the final manuscript. AG, SA, SZ, YS, CSL, IC, TA and SLZ performed the *in vivo* and *in vitro* experiments and data collection. SLZ, JGF and JRI added to the discussion, and reviewed/edited the manuscript. All authors were involved in data analysis and interpretation, critical manuscript revision, and gave final manuscript approval. They thank the rodent metabolic phenotyping core facility of the CRCHUM for assistance with the hyperinsulinemic-euglycemic clamp studies.

Abbreviations

ACR, albumin/creatinine ratio; Agt, angiotensinogen; Ang II, angiotensin II; Cat, catalase; DHE, dihydroethidium; ELISA, enzyme-linked immunosorbent assay; EMSA, electrophoretic mobility shift assay; ET-1, endothelin 1; GFR, glomerular filtration rate; HG, high glucose; hnRNP F, heterogeneous nuclear ribonucleoprotein F; hnRNP K, heterogeneous nuclear ribonucleoprotein K; HO-1, heme oxygenase-1; IRE, insulin-responsive element; IRPTCs, immortalized renal proximal tubular cells; Keap1, Kelch-like ECH-associated protein 1; NADPH oxidase, nicotinamide adenine dinucleotide phosphate oxidase; NG, normal glucose; Nrf2, nuclear factor erythroid 2-related factor 2; p44/42 MAPK, p44/42 mitogen-activated protein kinase; PAS, periodic acid Schiff; PI3-K, phosphatidylinositol 3-kinase; RAS, renin-angiotensin system; RE, responsive element; ROS, reactive oxygen species; RPTs, renal proximal tubules; RPTCs, renal proximal tubular cells; RT-qPCR, real time-quantitative polymerase chain reaction; SBP, systolic blood pressure; SGLT2, sodium-glucose co-transporter 2; siRNA, small interfering RNA; T1D/T2D, type 1/2 diabetes; Tg, transgenic; WB, Western blotting; WT, wild type

Figure Legends

Figure 1: Insulin prevents systemic hypertension and renal oxidative stress in Akita mice

(**A**) Longitudinal changes in mean SBP (measured 2 to 3 times per mouse per week in the morning without fasting). Baseline SBP was recorded daily over 5 days before initiation of measurement. (**B**) Cat immunostaining, (**C**) Semi-quantitation of Cat-immunostained areas, (**D**) Cat activity, **(E**) *Cat* mRNA level, (**F**) DHE (red) staining (left panel) and semi-quantitation of DHE fluorescence (right panel), (**G**) ROS generation by lucigenin assay, (**H**) NADPH oxidase activity, (**I**) *Nox4*, (**J**) *Nox1* and (**K**) *Nox2* mRNA expression in freshly-isolated RPTs from WT controls, Akita mice and Akita mice + insulin (Ins) implants. Values are mean ± SEM, n=8 per group. $^{*}p<0.05$; $^{**}p<0.01$ and $^{***}p<0.005$, WT vs Akita. $^{\dagger\dagger}p<0.01$, Akita vs Akita-Ins; NS, not significant. WT controls (open bars); Akita (solid bars) and Akita mice + Ins (grey bars).

Figure 2. Renal Agt, HO-1, Nrf2 and Keap1 expression in Akita mice

Renal Agt, HO-1, Nrf2, and Keap1 expression in Akita mice. (**A**) Agt, HO-1, Nrf2, and Keap1 immunostaining (magnification ×200). (**B**) WB of Agt and HO-1 in total lysates. (**C**) WB of Nrf2 and Keap1 in total lysates. (**D**) WB of Nrf2 and *p*-Nrf2 (s-40) in nuclear and cytoplasmic fractions of RPTs. (**E**) (i–iv) RT-qPCR of *Agt*, *HO-1, Nrf2*, and *Keap1* mRNA expression in RPTs of WT controls, Akita, and Akita mice + insulin (Ins). Values are mean ± SEM, n = 8 per group. $^{**}P < 0.01$; $^{***}P < 0.005$; WT controls (open bars); Akita (solid bars), and Akita mice + Ins (gray bars). NS, not significant.

Figure 3. Insulin effect on *Nrf2, Agt, hnRNP F* and *hnRNP K* gene promoter activity in IRPTCs

Cells stably transfected with (**A**) pGL4.20-*Nrf2*, (**B**) pGL4.20-*Agt,* (**C**) pGL4.20-*hnRNP F,* or (**D**) pGL4.20-*hnRNP K* gene promoter were incubated in NG or HG DMEM ± insulin for 24 h

with or without wortmannin, Ly-294,002, PD98059 or U0126 or transiently transfected with p42 MAPK or p44 MAPK siRNA (**E**, **F**, **G** and **H**). Luciferase activity in cells cultured in NG medium was considered as 100%. The results are expressed as percentage of control (mean ± SEM, n=3). $^{*}p<0.05$; $^{**}p<0.01$; $^{***}p<0.005$; NS, not significant. Similar results were obtained in 2 separate experiments.

Figure 4. Oltipraz effect on *Agt, Nrf2, hnRNP F* and *hnRNP K* gene expression in IRPTCs

Effect of oltipraz on promoter activity of (**A**) *Nrf2,* (**B**) *Agt,* (**C**) *hnRNP F* and (**D**) *hnRNP K* genes and their respective mRNA (**E-H**) and protein (**I** and **J**) levels in IRPTCs incubated in NG or HG medium ± insulin with or without PD98059. Promoter activity, mRNA, and protein levels in cells in NG medium are considered as 100% or arbitrary unit 1, respectively. The results are reported as percentages of control values (mean ± SEM, n = 3). $*P < 0.05$; $**P < 0.01$; $***P < 0.005$. Similar results were obtained in three separate experiments. Control IRPTCs in NG (open bars), IRPTCs treated with oltipraz (solid black bars), IRPTCs treated with oltipraz + Ins (horizontal striped bars), and IRPTCs treated with oltipraz + insulin + PD98059 (diagonal striped bars). DMSO, dimethyl sulfoxide; NS, not significant; RLU, relative luciferase unit.

Figure 5. SiRNA of *hnRNP F/K* or *Nrf2* and *hnRNP F/K* cDNA affect *Nrf2* and *Agt* gene promoter activity in IRPTCs

Effect of *hnRNP F* siRNA or *hnRNP K* siRNA or a combination of both on (**A**) promoter activity and (**B**) mRNA expression of *Nrf2* in IRPTCs incubated in NG or HG medium ± insulin. Effect of transfection of *Nrf2* cDNA (**C** and **D**) and *Nrf2* siRNA (**E** and **F**) on *Nrf2* and *Agt* promoter activity and their respective *Nrf2* and *Agt* mRNA levels (**G** to **J**) in IRPTCs. Promoter activity and mRNA levels in cells incubated in NG medium are expressed as 100% or arbitrary unit 1, respectively. Each point represents the mean±SEM (n=3) assayed in duplicate. $^{*}p<0.05$;

$^{**}p<0.01$; $^{***}p<0.005$; NS, not significant. Similar results were obtained in 2 to 3 separate experiments.

Figure 6. Identification of *hnRNP F/K-RE* or putative *IRE* in the *Nrf2* gene promoter

Identification of hnRNP F/K-RE or putative IRE in the Nrf2 gene promoter. Luciferase (Luc) activity of plasmids containing various lengths of Nrf2 gene promoter in (**A**) NG medium or (**B**) HG medium ± insulin in IRPTCs. Luciferase activities were normalized by cotransfecting the vector, pRc/RSV plasmid (Invitrogen, Inc.) containing beta-galactosidase cDNA. Control IRPTCs in NG (open bars), IRPTCs in HG (solid black bars), and IRPTCs treated with Ins in HG (horizontal striped bars). (**C**) Activity of 1 μg of the full-length Nrf2 gene promoter ± deletion of distal putative IRE (N-607 to N-592; 5′-ggggcccgggctccc-3′) or proximal putative IRE (N-463 to N-444 (5′-cgcgccccgcccccgcggga-3″) in IRPTCs in NG medium. (**D**) Activity of 1 μg of the full-length Nrf2 gene promoter with or without deletion of distal putative IRE or proximal putative IRE transfected with hnRNP F or hnRNP K cDNA or a combination of both in IRPTCs in NG medium. Values are mean ± SEM, n = 3. All experiments were repeated twice. (*P < 0.05; **P < 0.01; ***P < 0.005). (**E**) EMSA of putative biotinylated proximal IRE with RPTC nuclear proteins with or without excess unlabeled proximal WT IRE or mutated IRE. (**F**) Supershift EMSA. (i) Rabbit anti–hnRNP F or rabbit IgG and (ii) mouse anti–hnRNP K or mouse IgG was added to the reaction mixture and incubated for 30 minutes on ice before incubation with biotinylated probe. The results are representative of three independent experiments. NS, not significant; RLU, relative luciferase unit; SS, supershift band.

Figure 7. Renal Agt, hnRNP F/K, Nrf2, HO-1 and Keap1 expression in hyperinsulinemic-euglycemic mice

(**A**) Immunostaining of Agt, hnRNP F and hnRNP K and (**B**) Nrf2, HO-1 and Keap1 (magnification X 200). (**C**) WB of Agt, hnRNP F and hnRNP K and (**D**) Nrf2, HO-1 and Keap1 expression in isolated RPTs from WT mice after 3-h infusion with saline or Ins + D-glucose. (**E**) RT-qPCR of (i) *Agt*, (ii) *hnRNP F*, (iii) *hnRNP K,* (iv) *Nrf2,* (v) *HO-1* and (vi) *Keap1* mRNA expression in isolated RPTs from WT mice after 3-h infusion with saline (open bars) or insulin (Ins)+D-Glucose (solid black bars). Values are mean±SEM, n=8 per group. $^{*}p<0.05$; $^{**}p<0.01$; NS, not significant.

Table 1. Primer Sequences for RT-qPCR, Subcloning, and EMSA

Gene/Species	Forward/Reverse Primer Sequences	Reference Sequence
Angiotensinogen (mouse/rat)	F: 5′-CCACGCTCTCTGGATTTATC-3′ R: 5′-ACAGACACCGAGATGCTGTT-3′	NM_007428.3
HO-1 (mouse/rat)	F: 5′-CACCAAGTTCAAACAGCTCT-3′ R: 5′-CAGGAAACTGAGTGTGAGGA-3′	NM_010442.2
hnRNP F (mouse/rat)	F: 5′-AATTGTGCCAAACGGGATCA-3′ R: 5′-GCACCAGACCTCATCCTATCCA-3′	NM_133834.2
hnRNP K (mouse/rat)	F: 5′- CAGCTCCCGCTCGAATCTG-3′ R: 5′- ACCCTATCAGGTTTTCCTCCAA-3′	NM_001301341.1
KEAP1 (mouse/rat)	F: 5′-CATCCACCCTAAGGTCATGGA-3′ R: 5′-GACAGGTTGAAGAACTCCTCC-3′	NM_016679.4
Nrf2 (mouse/rat)	F: 5′-CGCCGCCTCACCTCTGCTGCCAGTAG-3′ R: 5′-AGCTCATAATCCTTCTGTCG-3′	NM_010902.3
Nox1 (mouse/rat)	F: 5′-GGTCACTCCCTTTGCTTCCA-3′ R: 5′- GGCAAAGGCACCTGTCTCTCT-3′	NM_172203.2
Nox2 (mouse/rat)	F: 5′-CCCTTTGGTACAGCCAGTGAAGAT-3′ R: 5′- CAATCCCGGCTCCCACTAACATCA-3′	NM_007807.5
Nox4 (mouse/rat)	F: 5′-TGGCCAACGAAGGGGTTAAA-3′ R: 5′-GATGAGGCTGCAGTTGAGGT-3′	NM_015760.4
β-Actin (mouse/rat)	F: 5′-ACGATTTCCCTCTCAGCTT-3′ R: 5′-TACAATGAGCTGCGTGTGGC-3′	NM_031144.3
hnRNP F gene promoter (rat)	F: 5′-AAAGGTACCTTTTTAAAGTCTTAAGCATTTG-3′ R: 5′-AAAAAGCTTCAGGGGAAACGCTTTTCG-3′	NC_005103.4
hnRNP K gene promoter (rat)	F: 5′-AAAGGTACCGGAGGCAACGGCGGACTCGC-3′ R: 5′-AAAAAGCTTACCAATTCACCATTGGTTTCGG-3′	NC_005116.4
Rat Nrf2 promoter	F: 5′-TAATTAGGTACCCTTGCCTCTTGCCCTAGCC-3′ F: 5′-TAATTAGGTACCCCCGAACCACGAGAGGAGG-3′ F: 5′-TAATTAGGTACCTTCGGCAAACAGCTGCTAATC-3′ F: 5′-TAATTAGGTACCAGCGTGGACTCATCCATCTC-3′ R: 5′-AAAAAACTCGAGTGCTGGGACTGTAGTCCTGGC-3′	−150 −400 −537 −820 +111
Rat Nrf2 promoter- hnRNP F/K-RE (*N*-607/-592)	F: 5′-CGATAGCAGCGCAGGTGTGTTTGCTC-3′ R: 5′-GAGCAAACACACCTGCGCTGCTATCG-3′	Site-directed mutagenesis primers
Rat Nrf2 promoter- hnRNP F/K-RE (*N*-463/-444)	F: 5′-CAAGGCCTCCTGCTACTTCAGCCCAC-3′ R: 5′-GTGGGCTGAAGTAGCAGGAGGCCTTG-3′	Site-directed mutagenesis primers
Rat Nrf2 promoter hnRNP F/K-RE (*N*-463/-444)	F: 5′-CTCGCGCCCCGCCCCCGCGGGAC-3′ R: 5′-GTCCCGCGGGGGCGGGGCGCGAG-3′	Biotinylated probe for EMSA
Rat Nrf2 promoter hnRNP F/K-RE (*N*-463/-444) WT	F: 5′-CTCGCGCCCCGCCCCCGCGGGAC-3′ R: 5′-GTCCCGCGGGGGCGGGGCGCGAG-3′	Competitor
hnRNP F/K-RE (M1)	F: 5′-CTCGCG**AAAA**GCCCCCGCGGGAC-3′ R: 5′-GTCCCGCGGGGGC**TTTT**CGCGAG-3′	Competitor
hnRNP F/K-RE (M2)	F: 5′-CTCGCGCCC**AAA**CCCCGCGGGAC-3′ R: 5′-GTCCCGCGGGG**TTT**GGGCGCGAG-3′	Competitor
hnRNP F/K-RE (M3)	F: 5′-CTCGCGCCCCG**AAAA**CGCGGGAC-3′ R: 5′-GTCCCGCG**TTTT**CGGGGCGCGAG-3′	Competitor
hnRNP F/K-RE (M4)	F: 5′-CTCGCG**AAAA**G**AAAA**CGCGGGAC-3′ R: 5′-GTCCCGCG**TTTT**C**TTTT**CGCGAG-3′	Competitor

Boldface letters indicate the nucleotides replacing the nucleotides in WT hnRNP F/K-RE.
Abbreviations: HO-1, heme oxygenase-1; Keap1, Kelch-like ECH-associated protein 1; RE, responsive element; RT-qPCR, real-time quantitative polymerase chain reaction.

Table 1

Table 2. Antibodies Used in This Study

Protein Target	Name of Antibody	Manufacturer, Catalog, and/or Name of Individual Providing the Antibody	Species Raised in; Mono or Polyclonal	Dilution for WB and or IHC	RRID
Agt	Angiotensinogen antibody	Specifically recognizing Agt were generated in our laboratory	Rabbit; polyclonal	WB; 1:2000 IHC; 1:200	AB_2631321
Cat	Catalase	Sigma-Aldrich	Rabbit; polyclonal	WB; 1:1000 IHC;1:200	AB_259018
HO-1	HO-1 antibody	Enzo Life Sciences (SPA-895(D))	Rabbit; polyclonal	WB; 1:2000 IHC; 1:200	AB_2248405
hnRNP F	hnRNP F antibody	Specifically recognizing(CTARRYIGIVK QAGLER) were generated in our laboratory	Rabbit; polyclonal	WB; 1:10,000 IHC; 1:200	AB_2631323
hnRNP K	hnRNP K (H-300)	Santa Cruz Biotechnology (sc-25373)	Rabbit; polyclonal	WB; 1:1000 IHC; 1:100	AB_2120388
hnRNP K	Anti–hnRNP K antibody (3C2)	Abcam (ab39975)	Mouse; monoclonal-chip grade	—	AB_732981
Keap1	Anti-Keap1	Abcam (ab66620)	Rabbit; polyclonal	WB; 1:1500 IHC; 1:200	AB_1141055
Nrf2	Anti-Nrf2	Abcam (ab31163)	Rabbit; polyclonal	IHC; 1:200	AB_881705
b-Actin	b-Actin clone AC-15	Sigma-Aldrich (A5441)	Mouse; monoclonal	WB; 1:20,000	AB_476744
pERK1/2	Phospho-p44/42 MAPK (Thr202/ Tyr204) (E10)	Cell Signaling (#9106)	Mouse; monoclonal	WB; 1:1000	AB_331768
ERK1/2	p44/42 MAPK	Cell Signaling (#9102)	Rabbit; polyclonal	WB; 1:2000	AB_330744
p-Nrf2	Nrf2 (S40)	Bioss (bs-2013R)	Rabbit; polyclonal	WB; 1:1000	AB_10855428

Abbreviations: IHC, immunohistochemistry; RRID, Research Resource Identifier.

Table 2

Table 3. Physiological Measurements

	WT	Akita	Akita + Insulin
Blood glucose (mmol/L)	7.46 ± 0.667	31.6 ± 0.76[a]	14.62 ± 3.57[b]
Systolic blood pressure (mm Hg)	109.17 ± 1.5	133.2 ± 4.86[a]	114.3 ± 4.16[c]
Body weight (g)	30.7 ± 0.73	22.41 ± 0.45[a]	24.35 ± 0.42[a]
Kidney weight (mg)	324 ± 11	520 ± 27[a]	467 ± 10[a,d]
Heart weight (mg)	140 ± 10	160 ± 10	150 ± 10
Tibia length (mm)	18.5 ± 0.15	16.3 ± 0.12[a]	17.3 ± 0.10[c,e]
Kidney/tibia length (mg/mm)	17.51± 0.8	31.91 ± 1.36[a]	26.99 ± 0.02[a,c]
Heart/tibia length (mg/mm)	7.6 ± 0.10	9.8 ± 0.31[e]	8.6 ± 0.10[d,f]
ACR (μg/μmol)	1.12 ± 0.17	5.64 ± 0.32[a]	1.96 ± 0.10[b]
GFR/body weight ($\mu L/min^{-1}g^{-1}$)	6.65 ± 0.12	16.3 ± 0.37[a]	7.79 ± 0.48[b]
Urinary Agt/creatinine ratio (ng/mg)	29.44 ± 4.3	289.75 ± 61.2[a]	167.6 ± 21.1[a,c]
UrinaryAng II/creatinine ratio (ng/mg)	1.40 ± 0.42	23.64 ± 12.04[e]	5.10 ± 5.01[a,b]
Serum Agt (ng/mL)	5221 ± 43.4	4609 ± 78.73	4114.13 ± 95.01
Glomerular tuft volume ($\times 10^3$ μm^3)	141.2 ± 4.52	182.03 ± 6.3[a]	135.7 ± 6.61[b]
RPTC volume ($\times 10^3$ μm^3)	6.9 ± 0.66	9.93 ± 0.27[a]	7.81 ± 0.37[c,f]
Tubular luminar area (μm^2)	44.7 ± 5.01	71.75 ± 4.02[a]	54.54 ± 6.03[c]

[a] $P < 0.005$ vs WT.
[b] $P < 0.005$ vs Akita.
[c] $P < 0.01$ vs Akita.
[d] $P < 0.05$ vs WT.
[e] $P < 0.01$ vs WT.
f $P < 0.05$ vs Akita.

Table 3

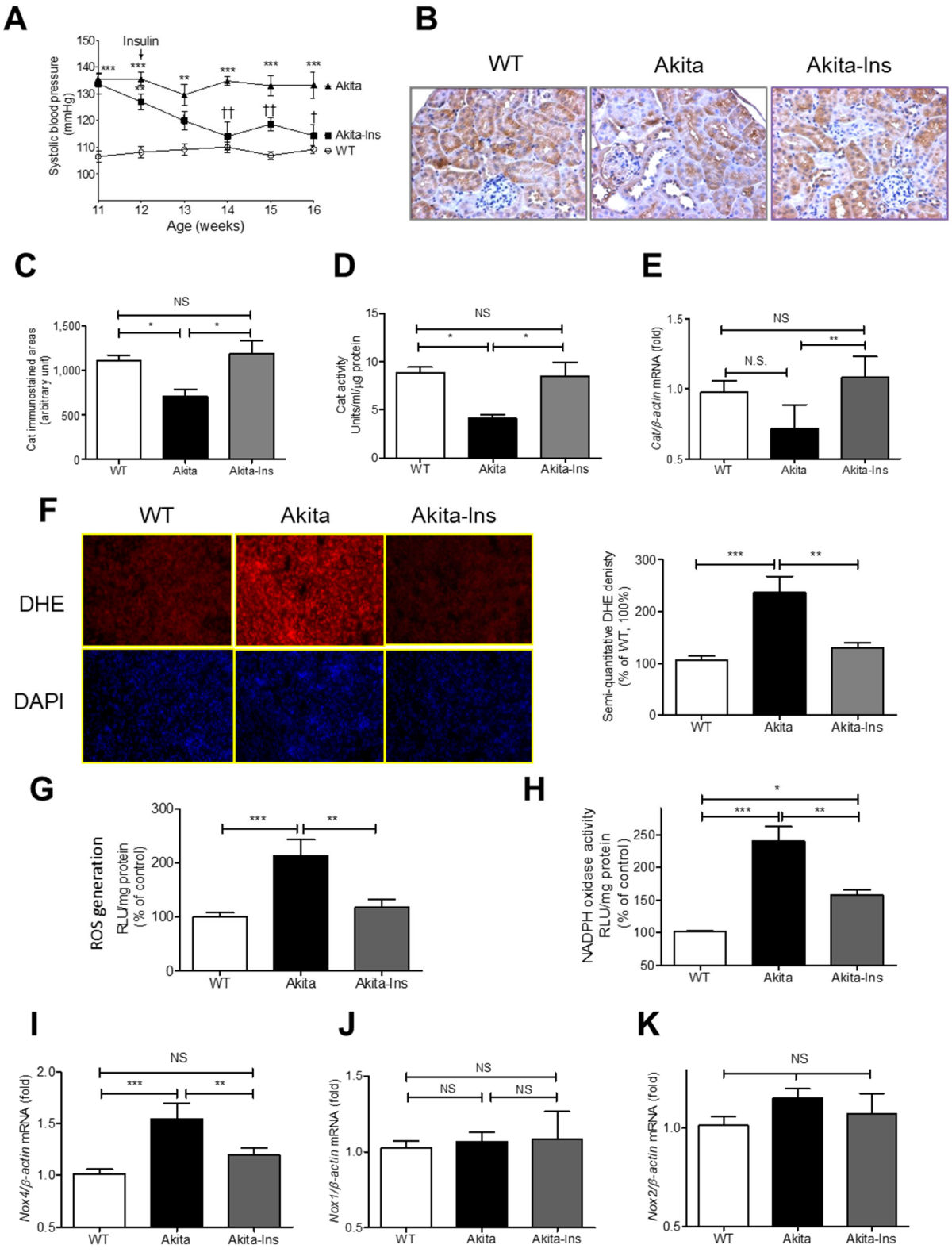
A
Insulin
Systolic blood pressure (mmHg)
Age (weeks)
Akita
Akita-Ins
WT
B
WT
Akita
Akita-Ins
C
Cat immunostained areas (arbitrary unit)
NS
D
Cat activity Units/ml/μg protein
E
Cat/β-actin mRNA (fold)
N.S.
F
DHE
DAPI
Semi-quantitative DHE denisty (% of WT, 100%)
G
ROS generation
RLU/mg protein (% of control)
H
NADPH oxidase activity RLU/mg protein (% of control)
I
Nox4/β-actin mRNA (fold)
J
Nox1/β-actin mRNA (fold)
K
Nox2/β-actin mRNA (fold)

Figure 1

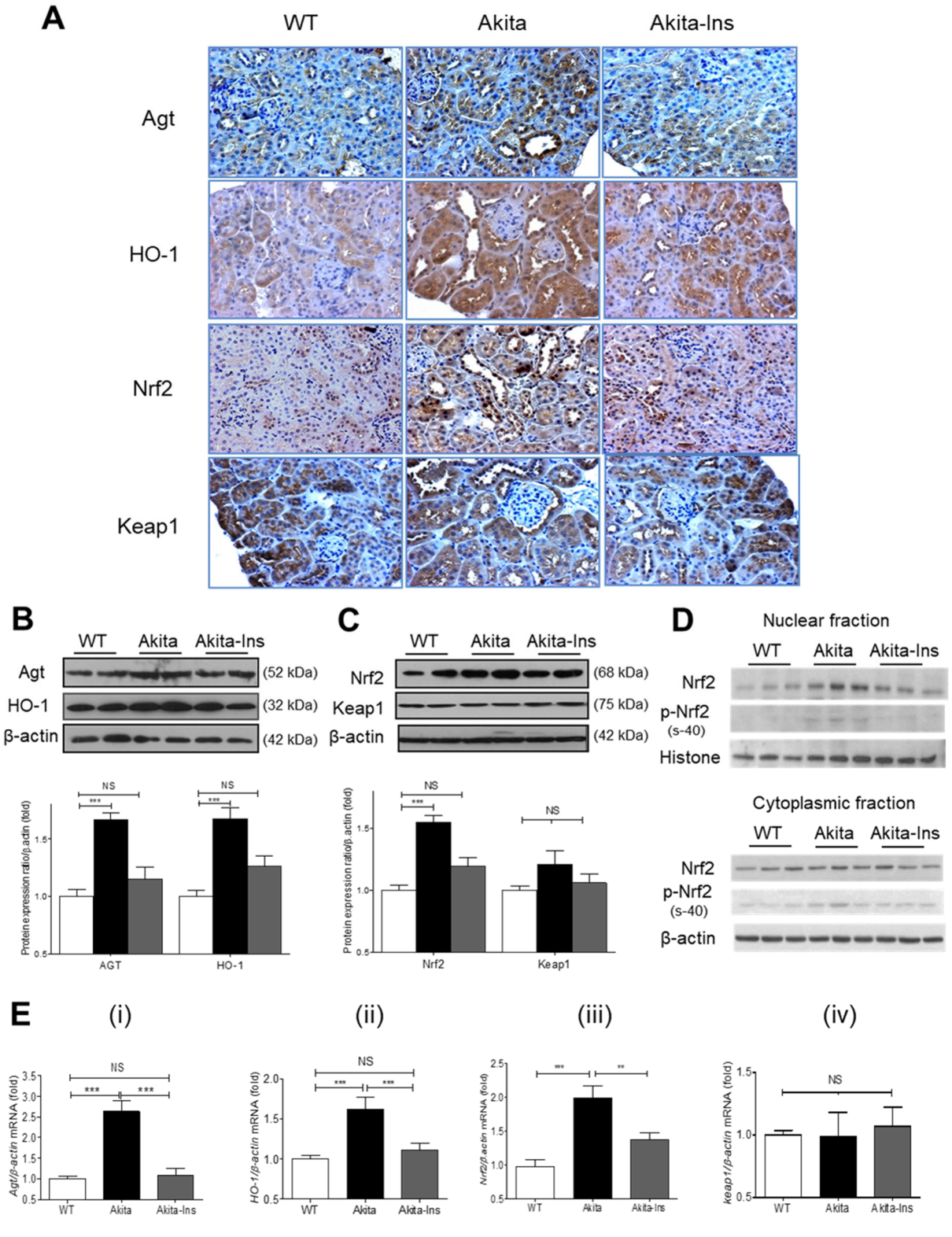
A
WT
Akita
Akita-Ins
Agt
HO-1
Nrf2
Keap1
B
WT
Akita
Akita-Ins
Agt
HO-1
β-actin
(52 kDa)
(32 kDa)
(42 kDa)
Protein expression ratio/β actin (fold)
NS
***
AGT
HO-1
C
WT
Akita
Akita-Ins
Nrf2
Keap1
β-actin
(68 kDa)
(75 kDa)
(42 kDa)
Protein expression ratio/β actin (fold)
NS
***
Nrf2
Keap1
D
Nuclear fraction
WT
Akita
Akita-Ins
Nrf2
p-Nrf2
(s-40)
Histone
Cytoplasmic fraction
WT
Akita
Akita-Ins
Nrf2
p-Nrf2
(s-40)
β-actin
E
(i)
(ii)
(iii)
(iv)
Agt/β-actin mRNA (fold)
HO-1/β-actin mRNA (fold)
Nrf2/β-actin mRNA (fold)
keap1/β-actin mRNA (fold)
NS
***
**
WT
Akita
Akita-Ins

Figure 2

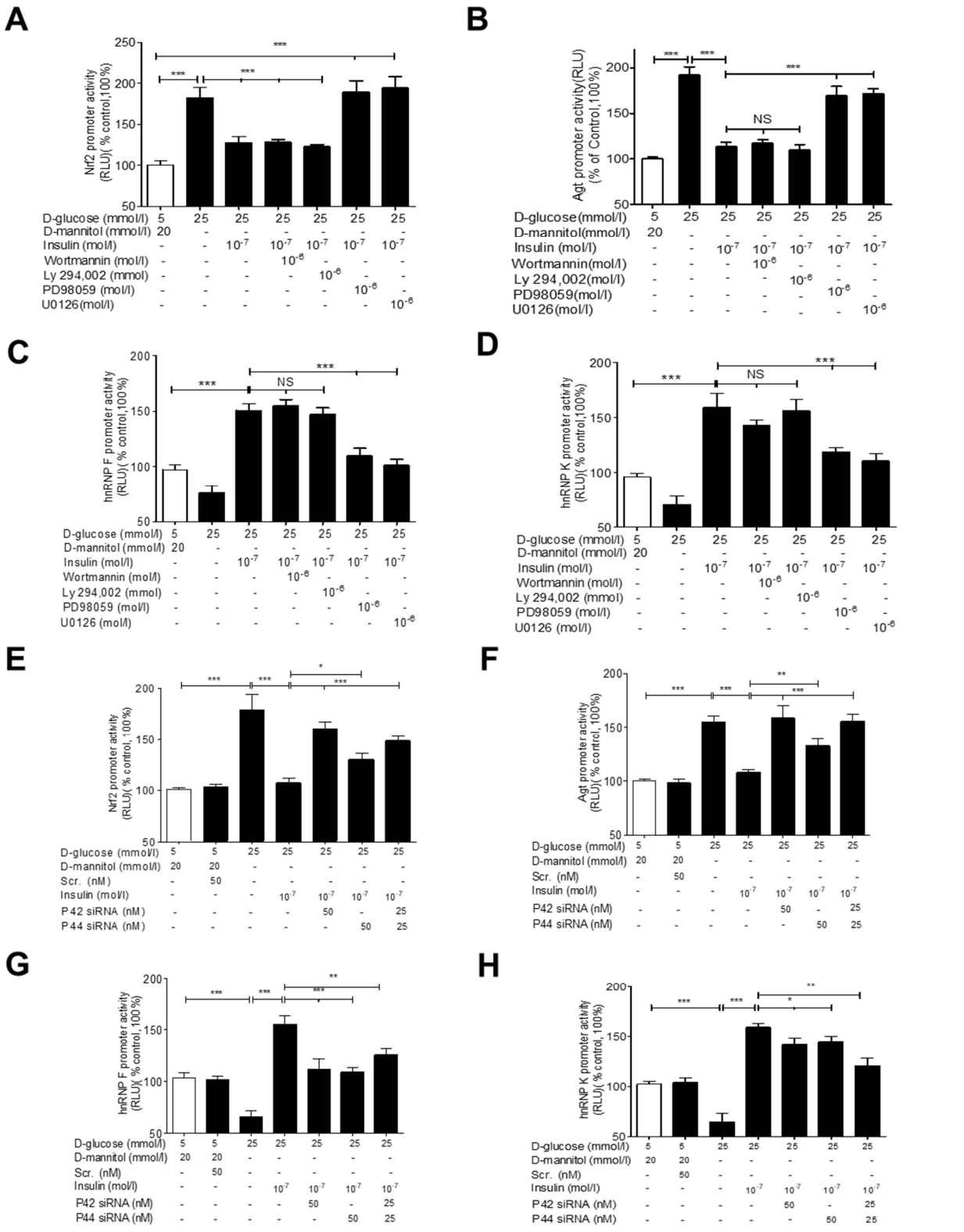
A
Nrf2 promoter activity (RLU)(% control,100%)
D-glucose (mmol/l) 5 25 25 25 25 25 25
D-mannitol (mmol/l) 20 - - - - - -
Insulin (mol/l) - - 10-7 10-7 10-7 10-7 10-7
Wortmannin (mol/l) - - - 10-6 - - -
Ly 294,002 (mmol) - - - - 10-6 - -
PD98059 (mol/l) - - - - - 10-6 -
U0126(mol/l) - - - - - - 10-6
B
Agt promoter activity(RLU) (% of Control,100%)
NS
D-glucose(mmol/l) 5 25 25 25 25 25 25
D-mannitol(mmol/l) 20 - - - - - -
Insulin (mol/l) - - 10-7 10-7 10-7 10-7 10-7
Wortmannin(mol/l) - - - 10-6 - - -
Ly 294,002(mol/l) - - - - 10-6 - -
PD98059(mol/l) - - - - - 10-6 -
U0126(mol/l) - - - - - - 10-6
C
hnRNP F promoter activity (RLU)(% control,100%)
NS
D-glucose (mmol/l) 5 25 25 25 25 25 25
D-mannitol (mmol/l) 20 - - - - - -
Insulin (mol/l) - - 10-7 10-7 10-7 10-7 10-7
Wortmannin (mol/l) - - - 10-6 - - -
Ly 294,002 (mmol) - - - - 10-6 - -
PD98059 (mol/l) - - - - - 10-6 -
U0126 (mol/l) - - - - - - 10-6
D
hnRNP K promoter activity (RLU)(% control,100%)
NS
D-glucose (mmol/l) 5 25 25 25 25 25 25
D-mannitol (mmol/l) 20 - - - - - -
Insulin (mol/l) - - 10-7 10-7 10-7 10-7 10-7
Wortmannin (mol/l) - - - 10-6 - - -
Ly 294,002 (mmol) - - - - 10-6 - -
PD98059 (mol/l) - - - - - 10-6 -
U0126 (mol/l) - - - - - - 10-6
E
Nrf2 promoter activity (RLU)(% control, 100%)
D-glucose (mmol/l) 5 5 25 25 25 25 25
D-mannitol (mmol/l) 20 20 - - - - -
Scr. (nM) - 50 - - - - -
Insulin (mol/l) - - - 10-7 10-7 10-7 10-7
P42 siRNA (nM) - - - - 50 - 25
P44 siRNA (nM) - - - - - 50 25
F
Agt promoter activity (RLU)(% control, 100%)
D-glucose (mmol/l) 5 5 25 25 25 25 25
D-mannitol (mmol/l) 20 20 - - - - -
Scr. (nM) - 50 - - - - -
Insulin (mol/l) - - - 10-7 10-7 10-7 10-7
P42 siRNA (nM) - - - - 50 - 25
P44 siRNA (nM) - - - - - 50 25
G
hnRNP F promoter activity (RLU)(% control, 100%)
D-glucose (mmol/l) 5 5 25 25 25 25 25
D-mannitol (mmol/l) 20 20 - - - - -
Scr. (nM) - 50 - - - - -
Insulin (mol/l) - - - 10-7 10-7 10-7 10-7
P42 siRNA (nM) - - - - 50 - 25
P44 siRNA (nM) - - - - - 50 25
H
hnRNP K promoter activity (RLU)(% control, 100%)
D-glucose (mmol/l) 5 5 25 25 25 25 25
D-mannitol (mmol/l) 20 20 - - - - -
Scr. (nM) - 50 - - - - -
Insulin (mol/l) - - - 10-7 10-7 10-7 10-7
P42 siRNA (nM) - - - - 50 - 25
P44 siRNA (nM) - - - - - 50 25

Figure 3

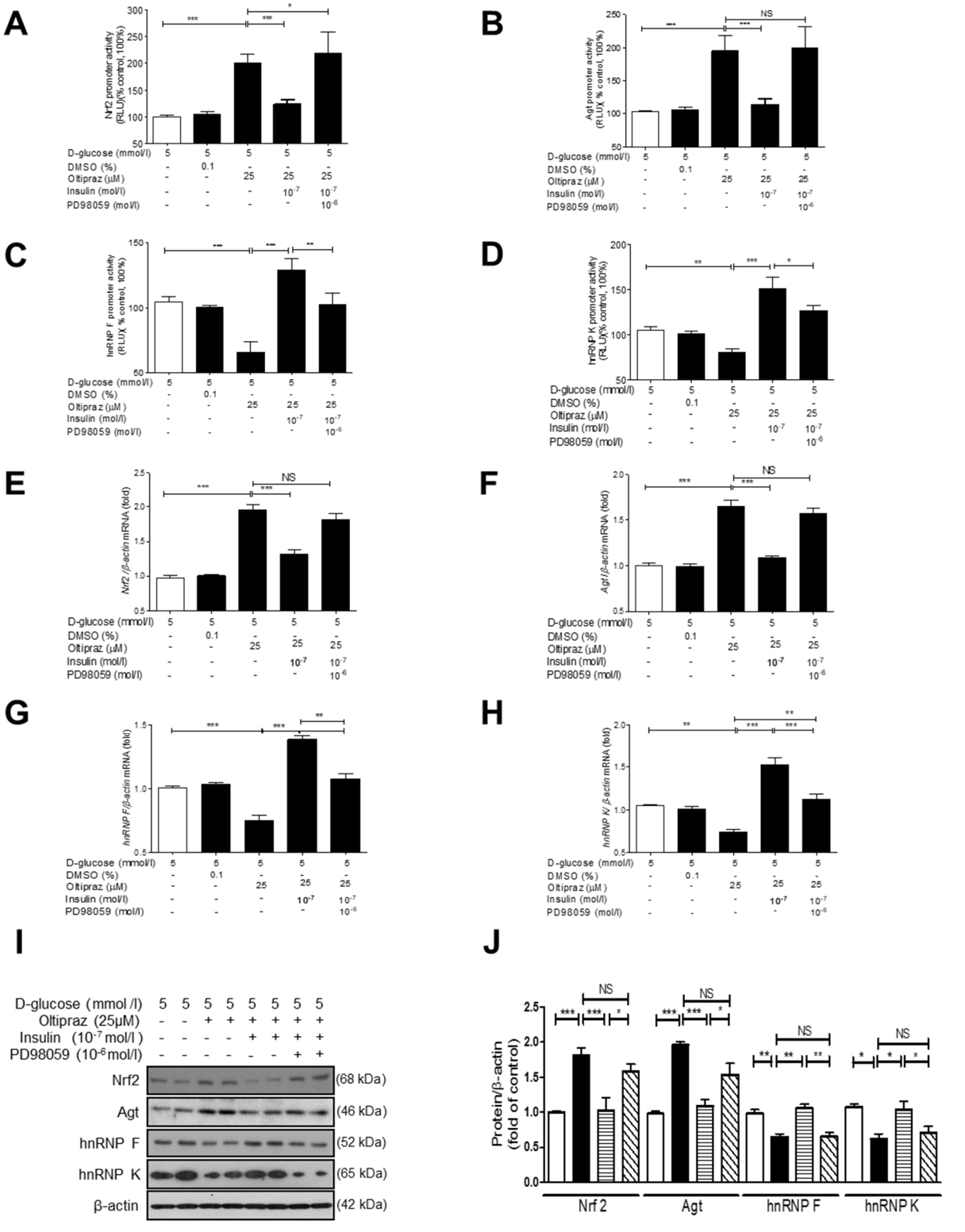
A
Nrf2 promoter activity (RLU)(% control, 100%)
B
Agt promoter activity (RLU)(% control, 100%)
C
hnRNP F promoter activity (RLU)(% control, 100%)
D
hnRNP K promoter activity (RLU)(% control, 100%)
E
Nrf2 /β-actin mRNA (fold)
F
Agt /β-actin mRNA (fold)
G
hnRNP F/β-actin mRNA (fold)
H
hnRNP K/ β-actin mRNA (fold)
D-glucose (mmol/l)
DMSO (%)
Oltipraz (μM)
Insulin (mol/l)
PD98059 (mol/l)
NS
I
D-glucose (mmol /l)
Oltipraz (25μM)
Insulin (10-7 mol/l)
PD98059 (10-6 mol/l)
Nrf2
Agt
hnRNP F
hnRNP K
β-actin
(68 kDa)
(46 kDa)
(52 kDa)
(65 kDa)
(42 kDa)
J
Protein/β-actin (fold of control)
Nrf 2
Agt
hnRNP F
hnRNP K

Figure 4

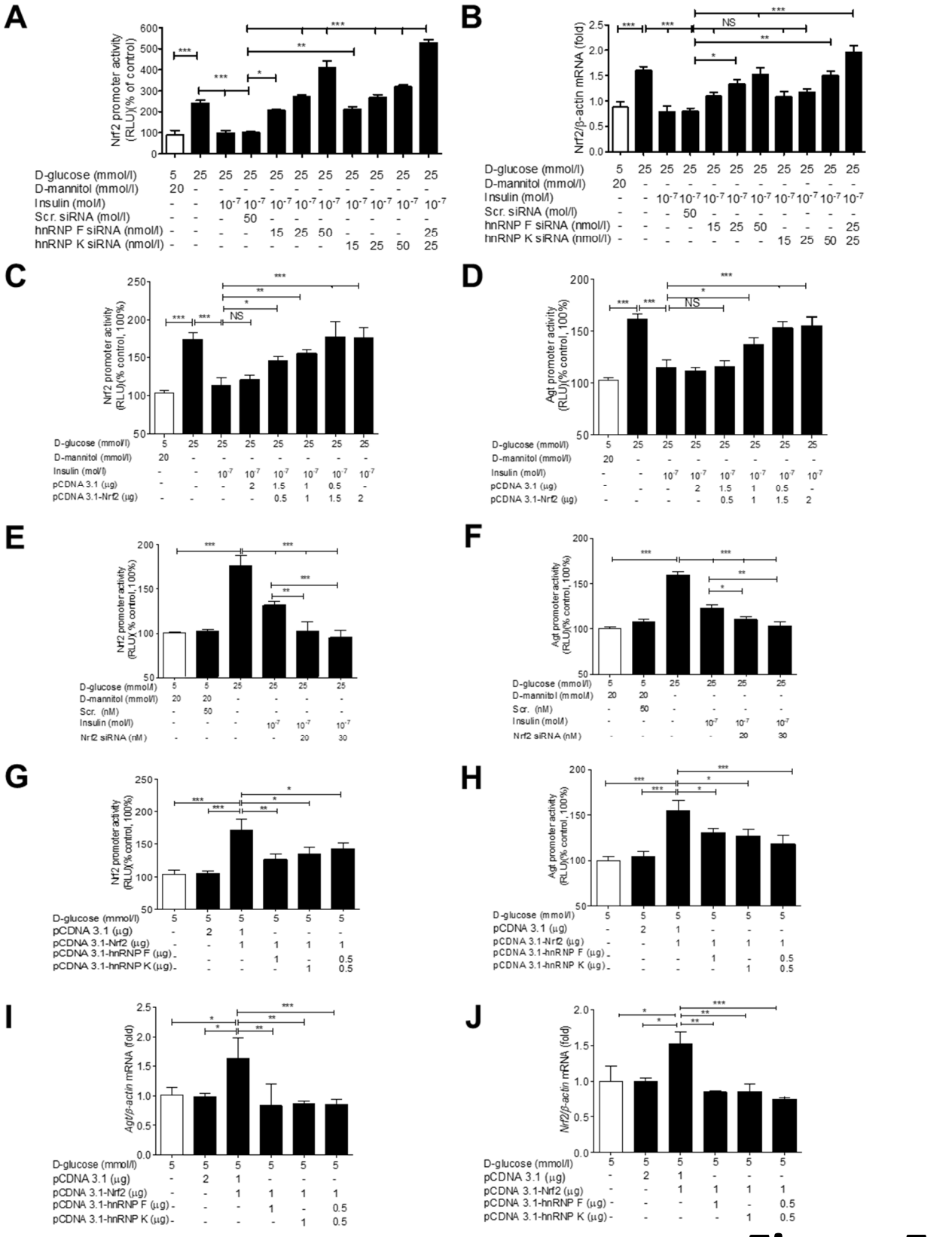
A
Nrf2 promoter activity (RLU)(% of control)
D-glucose (mmol/l) 5 25 25 25 25 25 25 25 25 25 25
D-mannitol (mmol/l) 20 - - - - - - - - - -
Insulin (mol/l) - - 10-7 10-7 10-7 10-7 10-7 10-7 10-7 10-7 10-7
Scr. siRNA (mol/l) - - - 50 - - - - - - -
hnRNP F siRNA (nmol/l) - - - - 15 25 50 - - - 25
hnRNP K siRNA (nmol/l) - - - - - - - 15 25 50 25
B
Nrf2/β-actin mRNA (fold)
NS
D-glucose (mmol/l) 5 25 25 25 25 25 25 25 25 25 25
D-mannitol (mmol/l) 20 - - - - - - - - - -
Insulin (mol/l) - - 10-7 10-7 10-7 10-7 10-7 10-7 10-7 10-7 10-7
Scr. siRNA (mol/l) - - - 50 - - - - - - -
hnRNP F siRNA (nmol/l) - - - - 15 25 50 - - - 25
hnRNP K siRNA (nmol/l) - - - - - - - 15 25 50 25
C
Nrf2 promoter activity (RLU)(% control, 100%)
NS
D-glucose (mmol/l) 5 25 25 25 25 25 25 25
D-mannitol (mmol/l) 20 - - - - - - -
Insulin (mol/l) - - 10-7 10-7 10-7 10-7 10-7 10-7
pCDNA 3.1 (μg) - - - 2 1.5 1 0.5 -
pCDNA 3.1-Nrf2 (μg) - - - - 0.5 1 1.5 2
D
Agt promoter activity (RLU)(% control, 100%)
NS
D-glucose (mmol/l) 5 25 25 25 25 25 25 25
D-mannitol (mmol/l) 20 - - - - - - -
Insulin (mol/l) - - 10-7 10-7 10-7 10-7 10-7 10-7
pCDNA 3.1 (μg) - - - 2 1.5 1 0.5 -
pCDNA 3.1-Nrf2 (μg) - - - - 0.5 1 1.5 2
E
Nrf2 promoter activity (RLU)(% control, 100%)
D-glucose (mmol/l) 5 5 25 25 25 25
D-mannitol (mmol/l) 20 20 - - - -
Scr. (nM) - 50 - - - -
Insulin (mol/l) - - - 10-7 10-7 10-7
Nrf2 siRNA (nM) - - - - 20 30
F
Agt promoter activity (RLU)(% control, 100%)
D-glucose (mmol/l) 5 5 25 25 25 25
D-mannitol (mmol/l) 20 20 - - - -
Scr. (nM) - 50 - - - -
Insulin (mol/l) - - - 10-7 10-7 10-7
Nrf2 siRNA (nM) - - - - 20 30
G
Nrf2 promoter activity (RLU)(% control, 100%)
D-glucose (mmol/l) 5 5 5 5 5 5
pCDNA 3.1 (μg) - 2 1 - - -
pCDNA 3.1-Nrf2 (μg) - - 1 1 1 1
pCDNA 3.1-hnRNP F (μg) - - - 1 - 0.5
pCDNA 3.1-hnRNP K (μg) - - - - 1 0.5
H
Agt promoter activity (RLU)(% control, 100%)
D-glucose (mmol/l) 5 5 5 5 5 5
pCDNA 3.1 (μg) - 2 1 - - -
pCDNA 3.1-Nrf2 (μg) - - 1 1 1 1
pCDNA 3.1-hnRNP F (μg) - - - 1 - 0.5
pCDNA 3.1-hnRNP K (μg) - - - - 1 0.5
I
Agt/β-actin mRNA (fold)
D-glucose (mmol/l) 5 5 5 5 5 5
pCDNA 3.1 (μg) - 2 1 - - -
pCDNA 3.1-Nrf2 (μg) - - 1 1 1 1
pCDNA 3.1-hnRNP F (μg) - - - 1 - 0.5
pCDNA 3.1-hnRNP K (μg) - - - - 1 0.5
J
Nrf2/β-actin mRNA (fold)
D-glucose (mmol/l) 5 5 5 5 5 5
pCDNA 3.1 (μg) - 2 1 - - -
pCDNA 3.1-Nrf2 (μg) - - 1 1 1 1
pCDNA 3.1-hnRNP F (μg) - - - 1 - 0.5
pCDNA 3.1-hnRNP K (μg) - - - - 1 0.5

Figure 5

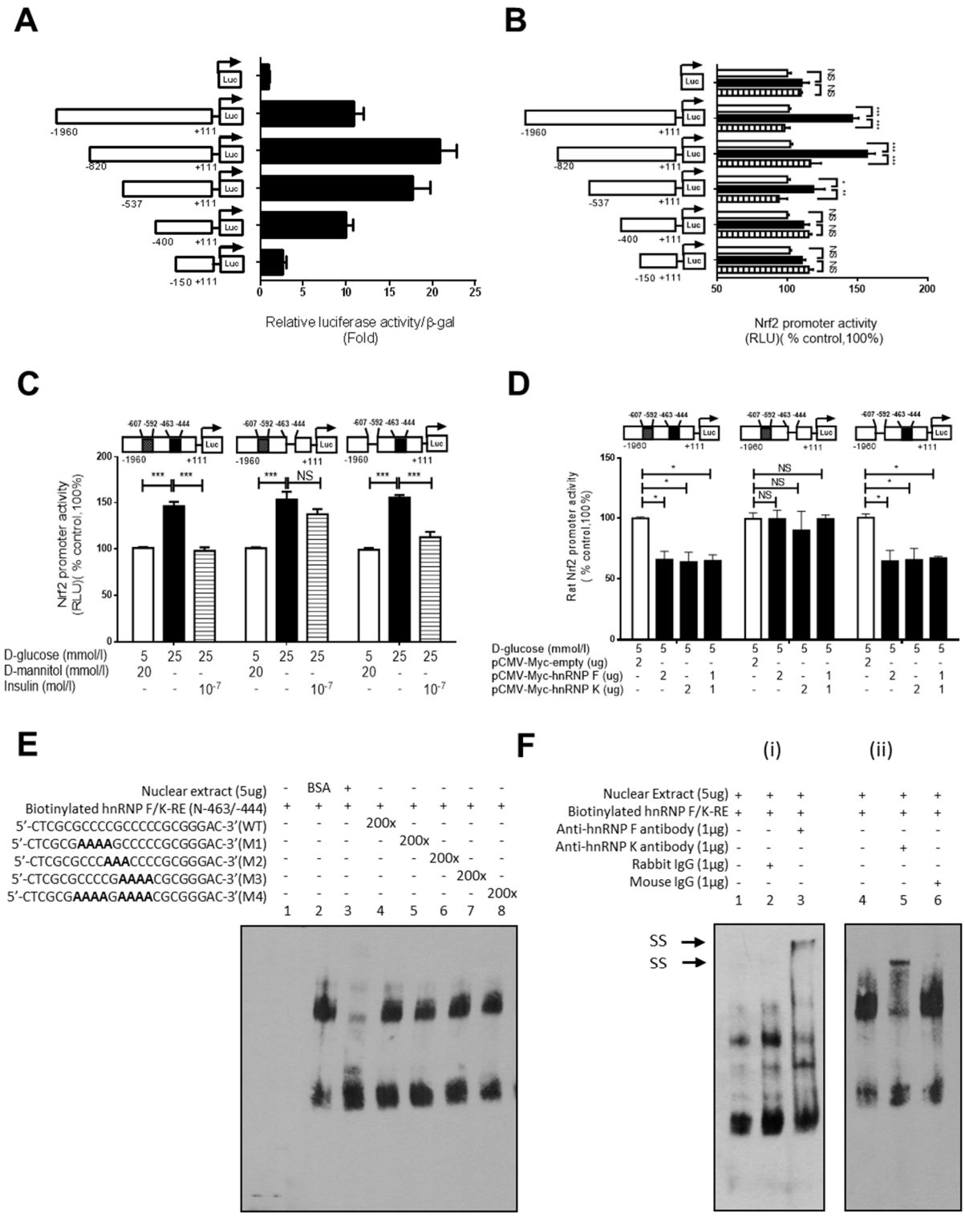
A
B
C
D
E
F
Relative luciferase activity/β-gal (Fold)
Nrf2 promoter activity (RLU)(% control,100%)
Nrf2 promoter activity (RLU)(% control,100%)
Rat Nrf2 promoter activity (% control,100%)
D-glucose (mmol/l)
D-mannitol (mmol/l)
Insulin (mol/l)
pCMV-Myc-empty (ug)
pCMV-Myc-hnRNP F (ug)
pCMV-Myc-hnRNP K (ug)
Nuclear extract (5ug)
Biotinylated hnRNP F/K-RE (N-463/-444)
5′-CTCGCGCCCCGCCCCCGCGGGAC-3′(WT)
5′-CTCGCGAAAAGCCCCCGCGGGAC-3′(M1)
5′-CTCGCGCCCAAACCCCGCGGGAC-3′(M2)
5′-CTCGCGCCCCGAAAACGCGGGAC-3′(M3)
5′-CTCGCGAAAAGAAAACGCGGGAC-3′(M4)
Nuclear Extract (5ug)
Biotinylated hnRNP F/K-RE
Anti-hnRNP F antibody (1μg)
Anti-hnRNP K antibody (1μg)
Rabbit IgG (1μg)
Mouse IgG (1μg)
(i)
(ii)
SS
SS

Figure 6

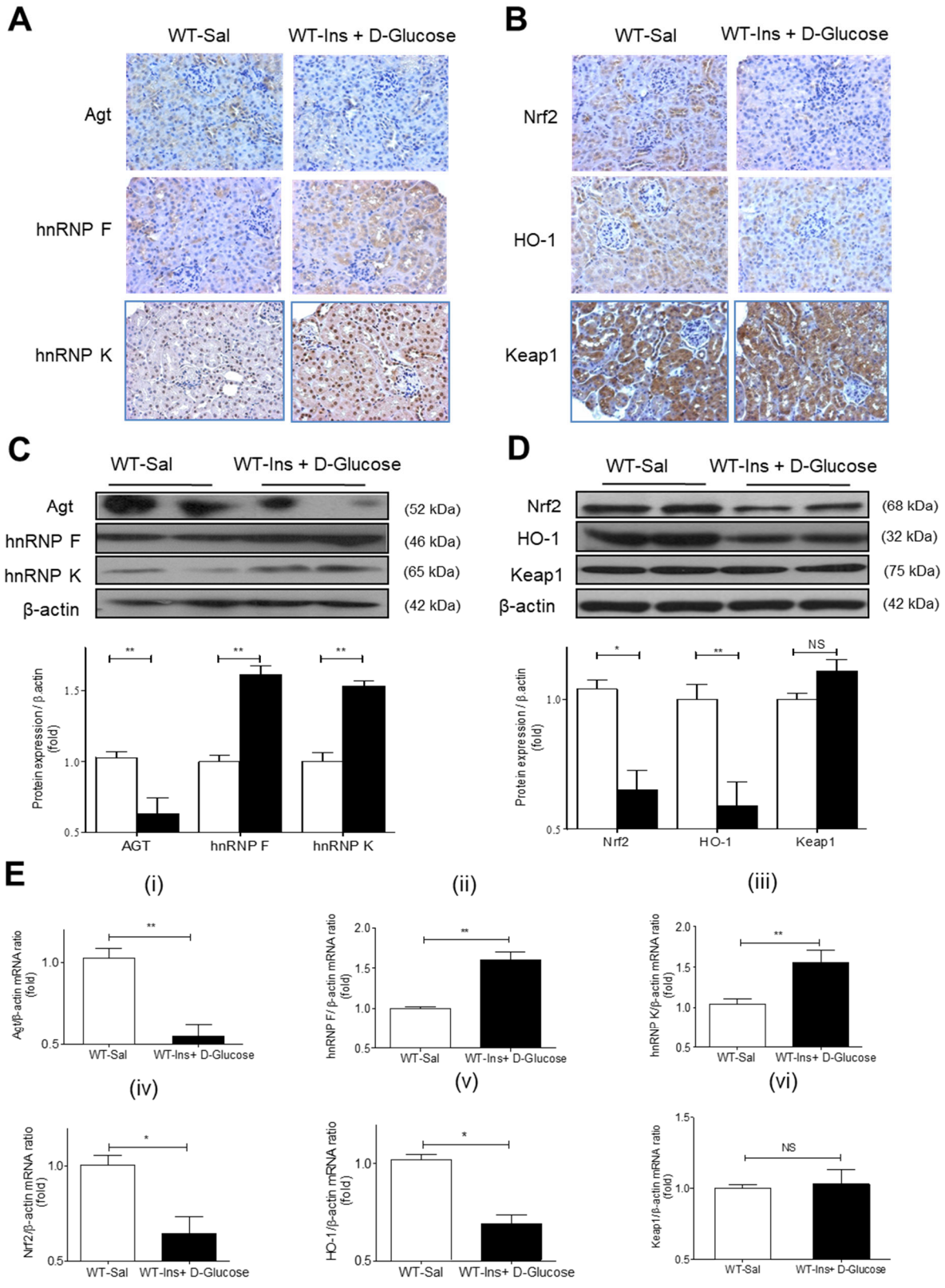
A
WT-Sal
WT-Ins + D-Glucose
Agt
hnRNP F
hnRNP K
B
WT-Sal
WT-Ins + D-Glucose
Nrf2
HO-1
Keap1
C
WT-Sal
WT-Ins + D-Glucose
Agt
hnRNP F
hnRNP K
β-actin
(52 kDa)
(46 kDa)
(65 kDa)
(42 kDa)
Protein expression / β actin (fold)
AGT
hnRNP F
hnRNP K
(i)
D
WT-Sal
WT-Ins + D-Glucose
Nrf2
HO-1
Keap1
β-actin
(68 kDa)
(32 kDa)
(75 kDa)
(42 kDa)
Protein expression / β actin (fold)
Nrf2
HO-1
Keap1
NS
(ii)
(iii)
E
Agt/β-actin mRNA ratio (fold)
hnRNP F / β-actin mRNA ratio (fold)
hnRNP K/β-actin mRNA ratio (fold)
WT-Sal
WT-Ins+ D-Glucose
(iv)
(v)
(vi)
Nrf2/β-actin mRNA ratio (fold)
HO-1/β-actin mRNA ratio (fold)
Keap1/β-actin mRNA ratio (fold)
NS

Figure 7

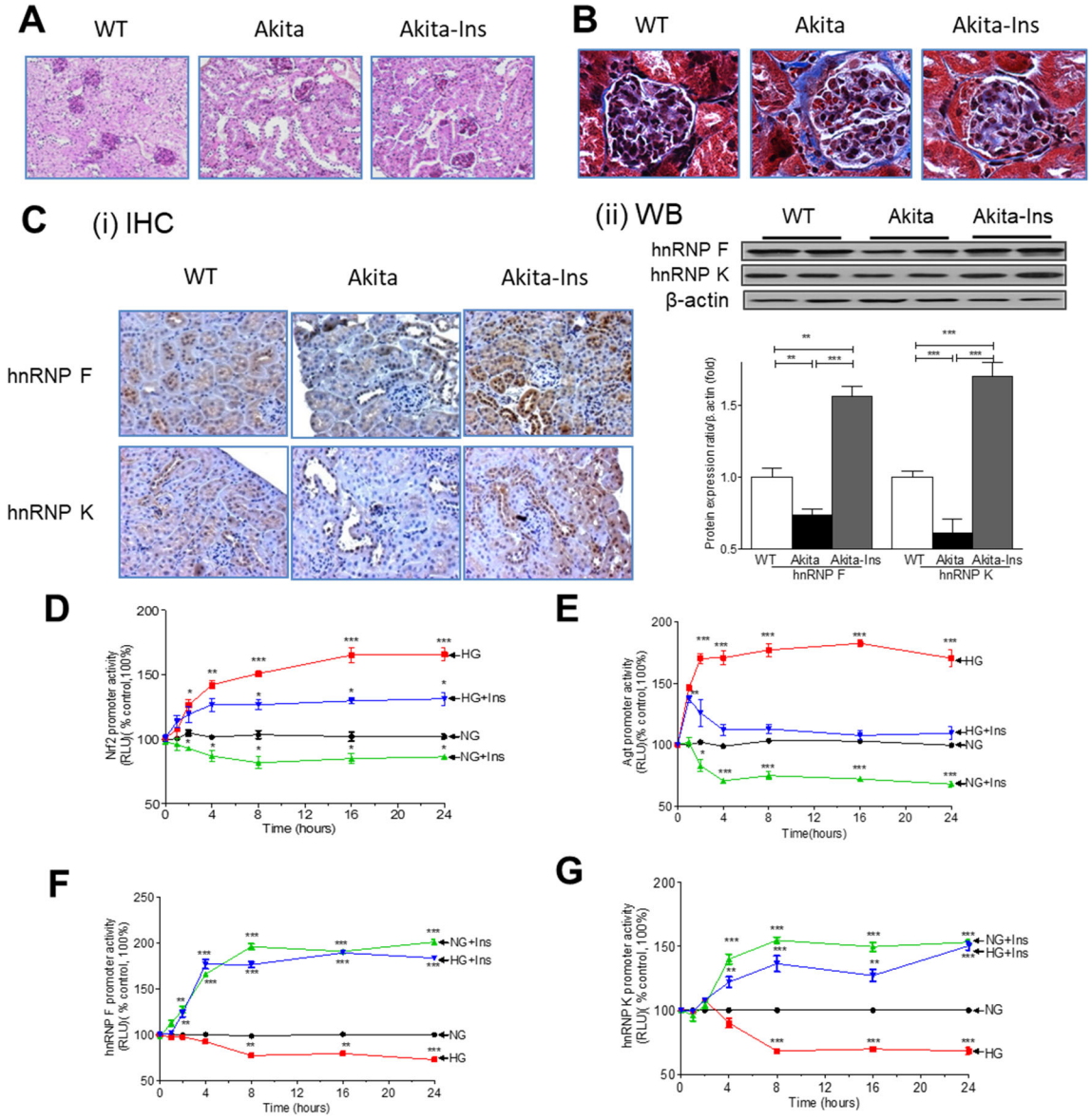

Figure 3-S1 Immunohistochemical staining and time-dependence of insulin effects on gene promoter activity in RPTCs. (A) PAS staining and **(B)** Masson's trichrome staining of collagenous components in kidneys of WT control, Akita and Akita mice treated with insulin implant (Akita-Ins). Magnification x100 and X600, respectively. **(C)** (i) Immunohistochemical staining and (ii) Western blotting and quantitationanalysis for hnRNP F and hnRNP K levels in RPTs from kidneys of WT control, Akita and Akita-Ins. Effects of insulin on *Nrf2* **(D)**, *Agt* **(E)**, *hnRNP F* **(F)** and *hnRNP K* **(G)** promoter activity in IRPTCs in normal glucose (NG, 5 mM D-glucose plus 20 mM D-mannitol) or high glucose (HG, 25 mM D-glucose DMEM) for 24 h. The results are expressed as mean ± SEM, n=3. **p<0.01; ***p<0.001. Similar results were obtained in two separate experiments.

Supplementary Figure 1

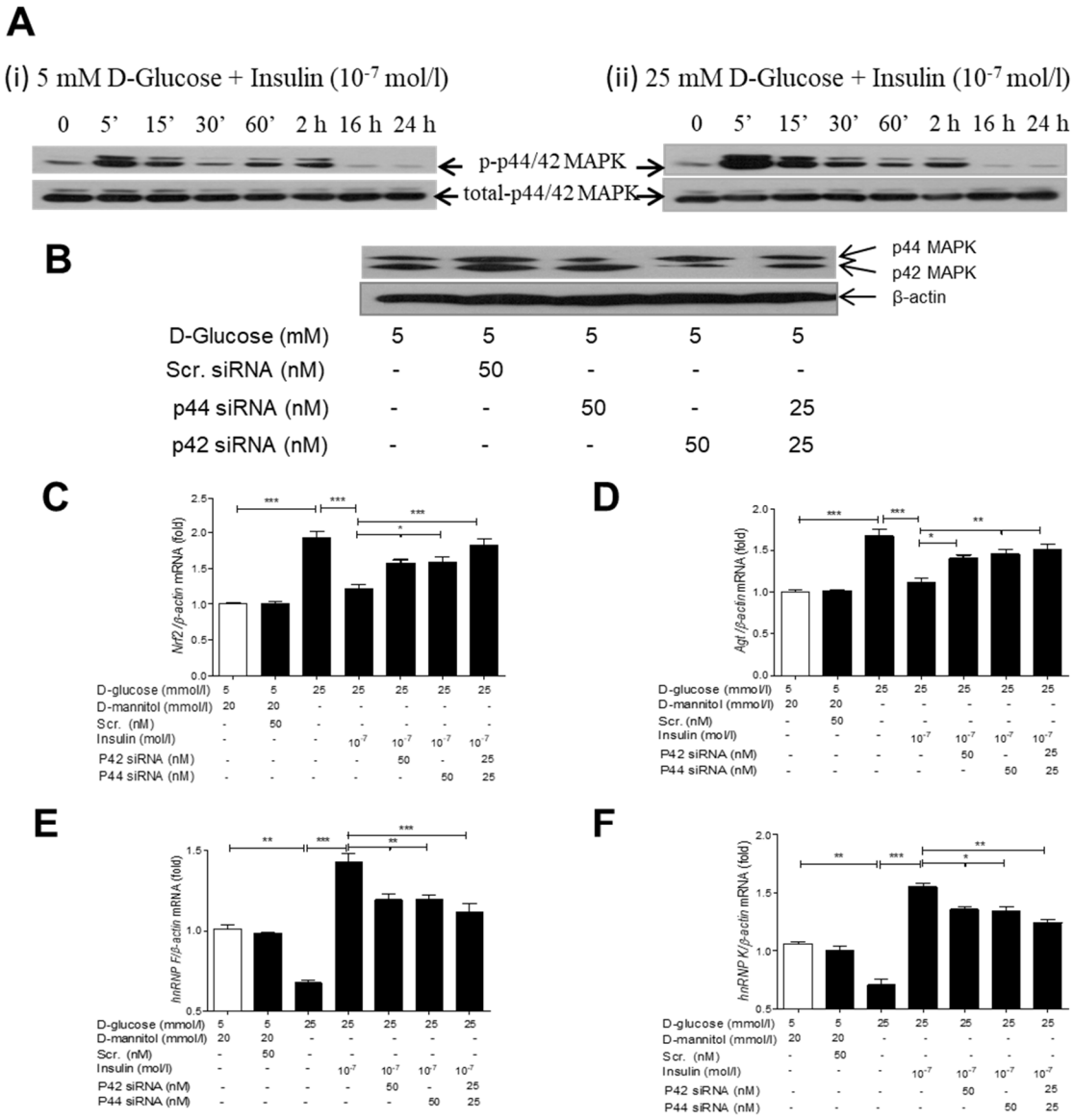

Figure 3-S2 Effect of insulin and siRNA of p44/42 MAPK on p44/42 MAPK and gene expression in IRPTCs. (A) Time-dependent of Insulin effect on p-44/42 MAPK and total p44/42 MAPK expression in IRPTCs cultured in normal glucose (NG, 5 mM D-glucose) (i) or high glucose (HG, 25 mM D-glucose) DMEM analyzed by Western blotting (WB). (B) Effect of transfection of specific siRNA of p42 MAPK and/or p44 MAPK on endogenous p44/42 MAPK expression analyzed by WB. Effect of transfection of specific siRNA of p42 MAPK and/or p44 MAPK on Nrf2 (C), Agt (D), hnRNP F (E) and hnRNP K (F) mRNA expression in IRPTCs cultured in HG quantified by RT-qPCR. mRNA levels in cells incubated in NG medium are expressed as arbitrary unit 1. Each point represent the mean ± SEM (n=3) assayed in triplicate. *p<0.05; **p<0.01; ***p<0.005. Similar results were obtained in 3 separate experiments.

Supplementary Figure 2

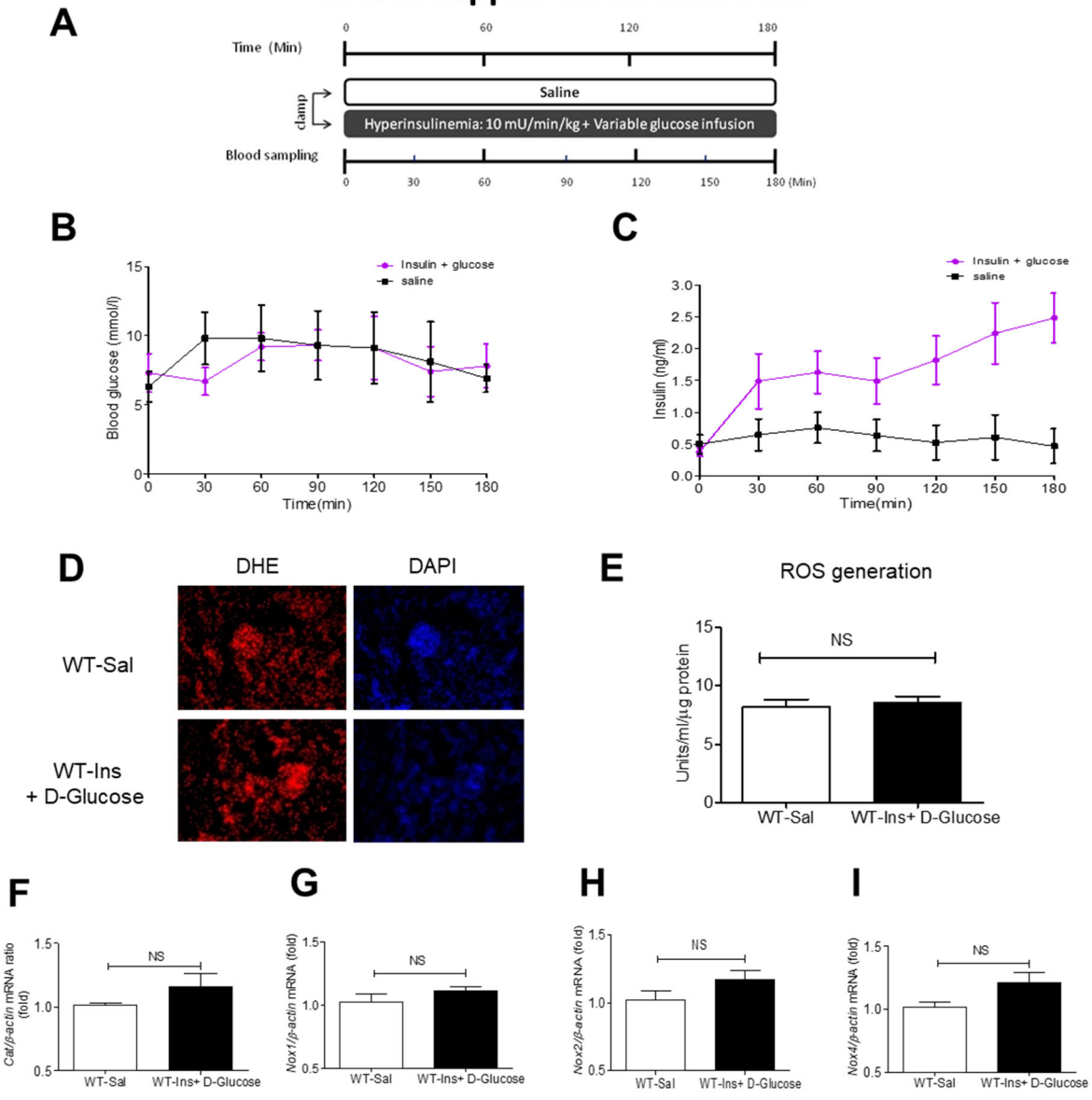

Figure 3-S3 Hyperinsulinemic-euglycemic clamp experiments performed on conscious male C57Bl/6 mice (age 12-14 weeks) after 4-h food restriction. (A) Experimental design of the hyperinsulinemic-euglycemic clamp. (B) Blood glucose and (C) serum insulin were measured by Accu-Check Performa System (Roche Diagnostics) and ELISA, respectively. (D) DHE staining, (E) ROS generation, (F) Cat mRNA and (G) Nox1, (H) Nox2 and (I) Nox4 mRNA level in RPTs from WT mice after 3-h infusion with saline or Ins + D-glucose. Values are mean ± SEM, n=8. ns, not significant. WT with saline infusion (open bars) and WT with Ins + D-glucose infusion (solid bars).

Supplementary Figure 3

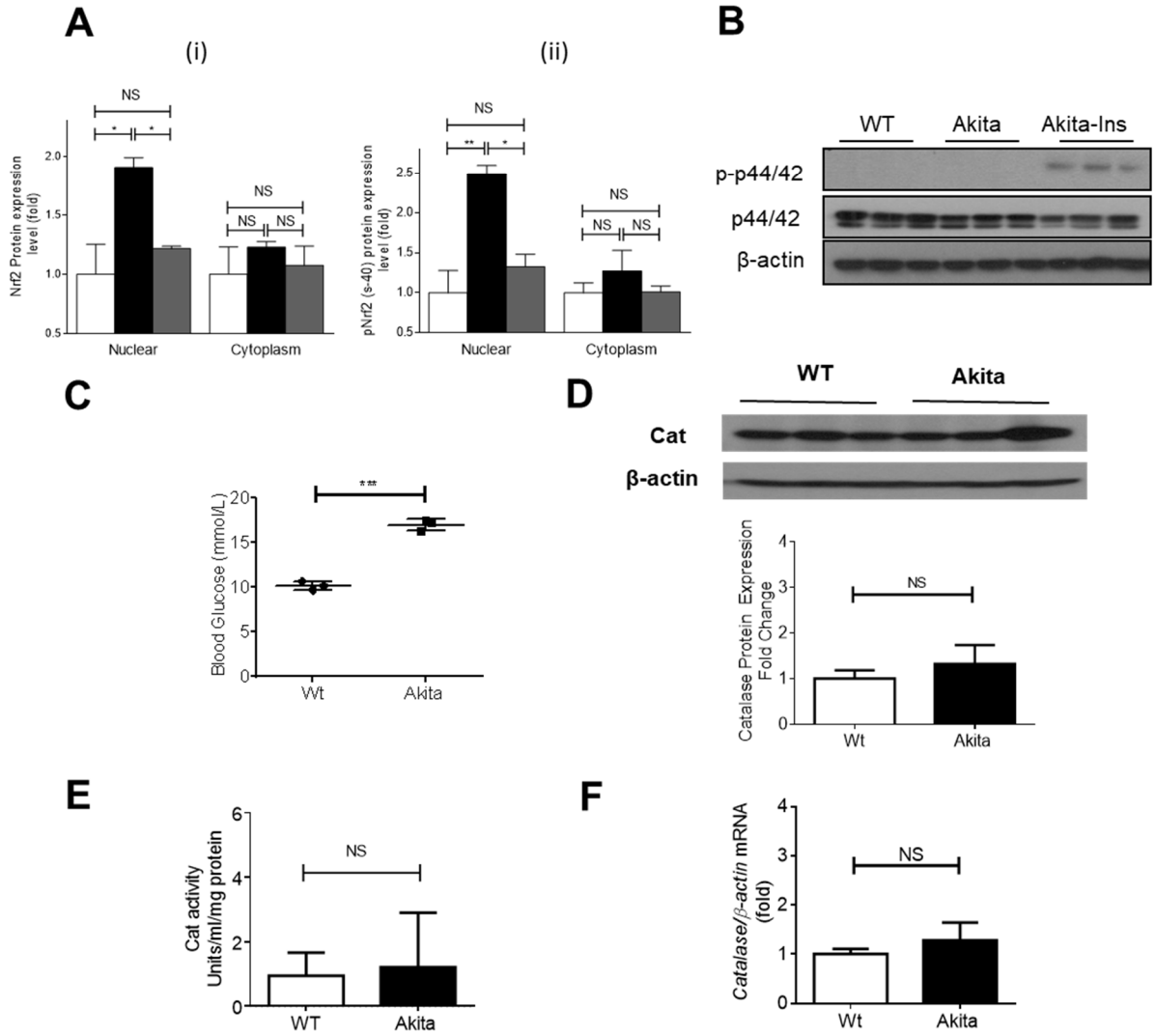

Figure 3- S4: **Nrf2 and p-Nrf2 expression and p44/42 MAPK phosphorylation in freshly isolated mouse RPTs. (A)** Quantitation of nuclear and cytoplasmic Nrf2 (i) and p-Nrf2 (s-40) (ii) expression and (**B**) WB of p44/42 MAPK phosphorylation in RPTs of WT, Akita and Akita mice treated with insulin at the age of 12 weeks and then euthanized at the age of 16 weeks. Values are mean ± SEM, n=3 per group. *p<0.05; **p<0.01; NS, not significant. WT (open bars); Akita (solid bars) and Akita mice + Ins (grey bars). **Catalase (Cat) expression and activity in freshly isolated RPTs of 4-weeks old mice. (C)** Blood glucose level in WT controls and Akita mice at the age of 4 weeks was measured in the morning after a 4-h fasting. **(D)** WB for Cat expression , **(E)** Cat activity and **(F)** *Cat* mRNA level in freshly isolated RPTs from WT and Akita mice at the age of 4 weeks. Values are mean ± SEM, n=3 per group. ***p<0.005; NS, not significant

Supplementary Figure 4

Online Supplemental Materials

Supplemental Table 1. Physiological measurements in non-Akita WT, Akita and Akita mice treated with insulin at the age of 20 weeks and then euthanized at the age of 24 weeks.

	WT	Akita	Akita + Insulin
Systolic blood pressure (mm Hg)	116 ± 1.22	133 ± 0.707 ***	127 ± 0.89 **††
Fasted (4h) Blood glucose (mmol/l)	10.44 ± 0.49	33.78 ± 0.22 ***	20.04 ± 2.21 ***†††
Body weight (g)	34.64 ± 2.32	25.53 ± 0.68 **	28.58 ± 0.97*
Kidney weight (KW) (mg)	331.4 ± 16.82	531 ± 18.47 ***	482 ± 19.85***
Tibia Length (TL) (mm)	21.5 ± 0.61	21.8 ± 0.57	21.9 ± 0.41
KW/BW ratio (mg/g)	10.08 ± 0.58	20,81 ± 0.52 ***	16.98 ± 1.02*** ††
KW/TL ratio (mg/mm)	15.76 ± 0.69	24.36 ± 0.83 ***	21.25 ± 0.45***†
ACR (µg/mg)	10.69 ±2.87	120±14.89 ***	82.55±25.53***

*p<0.05, **p<0.01 and ***p<0.001 vs. WT; †p<0.05, ††p<0.01 and †††p<0.001 vs. Akita

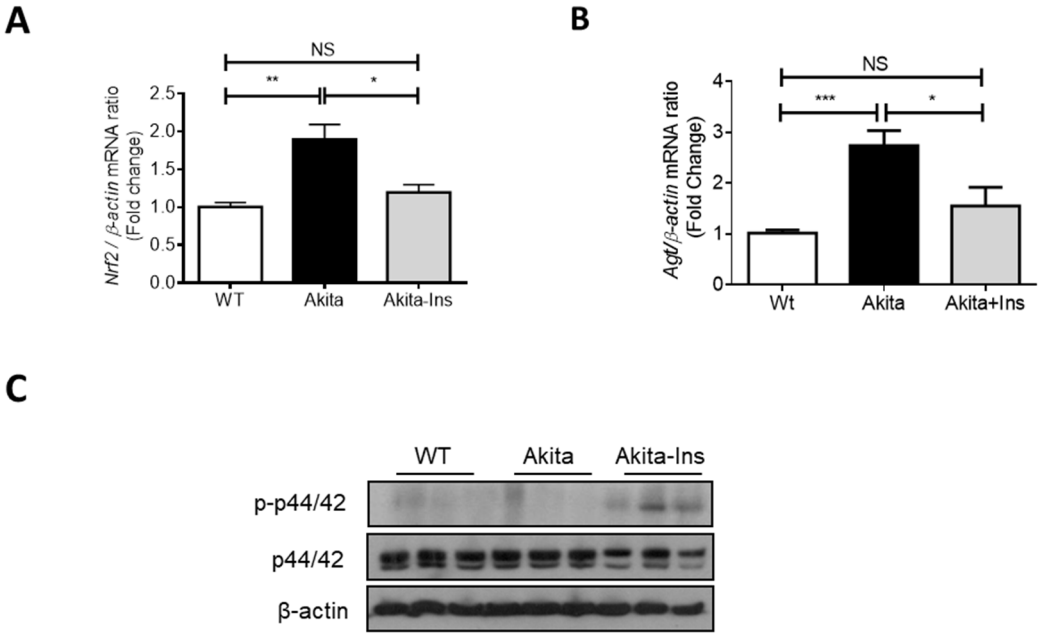

Table 3-1: **Supplimentary table 1:** Physiological measurements

Figure 3-S5 ***Nrf2* and *Agt* mRNA expression and p44/42 MAPK phosphorylation in freshly isolated mouse RPTs.** RT-qPCR of *Nrf2* **(A)** and *Agt* **(B)** mRNA expression and **(C)** WB of cytosolic p44/42 MAPK phosphorylation in RPTs of WT controls, Akita and Akita mice treated with insulin at the age of 20 weeks and then euthanized at the age of 24 weeks. Values are mean ± SEM, n=5 per group. *p<0.05; **p<0.01; ***p<0.005. WT controls (open bars); Akita (solid bars) and Akita mice + Ins (grey bars).

Supplementary Figure 5

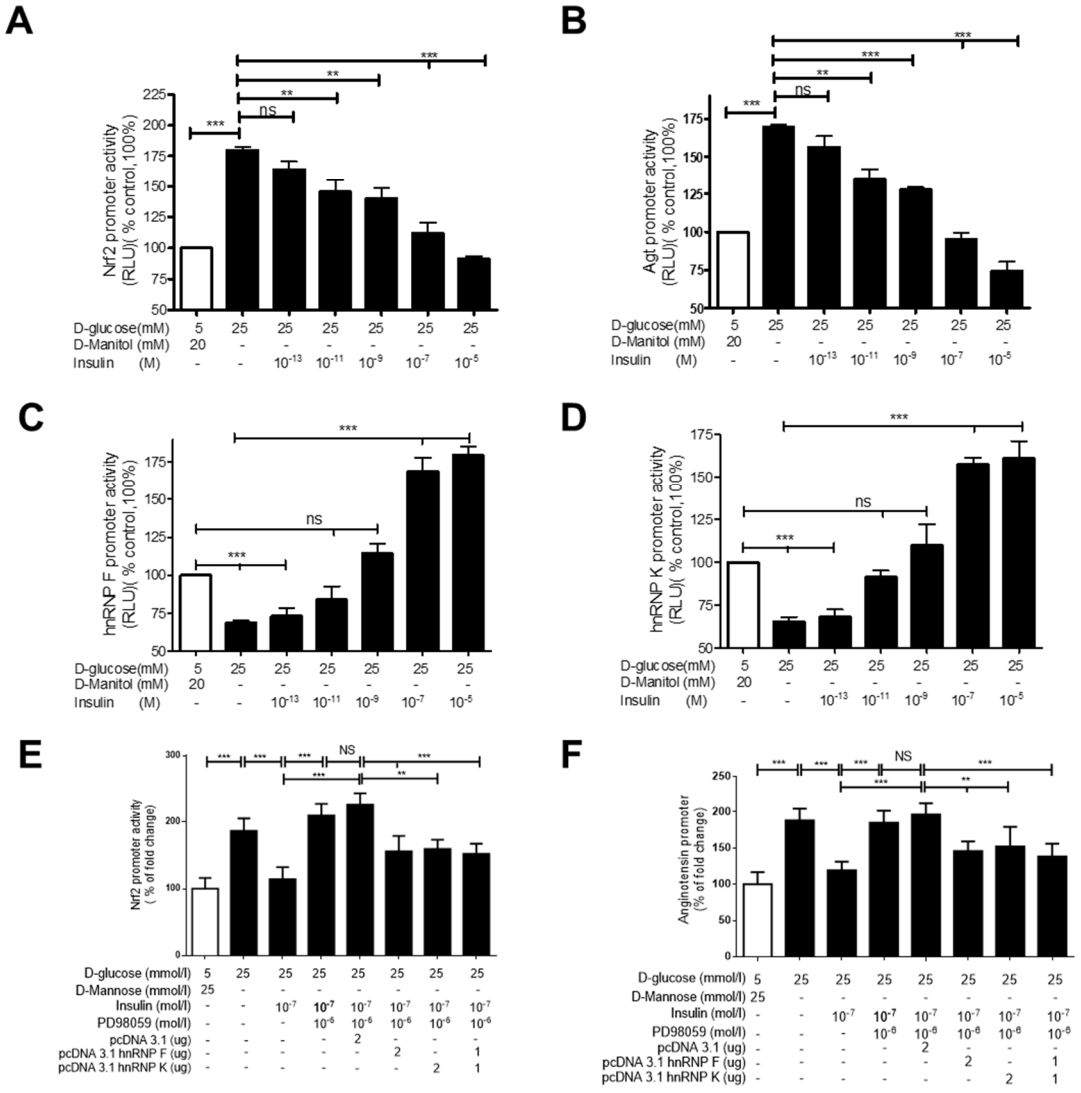

Figure 3-S6 Effect of insulin on *Nrf2*, *Agt*, *hnRNP F* and *hnRNP K* promoter activity in IRPTCs. Cells stably transfected with **(A)** pGL4-*Nrf2*, **(B)** pGL4-*Agt*, **(C)** pGL4-*hnRNP F* or **(D)** pGL4-*hnRNP K* promoter were incubated in normal glucose (NG) or high glucose (HG) DMEM ± various concentrations of insulin and PD98059 (**E** and **F**) with or without transiently transfection of pcDNA 3.1 *hnRNP F* or pcDNA 3.1 *hnRNP* K for 24 h. Cells were harvested and assayed for luciferase activity. The levels of luciferase activity in cells incubated in NG medium are expressed as percentage of control (100%). The inhibitory or stimulatory effect of insulin is compared with cells cultured in HG only. The results are expressed as mean ± SEM, n=3. ***p<0.005; ns, not significant. Similar results were obtained in two separate experiments.

Supplementary Figure 6

Chapter 3: Article 2

Accepted for publication in Scientific Reports. 2019, SREP-18-36519B

Heterogeneous Nuclear Ribonucleoprotein F Mediates Insulin Inhibition of Bcl2-Modifying Factor Expression and Tubulopathy in Diabetic Kidney

Anindya Ghosh[1], Shuiling Zhao[1], Chao-Sheng Lo[1], Hasna Maachi[1], Isabelle Chenier[1], Muhammad Abdul Lateef[1], Shaaban Abdo[1], Janos G. Filep[2], Julie R. Ingelfinger[3], Shao-Ling Zhang[1*] and John S.D. Chan[1*]

[1]Département de médecine
Université de Montréal
Centre de recherche du Centre hospitalier de l'Université de Montréal (CRCHUM)
900 Saint Denis Street, Montréal, QC
Canada H2X 0A9

[2]Département de pathologie et biologie cellulaire
Université de Montréal
Centre de recherche, Hôpital Maisonneuve-Rosemont
5415 boul. de l'Assomption, Montréal, QC
Canada H1T 2M4

[3]Harvard Medical School
Pediatric Nephrology Unit
Massachusetts General Hospital
15 Parkman Street, WAC 709, Boston, MA
USA 02114-3117

[1*]John S.D. Chan and Shao-Ling Zhang are joint senior authors to whom correspondence should be addressed.
Telephone: (514) 890-8000 Extension 15080 or 15633, Fax: (514) 412-7655
E-mail: john.chan@umontreal.ca and shao.ling.zhang@umontreal.ca

Running title: Insulin, Bmf and Diabetic Kidney

Keywords: Insulin; Bmf; HnRNP F; Tubulopathy; Diabetes

Subject categories: Pathophysiology of renal disease and progression

Title: 20 words; Abstract: 199 words; Text: 4,603

Abstract

We investigated the molecular mechanism(s) by which insulin prevents Bcl2-modifying factor (Bmf)-induced renal proximal tubular cell (RPTC) apoptosis and loss in diabetic mice. Transgenic mice (Tg) mice specifically overexpressing human BMF in RPTCs and non-Tg littermates were studied at 10 to 20 weeks of age. Non-diabetic littermates, diabetic Akita mice +/- insulin implant, Akita Tg mice specifically overexpressing heterogeneous nuclear ribonucleoprotein F (hnRNP F) in their RPTCs and immortalized rat renal proximal tubular cells (IRPTCs) were also studied. *BMF*-Tg mice exhibited higher systolic blood pressure, urinary albumin/creatinine ratio, RPTC apoptosis and urinary RPTCs than non-Tg mice. Insulin treatment in Akita mice and Akita mice overexpressing *hnRNP F* suppressed *Bmf* expression and RPTC apoptosis. In hyperinsulinemic-euglycemic wild type mice, renal *Bmf* expression was down-regulated with up-regulation of *hnRNP F*. *In vitro*, insulin inhibited high glucose-stimulation of *Bmf* expression, predominantly via p44/42 mitogen-activated protein kinase (MAPK) signaling. Transfection of *p44/42 MAPK* or *hnRNP F* small interfering RNA (siRNA) prevented insulin inhibition of *Bmf* expression. HnRNP F inhibited *Bmf* transcription via hnRNP F-responsive element in the *Bmf* promoter. Our results demonstrate that hnRNP F suppression of *Bmf* transcription is an important mechanism by which insulin protects RPTCs from apoptosis in diabetes.

Introduction

Although glomerulopathy is a hallmark of early injury in diabetic kidney disease (DKD), tubulopathy including tubular atrophy and tubulointerstitial fibrosis is a major feature of later stages, closely associated with loss of renal function(297, 298, 300, 359). Therefore, tubulopathy is a better predictor of disease progression than glomerular damage(360-362). Indeed, 71% of glomeruli from proteinuric diabetic patients were found to be attached to atrophic tubules at the glomerulotubular junction, including 8-17% atubular glomeruli (glomeruli without tubular attachment)(363, 364). The mechanisms underlying tubular atrophy are incompletely understood. One mechanism is apoptosis, which has been implicated in the subsequent loss of various renal cells, including renal proximal tubular cells (RPTCs)(365-370). Thus, tubular apoptosis may precede tubular atrophy.

Hyperglycemia, hyperlipidemia, oxidative stress and dysfunction of the intrarenal renin-angiotensin system (RAS) have all been implicated in the progression of DKD.We documented that reactive oxygen species (ROS) mediate high glucose (HG) stimulation of angiotensinogen (Agt, the sole precursor of all angiotensins) gene expression in RPTCs *in vitro*(305, 306). Hyperglycemia and Agt act in concert to induce hypertension and RPTC apoptosis in type 1 diabetic (T1D) *Agt*-Tg mice(307, 308). Conversely, catalase (CAT) overexpression attenuates RPTC apoptosis in T1D *CAT*-Tg mice(309) and T2D db/db *CAT*-Tgmice(310), supporting the view that hyperglycemia via enhanced ROS generation plays a central role in RPTC apoptosis in diabetes.

We used microarray analysis to identify the downstream target genes of ROS, and noted elevated expression of Bcl2 (B-cell lymphoma 2)-modifying factor (Bmf) gene in the RPTCs of

db/db mice; the elevated expression was, however, normalized in db/db *CAT*-Tg mice(249). *In vitro,* Bmf overexpression enhanced and knockdown with small interference RNA (siRNA) decreased RPTC apoptosis in HG milieu. Furthermore, Bmf expression is markedly enhanced and localized to apoptotic RPTCs in human diabetic kidneys(249). However, whether overexpression of Bmf would induce RPTC apoptosis and kidney injury *in vivo* has not been investigated.

Intensive insulin therapy has proven to be the most effective treatment for preventing nephropathy progression in T1D; however, the underlying mechanisms remain incompletely understood(18, 371). We previously reported that insulin inhibits high-glucose stimulation of renal rat *Agt* gene expression and RPTC hypertrophy through a putative insulin-responsive element (IRE) in the rat *Agt* gene promoter that interacts with 2 nuclear proteins, heterogeneous nuclear ribonucleoprotein F and K (hnRNP F/K) *in vitro(271, 272, 317)*. Overexpression of hnRNP F inhibited renal *Agt* gene expression and attenuated hypertension, kidney hypertrophy and RPTC apoptosis in Akita (T1D) and db/db-Tg mice(268, 270). We further reported that hnRNP F/K mediate insulin inhibition of renal *Agt* gene expression and that insulin stimulates hnRNP F/K expression through p44/42 MAPK signaling pathway but not through the phosphatidylinositol 3-kinase (PI-3K) pathway in diabetic mice(266, 267). These findings suggest that insulin inhibition of renal *Agt* gene transcription and RPTC apoptosis occurs via hnRNP F/K in diabetes.

In the present study, we investigated the impact of Bmf overexpression on RPTC apoptosis in *BMF*-Tg mice and examined whether hnRNP F mediates, at least in part, insulin

regulation of Bmf actions in Akita mice and in rat immortalized RPTCs (IRPTCs) cultured in HG milieu.

Results

RPTC-Specific Expression of Human Bcl2 Modifying Factor (*hBMF*) Transgene in Transgenic Mice.

hBMF-Tg mice were generated by inserting *myc-hBMF* cDNA with the stop codon into a pKAP2 plasmid containing the kidney-specific androgen-regulated protein (KAP) promoter (**Fig. 1a**). Southern blot analysis revealed the presence of the transgene in heterozygote and homozygote animals from line 148 (**Fig. 1b**). Tissue-specific analysis by RT-PCR confirmed *hBMF* mRNA expression in the kidney cortex and RPTs isolated from male *hBMF*-Tg mice, as well as in the kidney cortex of female *hBMF*-Tg mice implanted with testosterone pellet but not in other tissues from both male and female mice (**Fig. 1c**). *hBMF* transgene was detected in RPTs of male *hBMF*-Tg mice but not in non-Tg mice and can be differentiated from endogenous mouse *Bmf* using primers specific for *hBMF* and mouse *Bmf* in RT-PCR, respectively (**Fig. 1d**). WB of isolated RPTs with anti-Bmf or anti-cMyc antibody (**Fig. 1e**) and immunostaining of kidney sections with an anti-Bmf antibody (that recognizes both human and mouse Bmf) (**Fig. 1f**) confirmed significantly higher BMF expression in RPTCs from male *hBMF*-Tg mice than in non-Tg mice. Furthermore, immunofluorescence staining with anti-Bmf and anti-aquaporin-1 (APQ1, a proximal tubule marker) revealed RPTC-specific BMF expression and its co-localization with AQP1-positive RPTCs of male *hBMF*-Tg mice (**Fig. 1g and Supplementary Fig. 1c**). These data demonstrate that hBMF expression is RPTC-specific in *hBMF*-T gmice.

Overexpression of hBMF Increases Systolic Blood Pressure and Kidney Injury in Tg Mice

Longitudinal systolic blood pressure (SBP) measurements revealed consistently higher SBP in *hBMF*-Tg mice than in non-Tg mice from week 11 to 20 (**Fig. 2a**). Cross-sectional SBP measurements at week 20 showed significantly elevated SBP (on average by ~8 mm Hg) in *hBMF*-Tg mice as compared with non-Tg mice (**Table 1**).

Marked increases in urinary albumin/creatinine ratio (ACR) were observed in *hBMF*-Tg mice at 20 weeks of age (**Fig. 2b** and **Table 1**). Blood glucose, body weight (BW), kidney weight (KW), tibial length (TL), BW/KW, or BW/TL did not differ significantly between *hBMF*-Tg mice and non-Tg mice (**Table 1**). Periodic acid Schiff (PAS) staining of kidney sections revealed mild structural changes in *hBMF*-Tg compared to non-Tg mice and yielded higher statistically significant tubular injury scores (**Fig. 2c**). Moreover, more pronounced Masson's Trichrome staining and TGFβ1 immunostaining were detected in glomerulo-tubular areas of *hBMF*-Tg mice as compared to non-Tg controls and confirmed by semi-quantification (**Figs. 2d** and **2e**, respectively). RT-qPCR showed significantly increased mRNA levels of TGFβ1 (**Fig. 2f**), fibronectin (Fn1) **(Fig. 2g)** and collagen 1α (Col 1α) **(Fig. 2h)** in RPTs of *hBMF*-Tg mice compared to non-Tg mice, indicating that BMF overexpression induces tubulointerstitial fibrosis in kidneys of *hBMF*-Tg mice. Moreover, morphological measurements revealed significant increases in glomerular tuft volume and RPTC volume in *hBMF*-Tg mice as compared to non-Tg mice (**Table 1**).

Overexpression of BMF Stimulates RPTC Apoptosis and Increases Urinary RPTCs

The percentage of TUNEL-positive cells was significantly higher in *hBMF*-Tg mice as compared to non-Tg mice (**Fig. 3a** and **3b**). WB analysis showed increases in Bax and cleaved caspase-3 expression (**Fig. 3c** and **3d**) without detectable changes in Bcl2 and caspase-3 expression in RPT extracts of *hBMF*-Tg mice as compared to non-Tg mice. Furthermore, co-immunoprecipitation (co-IP) experiments revealed more BMF co-IP with Bcl2 whereas less Bcl2 co-IP with Bax in RPTs of *hBMF*-Tg mice than non-Tg mice (**Fig. 3e**). These data would indicate that in *hBMF*-Tg mice, BMF predominantly binds Bcl2 and dissociates it from Bax, thereby tipping the balance of the Bax/Bcl2 ratio towards caspase-3 activation and subsequently RPTC apoptosis.

As Bmf is known to enhance anoikis(250, 372), we investigated whether overexpression of BMF would increase the number of RPTCs in the urine as an indirect indicator of loss of RPTCs. Using flow cytometry, we detected a greater percentage of cells in the urine that stained positive for prominin-1, a proximal tubule marker(373) in *hBMF*-Tg than in non-Tg mice (**Fig. 3f** and **3g**). These data indicate that overexpression of BMF induces RPTC loss, followed by shedding into the urine in *hBMF*-Tg mice.

Insulin Inhibits Bmf Expression and RPTC Apoptosis in Akita Mice

We next tested whether insulin reduction of RPTC apoptosis in Akita mice is mediated, at least in part, via suppression of Bmf expression. As anticipated, Bmf expression was higher in RPTs of Akita mice than in WT mice and was inhibited by insulin (**Fig. 4a**). WB for Bmf protein expression in isolated RPTs confirmed these findings (**Figs. 4b** and **4c**). Co-immunostaining studies showed Bmf localization to TUNEL-positive RPTCs of Akita mice,

which was normalized by insulin treatment (**Fig. 4d**). The percentage of TUNEL-positive RPTCs was significantly higher in Akita than in WT mice and was normalized by insulin treatment (**Fig. 4e**). RT-qPCR analysis revealed increases in Bmf (**Fig. 4f**) and Bax mRNA expression (**Fig. 4g**), with decreases in Bcl-2 mRNA (**Fig. 4h**) in Akita mice. These changes in the Akita mice were normalized by insulin treatment with the exception of Bax mRNA. Consistently, the Bax/Bcl-2 mRNA ratio was significantly increased in Akita mice and was reversed by insulin treatment (**Fig. 4i**).

Insulin Inhibits Bmf Expression Independent of its Glucose Lowering Effect

We previously reported that hyperinsulinemia up-regulated hnRNP F expression in RPTCs independent of its glucose lowering effect[31]. To investigate whether insulin could also inhibit renal Bmf expression independent of its effect on lowering systemic blood glucose *in vivo*, hyperinsulinemic-euglycemic clamp experiments were performed on non-diabetic WT mice. Consistent with the previous report[31], hyperinsulinemia resulted in increases in hnRNP F immunostaining (**Supplemental Fig.1a**) and decreases in Bmf immunostaining (**Fig. 5a**) and Bmf mRNA (**Fig. 5b**) as compared with saline infusion. WB of Bmf expression (**Fig. 5c**) confirmed these observations, indicating that insulin suppression of renal *Bmf* expression occurs independently of its glucose lowering action.

HnRNP F Overexpression Inhibits Bmf Expression in Akita *hnRNP F*-Tg Mice

To explore the functional relationship between hnRNP F and Bmf expression in diabetes, we compared Akita *hnRNP F*-Tg mice to non-Tg mice and Akita mice[28]. Significant decreases in hnRNP F immunostaining (**Supplemental Fig. 1b**) and increases in Bmf immunostaining

were observed in kidneys of Akita mice as compared with non-Akita WT mice, whereas Bmf immunostaining was reduced in Akita *hnRNP F*-Tg mice (**Fig.5d**). WB of Bmf protein expression (**Fig. 5e**) and RT-qPCR of *Bmf* mRNA expression (**Fig. 5f**) confirmed these observations. These data would imply a role for hnRNP F in mediating insulin suppression of *Bmf* expression.

Insulin Inhibits *Bmf* Expression via HnRNP F in IRPTCs.

Confirming our previous findings(249), we found that HG stimulated *Bmf* mRNA expression in cultured IRPTCs and that insulin reversed this finding (**Fig. 6a**). Insulin treatment also prevented the stimulatory effect of HG on rat *Bmf* promoter (N-1370/+102) activity (**Fig. 6b**). Pharmacological blockade of p44/42 MAPK (with PD98059 and U0126) effectively prevented insulin inhibition of *Bmf* promoter activity, whereas blockade of PI-3-Kinase with wortmannin was without effect (**Fig. 6b**). Moreover, transfection with siRNA of *p44 MAPK* or *p42MAPK* also abolished insulin inhibition of *Bmf* promoter activity in HG, whereas scrambled (Scr) siRNA had no effect (**Fig. 6c**).

Furthermore, siRNA of *hnRNP F*, but not Scr siRNA abolished insulin inhibition of *Bmf* promoter activity in HG (**Fig. 6d**). Consistently, we detected 10-fold increase and 70% decrease of hnRNP F mRNA expression when IRPTCs were transfected with pCMV-*hnRNP F-HA* plasmid and siRNA of *hnRNP F*, respectively (**Fig. 6e**). In contrast, Bmf mRNA expression decreased by 60% and increased 175% when IRPTCs were transfected with pCMV-*hnRNP F-HA* and *hnRNP F* siRNA as compared to controls, respectively (**Fig. 6f**).

Identification of hnRNP F-*Response Element* (*RE*) in Rat *Bmf* Promoter

To identify putative hnRNP F-*RE* that mediate the inhibitory action of insulin on *Bmf* promoter activity, pGL4.20 plasmid containing different lengths of the rat *Bmf* promoter were transiently transfected into IRPTCs. pGL4.20-*Bmf* promoter (N-1370/N+102), pGL4.20-*Bmf* promoter (N-1260/N+102), pGL4.20-*Bmf* promoter (N-1045/N+102), and pGL4.20-*Bmf* promoter (N-965/N+102) displayed a 32-, 26-, 32- and 29-fold increase in activity compared with control pGL4.20 plasmid in IRPTCs in NG (**Fig. 7a**). Deletion of nucleotides N-1370 to N-365 significantly decreased pGL4.20-*Bmf* promoter (N-365/+102) activity to just 8-fold higher than plasmid pGL4.20 (**Fig. 7a**). Insulin prevented HG stimulation on pGL4.20-*Bmf* promoter (N-1370/N+102) and pGL4.20-*Bmf* promoter (N-1260/N+102) activity whereas insulin failed to affect pGL4.20-*Bmf* promoter (N-1045/N+102), pGL4.20-*Bmf* promoter (N-965/N+102) and pGL4.20-*Bmf* promoter (N-365/N+102) activity (**Fig. 7b**).

Intriguingly, *Bmf* promoter with deletion of nucleotides N-1086 to N-1081, pGL4.20-*Bmf* promoter (N-1370/N+102 Δ N-1086/N-1081) completely abolished the response to insulin in HG as compared to pGL4.2-*Bmf* promoter (N-1370/N+102) (**Fig. 7c**). In contrast, *Bmf* promoter with deletion of N-997 to N-991 and N-402 to N-395 did not alter the response to insulin (**Fig. 7c**). Furthermore, pGL4.20-*Bmf* promoter (N-1370/N+102) activity was significantly suppressed when co-transfected with pCMV-*hnRNP F*-HA, whereas it had no detectable effect on pGL4.20-*Bmf* promoter (N-1370/N+102 Δ N-1086/N-1081) in NG (**Fig. 7d**). Moreover, *Bmf* promoter with deletion of nucleotides N-997 to N-991 and N-402 to N-395 did not affect the inhibitory effect of pCMV-*hnRNP F*-HA on *Bmf* promoter activity. These

results point toward that nucleotides N-1086 to N-1081 is a putative core *RE* responding to insulin and hnRNP F.

Indeed, EMSA showed that the WT double-strand DNA fragment (N-1093 to N-1072) binds to IRPTC nuclear proteins, which could be displaced by the WT DNA fragment, but not by mutated DNA fragments (M1, M2 and M3) (**Fig. 7e**). Moreover, incubation with an anti-hnRNP F antibody, but not with rabbit IgG (control) induced a supershift (SS) of the *hnRNP F-RE* with nuclear proteins (**Fig. 7e**).

Discussion

The present study demonstrates that overexpression of hBMF specifically in the RPTCs enhances RPTC apoptosis and loss into the urine in *hBMF*-Tg mice, indicating a critical role for Bmf in mediating tubular cell apoptosis and loss. Our findings also indicate that insulin treatment prevents RPTC apoptosis and inhibits renal *Bmf* transcription via a novel putative *insulin-response element* (*IRE*) in the *Bmf* gene promoter that interacts with hnRNP F. These findings identify a novel mechanism by which insulin may prevent nephropathy progression in diabetes.

Bmf is a member of the BH3-only protein family[32]. Bmf binds to cytoskeletal structures and is sequestered to myosin V motors through association with dynein light chain 2. Certain damage signals, such as the detachment of adherent cells (anoikis) from their substratum trigger the release of Bmf, which through binding to pro-survival Bcl-2 proteins induces dissociation of the Bcl-2/Bax dimer, thereby allowing the pro-apoptotic action of Bax on mitochondria(250, 263, 372, 374). Bmf is expressed in various organs, including the kidney[33]. Mice deficient in

Bmf $^{-/-}$, however, do not display any obvious phenotypic abnormalities(256, 259). Recent studies by Pfeiffer *et al.* demonstrated that Bmf not only plays a major role in progressive pancreatic β-cell death in HNF1α-MODY, but also contributes to the pancreatic beta-cell function to maintain glucose homeostasis, independent of cell death signaling(375). However, little is known about the role of Bmf in the kidney or in the pathogenesis of diabetes. We previously reported the presence of increased Bmf expression in apoptotic RPTCs in db/db mice as well as in human diabetic kidneys(249).

To provide direct evidence for Bmf-mediated RPTC apoptosis *in vivo*, we generated Tg mice specifically overexpressing hBMF in their RPTCs. Our data demonstrate that overexpression of hBMF in RPTCs indeed induces RPTC apoptosis and loss into the urine in *hBMF*-Tg mice. Furthermore, overexpression of hBMF increased expression of Bax and cleaved (active) caspase-3 and enhanced Bax binding to Bcl2, consistent with Bax-mediated activation of the intrinsic (mitochondrial) pathway of apoptosis.

The mechanisms underlying increased SBP and ACR in *hBMF*-Tg mice are incompletely understood. The possibility that up-regulation of *TGFβ1* gene expression in RPTCs and its downstream targets Fn1 and Col 1α, leading to higher tubulointerstitial fibrosis that facilitates the development of hypertension has received considerable attention. Indeed, a strong correlation was found between interstitial fibrosis and the development of SBP via a loss or rarefaction of capillaries around the tubules(376, 377). Our observations of increased glomerular tuft volume, RPTC volume and GFR in *hBMF*-Tg mice lend additional support to this notion. Furthermore, the observed increases in ACR can be explained, at least in part, by a combination of loss of RPTCs and increased GFR(378).

The Akita mouse is an autosomal dominant spontaneous diabetic mouse model (mutation in *insulin2*) that exhibits many features resembling changes in T1D patients including hypoinsulinemia, hyperglycemia, hypertension and renal dysfunction(287, 343).

Insulin suppressed *Bmf* and stimulated *hnRNP F* expression in RPTCs of hyperinsulinemic-euglycemic mice after 3 h of hyperinsulinemia as compared to Akita mice after 4 weeks of insulin implantation. This rapid transcription is in agreement with previous reports that up-regulated and down-regulated genes in the skeletal muscle and liver were observed within 2 to 4 h under hyperinsulinemic-euglycemic condition(328, 329). These data demonstrate that insulin impacts RPT *Bmf* and *hnRNP F* expression, independent of its glucose-lowering effect.

Our data also revealed significantly higher expression of Bmf protein and mRNA in RPTs of 16 weeks old Akita than WT mice. Overexpression of hnRNP F significantly down-regulated *Bmf* expression in Akita *hnRNP F*-Tg mice, suggesting a role for hnRNP F in mediating insulin inhibition of *Bmf* expression in Akita mice. However, it is noteworthy that we could not exclude the off-target effects of random transgene insertion in mediating insulin suppression of Bmf expression in our hnRNP F-Tg mice. Addressing this issue would require mapping transgene insertion sites which is outside the scope of this present study. Generation of currently unavailable RPTC-specific hnRNP F knockout mice would provide more direct evidence of the role of hnRNP F on Bmf expression. We are now working on developing such a model for future work.

Combining studies with pharmacological inhibitors and siRNAs, we identified roles for the p44/42 MAPK signaling pathway and hnRNP F in mediating insulin suppression of renal

Bmf gene transcription. These findings clearly link hnRNP F to mediating insulin inhibition of *Bmf* gene expression in the diabetic mouse kidney. Nevertheless, additional studies employing RPTC-specific *hnRNP F* knockout mice are needed to firmly establish this pathway.

The mechanism by which hnRNP F down-regulates renal *Bmf* gene expression remains to be investigated. A likely mechanism is that hnRNP F suppresses *Bmf* transcription via binding to a putative *IRE* in the *Bmf* promoter. This is supported by the findings that transfection of *hnRNP F* cDNA considerably decreases *Bmf* promoter activity, whereas transfection of *hnRNP F* siRNA reverses insulin effect. DNA sequence analysis revealed 3 GC-rich regions in the *Bmf* promoter including nucleotides N-1086 to N-1081 (5'-AGGGGG-3'), N-997 to N-991 (5'-GAGGGGC-3') and N-402 to N-395 (5'-CCCCCGC-3'). Nucleotides N-1086 to N-1081 contain the sequence 5'-AGGGGG-3' which is homologous to the *IRE* sequence of N-402 to N-398 (5'-AGGGGG-3') and N-974 to N-969 (5′-AGGGGG-3') in the rat *Sirtuin-1* and *Ace2* promoter, respectively[29,47]. Deletion of N-1086 to N-1081in the *Bmf* promoter markedly reduced insulin- and hnRNP F-down-regulation of *Bmf* promoter activity in IRPTCs whereas deletion of N-997 to N-991 and N-402 to N-395 had no effect, indicating that the 5'- and 3'-flanking sequences of the core sequence might be important for hnRNP F binding. Moreover, biotinylated *IRE* (N-1093to N-1072) binds to nuclear proteins of RPTCs. Addition of anti-hnRNP F antibody yielded a supershift of biotinylated *IRE* complex with nuclear proteins on EMSA. These findings identify N-1093 to N-1072 as a putative *IRE* that interacts with hnRNP F and inhibits *Bmf* transcription.

It is noteworthy that hnRNP F not only regulates *Bmf* transcription as it also modulates the transcription of *Agt*[28], Sirtuin-1[29], *Nrf2*[31], *Ace2(269)* and possibly other genes(354). Thus,

the hnRNP F effect on Bmf expression might also be mediated by other (indirect) mechanisms. Furthermore, the role of hnRNP F in human pathophysiology remains to be explored. More studies are definitely needed along these lines.

In summary, our results demonstrate that insulin inhibits *Bmf* transcription and prevents RPTC apoptosis and loss via p44/42 MAPK signaling and hnRNP F expression (Fig. 8) These findings would imply that Bmf activation could aggravate tubulopathy via inducing RPTC loss in the diabetic kidney. However, it remains to be seen whether renal hnRNP F might be a potential target for the prevention of tubulopathy in the diabetic kidney.

Materials and Methods

Chemical and Reagents

D-glucose, D-mannitol, human insulin, PD98059 [a p44/42 MAPK inhibitor] and wortmannin (a PI-3K inhibitor) were procured from Sigma-Aldrich Canada Ltd. (Oakville, ON, Canada). U0126 (an inhibitor of p44/42 MAPK) was purchased from Cell Signaling Technology (New England BioLabs Ltd., Whitby, ON, Canada). Dulbecco's modified Eagle medium (DMEM, 5 mmol/L D-glucose, catalog no. 12320), penicillin/streptomycin and fetal bovine serum (FBS) were bought from Invitrogen, Inc. (Burlington, ON, Canada). Insulin implants (Linßit, with a release rate of approximately 0.1 unit/implant/day for 30 days) and pGL4.20 [Luc/Puro] vector containing luciferase reporter were obtained from Linshin (Scarborough, ON, Canada) and Promega Corporation (Sunnyvale, CA), respectively. The antibodies used are listed in **Supplementary Table 1**. Rat genomic DNA was used to clone the *Bmf* gene promoter N-1370 to N+102 by conventional polymerase chain reaction (PCR) with specific primers (**Supplementary Table 2**) and confirmed by DNA sequencing. The *Bmf* gene promoter then

was inserted into pGL4.20 vector via Xho I and Hind III enzyme restriction sites. Scrambled Silencer Negative Control small interfering RNA (siRNA), siRNAs of *p44/42 MAPK* and *hnRNP F* were obtained from Ambion, Inc. (Austin, TX). Oligonucleotides and biotin-labeled primers were sourced from Integrated DNA Technologies (Coralville, IA). Kits for LightShift Chemiluminescent electrophoretic mobility shift assay (EMSA) and QuickChange II Site-Directed Mutagenesis were purchased from Agilent Technologies (Santa Clara, CA) and Thermo Scientific (Life Technologies Inc., Burlington, ON, Canada), respectively. Restriction and modifying enzymes were from New England BioLabs, Invitrogen, Roche Biochemicals, Inc. (Dorval, QC, Canada), and GE Healthcare Life Sciences (Baie d'Urfé, QC, Canada).

Generation of Human BMF-Tg and Akita hnRNP F-Tg Mice

Tg mice specifically overexpressing human *myc-BMF* in their RPTCs were generated using a similar strategy to that described previously(197, 268, 309). In brief, full-length human *BMF* cDNA fused with Myc-tag was inserted into pKAP2 plasmid at the NotI site. The plasmid pKAP2 containing the KAP promoter that is responsive to androgen was a gift from Dr. Curt D. Sigmund (University of Iowa, Iowa City, IA)(379).

Akita *hnRNP F*-Tg mice were generated by cross-breeding *hnRNP F*-Tg mice with heterozygous Akita (C57BL/6-Ins2 Akita/J) mice (Jackson Laboratory, Ann Harbor, ME) as previously described[28].

Physiological Studies

Adult male non-Tg littermates (wild type (WT)) and *myc*-h*BMF*-Tg mice were studied

at the age of 10 to 20 weeks. Akita mice and Akita *hnRNP F*-Tg mice were studied at the age of 10 to 16 weeks. Male non-Akita littermates (controls) and Akita mice at the age of 10 weeks treated ± insulin implants and studied from week 12 until week 16(267). All animals had access to water and standard mouse chow ad libitum. Animal care and procedures followed the Principles of Laboratory Animal Care [National Institutes of Health (NIH) publication no. 85-23, revised 1985: http://grants1.nih.gov/grants/olaw/references/phspol.htm] and were approved by the Centre de recherche du centre hospitalier de l'Université de Montréal (CRCHUM) Animal Care Committee.

Mouse blood glucose levels after 4 to 5 h of fasting were measured by Accu-Chek Performa (Roche Diagnostics, Laval, QC, Canada). Morning SBP was monitored at least 2-3 times per week in each animal for 6 or 10 weeks with Visitech Systems BP-2000 tail-cuff (Apex, NC) (176, 266-269). The mice were acclimatized to the procedure for at least 15-20 min per day for 5 days before the first SBP measurements.

All animals were individually housed in metabolic cages for 8 h during day time for urine collection and blood was collected by cardiac puncture (centrifuged to obtain serum) before euthanasia at 16 or 20 weeks old. Urine samples were assayed for ACR by enzyme-linked immunosorbent assay (ELISA) (Albuwell and Creatinine Companion, Exocell, Inc., Philadelphia, PA). Immediately after euthanasia, the kidneys were removed, decapsulated, and weighed. Left kidneys were processed for histology and immunostaining and right kidneys for RPT isolation by Percoll gradient(176, 266-269). Aliquots of freshly isolated RPTs from individual mice were processed for isolation of total RNA and protein.

Fluorescein isothiocyanate-labeled inulin was used to estimate the glomerular filtration rate (GFR) as recommended by the Animal Models of Diabetic Complications Consortium (http://www.diacomp.org/), with slight modifications(176, 266-269).

In a separate series of studies, conscious male C57Bl/6 mice (aged 12 to14 weeks) after a 4-hour food restriction were used for hyperinsulinemic-euglycemic clamp experiments as previously described[31].

Morphologic Studies

Kidney sections of 4 μm thick from five to six animals/group were assessed by standard periodic acid–Schiff (PAS) or Masson's trichrome staining. Immunohistochemistry staining (IHC) was performed by the standard avidin-biotin-peroxidase complex method (ABC Staining, Santa Cruz Biotechnology, Santa Cruz, CA). Semi-quantitation of the relative staining was done by NIH Image J software (http://rsb.info.nih.gov/ij/).

Tubular injury score, mean glomerular tuft, tubular luminal area, and RPTC volumes were assessed on PAS–stained sections at ×200 magnification as described previously(176, 266-269). Briefly, PAS stained images (8-10 fields/kidney) were assessed for tubular injury in the cortex area that displayed tubular dilation, tubular atrophy, cast formation, vacuolization, degeneration, and loss of the brush border. The tubules were evaluated according to the following injury grade (0-3): 0= no tubular injury, 1= less than 25% tubules injured, 2 = 25%-50% injured, 3 = more than 50% tubules injured(380). The score corresponding to tubular injury was calculated for each group by summing and then averaging the grades for each field.

The mean glomerular volume (V_G) was determined by the method of Weibel and Gomez[381] with the aid of an image analysis software system (Motics Images Plus 2.0, Motic, Richmond, BC, Canada). The V_G was estimated by the mean glomerular tuft area (A_T) derived from the light microscopic measurement of 30 random sectional profiles of glomeruli from each group (n=6 animals per group) using the formula: $V_g = \beta / k \times A_T^{1.5}$, where $\beta = 1.382$ (shape coefficient for spheres) and $k = 1.1$ (size distribution coefficient).

Tubular luminal areas were measured on renal sections (six animals/ group; 4 to 5 sections per kidney, 4 random fields per section, 50 tubules around the glomerulus per field) with the same Motics Image Plus 2.0 image analysis software.

Outer cortical RPTs with similar cross-sectional views and clear nuclear structure were selected for cell volume measurement. Mean cell volume from 100 RPTCs was estimated by the Nucleator method(382).

Western Blotting

Western blotting (WB) was performed as described previously(176, 266-269). The relative densities of bands of Bmf, caspase-3, cleaved (active) caspase-3, Bax, Bcl2 and β-actin were quantified by NIH ImageJ software (http://rsb.info.nih.gov/ij/).

Real-Time Quantitative PCR

Real-time quantitative (q) PCR was used to quantify the mRNA levels of various genes in RPTs with the forward and reverse primers listed in **Supplementary Table 2**(176, 266-269).

Cell Culture

Rat IRPTCs (passages 13 through 18) were used(335). Rat *Bmf* gene promoter inserted into the plasmid pGL4.20 was stably transfected into IRPTCs as described previously(176, 266-269).

To investigate insulin effect, IRPTC stable transformants (75% to 85% confluence) were synchronized for 16 hrs in serum-free DMEM (5 mmol/L D-glucose). Then they were incubated in normal glucose (NG, 5 mmol/L D-glucose plus 20 mmol/L D-mannitol) or HG (25 mmol/L D-glucose) DMEM containing 1% depleted fetal bovine serum (FBS) and insulin (10^{-7} mol/L or 573 ng/mL) for up to 24 hours ± PD98059 or U0126 or wortmannin[31]. The cells were then harvested, and the *Bmf* gene promoter activity was measured by luciferase assay[31]. IRPTCs stably transfected with pGL4.20 served as controls. In addition, scrambled siRNA or siRNAs of *p44/42 MAPK* or *hnRNP F* were transfected into IRPTC stable transformants and cultured for 24 hours, their effects on *Bmf* gene promoter activity and mRNA expression were assessed.

Flow Cytometry Analysis of Urinary Cells

Urine was collected for 6 hrs from individual non-Tg or myc-h*BMF*-Tg mice placed individually in metabolic cages. Urines from 5 mice in each group were collected, pooled and centrifuged at 500 x g for 10 minutes to pellet down the cells in the urine. Pellets were rinsed with PBS and passed through a 35 μm cell strainer (#352235, Corning Inc., Corning, USA). Each cell suspension was then blocked with 2% FBS in PBS for 10 minutes then stained with DRAQ7 and anti-prominin-1 antibody conjugated with PE-Vio770 (MiltenyiBiotec, BergischGladbach, Germany, 1:25 dilution)[34] for 30 minutes at room temperature in the dark,

then washed with PBS; equal volumes of suspension from non-Tg or myc-h*BMF*-Tg mice were subjected to flow cytometry (LSR-II, BD Biosciences). Staining with DRAQ7 was used to assess viability. The data was analyzed using FlowJo V10 (FlowJo, LLC, Ashland, USA).

Statistical Analysis

Data are expressed as means ± SEM. Statistical analysis was performed with the Student *t* test or one-way ANOVA and the Bonferroni test, as appropriate (GraphPad Prism 5.0 software, http://www.graphpad.com/prism/Prism.htm). $P<0.05$ was considered to be statistically significant for all tests. (*$p \leq 0.05$; **$p \leq 0.01$; ***$p \leq 0.001$; NS, non-significant)

Acknowledgements

This manuscript or any significant part of it is not under consideration for publication elsewhere. The data, however, were presented, in part, as poster communications at the Annual Meeting of the American Society of Nephrology, New Orleans, LA October 31-November 5th, 2017.

Funding

This work was supported by grants from the Canadian Institutes of Health Research (MOP-84363 and MOP-106688 to JSDC, MOP-86450 to SLZ, and MOP-97742 to JGF), the Canadian Diabetes Association (NOD_OG-3-14-4472-JC to JSDC), the Kidney Foundation of Canada (KFOC 170006 to JSDC) and the National Institutes of Health (NIH) of USA (HL-48455 to JRI).

Disclosure

None reported.

Contribution Statement

JSDC is the guarantor of this work, has full access to all study data, takes responsibility for data integrity and the accuracy of data analysis. JSDC contributed to study conception and design, drafted and reviewed/edited the final manuscript. AG wrote the first draft of the manuscript and contributed to the discussion. AG, SZ, CSL, IC, HM, MAL, SA and SLZ performed the *in vivo* and *in vitro* experiments and data collection. SLZ, JGF and JRI added to the discussion, and reviewed/edited the manuscript. All authors were involved in data analysis and interpretation, critical manuscript revision, and gave final manuscript approval. They thank the rodent metabolic phenotyping core facility of the CRCHUM for assistance with the hyperinsulinemic-euglycemic clamp studies.

Competing Interests

The author(s) declare no competing financial and non-financial interests.

Figure Legends

Figure 1. Generation of *hBMF*-Tg mice. (**a**) Schematic map of the kidney androgen-regulated promoter (KAP2)-Myc-*hBMF* construct. The isolated 17-kb KAP2-myc-*hBMF* transgene (digested with *Spe*I and *Nde*I) was microinjected into 1-cell fertilized mouse embryos obtained from super ovulated C57Bl6 ✕ C3H mice. (**b**) Southern blotting of genomic DNA for founders with biotin-labeled *BMF* probe. Heterozygous and homozygous F_1, F_2 and F_3 were screened by PCR with specific primers (Table 1). Pc, plasmid positive control. NC, negative control. (**c**) RT-PCR product showing tissue expression of *hBMF* mRNA in male and in female Tg mice un-induced or induced with testosterone. *hBMF* and β-*actin* fragments are indicated. Female transgenic mice (line #148) mice were induced with placebo pellets or pellets containing 5 mg testosterone with a 21-day release schedule (Cat. #A-121, Innovative Research of America, Sarasota, FL) for 2 weeks prior to RNA isolation. Br, brain; Hr, heart; Lu, lung; Li, liver; Sp, spleen; Ki, kidney; PT, isolated proximal tubule. (**d**) Specific PCR analysis of *hBMF* transgene and mouse Bmf in offspring of non-Tg and *hBMF*-Tg line 148. (**e**) WB of Bmf and c-Myc protein expression in non-Tg and *hBMF*-Tg mice. (**f**) Representative immunostaining for Bmf expression in non-Tg and *hBMF*-Tg mice. (**g**) Representative colocalization of immunostaining for Bmf and aquaporin 1 (AQP1) in male non-Tg and *hBMF*-Tg mouse kidneys (x200). P: proximal tubule, G: glomerulus. Scale bar=50μm.

Figure 2. BMF overexpression induces systemic hypertension, glomerulo-tubular fibrosis and pro-fibrotic gene expression in Tg mouse kidneys at week 20. (**a**) Longitudinal changes in SBP (measured 2 to 3 times per mouse per week in the morning without fasting). Baseline

SBP was recorded daily over 5 days before initiation of measurements. (**b**) Urinary albumin/creatinine ratio (ACR) in non-Tg and *hBMF*-Tg mice. (**c**) PAS staining and tubular injury score. (**d**) Masson's trichrome staining and semi-quantification of staining. (**e**) TGF-β1 immunostaining and semi-quantification in non-Tg and *hBMF*-Tg mice. Scale bar=50μm. RT-qPCR of *TGF-β1* **(f)**, *FN1* **(g)** and *Col Iα* **(h)** mRNA in freshly-isolated RPTs from non-Tg and *hBMF*-Tg mice. Values are means ± SEM, n=6. *p<0.05; **p<0.01; ***p<0.005; NS, Not significant.

Figure 3. Overexpression of BMF induces RPTC apoptosis in mouse kidneys at age 20 weeks. (**a**) TUNEL (green fluorescence) Assay. Magnification x200. Arrowheads indicate apoptotic cells. P: proximal tubule, G: glomerulus. Scale bar=50μm. (**b**) Semi-quantitation of apoptotic cells in mouse kidneys. (**c**) WB of Bax, Bcl-2, caspase-3 and cleaved (c)-caspase-3, in freshly-isolated RPTs from non-Tg and *hBMF*-Tg mice and (**d**) densitometry analysis. Values are means ± SEM, n=6. **p<0.01; ***p<0.005; NS, Not significant. (**e**) Co-immunoprecipitation of Bcl-2 with Bmf and Bax with Bcl2 in RPT extracts from non-Tg and h*BMF*-Tg mice. The relative densities of bands of co-IP of Bmf/Bcl2 and Bcl2/Bax were quantified by NIH ImageJ software (http://rsb.info.nih.gov/ij/). (**f**) Analysis of urinary prominin-1 positive RPTCs in non-Tg and *hBMF*-Tg mice by flow cytometry (**g**) Quantitation of urinary RPTCs/total urinary cells in non-Tg and *hBMF*-Tg mice. Values are means ± SEM, n=3. ***p<0.005; NS, Not significant.

Figure 4. Insulin effect on Bmf expression and RPTC apoptosis in Akita mice at week 16. (**a**) Bmf immunostaining (magnification 200X) and semi-quantification of relative Bmf immunostaining by NIH Image J software (http://rsb.info.nih.gov/ij/). (**b**) Representative WB of Bmf and (**c**) densitometry analysis in freshly-isolated RPTs from WT, Akita and insulin-treated Akita mice. (**d**) Co-localization of Bmf expression and TUNEL-positive cells in Akita mouse kidneys. Kidney sections were subjected to TUNEL assay to visualize apoptotic cells (green) and then incubated with anti-Bmf antibody followed by anti-goat AlexaFluor 594 to demonstrate Bmf expression (red). Magnification 600X. Arrows indicate cells that stained positively for TUNEL and Bmf. G, glomerulus; and PT, proximal tubule. (**e**) Semi-quantitation of apoptotic cells in WT, Akita and insulin-treated Akita mice. RT-qPCR of Bmf (**f**), Bax (**g**), Bcl-2 (**h**) and ratio of Bax/Bcl-2 (**i**) mRNA in freshly isolated RPTs from WT, Akita and insulin-treated Akita mice. Values are means ± SEM, n=6. *p<0.05; **p<0.01; ***p<0.005; NS, Not significant.

Figure 5. Renal Bmf expression in hyperinsulinemic-euglycemic mice and in Akita *hnRNP* F-Tg mice. (**a**) Representative immunostaining of Bmf (magnification X 200), (**b**) RT-qPCR of *Bmf* mRNA expression and (**c**) representative WB and densitometry of Bmf expression in isolated RPTs from WT mice after 3-h infusion with saline (open bars) or insulin (Ins) + D-glucose (solid black bars). Values are mean ± SEM, n=8 per group. *p<0.05; ***p<0.005; NS, not significant. (**d**) Representative immunostaining for Bmf (magnification X 200). Semi-quantification of relative Bmf immunostaining in (a) and (d) was assessed by NIH Image J software (http://rsb.info.nih.gov/ij/), (**e**) Representative Bmf WB and densitometry analysis, and

(**f**) RT-qPCR of *Bmf* mRNA expression in isolated RPTs from WT, Akita and Akita *hnRNP* F-Tg mice at 20 weeks of age. Values are mean ± SEM, n=8 per group. $^{*}p<0.05$; $^{**}p<0.01$; NS, not significant.

Figure 6. Effect of siRNA of p44/42 *MAPK* or *hnRNP F* and *hnRNP F* cDNA on *Bmf* gene expression in IRPTCs. (**a**) Bmf mRNA expression in IRPTCs cultured in NG or HG in the presence or absence of insulin. **(b)** IRPTCs stably transfected with pGL4.20-rat *Bmf* gene promoter were incubated in NG or HG DMEM ± insulin for 24 h with or without pharmacological inhibitors or transiently transfected with siRNA of p42 *MAPK* or p44 *MAPK* (**c**) or with siRNA of *hnRNP F* (**d**). IRPTCs transiently transfected with pCMV empty or pCMV-*hnRNP F* plasmid and scrambled (Scr) siRNA or siRNA of *hnRNP F* to determine *hnRNP F* mRNA (**e**) or *Bmf* mRNA (**f**) expression. Luciferase activity in cells cultured in NG medium was considered as 100%. The results are expressed as percentage of control (mean ± SEM, n=3). Each value represents the mean ±SEM (n=3) assayed in duplicate. $^{**}p<0.01$; $^{***}p<0.005$; NS, not significant.

Figure 7. Identification of putative *IRE* or *hnRNP F-RE* in the *Bmf* gene promoter

(**a**) Luciferase activity of plasmids containing various lengths of *Bmf* gene promoter in NG medium or (**b)** HG medium ± insulin in IRPTCs. Luciferase activities were normalized by co-transfecting the vector pRC/RSV containing beta-galactosidase cDNA. Control IRPTCs in NG (open bars), IRPTCs in HG (solid black bars) and IRPTCs treated with insulin in HG (solid light grey).(**c**) The activity of 1μg of the full-length *Bmf* gene promoter ± deletion of putative *IRE*(N-

1086 to N-1081: 5'-AGGGGG-3'), (N-997 to N-991: 5'-GAGGGGC-3') and (N-402to N-395: 5'-CCCCCGC-3') in the *Bmf* gene promoter in IRPTCs in NG or HG medium ± insulin. (**d**) The activity of 1μg of the full-length *Bmf* gene promoter with or without deletion of putative *IRE* transfected with *hnRNP F* cDNA in IRPTCs in NG medium. Values are mean ± SEM, n=3. ($^{*}p<0.05$; $^{***}p<0.005$ NS, not significant). (**e**) EMSA of putative biotinylated *IRE* (N-1093 to N-1072) with RPTC nuclear proteins with or without excess unlabeled WT *IRE* or mutated *IRE*. For supershift rabbit anti-hnRNP F or rabbit IgG was added to the reaction mixture and incubated for 30 minutes on ice before incubation with biotinylated probe. The results are representative of 3 independent experiments. SS, supershift band.

Figure 8. Schematic diagram of mechanism of insulin action on inhibition of Bmf gene transcription and tubulopathy. Insulin stimulates p44/42 MAPK signaling and hnRNP F expression. HnRNP F binds to the hnRNP F-RE (N-1086/N-1081) in the Bmf promoter to inhibit Bmf expression and subsequently prevents Bmf-induction of tubulopathy in diabetic kidney.

Physiological measurements

	Non-Tg	h*Bmf*-Tg
Blood glucose (BG, mM) (n=10)	9.8±0.8	10.16±1.12
Systolic blood pressure (SBP, mmHg) (n=10)	113.57±1.3	121.12±1.4**
Body weight (BW, g) (n=10)	34.76±1.47	33,77±1.08
Kidney weight (KW, mg) (n=10)	363.0±23.3	340.8±16.07
KW/BW (mg/g) (n=10)	10.38±0.41	10.15±0.47
Tibia length (TL, mm) (n=10)	21.75±0.33	20.80±0.3
KW/TL (mg/mm) (n=10)	16.65±0.97	16.50±0.61
GFR/BW(ml/min/g) (n=10)	7.8±0.37	9.8±0.32*
Glomerular tuft volume ($*10^3\mu m^3$) (n=6)	139.6±5.6	166.7±7.24**
Tubular luminal area (μm^2) (n=6)	47.46±2.39	48.19±3.1
RPTC volume ($*10^3\mu m^3$) (n=6)	7.74±0.36	9.63±0.4**
ACR (µg/mg) (n=13)	22.37±2.95	60.62 ±9.53***

*p <0.05, **p < 0.01, ***p < 0.001 vs Non-Tg

Table 1

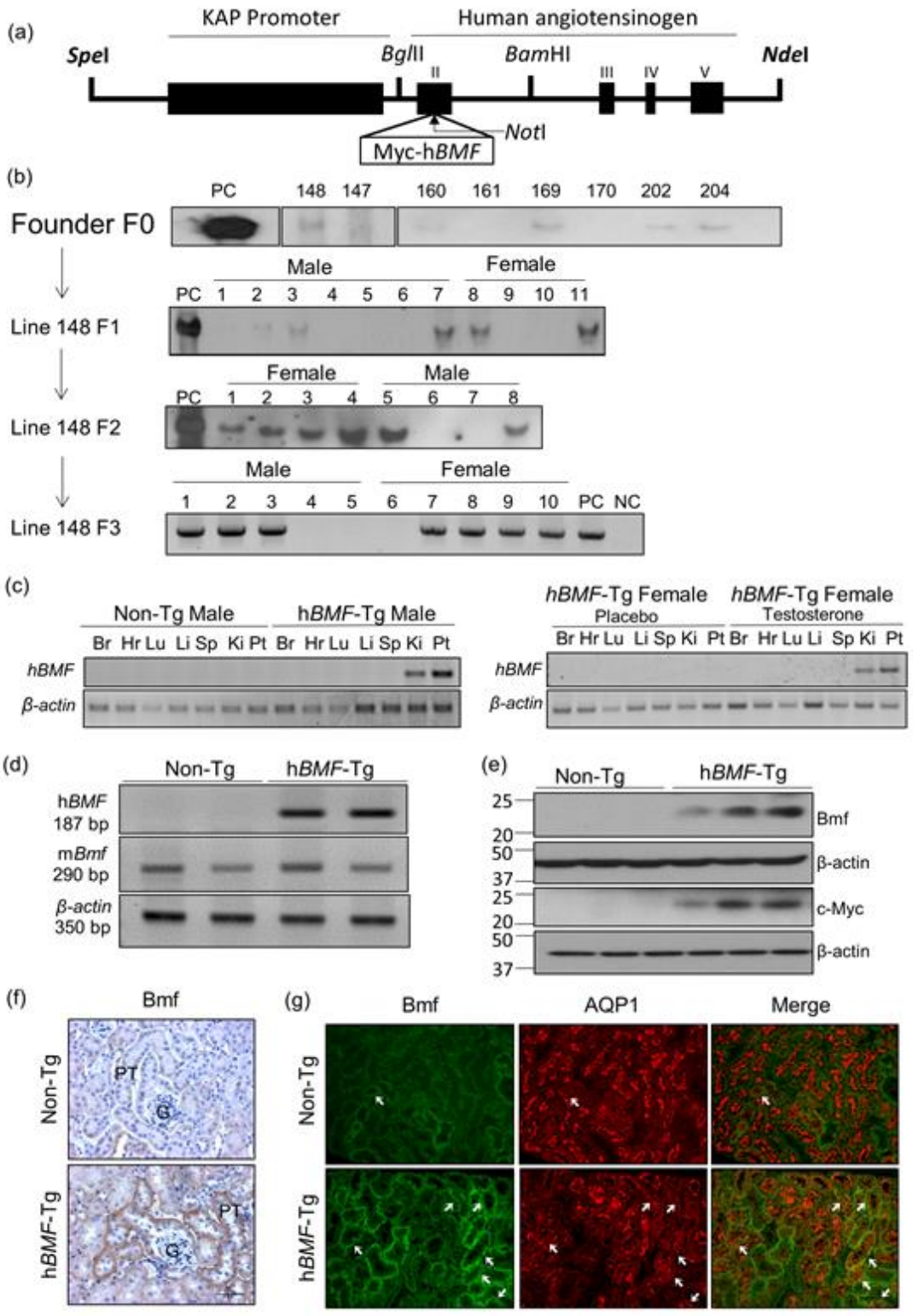
(a)
KAP Promoter
Human angiotensinogen
SpeI
BglII
BamHI
NdeI
II
III
IV
V
NotI
Myc-hBMF
(b)
PC
148 147 160 161 169 170 202 204
Founder F0
Male
Female
PC 1 2 3 4 5 6 7 8 9 10 11
Line 148 F1
Female
Male
PC 1 2 3 4 5 6 7 8
Line 148 F2
Male
Female
1 2 3 4 5 6 7 8 9 10 PC NC
Line 148 F3
(c)
Non-Tg Male
hBMF-Tg Male
Br Hr Lu Li Sp Ki Pt Br Hr Lu Li Sp Ki Pt
hBMF
β-actin
hBMF-Tg Female
Placebo
hBMF-Tg Female
Testosterone
Br Hr Lu Li Sp Ki Pt Br Hr Lu Li Sp Ki Pt
hBMF
β-actin
(d)
Non-Tg
hBMF-Tg
hBMF
187 bp
mBmf
290 bp
β-actin
350 bp
(e)
Non-Tg
hBMF-Tg
25
20
50
37
Bmf
β-actin
c-Myc
(f)
Bmf
Non-Tg
hBMF-Tg
PT
G
(g)
Bmf
AQP1
Merge
Non-Tg
hBMF-Tg

Figure 1

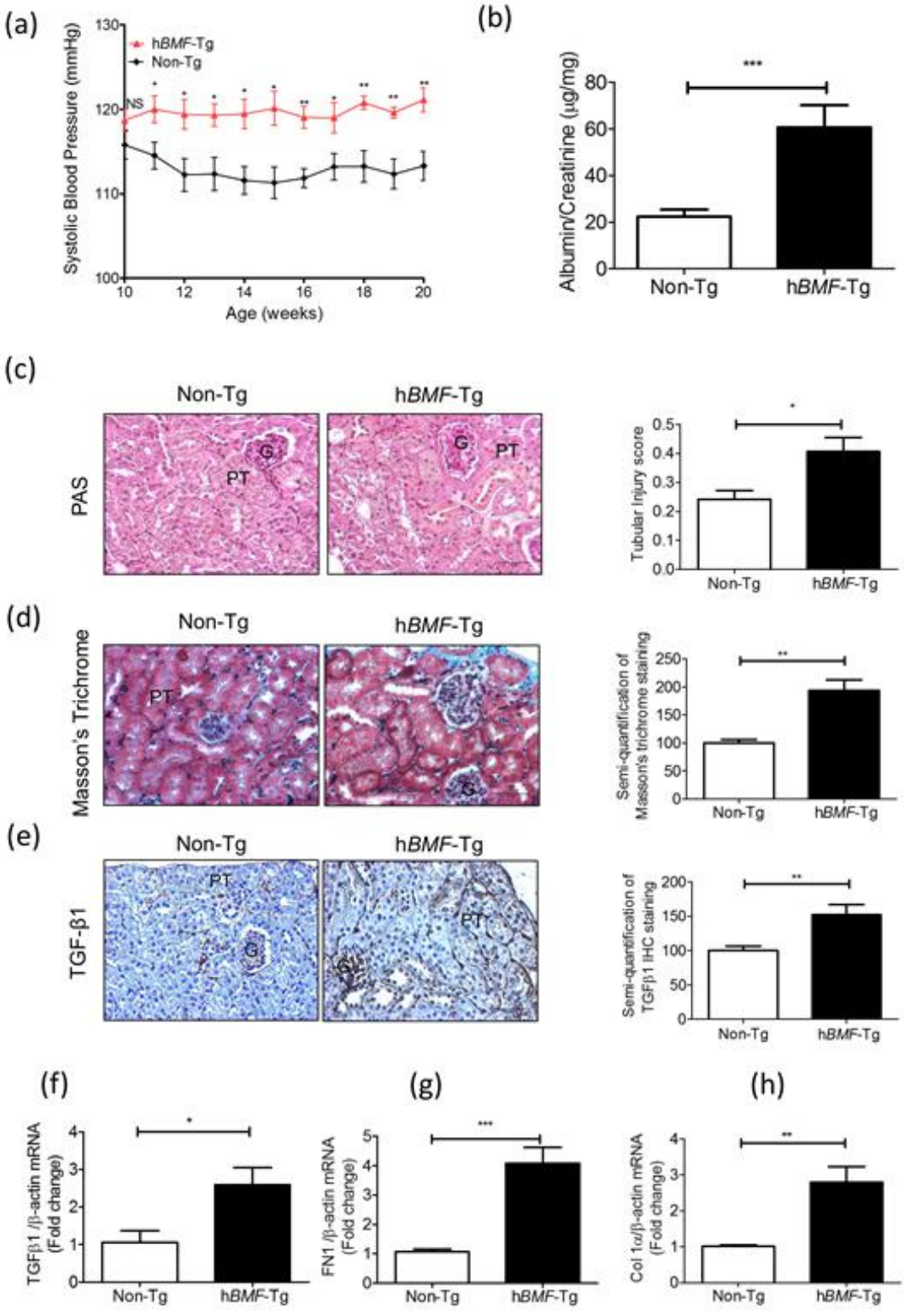
(a)
Systolic Blood Pressure (mmHg)
hBMF-Tg
Non-Tg
NS
Age (weeks)
(b)
Albumin/Creatinine (μg/mg)
Non-Tg
hBMF-Tg
(c)
Non-Tg
hBMF-Tg
PAS
G
PT
Tubular Injury score
(d)
Masson's Trichrome
Semi-quantification of Masson's trichrome staining
(e)
TGF-β1
Semi-quantification of TGFβ1 IHC staining
(f)
TGFβ1 /β-actin mRNA (Fold change)
(g)
FN1 /β-actin mRNA (Fold change)
(h)
Col 1α/β-actin mRNA (Fold change)

Figure 2

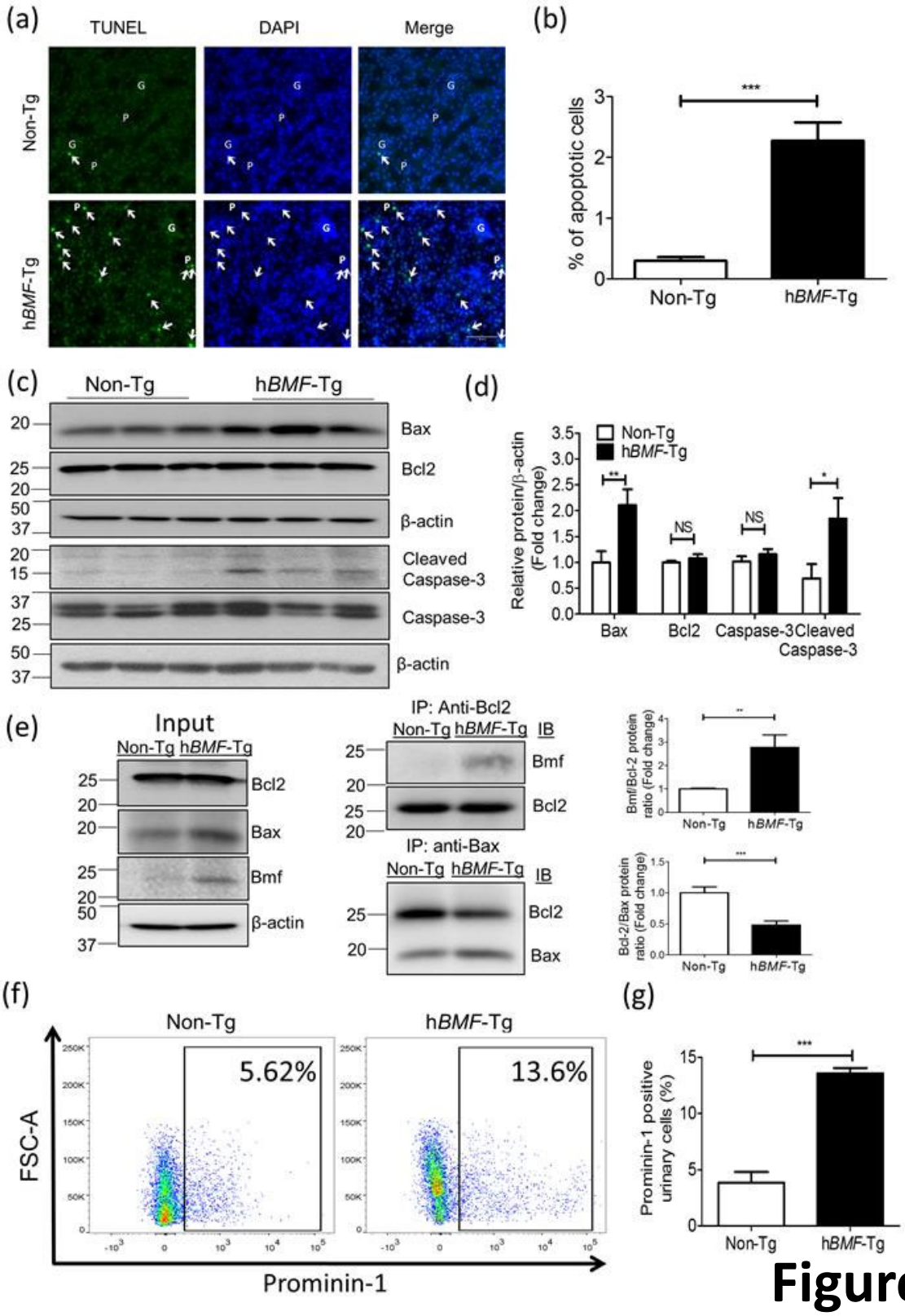
(a)
TUNEL
DAPI
Merge
Non-Tg
hBMF-Tg
(b)
% of apoptotic cells
***
Non-Tg
hBMF-Tg
(c)
Non-Tg
hBMF-Tg
Bax
Bcl2
β-actin
Cleaved Caspase-3
Caspase-3
β-actin
(d)
Relative protein/β-actin (Fold change)
Non-Tg
hBMF-Tg
NS
NS
Bax
Bcl2
Caspase-3
Cleaved Caspase-3
(e)
Input
Non-Tg hBMF-Tg
Bcl2
Bax
Bmf
β-actin
IP: Anti-Bcl2
IB
Bmf
Bcl2
IP: anti-Bax
Bcl2
Bax
Bmf/Bcl-2 protein ratio (Fold change)
Bcl-2/Bax protein ratio (Fold change)
(f)
Non-Tg
hBMF-Tg
5.62%
13.6%
FSC-A
Prominin-1
(g)
Prominin-1 positive urinary cells (%)
***

Figure 3

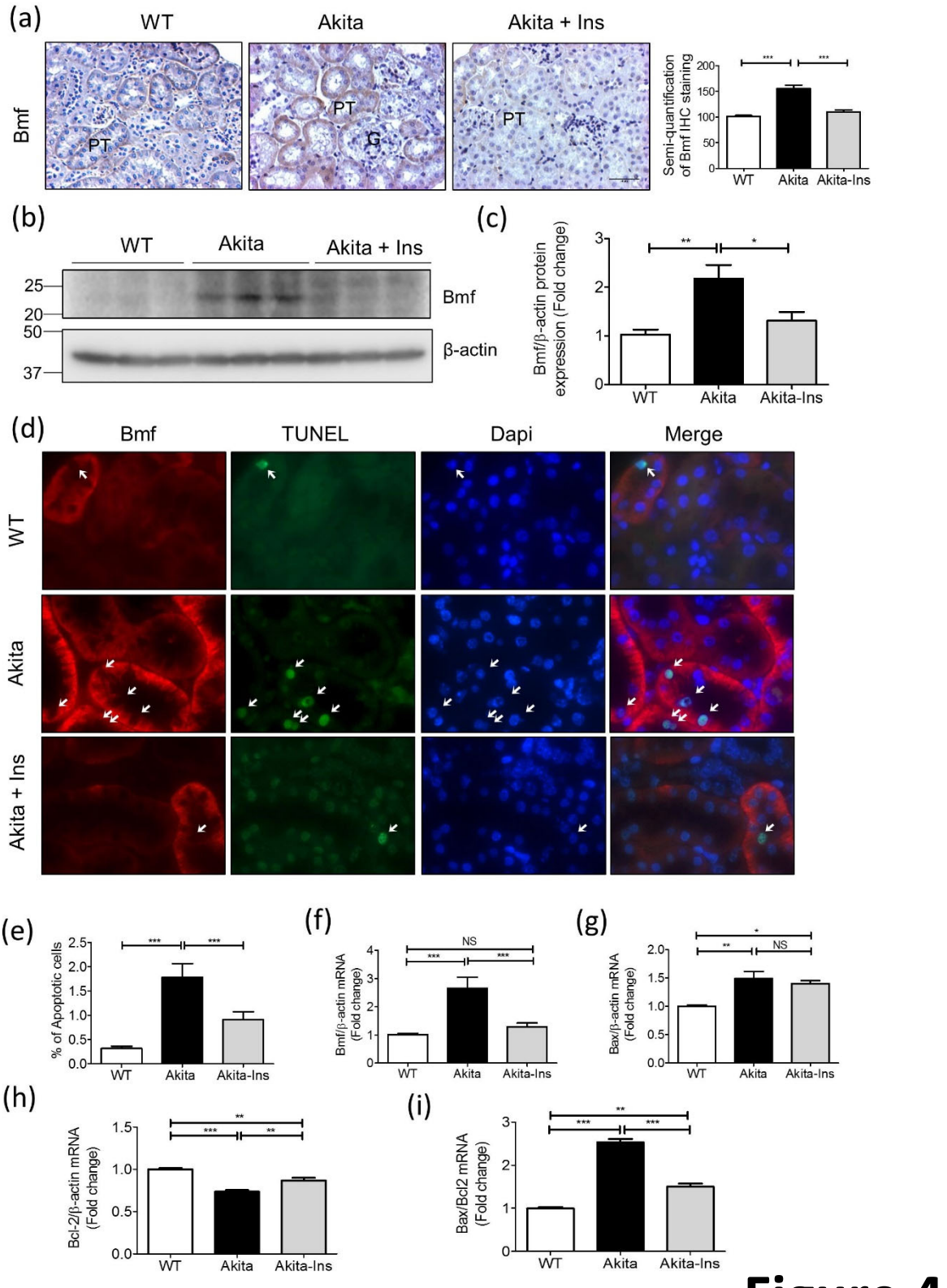
(a)
WT
Akita
Akita + Ins
Bmf
PT
G
Semi-quantification of Bmf IHC staining
WT
Akita
Akita-Ins
(b)
WT
Akita
Akita + Ins
25
20
50
37
Bmf
β-actin
(c)
Bmf/β-actin protein expression (Fold change)
(d)
Bmf
TUNEL
Dapi
Merge
WT
Akita
Akita + Ins
(e)
% of Apoptotic cells
(f)
Bmf/β-actin mRNA (Fold change)
NS
(g)
Bax/β-actin mRNA (Fold change)
(h)
Bcl-2/β-actin mRNA (Fold change)
(i)
Bax/Bcl2 mRNA (Fold change)

Figure 4

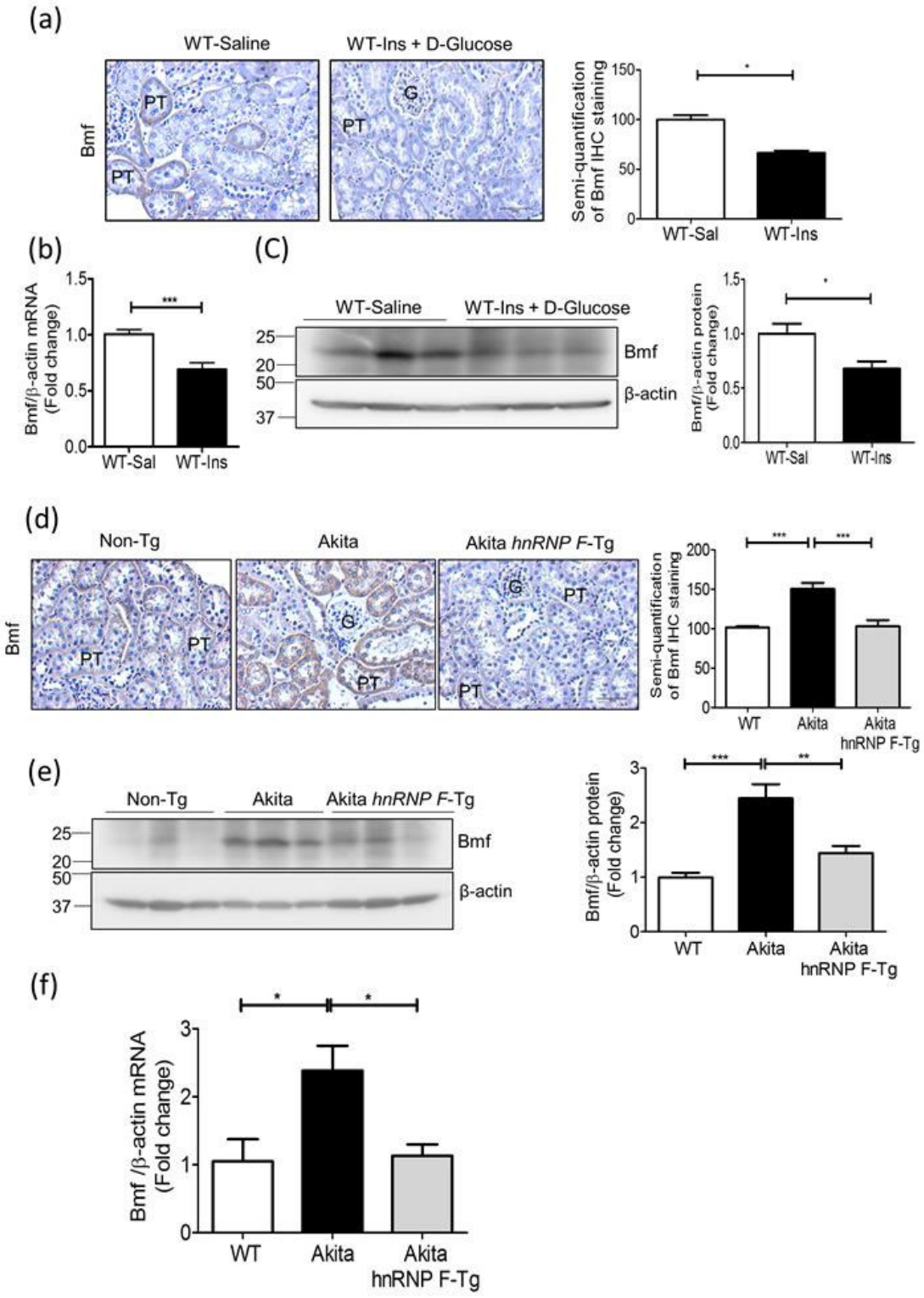
(a)
WT-Saline
WT-Ins + D-Glucose
Bmf
PT
G
Semi-quantification of Bmf IHC staining
WT-Sal
WT-Ins
(b)
Bmf/β-actin mRNA (Fold change)
(C)
WT-Saline
WT-Ins + D-Glucose
Bmf
β-actin
Bmf/β-actin protein (Fold change)
(d)
Non-Tg
Akita
Akita hnRNP F-Tg
WT
Akita hnRNP F-Tg
(e)
(f)
Bmf /β-actin mRNA (Fold change)

Figure 5

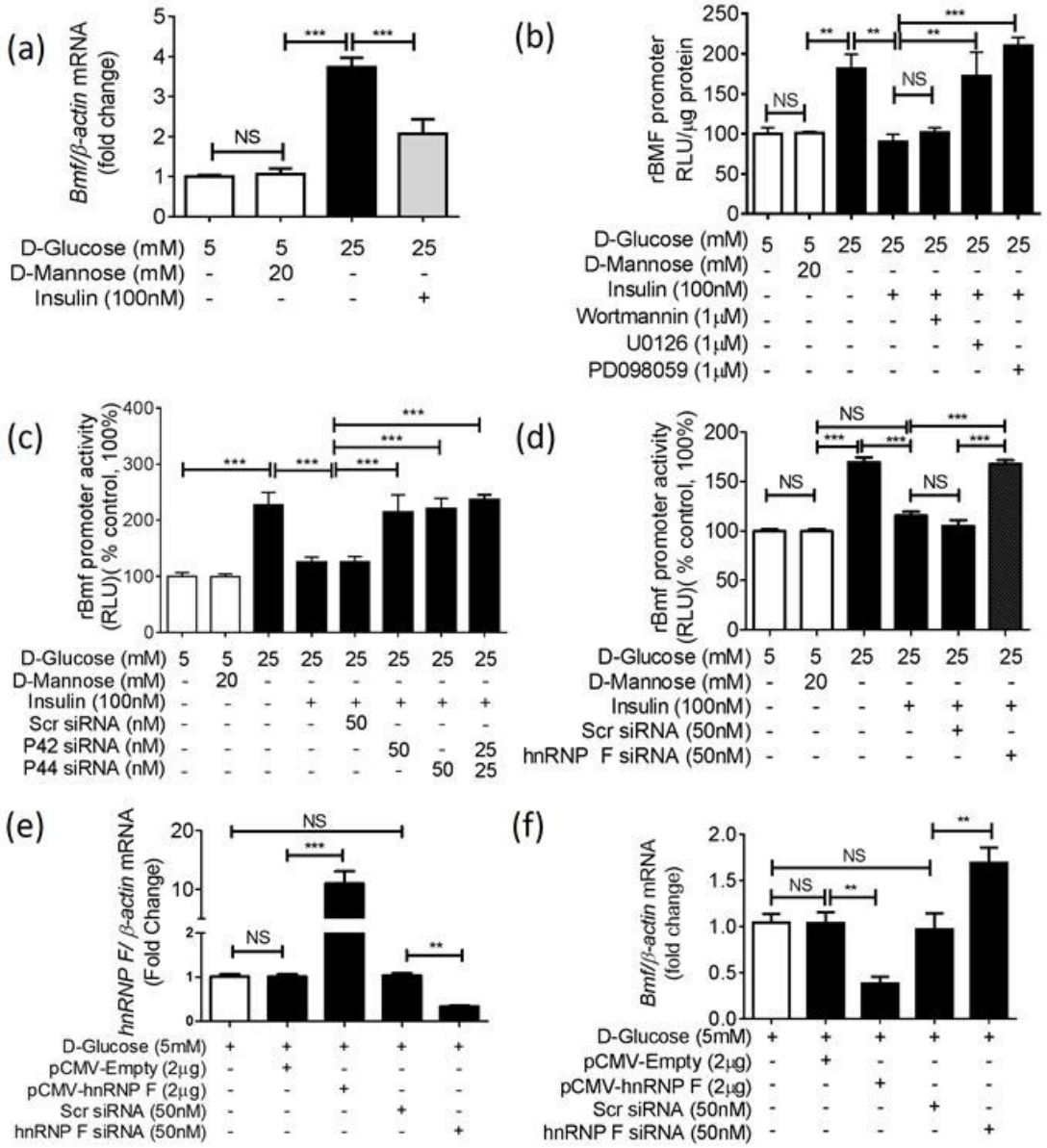
(a)
Bmf/β-actin mRNA (fold change)
NS
***
***
D-Glucose (mM) 5 5 25 25
D-Mannose (mM) - 20 - -
Insulin (100nM) - - - +
(b)
rBMF promoter RLU/μg protein
NS
**
**
**
NS
***
D-Glucose (mM) 5 5 25 25 25 25 25
D-Mannose (mM) - 20 - - - - -
Insulin (100nM) - - - + + + +
Wortmannin (1μM) - - - - + - -
U0126 (1μM) - - - - - + -
PD098059 (1μM) - - - - - - +
(c)
rBmf promoter activity (RLU)(% control, 100%)
***
***
***
***
***
***
D-Glucose (mM) 5 5 25 25 25 25 25 25
D-Mannose (mM) - 20 - - - - - -
Insulin (100nM) - - - + + + + +
Scr siRNA (nM) - - - - 50 - - -
P42 siRNA (nM) - - - - - 50 - 25
P44 siRNA (nM) - - - - - - 50 25
(d)
rBmf promoter activity (RLU)(% control, 100%)
NS
***
***
***
NS
NS
***
D-Glucose (mM) 5 5 25 25 25 25
D-Mannose (mM) - 20 - - - -
Insulin (100nM) - - - + + +
Scr siRNA (50nM) - - - - + -
hnRNP F siRNA (50nM) - - - - - +
(e)
hnRNP F/ β-actin mRNA (Fold Change)
NS
***
NS
**
D-Glucose (5mM) + + + + +
pCMV-Empty (2μg) - + - - -
pCMV-hnRNP F (2μg) - - + - -
Scr siRNA (50nM) - - - + -
hnRNP F siRNA (50nM) - - - - +
(f)
Bmf/β-actin mRNA (fold change)
NS
NS
**
**
D-Glucose (5mM) + + + + +
pCMV-Empty (2μg) - + - - -
pCMV-hnRNP F (2μg) - - + - -
Scr siRNA (50nM) - - - + -
hnRNP F siRNA (50nM) - - - - +

Figure 6

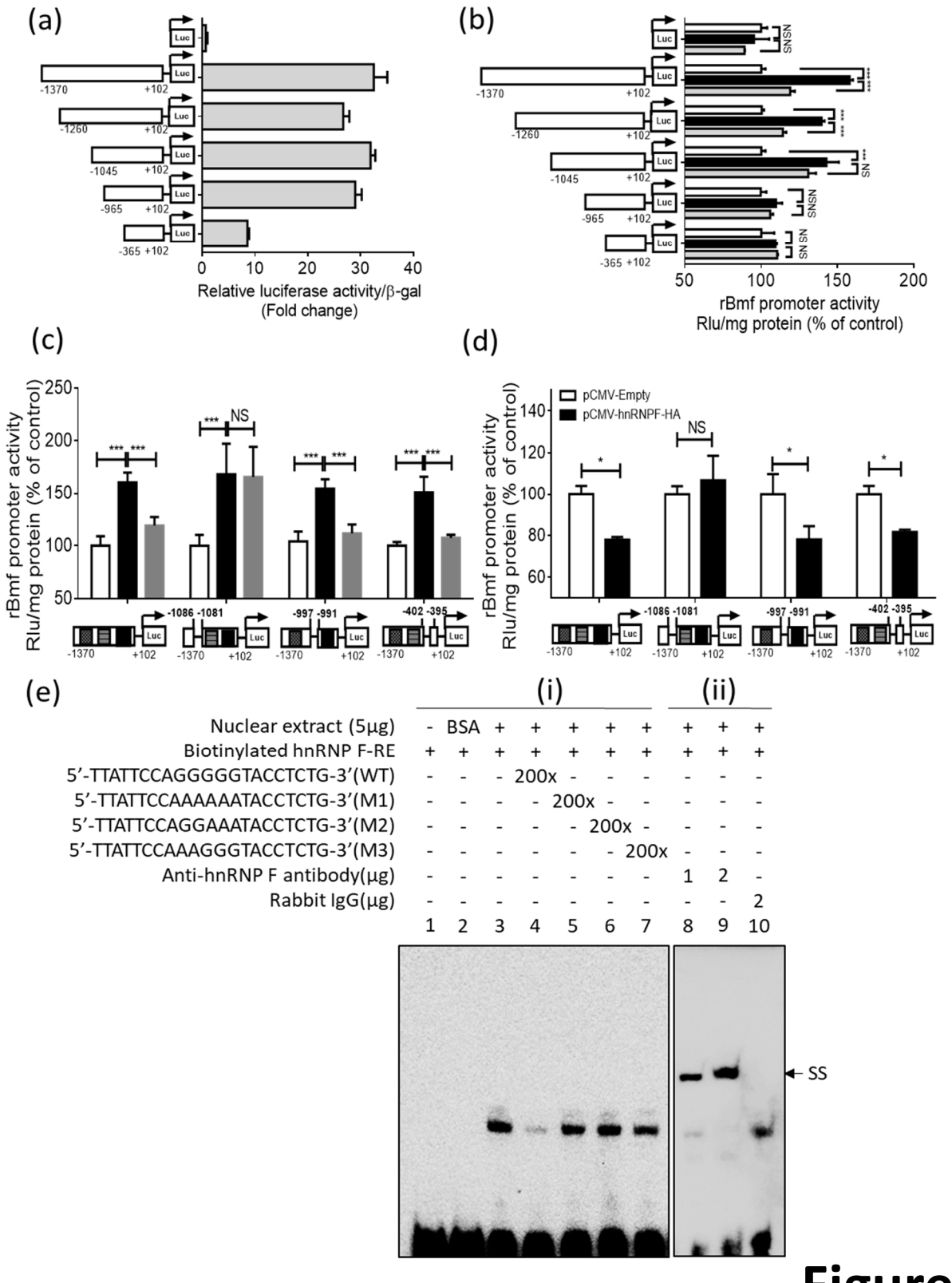
(a)
Luc
-1370 +102
-1260 +102
-1045 +102
-965 +102
-365 +102
0 10 20 30 40
Relative luciferase activity/β-gal
(Fold change)
(b)
SNSN
SN ***
50 100 150 200
rBmf promoter activity
Rlu/mg protein (% of control)
(c)
rBmf promoter activity
Rlu/mg protein (% of control)
250 200 150 100 50
NS
-1086 -1081
-997 -991
-402 -395
(d)
pCMV-Empty
pCMV-hnRNPF-HA
140 120 100 80 60
NS
(e)
(i)
(ii)
Nuclear extract (5μg) - BSA + + + + + + + +
Biotinylated hnRNP F-RE + + + + + + + + + +
5′-TTATTCCAGGGGGTACCTCTG-3′(WT) - - - 200x - - - - - -
5′-TTATTCCAAAAAATACCTCTG-3′(M1) - - - - 200x - - - - -
5′-TTATTCCAGGAAATACCTCTG-3′(M2) - - - - - 200x - - - -
5′-TTATTCCAAAGGGTACCTCTG-3′(M3) - - - - - - 200x - - -
Anti-hnRNP F antibody(μg) - - - - - - - 1 2 -
Rabbit IgG(μg) - - - - - - - - - 2
1 2 3 4 5 6 7 8 9 10
SS

Figure 7

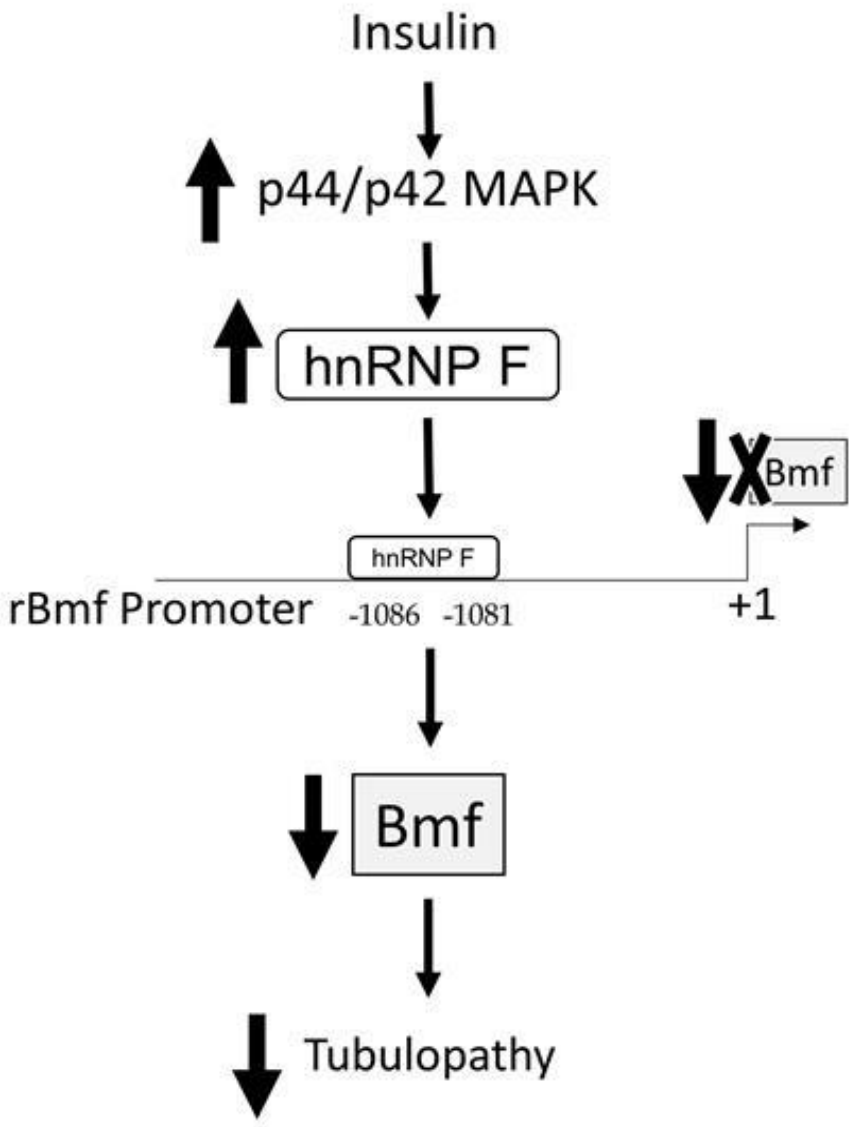
Insulin
p44/p42 MAPK
hnRNP F
Bmf
hnRNP F
rBmf Promoter
-1086
-1081
+1
Bmf
Tubulopathy

Figure 8

Supplemental Figure 1

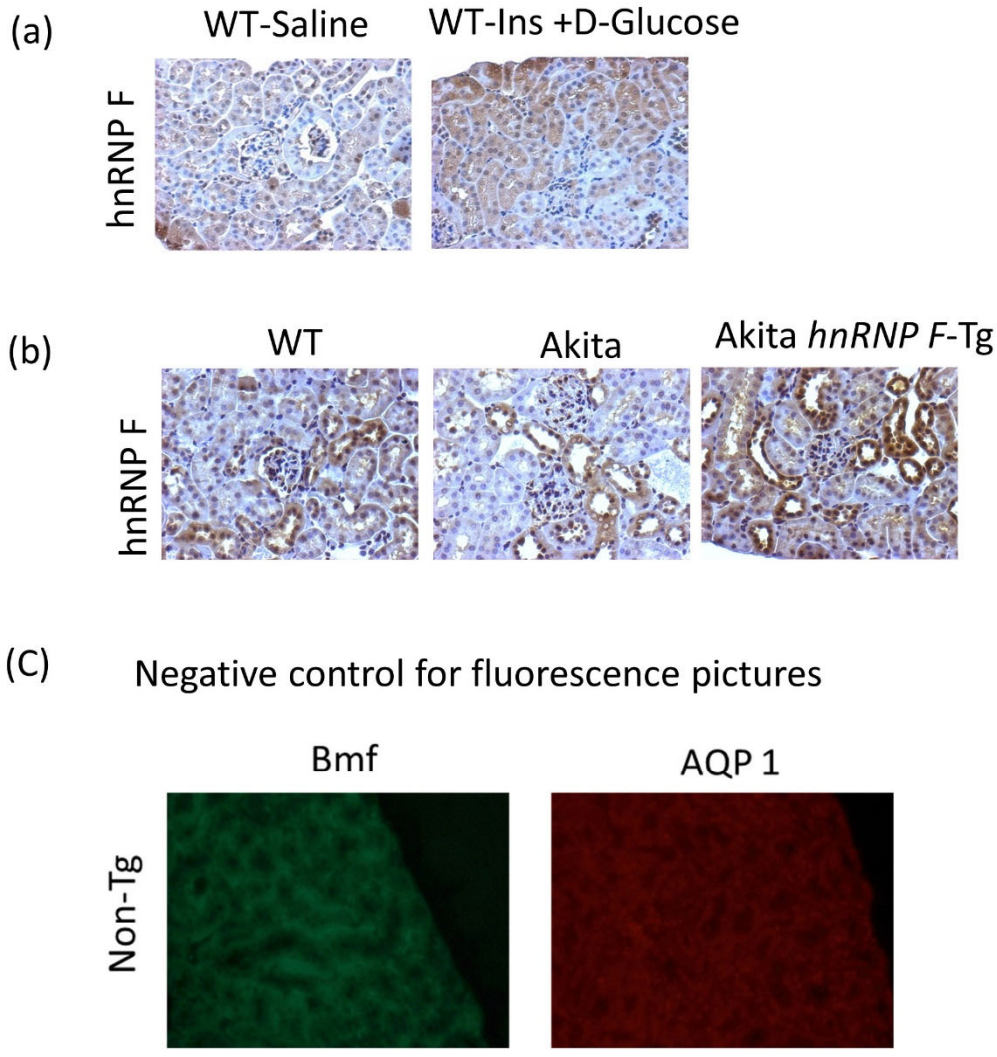

Figure S1: Immunohistochemical staining for hnRNP F levels in the RPTs from (a) WT mice after 3-h infusion with saline or insulin (ins) and (b) WT, Akita and Akita *hnRNP F*-Tg mice. (magnification X 200). (c) Negative control for fluorescence pictures in figure 1 (g) where primary antibodies were omitted from the reaction.

Supplimentary Figure 1

Antibodies

Protein Target	Name of Antibody	Manufacturer, Catalog, and/or Name of Individual Providing the Antibody	Species Raised in; Monoclonal or Polyclonal	Dilution for WB and or IHC
Bmf	Bmf antibody	N-19, sc-20181, Santa Cruz Biotechnology	Goat; polyclonal	IHC**:** 1:200
	Bmf antibody	9G10, Enzo Life Sciences	Rat; monoclonal	WB; 1:2000
	Bmf antibody	Abcam, Ab9655	Rabbit; polyclonal	IP: 1:100
HnRNP F	hnRNP F antibody	Specifically recognizing (CTARRYIGIVKQAGLER) were generated in our laboratory	Rabbit; polyclonal	WB; 1:10000 IHC; 1:200 EMSA;1-2 µg
AQP 1	AQP 1 antibody	H-55, sc-20810	Rabbit; polyclonal	WB; 1:2000
	AQP 1 antibody	1/22, sc-32737	Mouse; monoclonal	IF; 1:200
TGFβ	TGFβ antibody	Sc-146, Santa Cruz Biotechnology	Rabbit polyclonal	WB; 1:2000
Bax	Bax antibody	P-19, sc-526, Santa Cruz Biotechnology	Rabbit polyclonal	WB; 1:2000 IP; 1:100
Bcl-2	Bcl-2 antibody	C-2, SC-7382, Santa Cruz Biotechnology	Mouse; monoclonal	WB; 1:2000
	Bcl-2 antibody	D17C4, 3498S, Cell signaling	Rabbit; monoclonal	IP; 1:100
Caspase 3	Caspase 3 antibody	9662S, Cell signaling	Rabbit; polyclonal	WB; 1:2000
Cleaved caspase 3	Cleaved caspase 3 antibody	9661S (ASP175), Cell signaling	Rabbit; polyclonal	WB; 1:2000
β-Actin	β-Actin antibody	AB_476744, Sigma-Aldrich	Mouse; Monoclonal	WB; 1:20000
Prominin-1	PE-Vio-770 Prominin-1 antibody	Miltenyi Biotec, Clone: MB9-3G8	Rat; polyclonal	FACS; 1:25
c-Myc	c-Myc antibody	9E10, sc-40, Santa Cruz Biotechnology	Mouse; monoclonal	WB; 1:2000

Supplimentary Table 1

Primers and siRNA

Gene	Sequence	Species	Reference Sequence
BMF	F: CCCTTGGGGAGCAGCCCCCTG R: GCCGATGGAACTGGTCTGCAA	Mouse	NM_139258
BMF	F: GATTGTCCCCTCAGTCGGCT R: CTCGGTGCTGAAGGAACTGTC	Rat	NM_139258.2 NM_139258.3
Myc-hBMF	F: ATGGCATCAATGCAGAAGCTGATCTCAGAG R: AAGAGCTGAAGTCGGCTGAG		Detects Myc tagged human Bmf cDNA NM_001003943.1
TGF-β1	F: CCAAACTAAGGCTCGCCAGTC R: GGCACTGCTTCCCGAATGTC	Mouse	NM_011577.1
Col1α	F: ATCTCCTGGTGCTGATGGAC R: ACCTTGTTTGCCAGGTTCA	Mouse	NM_007742.3
FN1	F: GGCCTGAACCAGCCTACAG R: TGAGCTTAAAGCCAGCGTCA	Mouse	NM_010233.2
Bax	F: GTTTCATCCAGGATCGAGCAG R: CATCTTCTTCCAGATGGTGA	Mouse Rat	NM_007527.3 NM_017059.2
Bcl-2	F: CTGTGGATGACTGAGTACC R: GAGACAGCCAGGAGAAAT	Mouse Rat	NM_009741.5 NM_016993.1
hnRNP F	F: AGAGTGACCGGAGAAGCTGA R: GCTCTCCAGGCCACTGTAAG	Mouse Rat	NM_133834.2 NM_001037286.1
β-actin	F: ATGCCATCCTGCGTCTGGAC R: AGCATTTGCGGTGCACGATGG	Mouse Rat	NM_007393.3 NM_031144.2
Rat Bmf Promoter	F: AAAAAACTCGAGCCTCGTTTTCCCCCAAATCCATC F: GGCAAACTCGAGGACCCAGGTTCAATTCC F: GGCAAACTCGAGCTGACCTAAATCTACCTG F: GACCTGCTCGAGTACTTTATTC F: GCTTTCTGGAAGTCCCGCA R: AAAAAAAGCTTCTGCGGTGGGAGGTGGTG	Rat	-1370 Xho 1 -1260 Xho1 -1045 Xho1 -965 Xho1 -351 Xho1 +102 HindIII
Site directed mutagenesis primers for Rat Bmf Promoter hnRNP F binding element	F: GAGGATGCCTGATAGCTCAATACTGACCTTGCTT R: AAGCAAGGTCAGTATTGAGCTATCAGGCATCCTC F: CCTCATCCTGTTATTCCTACCTCTGCAATCTGACC R: GGTCAGATTGCAGAGGTAGGAATAACAGGATGAGG F: GACCAGCAACTCCTTTTTTTATACAAGTCGCGGCT R:AGCCGCGACTTGTATAAAAAAAGGAGTTGCTGGTC	Rat	Bmf (-1370/+102) Δ997-991 Bmf (-1370/+102) Δ1086-1081 Bmf (-1370/+102) Δ402-395
Rat Bmf promoter hnRNP F-RE probe	F: TTATTCCAGGGGGTACCTCTG R: CAGAGGTACCCCCTGGAATAA		Biotinylated probe for EMSA (-1086)
HnRNP F RE (WT)	F: TTATTCCAGGGGGTACCTCTG R: CAGAGGTACCCCCTGGAATAA		competitor
HnRNP F RE (Mut 1)	F: TTATTCCAaaaaaTACCTCTG R: CAGAGGTAttttTGGAATAA		competitor
HnRNP F RE (Mut 2)	F: TTATTCCAGGaaaTACCTCTG R: CAGAGGTAtttCCTGGAATAA		competitor
HnRNP F RE (Mut 3)	F: TTATTCCAaaGGGTACCTCTG R: CAGAGGTACCCttTGGAATAA		competitor
si hnRNP F (ID:s133896)	F: CAUGCAGCACAGAUACAUAtt R: UAUGUAUCUGUGCUGCAUGtt	Rat	siRNA

Supplimentary Table 2

Chapter 4: Discussion

The global prevalence of diabetes is on the rise. Diabetic kidney disease (DKD) or diabetic nephropathy (DN) is the most common cause of developing ESRD in diabetic patients. Hyperglycemia, hyperlipidemia, ROS generation, antioxidant deficiencies and RAS dysfunction have long been implicated in DKD. Although a lot of progress have been made in recent years, the underlying molecular mechanisms are still far from being fully understood. Hyperglycemia and RAS activation have been identified as major risk factors for DKD progression. Current available therapeutics mainly target these two arms to provide renoprotection against DKD. However, none of the drug developed to date for kidney disease have the potential to cure DKD, mainly because of the complexity of the kidney as an organ system with multiple types of cells performing different functions. Thus, this thesis is focused to offer new insights for better understanding the relationships between oxidative stress, RAS activation, tubular injury and the underlying mechanisms of insulin action to identify appropriate therapeutic targets.

In this study, data obtained by the researcher's group has shed light on the underlying molecular mechanisms to explain how enhanced ROS production in diabetes can alter intrarenal RAS activation to induce hypertension and tubular apoptosis leading to DKD. Previously, the research group have demonstrated that ROS-induced Nrf2 can enhance Agt expression which can be prevented by selective overexpression of Cat in RPTCs or using Nrf2 inhibitor trigonelline *in vivo*. In the current study a novel finding is that insulin can inhibit Nrf2 expression directly via a novel putative IRE that binds to hnRNP F/K and prevents Nrf2-induced *Agt* gene expression and subsequently, prevents systemic hypertension and kidney injury in Akita mice. Another promising finding is that in RPTCs overexpression of Bmf, a proapoptotic protein, is sufficient to induce RPTC apoptosis and renal injury. Finally, the results have demonstrated that insulin can attenuate enhanced Bmf expression in Akita mice via IRE in the Bmf promoter that binds to hnRNP F. The researchers' results cast a new light on the understanding of the events leading to DKD and offer multiple therapeutic targets including Nrf2, hnRNP F, hnRNP K and Bmf.

4.1 Genetically Modified Akita Mice Model (T1D)

The Akita mouse is a genetic model of insulin deficiency (T1D), which carries the *Ins2*$^{+/C96Y}$ mutation, an autosomal dominant single nucleotide substitution in the Ins2 gene. This mutation causes misfolding of Insulin2 which results in pancreatic β cell failure and development of hyperglycemia, as early as 4 weeks of age (343). Within 13 to 30 weeks, male Akita mice present signs of renal dysfunction, hypertension and the presence of increased oxidative stress markers in their RPTs which closely resemble the early to moderately advanced renal morphological changes in human T1D patients (383, 384). In this thesis, 12- 20 weeks old Akita mice were used. In line with previous studies by several groups including Dr. Chan's group (146, 266, 314, 344, 383, 384), increased GFR, systolic blood pressure (SBP), urinary albumin/creatinine (ACR), urinary Agt and AngII levels, and kidney weight/tibia length in Akita mice were found, as compared to in non-Akita WT littermate. Histologically, Akita mice showed increased RPTC apoptosis and tubular atrophy, tubular luminal dilatation and increased ECM in tubules and glomeruli. In gene expression, it was observed that Akita mice have increased expression of several genes including Agt, Nrf2, NQO1, HO-1 and Bmf. This was associated with marked increases in ROS generation, NADPH oxidase activity and Nox4 mRNA expression as well as diminished Cat expression and activity in the RPTCs of Akita mice. Thus, Akita mice serve as an excellent model to study early DN progression.

Genetically modified T1D model of Akita mice provides several advantages. Consistent with previous observations of Dr. Chan's group with STZ induced T1D mice model, Agt mRNA expression was upregulated in Akita mice model (266). STZ damages pancreatic β cells, resulting in decreased insulin production and increased hyperglycemia. However, STZ being a cytotoxic drug, had several hepatotoxic and nephrotoxic side effects (385-389). It was responsible for renal proximal tubular damage and promote acidosis (388). High dose of STZ was associated with nitrosourea toxicity (cause type B lactic acidosis) while multiple lower doses elicited immune and inflammatory reactions. Besides, mice were more resistant to STZ-induced diabetes than rats (389). Using Akita mice model, toxicity and complications associated with STZ were avoided. Moreover, Akita mice have more substantial hyperglycemia and higher blood pressure than STZ induced mice, which is characteristic of humans with DN.

The underlying mechanisms of elevated blood pressure in Akita mice are still unknown. The present study indicates that activation of intrarenal RAS by oxidative stress may lead to the development of hypertension and renal injury. This hypothesis is supported by the present findings of significantly elevated Agt expression in RPTCs, and urinary Agt and AngII levels in Akita mice. Cat overexpression or insulin treatment in Akita mice normalised these changes (176, 267). These observations were consistent with the clinical findings of elevated intrarenal Agt gene expression in the diabetic and hypertensive patients (188, 390-393). Agt was converted into AngII, which then acts via AT_1R to induce hypertension by various pathways described in Table 1-5 including increased sodium reabsorption through direct stimulation of Na^+-K^+-ATPase and NHE-3 transporters in RPTs (394, 395), enhanced ROS production by NADPH oxidases, or by direct vasoconstriction of glomerular efferent arterioles. Our observation of increased GFR in Akita mice supported this notion.

Another possibility that downregulation of Ace2 gene expression and consequent higher AngII/Ang1-7 ratio facilitating hypertension development in Akita mice has received considerable attention (396, 397). Indeed, another study by Dr. Chan's group demonstrated that Akita mice have decreased Ace2 and urinary Ang1-7 levels, while increasing ACE, and urinary Agt and AngII levels when compared to non-Akita WT mice. Agt-Tg mice have markedly elevated ACE and decreased Ace2 expression in the kidney. Overexpression of Cat in Agt-Tg mice or in Akita mice could reverse these changes (146, 334). Higher ACE and lower ACE2 level were also observed in the kidneys of diabetic and hypertensive patients compared to normal human kidney (398, 399). Furthermore, AngII was found to increase ACE and downregulate Ace2 in HK cells in vitro (398). Taken together these observations support the idea that intrarenal RAS activation upregulates ACE and downregulates Ace2 via increased oxidative stress in RPTCs which contributes to the development of hypertension.

Agt-Tg mice overexpressing Agt in the RPTCs develop systemic hypertension. Even though treatment with apocynin did not decrease the blood pressure in Agt-Tg mice (400), overexpression of Cat in Agt-Tg mice normalised systolic blood pressure (334). Cat overexpression probably lessens oxidative stress regardless of its source, whereas apocynin acts only on NADPH oxidase dependent ROS production. Similar reduction of hypertension is

observed in Akita-Cat-Tg mice, indicating Cat-induced H_2O_2 degradation may be effective in blood pressure reduction (176). However, no hypotension was observed in Cat-Tg mice, and Cat-deficient mice did not show hypertension, indicating intrarenal H_2O_2 may not be related to blood pressure in normal physiological conditions because Cat effectively converts H_2O_2 to water and O_2.

4.2 Antioxidant Therapies for DKD

Excessive oxidative stress can be countered by lowering ROS in two different approaches – either by direct scavenging (SODs, Catalase, GSH) or reducing their production at the source (Nox inhibitors). Although antioxidant therapies have shown to be effective against diabetic complications in animal models, including attenuation of proteinuria, oxidative stress and kidney injury, growing clinical evidence have been mostly ineffective and disappointing.

Three large clinical studies, HOPE (Heart Outcomes Prevention Evaluation) (401), GISSI (Italian group for the study of the survival of myocardial infarction) (135) and the Physician's Health Study II (132), did not find any benefit after administration of vitamins E and C. As opposed to expectation, HOPE and GISSI reported that vitamin E promoted the risk of developing heart failure. AST-120A, an orally administered spherical carbon adsorbent that can adsorb various small molecule uremic toxins with anti-oxidative properties, failed to show any beneficiary effect in two placebo-controlled global trials (402, 403). Recent meta-analysis of 26 studies also failed to show any benefit of antioxidant treatments on cardiovascular disease (CVD), cancer or mortality in healthy individuals (404). The underlying challenge of antioxidant therapies might be that the effects of antioxidants examined to date are insufficient, possibly due to the fact that they provide a limited anti-oxidative potential(405). Undoubtedly, a new novel therapeutic approach is needed to counter diabetic complications in multiple levels. In this background Keap1-Nrf2 system has drawn special attention recently for its anti-oxidative properties.

4.3 Effect of Catalase Overexpression in Diabetic Mice.

In cells, cytoprotective antioxidants such as superoxide dismutase (SOD) convert harmful superoxide into hydrogen peroxide (H_2O_2). Catalase and GST can convert H_2O_2 to

water and oxygen to prevent tissue injury by oxidative stress. ROS induces Nrf2, which is reported to activate the expression of many genes including antioxidants and phase 2 detoxifying enzymes to boost antioxidant defense system (406).

Previously, Dr. Chan's group crossed RPTC specific Cat-Tg mice with Akita mice to elucidate whether overexpressing Cat in RPTC can reverse the oxidative stress-induced pathological changes that occur in Akita mice, including hypertension and kidney injury. As expected, under normal physiological conditions, selective overexpression of Cat in RPTCs did not change any physiological or histological parameters in comparison to non-Tg littermate. However, when overexpressed in Akita mice, Cat attenuated but did not normalise most of the physiological and histological changes that have been observed in Akita mice. Although Cat overexpression did not reduce blood glucose levels, it successfully attenuated SBP, GFR; urinary ACR, Agt and AngII levels; kidney and heart weight in comparison to Akita mice. Moreover, catalase overexpression increases catalase expression and activity while attenuating ROS generation, NADPH oxidase activity and Nox4 expression in Akita mice. In accordance with several studies including the present, these evidences further confirm that hyperglycemia-induced oxidative stress was the major mediator of renal pathologies observed in Akita mice (146, 384).

Ho YS *et al.* reported that catalase deficient mice develop normally but show differential sensitivity to oxidant tissue injury (407). Kang YJ *et al.* reported Tg mice overexpressing catalase in heart protected against doxorubicin-induced cardiotoxicity (408). However, little is known about whether overexpression of Cat in the RPTC could protect against hyperglycemia-induced renal injury. The finding confirms the protective effect of Cat in the kidney against oxidative stress-induced renal injury in Akita mice. These are also in line with observations that Cat deficiency renders kidneys more vulnerable to oxidative stress (409).

Cat overexpression in RPTCs prevents hypertension, tubulointerstitial fibrosis and RPTC apoptosis in nondiabetic AGT/Cat-Tg or diabetic Cat-Tg mice (146, 310, 334), as well as supresses Agt, Nrf2 and HO-1 mRNA and protein expression, Nrf2 nuclear translocation and Nrf2 stimulation of Agt gene expression in Akita mice (176). These results provide evidence that increased ROS generation can directly upregulate Agt via Nrf2, thereby promoting

hypertension by the above described pathways in Akita mice. These findings are consistent with report by Ungvari Z *et al.* that hyperglycemia induces Nrf2 expression and its target genes, such as NQO1 in endothelial cells (410).

4.4 Nrf2 Activation: The Double-Edged Sword

Several signaling pathways, including those involved in Nrf2 transcription factor were activated to counter accumulating ROS and electrophiles. Exposure to pharmacological activators, such as oltipraz or bardoxolone methyl (CDDO-Im) or oxidative stress, triggers Nrf2 to translocate to the nucleus, where it heterodimerizes with sMAF proteins to initiate the transcription of antioxidant response element (ARE)–containing target genes to mitigate ROS pathways for maintaining homeostasis. Functional AREs are localised in upstream promoter regions of various genes that encode antioxidants, detoxification enzymes, and in genes involved in a multitude of cellular processes, including redox regulation, protein homeostasis, DNA repair, carbohydrate and lipid metabolism, iron homeostasis, transcriptional regulation, and mitochondrial function (406, 411, 412). The best known function of Nrf2 is to maintain redox homeostasis, mainly via the synthesis and redox cycling of glutathione (GSH) and thiol-based antioxidant enzymes including GCLC, GCLM, GSTs, GPX2, GPX4, TXN1 (412). We reported that Nrf2 can regulate major components of RAS system including Agt, Ace2, MasR (175, 176). The variety of Nrf2 targets indicates the vital role of Nrf2 in facilitating cellular function.

Consistently, it has been observed that high glucose (HG), H_2O_2 and Oltipraz could activate Nrf2 and its target gene such as HO-1, as well as Agt. In vivo, the data indicates higher Nrf2 and HO-1 expression in Akita mice (176). Contrary to expectations, Han *et al.* demonstrated that primary RPTCs treated with HG and H_2O_2, results in a decrease in the activity of Cat and glutathione. Treatment with AGEs inhibitor or antioxidant such as rotenone and apocynin was able to restore Cat activity (413). Cat activity was consistently found to be decreased in the liver and kidneys but elevated in heart and brain of diabetic rats (414). Osorio H *et al.* reported a decreased Cat activity in cortex and medulla from STZ-induced diabetic rats (415). Interestingly, consistent with other reports that Cat activity and expression were attenuated in diabetic rats (416), Dr. Chan's group observed that significantly decreased catalase

expression and activity but not mRNA expression, in RPTCs form Akita mice (16 and 20 weeks) in comparison to WT mice. In addition, no significant change in Cat expression or activity were found in RPTCs of younger Akita mice (4 weeks). This led the researchers to speculate that the lower Cat expression and activity are due to exhaustion of the scavenging system.

The precise mechanisms of how hyperglycemia upregulates Nrf2 and Agt expression are incompletely understood. One possibility is that ROS generation leads to the modification of reactive cysteines (Cys-151) in keap1, promoting Nrf2 dissociation from keap1 and subsequent translocation into the nucleus, where it can bind to Nrf2-binding sequences at the Agt gene promoter region and increasing Agt gene expression. Indeed, data from Dr. Chan's group with *in vitro* studies in rat RPTCs confirm that HG, H_2O_2, oltipraz and transient transfection of Nrf2 cDNA could stimulate Nrf2 and Agt expression. These can be reversed by pharmacological or genetic knockdown of Nrf2 with trigonelline or Nrf2 siRNA, respectively (176, 267). This results can be explained by the presence of Nrf2-REs in both Nrf2 (352) and Agt (417) gene promoters. Consistently, deletion of putative distal Nrf2-RE and proximal Nrf2-RE completely abolished the stimulatory effect of oltipraz on Agt gene transcription. All these data support the hypothesis that Nrf2 stimulates Agt gene transcription. Further support for this hypothesis came from the *in vivo* studies. administration of oltipraz in WT mice, stimulated Nrf2, Agt and HO-1 gene expression which could be reversed by co-administration of trigonelline in the kidney RPTCs. Moreover, Dr. Chan's group reported that oltipraz stimulated Nrf2 but not Agt expression in the liver of WT mice (176). This suggests a tissue specific Nrf2 regulation of Agt gene expression.

Several basic and pre-clinical research reported the Nrf2-Keap1 signaling pathway as beneficial and protective against diabetic nephropathy. Genetic Nrf2 deletion in STZ-induced diabetic mice was reported to worsen inflammation, oxidative stress and nephropathy (322, 418, 419). Yamamoto's group developed $Keap1^{flox/-}$ mice, which have constitutively higher levels of Nrf2, markedly supressed onset of diabetes when crossed with *db/db* mice, improving both insulin secretion and insulin resistance. $Keap1^{flox/-}$ mice havea also been reported to prevent high fat diet induced diabetes (420). Nrf2 activators, such as sulforaphane or cinnamic aldehyde reduces albuminuria, oxidative damage and preserve renal function in STZ-induced diabetic

mice, indicating Nrf2 as a potential therapeutic target in DN (323). Oltipraz and curcumin improved insulin sensitivity and glucose tolerance in high fat diet induced obesity model (421, 422). CDDO-Im and CDDO-Me (bardoxolone methyl (BM) analogue), have been reported to improve glucose tolerance, insulin sensitivity lower plasma triglycerides and free fatty acid levels and decrease hepatic lipid accumulation in both high-fat diet induced and genetic models of obesity (420, 423, 424). Recently, Yamamoto's group observed that CDDO-Im administration in early phase of renal ischemia reperfusion injury (IRI) in mice, prevents tubular damage progression (406).

On the contrary, studies with Lep$^{ob/ob}$-Keap1-knockdown (KD) mice and Keap1 KD mice on high fat diet showed enhanced diabetic phenotype with worsened insulin resistance and glucose tolerance as well as increased markers of metabolic syndrome (425, 426). Akita-Nrf2 KO mice or pharmacological inhibition of Nrf2 in Akita mice has been reported to attenuate hypertension, renal injury, tubulointerstitial fibrosis, and the urinary ACR, compared to in WT mice. Moreover, loss of Nrf2 in Akita mice resulted in increased RPTC Ace2 and MasR expression, urinary Ang 1-7 levels, and decreased expression of Agt, ACE, and profibrotic genes (175). These contradictory results indicated that dietary and genetic factors regulating Nrf2 may affect the onset and progression of diabetes differently (427). Zoja *et al.* used BM analogue RTA 405 in Zucker diabetic fatty (ZDF) rats and reported that BM is associated with increased albuminuria, blood pressure, weight loss, liver toxicity and increased mortality (315). Recent studies with lower doses of dh404 (BM analogue) in rodents showed a renoprotective effect whereas higher doses were associated with worsening proteinuria and renal dysfunction (312, 428). However, a study with RTA 405 and dh404 in ZDF rats, sponsored by Reata Pharmaceuticals, reported heightened urinary albumin/creatinine ratio, but no adverse effects in the liver. Although they found that these analogues were well tolerated without adverse effects, they failed to show their protective effects (429). These data raise serious concerns on the use of Nrf2 activators in type 2 diabetic nephropathy.

Clinical trials of BM for kidney disease- BEAM and BEACON studies: BM was thought to be a potential therapeutic target for CKD and diabetic individuals due to the observation that BM treatment can increase eGFR in cancer patients (430). This encouraging

observation led to the phase IIa clinical trial to evaluate the safety and renoprotective efficacy of BM in T2D and stage 3b-4 CKD patients (431). Data from this short-term study (8 weeks) showed increased estimated GFR (eGFR) and creatinine clearance while serum creatinine and blood urea nitrogen were both decreased without any serious adverse effects. These findings were verified in a large phase IIb trial known as BEAM study with 227 patients with moderate to severe CKD for 52 weeks. BM treatment increased eGFR in a dose-dependent manner in patients at 24 weeks, with persistence up to 52 weeks. Interestingly, a paradoxical increase in albuminuria, weight loss and increased blood pressure was reported in some patients (432). These results motivated de Zeeuw *et al.* to conduct large scale phase III clinical trial with 2185 patients from different countries with stage 4 CKD and T2D (known as BEACON study). Just after 9 months BEACON trial was terminated because BM treatment did not reduce the risk of ESRD but was associated with increased risk of heart failure, and mortality. In fact, investigators observed significantly increased blood pressure, urinary albumin-to-creatinine ratio (ACR) and body weight without favourable effects on the eGFR in BM treated group which might be responsible for the higher risk of cardiovascular disease and mortality (433).

Finally, after the BEACON trial was terminated, *post hoc* analyses suggested that the adverse effects, including increased heart failure, in the treatment group was not due to direct BM toxicity but due to fluid overload and it might be mediated through the endothelin 1 (ET-1) pathway (355). Preclinical data suggested that BM administration was associated with a decrease in ET-1 secretion and ET_A receptor expression. It was argued that acute modulation of endothelin signaling pathway in the stage 4 CKD patient population may have promoted acute sodium and water retention, resulting in increased blood pressure and fluid overload (355). Moreover, two major risk factors were identified as predictors of fluid overload events: elevated baseline B-type natriuretic peptide (BNP) and prior hospitalization for heart failure (356).

Although this analysis provides a valuable hypothesis, the following points raise certain doubts: firstly, the endothelin pathway in heart had a different function with regards to the kidney as, in the heart, ET-1 promotes cardiac hypertrophy and heart failure via activating ET_A receptor. Suppression of ET_A receptor should therefore protect from heart failure (434). Secondly, BM in BEACON study increases albuminuria and worsens blood pressure, while

selective ET_A antagonists are expected to do the reverse, as found in ASCEND trial (358). Thirdly, without important measurements from BEACON study, such as urinary ET-1 levels, evidence comes from *in vitro* and animal studies which might not be the same as human CKD patients.

These conflicting results of Nrf2 activation, and failed BEACON trial suggest that Nrf2 over-activation may not always be beneficial in diabetic patients. Moreover, a recent study reported that the Nrf2-Keap1 pathway regulates both mitochondrial and cytosolic ROS production through NADPH oxidase (435). Another study with unilateral ureter obstruction in Nrf2-deficient mice suggested that Nrf2 dependent inflammasome activation can contribute to the pathogenesis of kidney via infiltration of M1 macrophages (436). Furthermore, Suzuki *et al.* created tubular specific keap1-deficient mice and observed that hyperactivation of Nrf2 in developing kidney causes nephrogenic diabetes insipidus and hydronephrosis, but not in adulthood (437).

Due to these paradoxical observations, Dr. Chan's group investigated the relationship between Nrf2 in hypertension and nephropathy development. It was demonstrated for the first time that ROS induced Nrf2 activation can promote Agt activation, and thus, RAS activation, leading to hypertension and renal injury (175, 176). Hence, taken together, these observations strongly indicate the possible dual role of Nrf2 activation in the diabetic kidney, with stimulation of both protective antioxidants and pathogenic hypertensinogenic genes such as Agt, and inflammasome activation. Furthermore, timing (412, 437), length and the level of Nrf2 activation (312, 428), as well as careful evaluation of risk factors (356) in individual patient must be considered for further trials.

Based on detailed analysis and excluding risk factors mentioned in BEACON study, a phase 2 trial for BM (TSUBAKI; NCT02316821) with 120 patients having T2D and CKD (stage G3-G4) was initiated in Japan in 2015. No cardiovascular events were observed including heart failure for 16 weeks of treatment after appropriate patient selection and close monitoring. eGFR was improved and there was no sign of body fluid retention in treated patients (438). BM is currently being tested in a phase 2/3 trial (CARDINAL; NCT03019185) in patients with CKD due to Alport syndrome, a phase 3 trial (AYAME; NCT03550443) in patients with CKD (stage

G3-G4) in Japan and another phase 2 trial (PHOENIX; NCT03366337) for patients with autosomal dominant polycystic kidney disease. Preliminary results from CARDINAL trials indicates improved eGFR in the patients (438).

Although several Nrf2 activator have advanced to clinical trials for the treatment of various pathologies, only dimethyl fumarate (TECFIDERA™) has been approved by FDA for clinical use to treat multiple sclerosis, while there is no specific Nrf2 inhibitors for clinical use. To overcome the "dark side" of Nrf2 there is a need to develop targeted Nrf2 inhibitors to help minimize the off-target effects when prolonged or uncontrolled activation of Nrf2 which causes tissue damage. With the recent discoveries of Keap1 independent regulatory pathways of Nrf2 have opened new possibilities for the development of safe and specific therapeutics (412). Rojo de la Vega *et al*. discussed several areas of opportunity to develop targeted Nrf2 inhibitors including transcriptional down-regulators of Nrf2 (439). In this thesis, we have identified hnRNP F/K as transcriptional inhibitor of Nrf2 which might be translated beyond diabetes and provide protection against multiple pathological conditions. The present study suggests that there is a role for Nrf2 inhibitors in clinical medicine but require further investigation on its safety and long term use (440).

4.5 Akita Mice Treated with Insulin

In the first part of this study, Akita mice were treated with insulin to investigate whether insulin could directly downregulate Nrf2 gene transcription and prevent Nrf2 stimulation of Agt gene expression via hnRNP F/K, and subsequently protect against the development of hypertension and renal injury in Akita mice. Here, a novel inhibitory mechanism of insulin was identified: it could inhibit renal Nrf2 gene transcription through a novel IRE sequence in the Nrf2 promoter, independent of its glucose lowering effects. Our observations suggested that hnRNP F/K play a critical role in modulating oxidative stress and RAS activation.

To date, intensive insulin therapy is the most effective treatment for preventing the progression of nephropathy in T1D, though the underlying mechanisms remain unclear (18, 301, 338). Most patients in the US with T1D fail to achieve hemoglobin $A1_C$ targets (441). Moreover, insulin treatment increases the risk of hypoglycemia, obesity, inflammation-related pain and

metabolic syndrome (442). Therefore, novel targets or agents that will complement insulin action and reduce adverse effects are urgently needed (443). In this study, we have identified and provided evidence that hnRNP F and K might be a potential therapeutic target.

Previously, it has been demonstrated by Dr. Chan's group that insulin prevents hypertension and renal injury by inhibiting Agt transcription via hnRNP F/K upregulation in Akita mice (266). Consistently, in this study it was found that, in addition to lowering blood glucose, implanting insulin in 12 weeks old Akita mice for 4 weeks could increase body weight and normalise SBP, kidney weight/tibia length, ACR, GFR, urinary Agt and AngII levels in comparison to Akita mice. Histologically, insulin administration could attenuate renal damages observed in Akita mice, such as tubular cell atrophy, tubular lumen dilation, and accumulation of ECM in glomeruli and tubules. These data indicated the effect of insulin treatment on preventing tubulointerstitial fibrosis in Akita mice. Moreover, insulin treatment in Akita mice attenuated ROS generation, NADPH oxidase activity and Nox4 expression, while it restored catalase expression and activity compared to Akita mice. In line with previous findings, Agt expression was normalised by insulin treatment in Akita mice. Furthermore, for the first time, it was reported that insulin administration in Akita mice could decrease Nrf2 expression and its target gene HO-1 expression, as well as inhibit nuclear accumulation of Nrf2. These data demonstrated that insulin could prevent hypertension via the inhibition of intrarenal Nrf2 and Agt expression and RAS activation.

Interestingly, it was observed that implanting insulin in 20 weeks-old Akita mice for 4 weeks could also increase body weight and attenuate blood glucose, SBP, kidney weight/tibia length ratio but not ACR. Moreover, insulin treatment decreased Nrf2, Agt expression and stimulated p44/42 MAPK phosphorylation in RPTs of Akita mice at 24 weeks. The findings were consistent with those of Lizotte *et al.* who reported that insulin treatment in 4-5-months old Akita mice for 2 months increases body weight, and effectively lowers blood glucose but not the ACR (344). However, in contrast to our study in 16 weeks-old Akita mice, they did not observe an improvement in GFR or in renal fibrosis markers in 7 months old mice implanted with insulin. Furthermore, they reported more podocyte foot process effacement and loss. They explained that it might be due to glycemic memory and irreversible progression of DN. In the

current study, it was found that up to 24 weeks Aki ta mice responded to insulin signaling in RPTs. However, whether insulin is effective even in older Akita mice to reverse histopathological factors, remains to be investigated.

4.6 Insulin Signaling and Nrf2

To investigate the underlying signaling pathway of insulin action on Nrf2, immortalised rat RPTC cells were used *in vitro*. Consistent with previous findings (266, 347), it was observed that HG could increase Nrf2 and Agt promoter activity and decreases hnRNP F and hnRNP K promoter activity. Insulin could reverse these changes in the presence of HG. Using pharmacological inhibitors against ERK 1/2 (p44/p42 MAPK) but not the PI3-Kinase pathway, prevented insulin inhibition of Nrf2 and Agt promoter activity and the stimulation of hnRNP F and hnRNP K promoter activity. This observation was further confirmed by knocking down the gene expression of p44/p42 MAPK by transient transfection with p44 MAPK siRNA or p42 MAPK siRNA or both, which reversed the insulin inhibition of Nrf2 and Agt while stimulating hnRNP F and hnRNP K promoter activity, as well as mRNA expression. The *in vivo* observations that insulin implanted Akita mice at 16 or 24 weeks increases phosphorylated p44/42 MAPK further confirmed our *in vitro* findings.

Currently, the exact mechanism of how insulin decreases nuclear Nrf2 translocation in Akita mice is not understood. Zheng *et al.* reported that mutation of three consensus Serine residues (s215, s408 and s577) for MAPK phosphorylation in Nrf2 by MAPKs had a limited impact on mediating Nrf2 translocation and activity in HEK 293T cells (346). One explanation could be that insulin activates p44/p42 MAPK following binding to insulin receptors, then phosphorylates Nrf2, thereby modulating or hindering its nuclear translocation and activity. This possibility was supported by our data that insulin administration increases p44/42 MAPK phosphorylation and decreases nuclear accumulation of Nrf2 and p-Nrf2 (s-40) without effecting cytoplasmic Nrf2 and p-Nrf2 (s-40). Its has been shown that during oxidative stress, PCK-δ could phosphorylate Nrf2 at s-40 to enhance its nuclear translocation (350). Furthermore, Hu *et al.* reported that MAPK1 could act as a transcriptional repressor for interferon gamma-induced genes via binding to G/C AAA G/C sequence (351). Another possibility is that insulin could directly or indirectly increase the nuclear export of Nrf2 or nuclear degradation of Nrf2.

GSK-3β/Fyn signaling has been reported to decrease Nrf2 nuclear accumulation by increasing nuclear export (444). In addition, phosphorylation of Nrf2 by p38 MAPK has been reported to increase in the interaction between Nrf2 and Keap1, which attenuates Nrf2 activity (445). Insulin signaling could also modulate GSK-3 β and p38 MAPK pathways, thereby modulating nuclear accumulation of Nrf2 (31, 283, 446). However, this study was mainly focused in the transcriptional regulation of Nrf2 by insulin. Clearly, additional studies are needed to clarify the precise mechanism how insulin regulate Nrf2 post-translationally.

To investigate whether insulin inhibits Nrf2 gene expression, and Nrf2 stimulation of Agt via hnRNP F/K *in vitro*, Nrf2 activator oltipraz and pcDNA3.1-Nrf2 transfection as well as Nrf2 siRNA were used. Nrf2 overexpression prevented, whereas Nrf2 siRNA enhanced-insulin inhibition of Nrf2 and Agt gene transcription *in vitro*. These effects could be explained by the presence of Nrf2-RE in both Nrf2 (352) and Agt promoters. Consistent with the previous reports, the data indicates auto-feedback effects of Nrf2 (352).

In contrast, Nrf2 activation with oltipraz diminished hnRNP F/K activity whereas silencing Nrf2 enhanced hnRNP F/K expression which were reversed by insulin via the p44/42 MAPK pathway. These results strongly indicated the possibility of having or Nrf2 response element in the hnRNP F/K promoters. Nrf2 would bind to the Nrf2 response element(s) in hnRNP F/K promoters and subsequently inhibited their transcription. Nevertheless, more work is required to confirm the presence or absence of Nrf2 response element(s) in hnRNP F/K promoters.

4.7 Promoter Studies and IREs

To understand the precise mechanism of how hnRNP F/K mediated insulin action on Nrf2, we hypothesized that hnRNP F/K binds to the putative insulin response elements (IRE) in the Nrf2 promoter and supresses its gene transcription. It was found that transfection with hnRNP F or hnRNP K siRNA, or both, reversed the inhibitory effect of insulin on Nrf2 promoter activity (i.e. increased Nrf2 expression). On the other hand, overexpression of hnRNP F/K directly decreased Nrf2 promoter activity and mRNA expression. These findings strongly confirmed the hypothesis.

In this study, found 2 GC rich regions were found from the analysis of rat Nrf2 promoter (N-1960/N+111) which are nucleotides N-463 to N-444 (5′-cgcgccccgccccccgcggga-3′) and N-607 to N-592 (5′-ggggcccgggctccc-3′). Previously, it had been reported that hnRNP F could bind to poly G sequences whereas hnRNP K bound to poly C sequences (269, 270, 275, 447, 448). Furthermore, nucleotide N-463 to N-444 in Nrf2 promoter contained core sequence 5'-ccccgcccc-3' which was homologous to the IRE with core sequence (*N*-882 to *N*-855, 5′-cctccct**tcccgccct**tcactttctagt-3′) of rat Agt promoter (271, 272). To demonstrate that insulin acted via these 2 regions in Nrf2 promoter, regions between N-463 to N-444 and N-607-N-592 region were deleted using site-directed mutagenesis cloning and was observed that the deletion of N-463 to N-444 region, but not the region between N-607 to N-592, abolished the insulin and hnRNP F/K mediated downregulation of Nrf2 promoter activity in IRPTCs. To confirm this observation, DNA-protein binding gel shift assay (or EMSA) with biotinylated-labeled IRE (N-463 to N-444) was performed. We demonstrated that proteins from IRPTC nuclear extract could bind to this IRE sequence and the addition of anti hnRNP F or hnRNP K antibody yielded a supershift band. This data strongly confirms the hypothesis that insulin can directly regulate Nrf2 expression via binding of hnRNP F/K to the IRE sequence (N-463 to N-444) of the Nrf2 promoter.

At this moment, it is not known whether hnRNP F and hnRNP K could form a dimer and then binds to this sequence or if they could bind individually and modulate Nrf2 transcription. As mentioned earlier in the introduction, hnRNP K contain multiple K interactive domains that act as a binding site for other factors (274). Previously, Dr. Chan's group reported that hnRNP K could interact with hnRNP F using co-immunoprecipitation (272). Furthermore, several studies have described that hnRNP F act as a splicing factor and regulate alternative splicing by remodeling RNA structure (278, 279). Whether hnRNP F can regulate Nrf2 post-transcriptionally, further studies are required.

4.8 Insulin on Gene Expression is Independent of Glucose Lowering Effect

4.8.1 Hyperinsulinemic Euglycemic Clamp

One of the major disadvantages of the current study design with Akita mice implanted with insulin was that we could not differentiate between a 'glucose-lowering effect' and a 'direct effect' of insulin on renal Nrf2, Agt, hnRNP F, hnRNP K and Bmf gene expression *in vivo*. To demonstrate the direct action of insulin on renal Nrf2, Agt, hnRNP F, hnRNP K and Bmf gene expression, a hyperinsulinemic-euglycemic clamp in wild type mice was performed (449). This test is widely used and referred as the gold standard for assessing insulin resistance and sensitivity in humans (450). In this study hyperinsulinemic-euglycemic clamp technique was used to evaluate insulin action on gene expression and insulin sensitivity, independent of its glucose lowering effect *in vivo*. In this technique, plasma insulin concentration is acutely raised by infusion which is accompanied by variable glucose infusion to maintain the basal plasma glucose level and to prevent hypoglycemic shock during the period of the experiment (449) Generally, experiments have a duration of three hours, where insulin level can be elevated up to 6 fold compared to control group (saline-infused group).

In this study, insulin suppressed Agt, Nrf2, and HO-1 expression and stimulated hnRNP F/K expression in the isolated proximal tubules from the hyperinsulinemic-euglycemic mice. This was a rapid insulin effect of 3 hours when compared to insulin implants in Akita mice (after 4 weeks of insulin implantation). The results were consistent with several studies which found similar rapid change in gene transcription in muscles and liver within 2 to 4 hours under euglycemic-hyperinsulinemic conditions (14, 15). Our data indicated that insulin could directly impact renal Nrf2 and Agt gene expression, in addition to its glucose-lowering action, thus confirming the hypothesis.

4.8.2 Studies with SGLT2 inhibitor

To further demonstrate that, in addition to lower blood glycemia, insulin could directly affect gene transcription, an SGLT2 inhibitor Canagliflozin (Cana) were used to treat 12 weeks

old Akita mice for 4 weeks. It was found that although Cana could reverse blood glycemia to normal levels and increase body weight, it failed to lower renal hypertrophy, SPB, GFR or ACR after 4 weeks of treatment in Akita mice (Unpublished data Table 5-1 and Figure 5-6). In contrast, insulin treatment could normalise all the above-mentioned parameters, including SPB, GFR and ACR in Akita mice. This indicated hypertension lowering effect of insulin was independent of its glucose lowering effect. This observation is in line with the study of Linda *et al.* who demonstrated that, although SGLT2 inhibitor empagliflozin (EMPA) could attenuate fibrosis, it failed to reduce ACR in db/db mice (451). In contrast, Vallon *et al.* reported that EMPA could strongly attenuate blood glycemia and it decreased without completely eliminating GFR, ACR and SBP in Akita mice. This discrepancy resulted probably because they started feeding EMPA to Akita mice at 4 weeks of age for 15 weeks. It is clear from several studies (343) including the current one, that at 4 weeks of age glycemia just starts to elevate in Akita mice. Controlling plasma glycemia at very young age thus provides protection from glycemia induced damage in adult Akita mice.

In addition, it was found that Cana treatment failed to reverse the expression of Agt and Nrf2 in RPTs and urinary Agt levels in Akita mice (Unpublished figure 5-7). This observation most likely explains the increased SBP in Cana treated Akita mice. This data strongly confirms the hypothesis that insulin could decrease RAS activation and hypertension by attenuating Nrf2 and Agt expression.

4.9 Potential Activator of hnRNP F/K: Hordenine

Recently, Su *et al.* evaluated the anti-diabetic effect of hordenine (HOR), a phenethylamine alkaloid and a natural constituent of many plants, in STZ-induced diabetic mice (452). STZ treatment in mice developed high blood glucose, ACR, fibrosis, inflammation and renal dysfunction compare to WT control. HOR treatment alone was sufficient to attenuate albuminuria, ACR, fibrosis and improved renal histology at the same level as insulin with the exception of fasted blood glucose. Combination treatment was even more potent to protect from STZ-induced adverse effects in these mice. Consistent with the present research hypothesis, they reported STZ induced diabetic mice had increased renal Nrf2 expression. Although ROS was

high in STZ-induced diabetic mice, elevated Nrf2 did not increase the expression of various antioxidants. In fact, they observed a decrease of various antioxidants, suggesting a changing pattern of Nrf2 induced gene activation. HOR treatment attenuated Nrf2 expression and restore other antioxidant levels at the same level as insulin in STZ-induced diabetic mice.

In line with the current finding, insulin administration in these STZ-induced diabetic mice significantly increased hnRNP F and hnRNP K expression. Surprisingly, they found that HOR treatment can also significantly increase hnRNP F and hnRNP K expression in STZ-induced diabetic mice. In the HOR treated group, there was an even greater increase in HnRNP F expression than that of the insulin treated group. In the combination treatment group, the levels of hnRNP F and K expression were almost doubled than that of HOR or insulin treated group alone. This data strongly suggested that HOR could be potential hnRNP F/K activator. Moreover, HOR and insulin functioned synergistically to enhance renoprotective effects.

These observations of Su *et al*. further confirmed the findings that hnRNP F/K activation could attenuate Nrf2 expression and attenuated kidney injury. However, they did not study the hypertension or RAS activation. It would be interesting to see what kind of effect HOR might have on RAS activation or in hypertension.

4.10 Transgenic mice overexpressing hBMF in the RPTC

In chapter 3 it has been demonstrated that RPTC specific overexpression of *hBMF* increases RPTC apoptosis and loss in the urine and induced renal dysfunction in *hBMF*-Tg mice, indicating a critical role for Bmf in mediating tubular cell apoptosis and loss. The findings further indicated that insulin treatment prevented RPTC apoptosis and inhibited renal Bmf transcription via hnRNP F that binded to a putative IRE in the Bmf gene promoter. These findings identified a novel mechanism by which insulin prevented RPTC apoptosis and loss in diabetic kidneys.

To demonstrate whether overexpression of Bmf can induce RPTC apoptosis, Tg mice overexpressing human BMF in the RTPCs were created. *Myc-hBMF* cDNA with the stop codon was inserted into a construct containing the kidney androgen regulated promoter, pKAP2. The KAP promoter can drive the targeted gene to express in the RPTCs in response to testosterone

stimulation. For the present study, male Tg mice were chosen, which had enough endogenous testosterone to induce Tg gene expression. The presence of *hBMF* transcript specifically in the kidney and proximal tubules in male mice and testosterone implanted female mice were confirmed by RT-PCR. Moreover, transgenic mice were validated by immunoblotting and immunostaining, using anti-Bmf antibody and anti-cMyc antibody. Furthermore, co-immunofluorescence staining with AQP1 confirmed RPTC specific overexpression of *hBMF*. These data confirmed that *hBMF*-Tg mice specifically overexpressed hBMF in the proximal tubules.

4.11 Effect of Bmf Overexpression in RPTC

In *hBMF*-Tg mice, significant increases in SBP, ACR, GFR, and RPTC volume compared to non-Tg mice were observed. Histologically, in *hBMF*-Tg mice, PAS staining revealed mild structural changes, but statistically significant tubular injury score compared to non-Tg mice. Semi-quantification of Masson's trichrome staining and TGF-β1 staining suggested the presence of tubule-interstitial fibrosis in *hBMF*-Tg mice which was confirmed by the presence of increased TGF-β1, fibronectin and collagen 1α. Moreover, significantly higher TUNEL positive cells in kidney sections of *hBMF*-Tg mice were observed when compared to non-Tg mice. WB analysis showed increased Bax and cleaved caspase 3 expression, whereas no significant change in anti-apoptotic Bcl2 expression was observed in RPT extracts of *hBMF*-Tg mice as compared to non-Tg mice. Furthermore, co-IP experiments revealed more Bmf binds to Bcl2, whereas less Bax binds to Bcl2 in Bmf-Tg mice compared to non-Tg mice. These data indicated that, in *hBMF*-Tg mice, Bmf predominantly binds to Bcl2 and dissociates it from Bax, thereby tipping the balance of the Bax/Bcl2 ratio towards caspase-3 activation. Finally, flow cytometry revealed the presence of more RPTCs in the urine of *hBMF*-tg mice compared to non-Tg mice.

Bmf is a member of proapoptotic BH3-only protein family (242). Under physiological conditions, Bmf binds to cytoskeletal structures and is sequestered to myosin V motors through association with dynein light chain 2. Certain stress signals, such as oxidative stress, anoikis, trigger the release of Bmf, which then directly or indirectly (via binding to Bcl2) activates Bax

to translocate into mitochondria and trigger intrinsic pathway of apoptosis (250, 251). Bmf is expressed in various organs including the kidney (250).

Among proapoptotic BH3-only proteins implicated in the cell death, the role of Bmf remains poorly understood. Mice deficient in Bmf $^{-/-}$ did not show any obvious phenotypic abnormalities (251, 256). However, little is known about the role of Bmf in kidney or in the pathogenesis of diabetes. In response to bioenergetic stress AMPK had been reported to induce Bmf dependent apoptosis in INS-1 cells (453). Dr. Chan's group have previously reported increased Bmf expression in apoptotic RPTCs in db/db mice, as well as in human diabetic kidneys (249). Recently, Alkhalifah *et al.* reported that Bmf play a major role in beta cell mass reduction in the pancreases and contributes to the pathogenesis of MODY3, a non-insulin dependent diabetes mellitus (NIDDM) (454). Pfeiffer *et al.* demonstrated that Bmf not only plays a major role in progressive pancreatic β-cell death in HNF1α-MODY, but also contributes to the pancreatic beta-cell function to maintain glucose homeostasis, independent of cell death signaling (375). These studies indicated that Bmf might be a key player in the pathogenesis of diabetes. Here, for the first time, our data provided strong evidence that overexpression of Bmf in the kidney was associated with tubular cell apoptosis, increased hypertension and renal dysfunction.

The underlying mechanisms of increased SBP and ACR in *hBMF*-Tg mice are still incompletely understood. The possibility that up-regulation of TGFβ1 gene expression in RPTCs and its downstream targets Fn1 and Col 1α, leading to higher tubulo-interstitial fibrosis that facilitates the development of hypertension, has received considerable attention. Indeed, strong correlation has been found between interstitial fibrosis and development of SBP via a loss or rarefaction of capillaries around the tubules (376, 377). Our observations of enhanced glomerular tuft volume, RPTC volume and GFR in *hBMF*-Tg mice lend additional support to this notion. Furthermore, the observed increases in ACR could be explained, at least in part, by a combination of loss of RPTCs and increased GFR (378).

An accumulating number of evidence indicates the role of the RPTCs as a prime mover in the pathogenesis and progression of DKD (297, 455). In diabetes, structural changes in RPTC such as tubulointerstitial fibrosis, tubular atrophy and peritubular capillary rarefaction correlate

closely with progressive renal decline (297-300). In addition, several studies have reported that proximal tubular injury can lead to glomerular injury (297, 376, 456) . Grgic *et al.* developed a mouse model of site directed injury to proximal tubules by expressing diptheria toxin receptors in the proximal tubules. Repeated insult by the toxin was sufficient to trigger pathological changes associated with DKD, including tubular atrophy, interstitial fibrosis, capillary rarefaction as well as glomerulisclerosis and proteinuria (376). Hasegawa *et. al.* provided evidence of retrograde trafficking between RPTCs and the glomerulus, showing that nicotinamide mononucleotide (NMN) derived from RPTCs diffuses back to the glomerulus to induce podocyte foot process effacement and albuminuria (456). As podocyte injury implicated not only to albuminuria but also in the progression of glomerulosclerosis and tubuloglomerular junction pathology (457), triggering of glomerular pathology by RPTCs strengthen the importance of proximal tubules in disease development. These finding are in line with our observation that overexpression of Bmf in the RPTCs is not only associated with tubular apoptosis but also induces albuminuria, GFR, hypertension and tubulopathy and supports the concept of RPTC injury and loss as a vital mediator of renal dysfunction.

4.12 Regulation of Bmf by Insulin

The previous observation by Dr. Chan's group that insulin treatment in STZ induced diabetic mice could attenuate Bmf expression (249) led us to investigate whether insulin mediated suppression of apoptosis occurs at least in part, via suppression of Bmf expression. As expected, Bmf expression was higher in 16 weeks old Akita mice and was inhibited by insulin. Co-immunostaining studies showed increased Bmf expression in TUNEL positive RPTCs in Akita mice which was attenuated by insulin treatment. Furthermore, Akita mice had increased Bmf and Bax mRNA expression, while decreased in Bcl-2 mRNA. Insulin treatment normalized these changes except for Bax mRNA. This observation suggested that insulin induced decrease in Bmf protein will promote Bax-Bcl2 binding thereby inhibiting caspase 3 activation and apoptosis. This notion is supported by research data showing that Bmf overexpression increased the binding of Bmf with Bcl2 while promoting its dissociation from Bax. Overall, these data confirmed the research hypothesis.

To show whether insulin could regulate Bmf expression independent of its glucose lowering effect, hyperinsulinemic-euglycemic mice were used as previously mentioned. Confirming the hypothesis, insulin down-regulate Bmf expression, independent of its glucose lowering effects as it was observed that, insulin supresses Bmf mRNA and protein expression.

Furthermore, in a separate study with Akita mice and Sglt2 inhibitor Cana, it was found that although Cana treatment in Akita mice could lower blood glucose, it could not decrease the gene expression of Bmf and was unable to prevent caspase-3 activation (Unpublished figure 5-8). In contrast, here it has been demonstrated that insulin treatment could successfully decrease Bmf and inhibit tubular apoptosis. These data strongly suggest that insulin could supress Bmf gene expression independently of its glucose lowering effects.

To explore if hnRNP F was involved in insulin suppression of Bmf, Akita hnRNP F-Tg mice overexpressing hnRNP F in RPTC were compared with Akita and WT mice (458). Indeed, overexpression of hnRNP F significantly down-regulated Bmf expression in Akita hnRNP F-Tg mice, suggesting a role for hnRNP F in mediating insulin inhibition of Bmf expression in Akita mice.

Confirming previous findings (249), it was observed that HG stimulated Bmf mRNA expression *in vitro* in IRPTCs which was reversed by insulin treatment. By combining studies with pharmacological inhibitors and gene knockdown with siRNAs, the p44/42 MAPK pathway and hnRNP F in mediating insulin suppression of renal Bmf gene transcription were identified. These findings clearly link hnRNP F to mediating insulin inhibition of Bmf gene expression in the diabetic mouse kidney. However, the precise mechanism by which hnRNP F down-regulates renal Bmf gene expression remains to be investigated. We hypothesized that hnRNP F binds to putative IRE in the Bmf promoter to suppress Bmf transcription. As anticipated, hnRNP F cDNA transfection was found to considerably decreased Bmf gene promoter activity, and that downregulation of hnRNP F with siRNA reversed insulin effect. DNA sequence analysis discerned 3 GC-rich regions, nucleotides N-1086 to N-1081 (5'-AGGGGG-3'), N-997 to N-991 (5'-GAGGGGC-3') and N-402 to N-395 (5'-CCCCCGC-3') in the Bmf gene promoter. Nucleotides N-1086 to N-1081 contain the core sequence 5'-AGGGGG-3' which was homologous to the core sequence of IRE N-402 to N-398 (5'-AGGGGG-3') of the rat Ace2

gene promoter (269) and IRE N-974 to N-969 (5′-AGGGGG-3’) of rat Sirtuin-1 (270). Deletion of N-1086 to N-1081, but not N-997 to N-991 and N-402 to N-395 in the Bmf promoter, markedly reduced insulin and hnRNP F mediated down-regulation of Bmf promoter activity in IRPTCs, indicating that the 5’- and 3’-flanking sequences of the core sequence might be important for hnRNP F binding. Moreover, biotin-labeled IRE (N-1093 to N-1072) specifically bound to RPTC nuclear proteins, and the addition of anti-hnRNP F antibody produced a supershift of biotin-labeled IRE binding with nuclear proteins on EMSA. These data identified N-1093 to N-1072 as a putative IRE that binds hnRNP F and inhibits Bmf transcription. It is noteworthy that hnRNP F is not restricted to regulating Bmf expression for it modulates the expression of Agt (268), Ace2 (269), Nrf2 (459), Sirtuin-1 (270) and possibly other genes (354). Whether hnRNP F is also involved in the alternative splicing of Bmf, need to be further studied.

To summarise, in chapter 3, the data demonstrated that Bmf activation could amplify tubulopathy and renal dysfunction via increasing RPTC apoptosis and loss. On the other hand, insulin can down-regulate Bmf expression via hnRNP F expression and p44/42 MAPK signaling pathway.

4.13 Regulation of Bmf by Nrf2

In previous study, Dr. Chan’s group provided evidence that hyperglycimia induced ROS generation could increase Bmf expression both *in vivo* and *in vitro*. In diabetic db/db mice model, Bmf expression was upregulated and proximal tubule specific over expression of catalase in db/db-catalase transgenic mice can attenuate Bmf expression. Furthermore in vitro, high glucose induced Bmf expression in the RTPCs was inhibited by rotenone, CAT, DPI, and apocynin (249). These data strongly supported ROS mediated Bmf expression. Increased oxidative stress is also responsible for Nrf2 activation. This led us to hypothesize that Nrf2 activation under high glucose condition might be responsible Bmf expression. To test the hypothesis, rat and human Bmf gene promoter were analysed and the presence of Nrf2 binding site in Bmf promoter region was found, as shown in unpublished figure 5-3 and figure 5-4. Furthermore, genetical and pharmacological activation or inhibition of Nrf2 *in vitro* in RPTCs resulted in significant dose dependent increase or decrease in Bmf mRNA expression and

promoter activity, respectively (figure 5-5). These data support our hypothesis that Nrf2 can modulate Bmf activity. Further evidence came from the *in vivo* studies in proximal tubules specific Nrf2-Tg mice. Overexpression of Nrf2 in the proximal tubules of 20 weeks old Nrf2-Tg mice, resulted in increased Bmf mRNA expression in compare to non-Tg controls (Figure 5-2d). These data further bolster the idea of the dark side of Nrf2 activation (412, 439). As here we have showed that Bmf is responsible for tubular apoptosis and kidney damage, this might also give the explanation for some studies where chronic Nrf2 activation worsen diabetic kidney pathologies.

4.14 Limitations of the study

4.14.1 Limitations of Akita mice model

Akita model has certain disadvantages. Female Akita mice do not develop hyperglycemia as their male counter part and are resistant to DN (343). For this reason, male Akita mice were used for the present study. C57BL/6 strain of Akita mice were used, which develop only modest levels of albuminuria and modest morphological changes. This mutation in other backgrounds such as DBA/2, FVB or 129/SvEv develop similar levels of hyperglycemia but differ in their manifestation of nephropathy (285, 288). However, due to unavailability of these background with $Ins2^{+/C96Y}$ mutation commercially, Akita mice with a C57BL/6 background were used in this study.

4.14.2 hnRNP F/K Knockout Mice

Previously, Dr. Chan's group have shown that overexpression of hnRNP F in Akita mice or in db/db mice could attenuate hypertension and renal injury (268-270). Moreover, they also reported that administration of insulin attenuated Agt expression via hnRNP F/K. Consistently, in this study strong evidence has been provided that insulin mediated hnRNP F/K can directly regulate Nrf2 and Bmf gene expression. However, RPTC specific hnRNP F knockout mice are needed to verify the observations that insulin mediated renoprotection is at least in part by hnRNP F. Indeed, such studies are underway in Dr. Chan's laboratory.

4.14.3 Role of Other BH3-only Proteins in Diabetic Kidneys

Bim another BH3-only protein that share functional and regulatory similarities with Bmf (252). In fact, as mentioned in the introduction, Bim is the most potent killer among all the BH-3 only protein family(242). Bim had been reported to be a key mediator of pro-inflammatory cytokine-induced β-cell apoptosis in autoimmune diabetes. Moreover, Bim regulates apoptotic pathway and mitochondrial function in hepatocytes and pancreatic islets from human with T2D have high expression of Bim (460). However, in the previous study, using microarray analysis Dr. Chan's group found that Bmf but not Bim, was significantly upregulated in the kidney proximal tubules of db/db mice in compare to db/m control mice. Furthermore, in human diabetic kidney we found increased expression of Bmf (249). In this study evidence has been provided that Bmf is involved in kidney pathology. Currently, there are no evidence on whether Bim is involved in the kidney pathology. More studies are needed to elucidate the role of BH-3-only proteins in the kidney.

4.15 Conclusion

The main purpose of the current study was to elucidate the underlying mechanisms of how insulin can counter ROS induced hypertension and renal dysfunction in diabetes and to identify downstream potential therapeutic targets to counter DN progression.

This study had shown that, insulin treatment in Akita mice could attenuate renal Nrf2, Nrf2 stimulation of Agt expression and reduced hypertension and kidney injury. Furthermore, it has been shown that insulin can down-regulate Nrf2 expression directedly independent of its glucose lowering effects via hnRNP F and hnRNP K. Finally, for the first time we have reported that overexpression of a pro-apoptotic protein Bmf in RPTC could cause RPTC apoptosis and renal dysfunction. In addition, it has been elucidated that insulin can attenuate Bmf expression via hnRNP F. These observations are summarized in figure 4-1.

The most obvious finding to emerge from this study is that in diabetes, ROS induced increased Nrf2 expression directly stimulates Agt expression which leads to activation of RAS resulting hypertension and renal dysfunction. The second major finding is that insulin can stimulate hnRNP F/K via p44/p42 pathway which then can bind to the IRE region of Nrf2 and

Bmf gene promoter to supress their activation thus protect from hypertension, RPTC apoptosis, and renal dysfunction.

The evidence from this study suggest hnRNP F/K, Nrf2 and Bmf as potential therapeutic target against diabetic nephropathy.

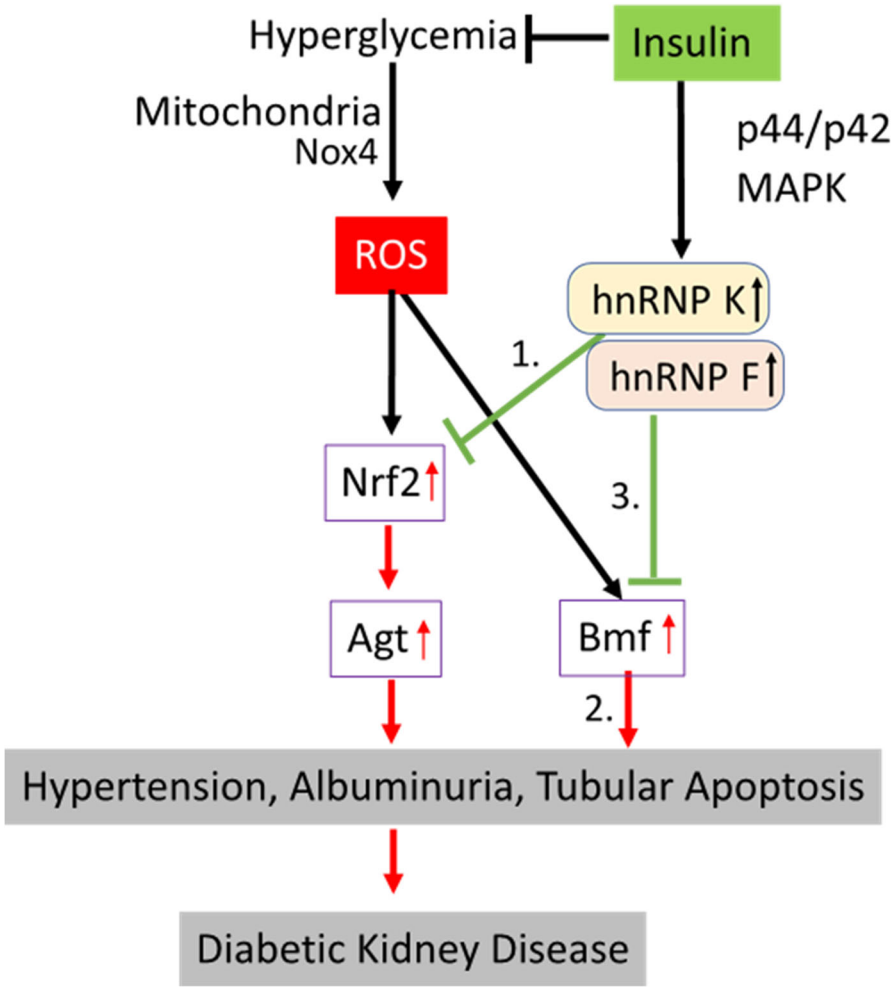

Figure 4-1: Proposed model. In diabetic condition, hyperglycimia induces ROS generation in the renal proximal tubules mainly via mitrochondrial pathways and Nox 4 activation. This increased ROS then activates Nrf2, which translocates to nucleus and binds to the Nrf2 response elements on various genes including Agt. Increased Agt elevates hypertentension and progression of DKD. Here we confirmed that 1. Insulin down-regulated Nrf2 expression via hnRNP F/K mediated IRE binding in the Nrf2 promoter. 2. Overexpression of Bmf caused RPTC apoptosis and renal dysfunction. 3. Insulin could down regulate Bmf expression via hnRNP F mediated IRE binding in the Bmf promoter.

Chapter 5: Unpublished Results and Research Perspectives

5.1 Generation of Nrf2 transgenic mice

To better understand role of Nrf2 in hypertension and nephropathy progression, transgenic mice overexpressing rat-Nrf2 in the RPTCs have been genarated. Rat Nrf2 cDNA was cloned from rat kidney, fused with FLAG tag and inserted into a construct containing the kidney androgen regulated promoter, pKAP2 (figure 5-1A). The isolated KAP2-rNRF2-FLAG transgene was then microinjected into one-cell fertilised mouse embryos. First positive Tg founders were then crossed with WT C56BL/6 mice for F1 generation (figure 5-1B). Breeding was continued until homozygous F3 and F4 Tg mice were found. 20 weeks old male rNRF2-Tg

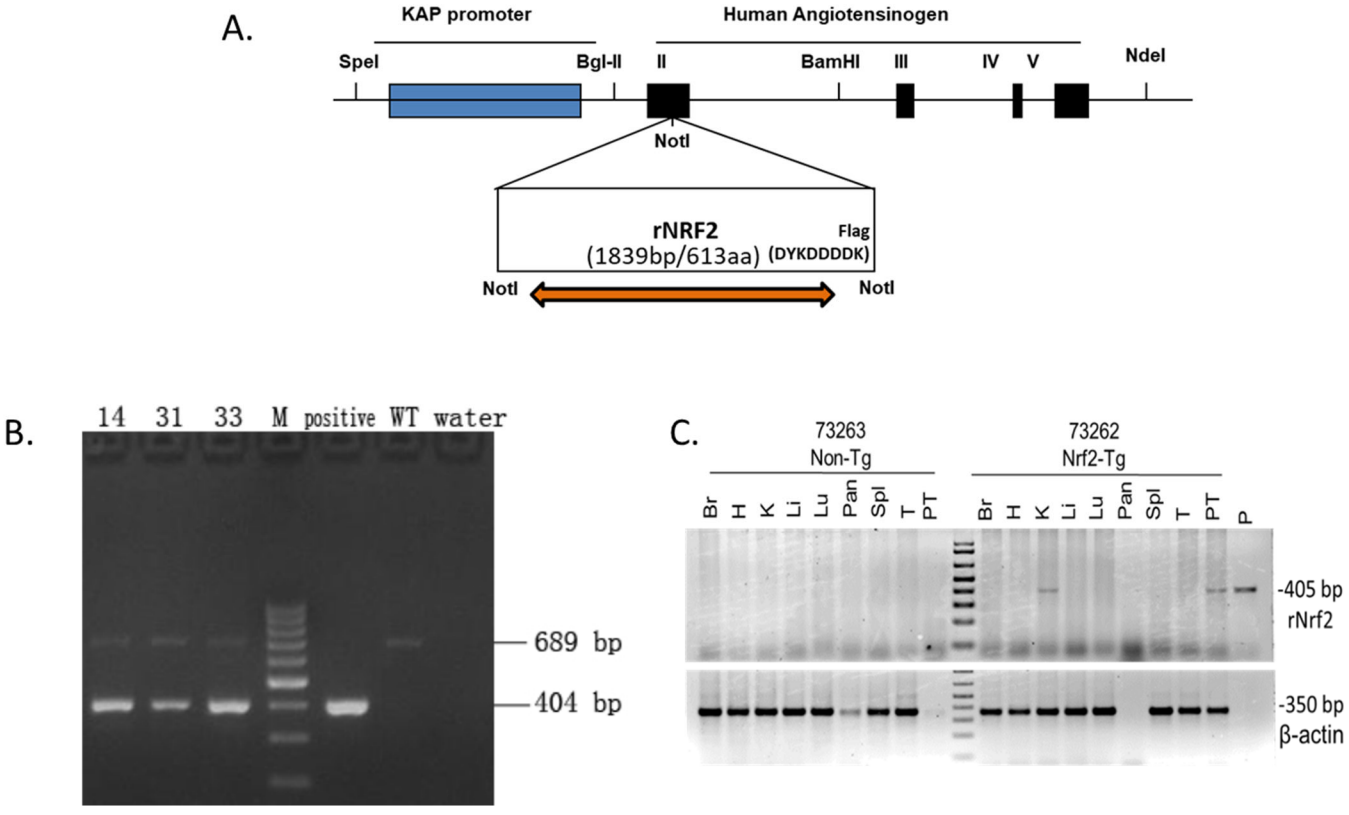

Figure 5-1: Generation of KAP2-rNRF2-Tg mice. A. Schematic map of the KAP2-rNRF2-Flag construct. B. Genotyping results for F1 generation. C. PCR analysis for tissue specific expression of rNRF2 transgene in male rNRF-Tg and non-Tg control mice. Br-brain, H-heart, K-kidney, Li-liver, Pan-pancreases, Spl-spleen, T-testis, PT-proximal tubules, P-positive control.

and non-Tg control mice were sacrificed and different organs were isolated to determine tissue specific expression of transgenic rNRF2 (Figure 5-1C.). We found transgenic male rNRF2 expresses the transgene only in kidney and proximal tubules but not in other organs. These data validated out rNrf2 transgenic mice.

Next, the proximal tubules from non-Tg or rNRF2-Tg mice (n=4) were isolated and assased mRNA expression of various genes including Nrf2 and Nrf2 target gene NQO1 as well as Agt and Bmf by qRT-PCR. As expected, Nrf2, NQO1 and Agt expression in rNRF2-Tg mice significantly increased than in not-Tg mice (figure 5-2). This observation further validated rNRF2-Tg mice. Interestingly, renal Bmf gene expression was found significantly upregulated suggesting Nrf2 can modulate Bmf expression. This observation led us to investigate whether Nrf2 can increase Bmf expression directly via Nrf2-RE in Bmf promoter.

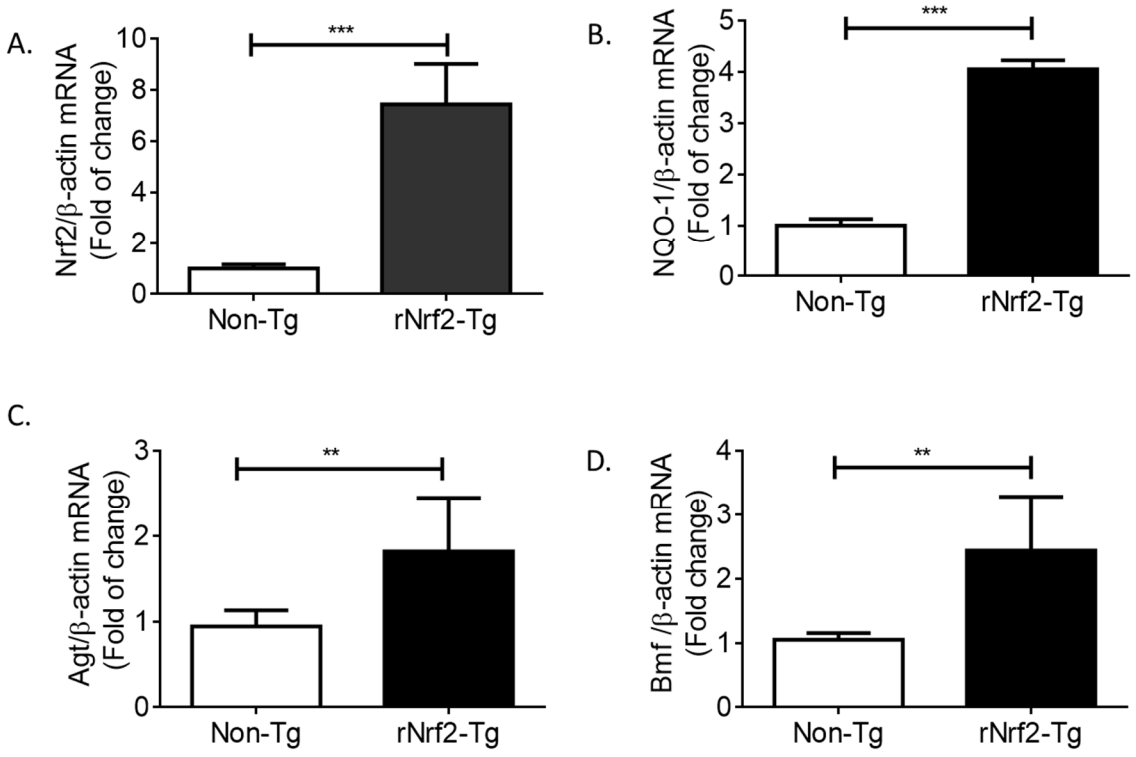

Figure 5-2: Gene expression Pattern in rNRF2-Tg mice. qRT-PCR was done in isolated proximal tubules of rNRF2-Tg and non-Tg mice for A. *Nrf2*, B. *NQO1*, C. *Agt*, and D. *Bmf* gene. Values are means ± SEM, n=5. **p<0.01; ***p<0.005;

5.2 Bmf Promoter analysis

Detailed promoter analysis was done using various bio-informatics tools revealed the presence of Nrf2-RE in both human and rat Bmf promoter. In addition, we found the presence of transcription factor Foxo and p53 binding sites. Recently, Hornsveld et al. reported that FoxO3 is responsible for transcriptional activation of Bmf (461). Contreras *et al.* reported that deacetylation of p53 can supress Bmf expression (462). No one reported if Nrf2 could regulate Bmf expression. Here we tested whether Nrf2 can directly regulate Bmf expression. Rat and human Bmf promoter analysis were shown in Figure 5-3. Detailed rat-Bmf promoter analysis were shown in Figure 5-3.

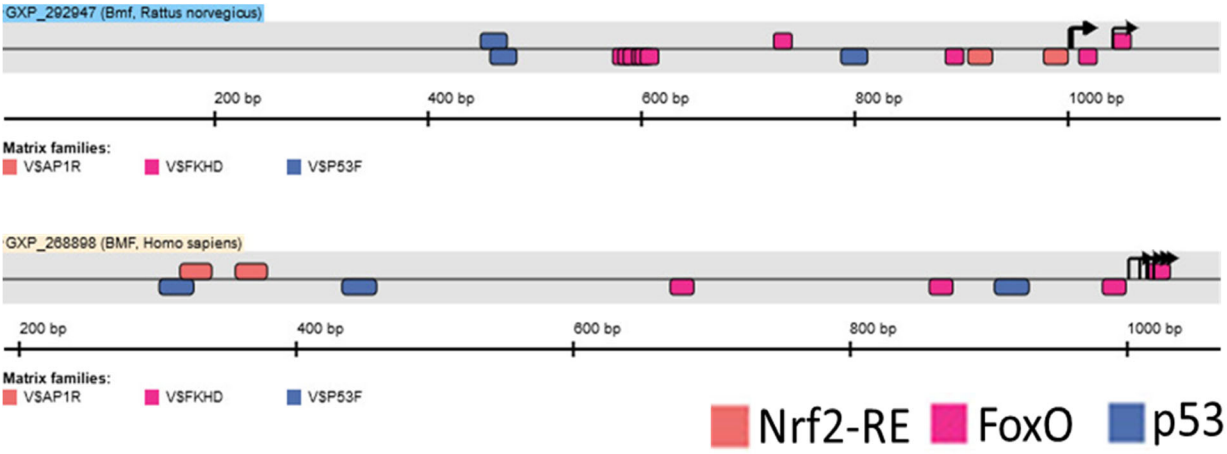

Figure 5-3: Bmf-promoter analysis. Rat and human Bmf promoter were analysed for Nrf2, FoxO and p53 binding sites using Genomatix software (www.genomatix.de). Schematic map showing Nrf2, Foxo and p53 binding sites.

RAT BMF Promoter -1370/+102

-1370 CCTCGTTTTCCCCCAAATCCATCTTCTGCAAAGTCTTTGCTACCGGCCCGCTAGGAAATACAAATTCCTT

-1300 GGGGCTGAAGAGATGGCTCAGTGGTTAAACGCACTAGTTGCTCTTCCAGAGGACCCAGGTTCAATTCCAA
Nrf2

-1230 GGACCCACGTGGCAGCTCATAGACATCTGTAACTCCAGTTCCAGAAGACCTGCTGTCACAAAGACATATG
p53

-1160 CAAAACACTAATGCACATGAAATAAAAATAAACAAATTATTTTTAAAGGTACAAATTCCTCATCCTGTTA
Foxo3 Foxo3 Nrf2

-1090 TTCCAGGGGGTACCTCTGCAATCTGACCTAAATCTACCTGCCCTCCATACCTTCACATCCTAAACCATGG
hnRNP F

-1020 TGAGGATGCCTGATAGCTCAATAGAGGGGCCTGACCTTGCTTCCCAGACCTGCTCAGTACTTTATTCTAG
hnRNP F Nrf2 p53

-950 CTCCCTGCCTTCTCCGGCTCACGACTGTTTCATTTGGTTTTTATTTAGTGAAAAATTCCCCATTCTTCAA

-880 GGCCCTATCCCAAAGTCTTTGCATATTATCCCTAAAATAGCACCATTCACGTTGGTTCCCATCATTCACA

-810 AGTAGAGTATAAGTTCATTGAGGTCAGGCACAGAAGTCTGACACTTAGACCAGTGCTTGGCACACAGTAG

-740 GTGTTCAAAAAAATGTGCACCCATCCCTAGATAGTATACGAGATGCGTTTTGCTTTCCTAGCAGCCTAAG

-670 AACAGCCCTCTGATGCTACCCAGGCTGCCCTTTTGATTTCTCCTCTTACAGAGTCTTTATAGCAATGATC

-600 TTGCATAGTCTAGACGAGAGGACATGGCCTTTCTTTGCACTTGATGGATCCAAATGTCATTTAGTTCTAG

-530 ATGCAGACACACGTGTTCTCCTCTAGCTTTCCTCAGACACGCCCAACAGGCAAGAGGGCGGGCTTTTTGT
p53

-460 TTTGTTTTGTTTTTTGTTTGTTTTGTTTTTCTCATTAGAGACCAGCAACTCCTTTTTTCCCCCGCTATAC
hnRNP F

-390 AAGTCGCGGCTGAAATCTCCCAGTCTCCTCCTGAGCCGGCTTTCTGGAAGTCCCGCAAAAATTCAGCCCA

-320 TTTCCAAGTAGACAAAAGTCACTTAGGCGTCTTGTGCCCCCAACCTAGTGGAGAACCCAGGGACTCTCTG

-250 TCATTTCTGGGGCTTGCATTCGGAACCGAATCCTCACCCTTTACAGAGCTCCAATTGCGCTTCTGGCGGA

-180 GGTCAGAAATGTGCCCGGCCCCTTATAATGTTTCCAAGGGAAGGTTCGTACATTGGTGACTGTCCCTGGC

-110 AGCTGCCCAGCTTGAGACTTGGAGCTCCACTTGCCATTGGTCAGTGGTTGGAGTGACGCAAAGAAGGGCG
p53

-40 GGGCCTCATCAGCTGTTTGCGGGATGCCCGGAGCGGGCGTATTTTGGAAACAATACCGCGCGGTGCGCGG
+1 Transcriptional start site

+30 TGGCCTCCTCCCGCGCCAGCTCACGCCCACAGCAGTCGCTGCCCGAGCCCGCGCCACCACCTCCCACCGC

+100 AG

Figure 5-4. Rat Bmf promoter (N-1370/+102) sequence were analysed for the putative binding site for Nrf2, hnRNP F, FoxO3 and p53 response element.

5.3 Role of Nrf2 in the regulation of Bmf

In vitro, both pharmacological and genetic approach were used to investigate whether Nrf2 can promote Bmf expression. It was found that Nrf2 activator oltipraz and pCMV-rNrf2 could significantly increase Bmf mRNA and rat Bmf promoter (N-1370/+102) activity in IRPTC cells. Trigonelline and rat Nrf2 siRNA reversed the HG or oltipraz induced Bmf expression. These observations strongly indicated Nrf2 could directly regulate Bmf expression.

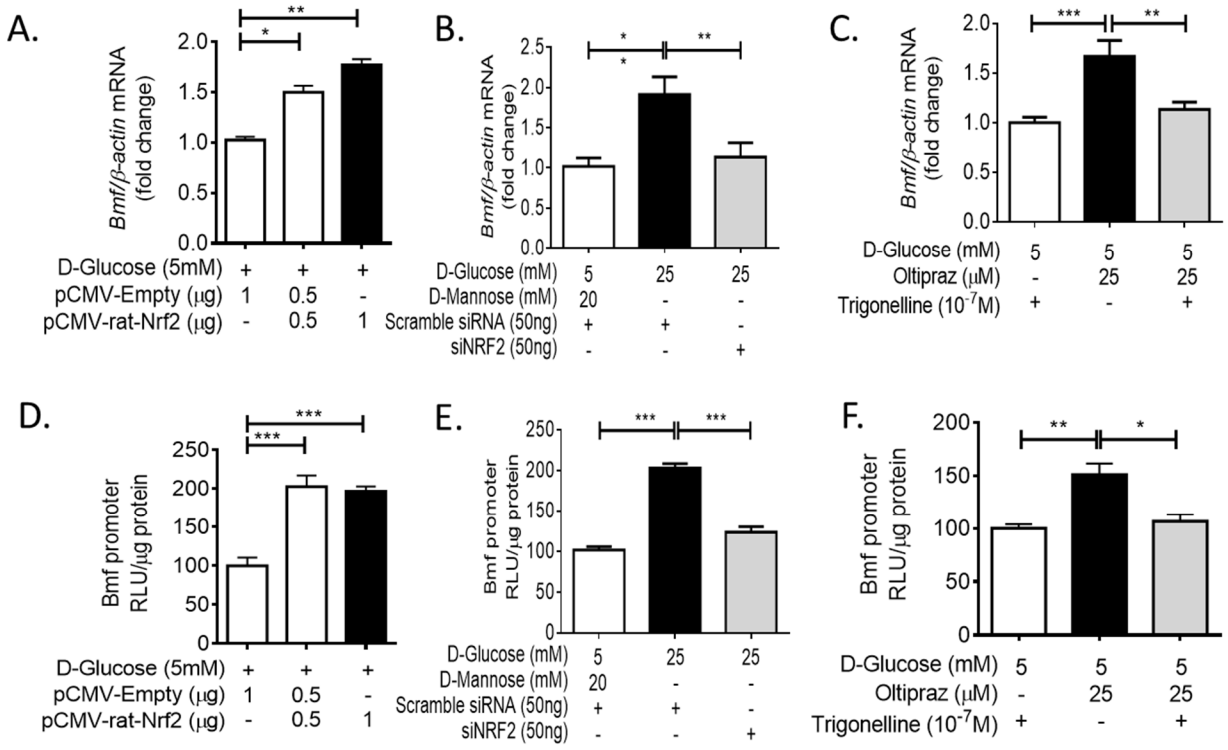

Figure 5-5: Role of Nrf2 in Bmf expression. A.,B.,C.: Bmf mRNA expression in response to rat Nrf2-plasmid, siRNA-Nrf2 and Nrf2 activator oltipraz with or without Nrf2 inhibitor Trigonelline, respectively in IRPTC cells. D.,E.,F.: Luciferase assay in IRPTC cells stably transfected with pGL4.20 plasmid containing rat Bmf promoter (N-1370/+102) region. Each value represents the means ± SEM, (n=3) assayed in duplicate. *p<0.05; **p<0.01; ***p<0.005;

5.4 Adminstration of SGLT2 Inhibitor Canagliflozin in Akita mice

Akita mice were administrated Cana with water at 12 weeks of age and continued for 4 weeks. It was observed that Cana treatment could successfully attenuate blood glucose and kidney hypertrophy but have no effect on SBP, GFR and ACR as well as in body weight (table 5-1). Furthermore, IHC, WB and qPCR analysis showed that Cana treatment in Akita mice could not decrease Agt or Nrf2 expression as well as urinary Agt (figure 5-7). In addition, Cana treatment did not reduce cleaved caspase 3 or Bmf expression in Akita mice. (figure 5-8)

	WT (7)	Akita (7)	Akita-Cana (6)
Body weight (g)	29.63±0.611	22.56±0.302***	23.98±0.388***
Blood glucose (mmol/L)	7.92±0.484	30.98±0.549***	12.36±1.233**†††
Systolic blood pressure (mmHg)	110.4±1.33	130.1±4.3***	132.9±3.28***
Kidney weight/Tibia length (mg/mm)	11.93±0.471	24.07±1.1***	20.1±0.507***††
GFR	7.48±0.428	17.11±0.828***	19.24±0.885***
ACR (μg/mg)	18.23±3.315	85.83±24.63***	80.9±20.79*

Table 5-1. Physiological parameters

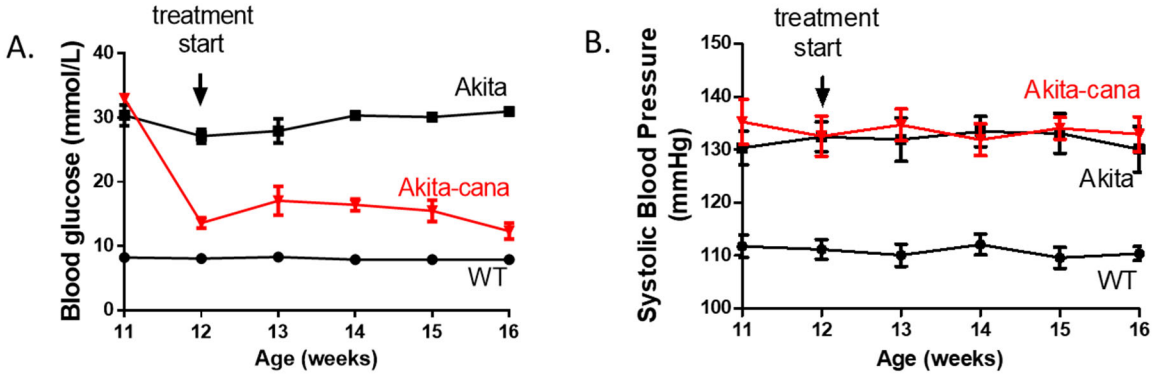

Figure 5-6: Physiological measurements. A. Measurement of blood glucose and B. Systolic blood pressure in WT, Akita and Akita mice treated with canagliflozin. n = 6-7 mice/group.

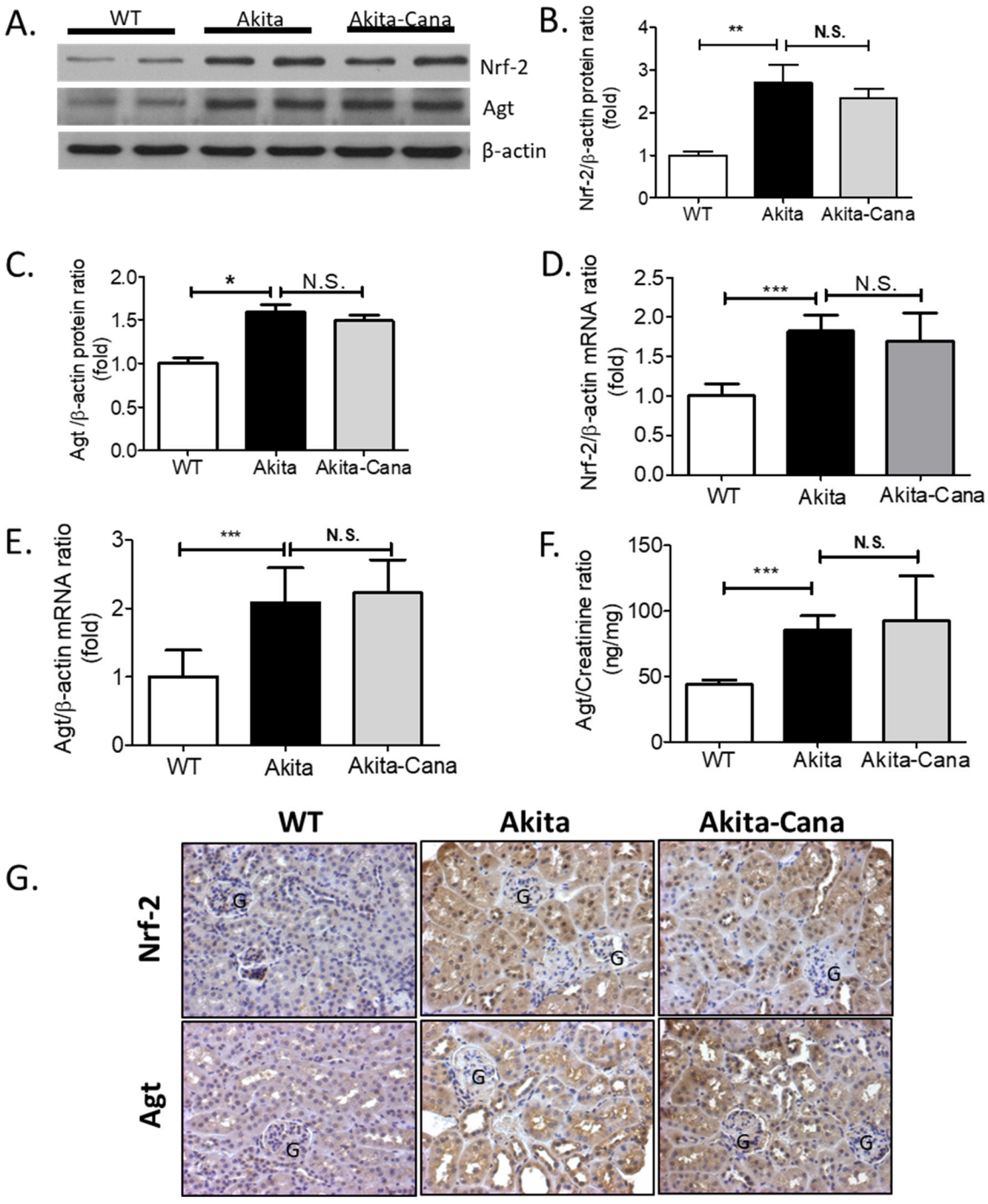

Figure 5-7: Nrf2 and Agt gene expression. (A)., WB and its quantification of Nrf2 (B.) and Agt (C) in isolated RPTs of WT, Akita and Akita-Cana group. (D.), (E) mRNA and (G) IHC expression for Nrf2 and Agt, respectively in WT, Akita and Akita-Cana group. (F) Urinary Agt concentration. Each value represents the means ± SEM, (n=6), *p<0.05; **p<0.01; ***p<0.005;

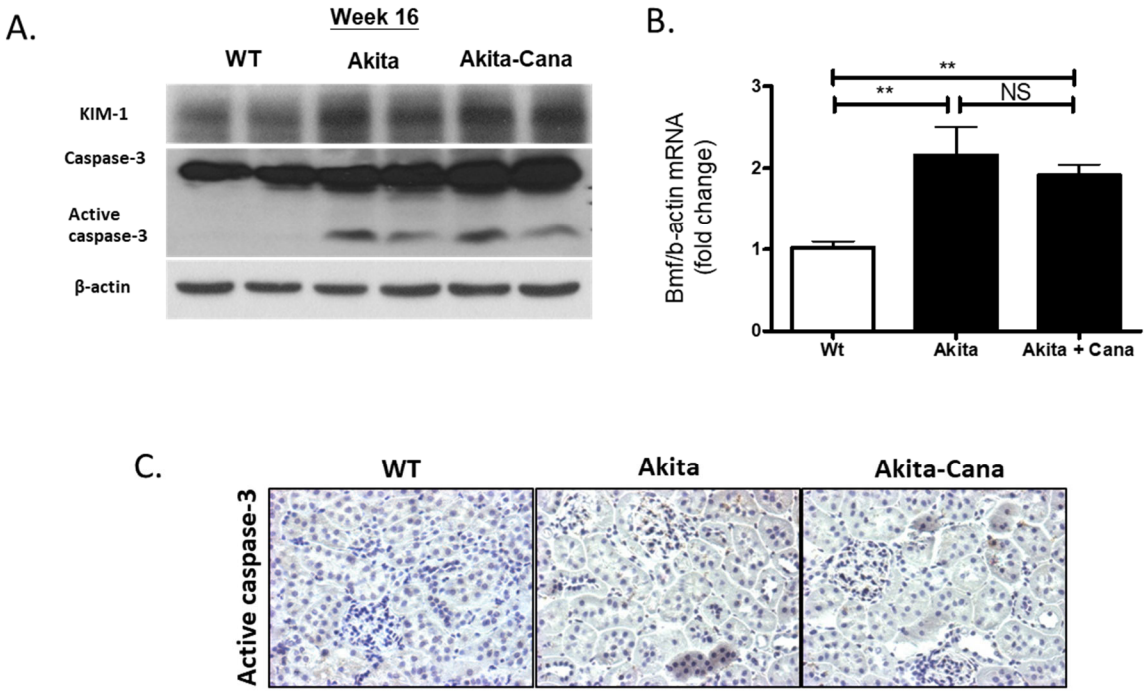

Figure 5-8. Caspase 3 and Bmf expression. A. WB for kidney damage marker KIM-1, caspase and active caspase-3, B. qRT-PCR to determine mRNA expression of Bmf and C. IHC to detect active caspase3 in WT, Akita or Akita treated with Cana. Each value represents the means ± SEM, (n=6), **p<0.01; NS= non significant;

This observation suggested that Cana treatment for 4 weeks in Akita mice attenuated blood glucose level but did not improve hypertension or kidney injury.

5.5 Future Experiments

5.5.1 Generation of Nrf2KO: KAP2-rNrf2-Tg Mice

To elucidate the role of Nrf2 in the kidney, Nrf2KO: KAP2-rNrf2-Tg mice will be genarated where rNrf2 will be overexpress in the proximal tubules of general Nrf2KO mice. As mentioned earlier, now we have rNrf2-Tg mice. Nrf2 KO mice were commercially purchased from Jackson. Currently we are in process to cross these mice as shown below. We hope this mice model will shed light on the role of Nrf2 in diabetic nephropathy.

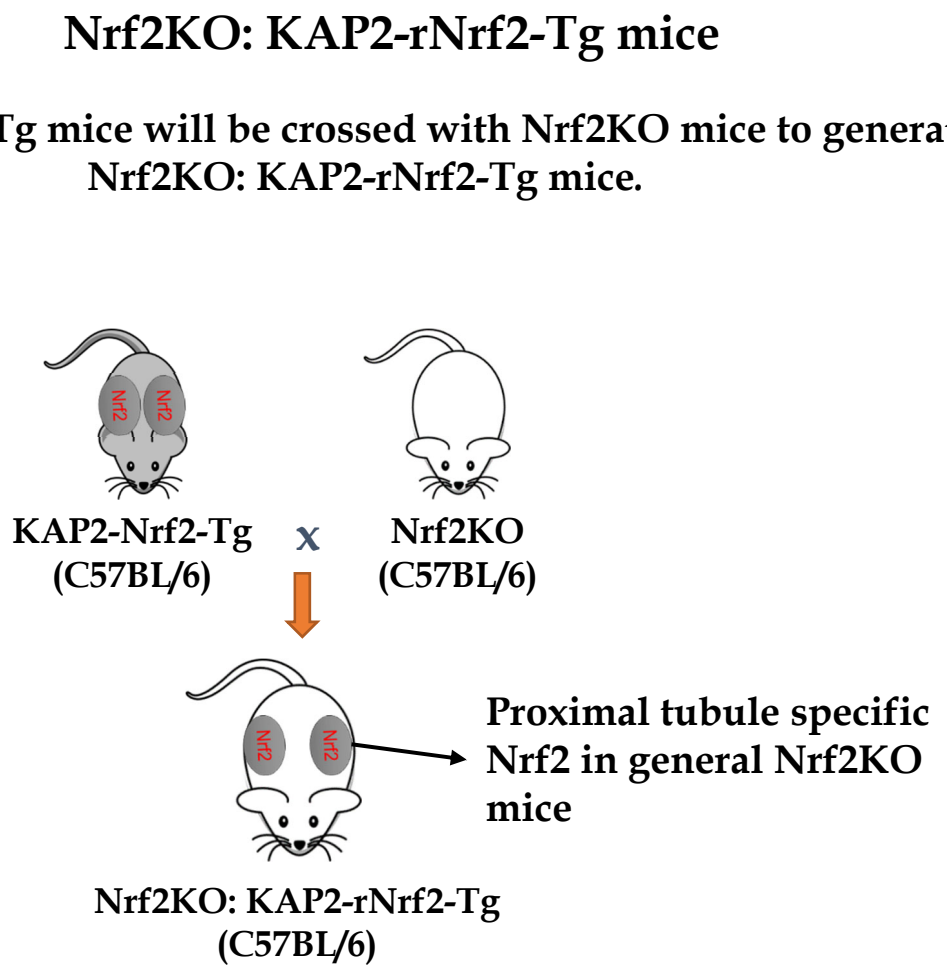

Figure 5-9 Diagram to generate Nrf2KO: KAP2-rNrf2-Tg mice.

5.5.2 Generation of Akita-Erk1$^{-/-}$:Pax8-Cre-Erk2$^{-/-}$ Mice

To further provide evidence that insulin-mediated renoprotective effects in Akita mice were via modulating hnRNP F, hnRNP K, Agt, Nrf2 and Bmf expression in a Erk1/2 dependent manner, we are currently in the process of generating Akita-Erk1$^{-/-}$:Pax8-Cre-Erk2$^{-/-}$ mice. Erk1$^{-/-}$ mice are viable, fertile and available commercially, whereas Erk2$^{-/-}$ mice are embryonic lethal due to placental defects (463). Presently, we have generated kidney tubular epithelial cell specific Pax8-Cre-Erk2$^{-/-}$ mice by cross-breeding kidney specific Pax8-Cre mice with floxed Erk2$^{fl/fl}$ mice. This mouse will be crossed with general Erk1$^{-/-}$ mice to generate Erk1$^{-/-}$:Pax8-Cre-Erk2$^{-/-}$ Mice. Finally Akita mice will be cross-bred with this mouse to generate Akita-Erk1$^{-/-}$:Pax8-Cre-Erk2$^{-/-}$ Mice. The plan for developing this mouse model is shown below.

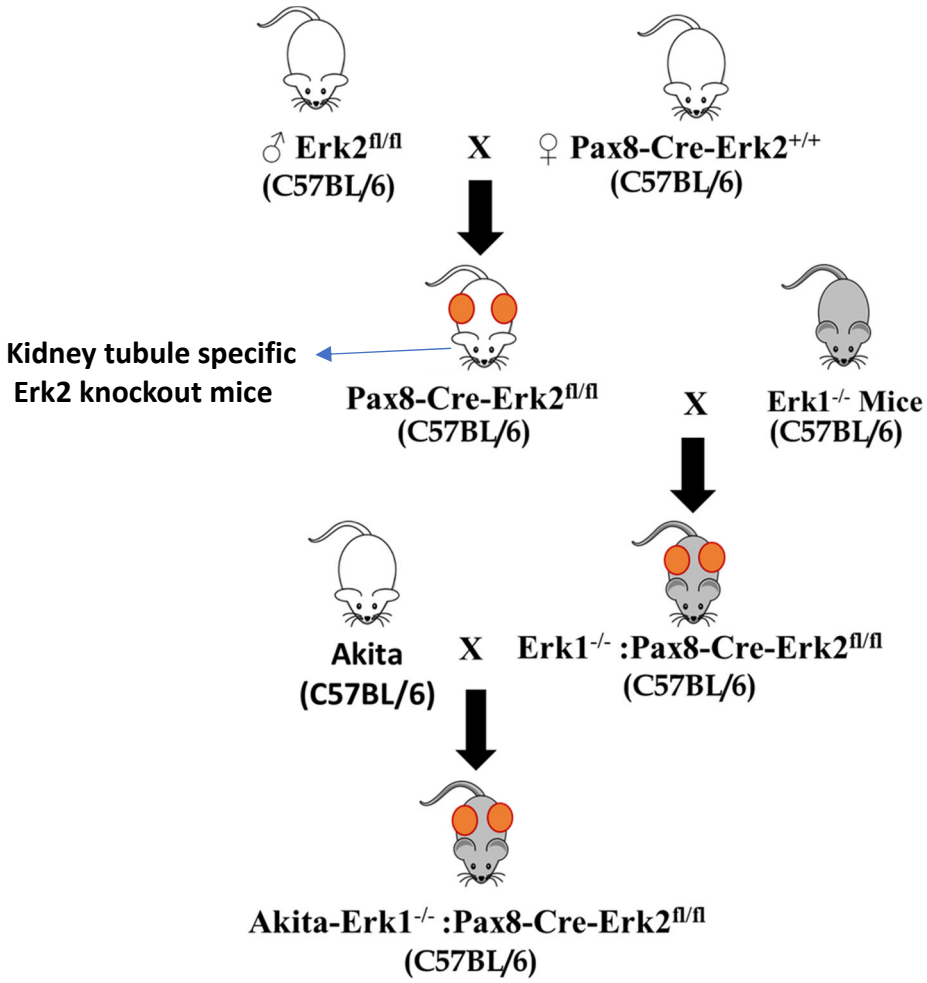

Figure 5-10 Diagram to generate Akita-Erk1$^{-/-}$:Pax8-Cre-Erk2$^{-/-}$ mice.

Our preliminary data with Erk1$^{-/-}$ mice and Pax8-Cre-Erk2$^{-/-}$ mice provides further evedence that Erk 1/2 signaling modulates hnRNP F and K expression in the kidney *in vivo*.

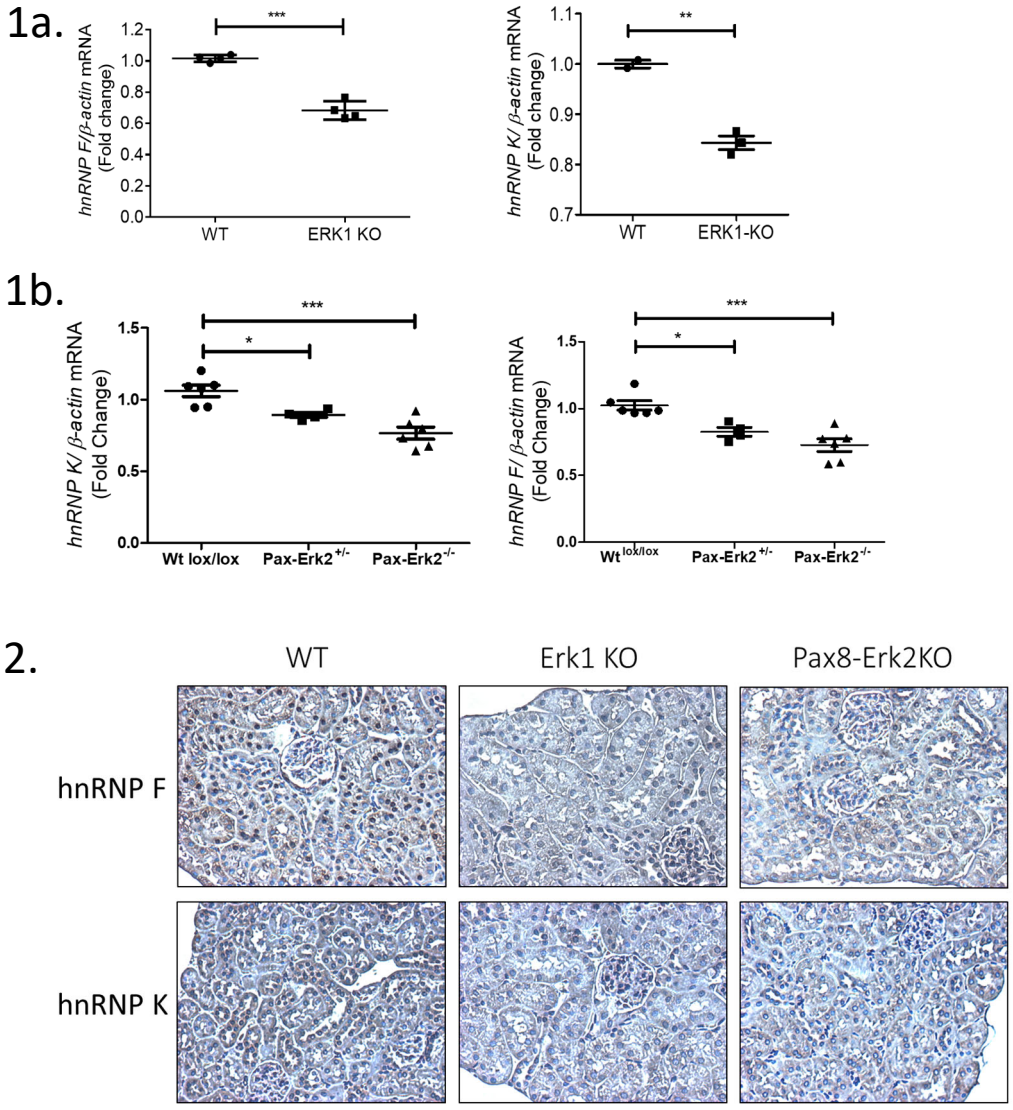

Figure 5-11. hnRNP F/K expression in Erk1 KO and Pax8-Cre-Erk2 KO mice. (1a.) Isolated proximal tubules from Erk1 KO mice, (1b.) Pax8-Cre-Erk2 heterozygote mice and Pax8-Cre-Erk2 KO mice were analysed by qRT-PCR for hnRNP F/K mRNA expression. (2) IHC staining of hnRNP F/K in the kidney section of Erk1 KO and Pax8-Erk2 KO mice.

Chapter 6: References

1. Goldman R, Zajac J, Shrestha A, Patel P, Poretsky L. The Main Events in the History of Diabetes Mellitus. In: Poretsky L, editor. Principles of Diabetes Mellitus. Cham: Springer International Publishing; 2017. p. 3-19.
2. MacCracken J, Hoel D, Jovanovic L. From ants to analogues. Postgraduate Medicine. 1997;101(4):138-50.
3. Medvei VC. The Mediaeval Scene. In: Medvei VC, editor. A History of Endocrinology. Dordrecht: Springer Netherlands; 1982. p. 79-95.
4. Medvei VC. The 18th Century and the Beginning of the 19th Century. In: Medvei VC, editor. A History of Endocrinology. Dordrecht: Springer Netherlands; 1982. p. 149-211.
5. Ahmed AM. History of diabetes mellitus. Saudi Med J. 2002;23(4):373-8.
6. Medvei VC. The First Four Decades of The 20th Century — Part II. In: Medvei VC, editor. A History of Endocrinology. Dordrecht: Springer Netherlands; 1982. p. 437-98.
7. Minkowski O. Historical development of the theory of pancreatic diabetes by Oscar Minkowski, 1929: introduction and translation by Rachmiel Levine. Diabetes. 1989;38(1):1-6.
8. Bliss M. The Discovery of Insulin. Chicago: University of Chicago Press; 1982.
9. Drejer K. The bioactivity of insulin analogues from in vitro receptor binding to in vivo glucose uptake. Diabetes Metab Rev. 1992;8(3):259-85.
10. American Diabetes A. Diagnosis and classification of diabetes mellitus. Diabetes Care. 2010;33 Suppl 1:S62-9.
11. Nyaga DM, Vickers MH, Jefferies C, Perry JK, O'Sullivan JM. The genetic architecture of type 1 diabetes mellitus. Mol Cell Endocrinol. 2018.
12. Matboli M, Shafei A, Ali M, Kamal KM, Noah M, Lewis P, et al. Emerging role of nutrition and the non-coding landscape in type 2 diabetes mellitus: A review of literature. Gene. 2018.
13. International Diabetes Federation. IDF Diabetes Atlas, 8th edn. Brussels, Belgium: International Diabetes Federation, 2017. http://www.diabetesatlas.org.
14. Yamamoto JM, Kellett JE, Balsells M, Garcia-Patterson A, Hadar E, Sola I, et al. Gestational Diabetes Mellitus and Diet: A Systematic Review and Meta-analysis of Randomized

Controlled Trials Examining the Impact of Modified Dietary Interventions on Maternal Glucose Control and Neonatal Birth Weight. Diabetes Care. 2018;41(7):1346-61.

15. Bellamy L, Casas JP, Hingorani AD, Williams D. Type 2 diabetes mellitus after gestational diabetes: a systematic review and meta-analysis. Lancet. 2009;373(9677):1773-9.

16. Landon MB, Spong CY, Thom E, Carpenter MW, Ramin SM, Casey B, et al. A multicenter, randomized trial of treatment for mild gestational diabetes. The New England journal of medicine. 2009;361(14):1339-48.

17. Wild S, Roglic G, Green A, Sicree R, King H. Global Prevalence of Diabetes. Estimates for the year 2000 and projections for 2030. 2004;27(5):1047-53.

18. The Diabetes Control and Complications Trial Research Group. The Effect of Intensive Treatment of Diabetes on the Development and Progression of Long-Term Complications in Insulin-Dependent Diabetes Mellitus. New England Journal of Medicine. 1993;329(14):977-86.

19. Ogden CL, Carroll MD, Kit BK, Flegal KM. Prevalence of childhood and adult obesity in the United States, 2011-2012. Jama. 2014;311(8):806-14.

20. Gregg EW, Li Y, Wang J, Rios Burrows N, Ali MK, Rolka D, et al. Changes in Diabetes-Related Complications in the United States, 1990–2010. New England Journal of Medicine. 2014;370(16):1514-23.

21. Chan JC, Malik V, Jia W, Kadowaki T, Yajnik CS, Yoon KH, et al. Diabetes in Asia: epidemiology, risk factors, and pathophysiology. Jama. 2009;301(20):2129-40.

22. Fowler MJ. Microvascular and Macrovascular Complications of Diabetes. Clinical Diabetes. 2008;26(2):77-82.

23. Carstensen B, Jorgensen ME, Friis S. The epidemiology of diabetes and cancer. Current diabetes reports. 2014;14(10):535.

24. Wong E, Backholer K, Gearon E, Harding J, Freak-Poli R, Stevenson C, et al. Diabetes and risk of physical disability in adults: a systematic review and meta-analysis. Lancet Diabetes Endocrinol. 2013;1(2):106-14.

25. Roy T, Lloyd CE. Epidemiology of depression and diabetes: a systematic review. J Affect Disord. 2012;142 Suppl:S8-21.

26. Tanner GA. Kidney Function. In: Rodney A. Rhoades, David R. Bell, editor. Medical physiology : principles for clinical medicine. Philadelphia: Lippincott Williams & Wilkins; 2009. p. 391-418.

27. Boron WF, Boulpaep EL. Medical Physiology E-Book: Elsevier Health Sciences; 2016.
28. Koeppen BM, Stanton BA. 2 - Structure and Function of the Kidneys. In: Koeppen BM, Stanton BA, editors. Renal Physiology (Fifth Edition). Philadelphia: Mosby; 2013. p. 15-26.
29. Renal System. Encyclopædia Britannica, : Encyclopædia Britannica Inc.; [updated June 15, 2018. Available from: https://www.britannica.com/science/human-renal-system
30. Pozzi A, Zent R. Hold tight or you'll fall off: CD151 helps podocytes stick in high-pressure situations. The Journal of Clinical Investigation. 2012;122(1):13-6.
31. Hale LJ, Coward RJ. Insulin signalling to the kidney in health and disease. Clin Sci (Lond). 2013;124(6):351-70.
32. Feher J. 7.2 - Functional Anatomy of the Kidneys and Overview of Kidney Function. In: Feher J, editor. Quantitative Human Physiology (Second Edition). Boston: Academic Press; 2017. p. 698-704.
33. Arif E, Nihalani D. Glomerular Filtration Barrier Assembly: An insight. Postdoc J. 2013;1(4):33-45.
34. Menon MC, Chuang PY, He CJ. The Glomerular Filtration Barrier: Components and Crosstalk. International Journal of Nephrology. 2012;2012:9.
35. Gluhovschi C, Gluhovschi G, Petrica L, Timar R, Velciov S, Ionita I, et al. Urinary Biomarkers in the Assessment of Early Diabetic Nephropathy. J Diabetes Res. 2016;2016:4626125.
36. Kriz W, Shirato I, Nagata M, LeHir M, Lemley KV. The podocyte's response to stress: the enigma of foot process effacement. Am J Physiol Renal Physiol. 2013;304(4):F333-47.
37. Glomerular Disease Primer : The Normal Kidney: National Institute of Diabetes and Digestive and Kidney Diseases (NIDDK); 2018 [cited 2018. Available from: https://www.niddk.nih.gov/research-funding/at-niddk/labs-branches/kidney-disease-branch/kidney-diseases-section/glomerular-disease-primer/-normal-kidney/Pages/normal-kidneys.aspx.
38. Brinkkoetter PT, Ising C, Benzing T. The role of the podocyte in albumin filtration. Nat Rev Nephrol. 2013;9(6):328-36.
39. Kriz W, Kaissling B. Chapter 20 - Structural Organization of the Mammalian Kidney. In: Alpern RJ, Moe OW, Caplan M, editors. Seldin and Giebisch's The Kidney (Fifth Edition): Academic Press; 2013. p. 595-691.

40. A standard nomenclature for structures of the kidney. Kidney International. 1988;33(1):1-7.
41. Zhai XY, Birn H, Jensen KB, Thomsen JS, Andreasen A, Christensen EI. Digital three-dimensional reconstruction and ultrastructure of the mouse proximal tubule. J Am Soc Nephrol. 2003;14(3):611-9.
42. Park J, Shrestha R, Qiu C, Kondo A, Huang S, Werth M, et al. Single-cell transcriptomics of the mouse kidney reveals potential cellular targets of kidney disease. Science. 2018.
43. Lee JW, Chou CL, Knepper MA. Deep Sequencing in Microdissected Renal Tubules Identifies Nephron Segment-Specific Transcriptomes. J Am Soc Nephrol. 2015;26(11):2669-77.
44. Reilly RF, Ellison DH. Mammalian Distal Tubule: Physiology, Pathophysiology, and Molecular Anatomy. Physiological Reviews. 2000;80(1):277-313.
45. Rozansky DJ, Cornwall T, Subramanya AR, Rogers S, Yang Y-F, David LL, et al. Aldosterone mediates activation of the thiazide-sensitive Na-Cl cotransporter through an SGK1 and WNK4 signaling pathway. The Journal of Clinical Investigation. 2009;119(9):2601-12.
46. Peti-Peterdi J, Harris RC. Macula densa sensing and signaling mechanisms of renin release. J Am Soc Nephrol. 2010;21(7):1093-6.
47. Feher J. 7.6 - Regulation of Fluid and Electrolyte Balance. In: Feher J, editor. Quantitative Human Physiology (Second Edition). Boston: Academic Press; 2017. p. 740-51.
48. Vallon V. Tubuloglomerular Feedback and the Control of Glomerular Filtration Rate. Physiology. 2003;18(4):169-74.
49. Tubular Reabsorption: Rice University; [Available from: https://opentextbc.ca/anatomyandphysiology/chapter/25-6-tubular-reabsorption/.
50. Webster AC, Nagler EV, Morton RL, Masson P. Chronic Kidney Disease. The Lancet. 2017;389(10075):1238-52.
51. Chapter 1: Definition and classification of CKD. Kidney International Supplements. 2013;3(1):19-62.
52. Kearney PM, Whelton M, Reynolds K, Muntner P, Whelton PK, He J. Global burden of hypertension: analysis of worldwide data. The Lancet. 2005;365(9455):217-23.
53. 2017 Annual Data Report. United States Renal Data System2018 [Available from: https://www.usrds.org/2017/view/Default.aspx.

54. ESRD Quaterly Update.: United States Renal Data System; 2018 [Available from: https://www.usrds.org/qtr/default.aspx.

55. Saran R, Robinson B, Abbott KC, Agodoa LYC, Bhave N, Bragg-Gresham J, et al. US Renal Data System 2017 Annual Data Report: Epidemiology of Kidney Disease in the United States. Am J Kidney Dis. 2018;71(3S1):A7.

56. Chronic Kidney Disease (CKD): Clinical Practice Recommendations For Primary Care Physicians And Healthcare Providers. American Society of Nephrology: Henry Ford Health System; 2011 [Available from: https://www.asn-online.org/education/training/fellows/HFHS_CKD_V6.pdf.

57. Skorecki K, Chertow GM, Marsden PA, Taal MW, Yu ASL. Brenner & Rector's the Kidney: Elsevier; 2016.

58. Lopez-Giacoman S, Madero M. Biomarkers in chronic kidney disease, from kidney function to kidney damage. World J Nephrol. 2015;4(1):57-73.

59. Reutens AT, Atkins RC. Epidemiology of diabetic nephropathy. Contributions to nephrology. 2011;170:1-7.

60. Nephropathy in Diabetes. Diabetes Care. 2004;27(suppl 1):s79-s83.

61. Gross JL, de Azevedo MJ, Silveiro SP, Canani LH, Caramori ML, Zelmanovitz T. Diabetic Nephropathy: Diagnosis, Prevention, and Treatment. Diabetes Care. 2005;28(1):164-76.

62. Anders H-J, Huber TB, Isermann B, Schiffer M. CKD in diabetes: diabetic kidney disease versus nondiabetic kidney disease. Nature Reviews Nephrology. 2018;14(6):361-77.

63. Reidy K, Kang HM, Hostetter T, Susztak K. Molecular mechanisms of diabetic kidney disease. The Journal of Clinical Investigation. 2014;124(6):2333-40.

64. Tervaert TW, Mooyaart AL, Amann K, Cohen AH, Cook HT, Drachenberg CB, et al. Pathologic classification of diabetic nephropathy. J Am Soc Nephrol. 2010;21(4):556-63.

65. Vallon V. The Mechanisms and Therapeutic Potential of SGLT2 Inhibitors in Diabetes Mellitus. Annual Review of Medicine. 2015;66(1):255-70.

66. Mauer SM, Steffes MW, Connett J, Najarian JS, Sutherland DER, Barbosa J. The Development of Lesions in the Glomerular Basement Membrane and Mesangium After Transplantation of Normal Kidneys to Diabetic Patients. Diabetes. 1983;32(10):948-52.

67. Mauer SM, Goetz FC, McHugh LE, Sutherland DER, Barbosa J, Najarian JS, et al. Long-Term Study of Normal Kidneys Transplanted Into Patients With Type I Diabetes. Diabetes. 1989;38(4):516-23.

68. Dronavalli S, Duka I, Bakris GL. The pathogenesis of diabetic nephropathy. Nature Clinical Practice Endocrinology &Amp; Metabolism. 2008;4:444.

69. Brownlee M. Biochemistry and molecular cell biology of diabetic complications. Nature. 2001;414:813.

70. Raptis AE, Viberti G. Pathogenesis of diabetic nephropathy. Experimental and clinical endocrinology & diabetes : official journal, German Society of Endocrinology [and] German Diabetes Association. 2001;109 Suppl 2:S424-37.

71. Forbes JM, Cooper ME, Oldfield MD, Thomas MC. Role of advanced glycation end products in diabetic nephropathy. J Am Soc Nephrol. 2003;14(8 Suppl 3):S254-8.

72. Makita Z, Radoff S, Rayfield EJ, Yang Z, Skolnik E, Delaney V, et al. Advanced Glycosylation End Products in Patients with Diabetic Nephropathy. New England Journal of Medicine. 1991;325(12):836-42.

73. Tanji N, Markowitz GS, Fu C, Kislinger T, Taguchi A, Pischetsrieder M, et al. Expression of advanced glycation end products and their cellular receptor RAGE in diabetic nephropathy and nondiabetic renal disease. J Am Soc Nephrol. 2000;11(9):1656-66.

74. Wendt TM, Tanji N, Guo J, Kislinger TR, Qu W, Lu Y, et al. RAGE drives the development of glomerulosclerosis and implicates podocyte activation in the pathogenesis of diabetic nephropathy. Am J Pathol. 2003;162(4):1123-37.

75. Tan AL, Sourris KC, Harcourt BE, Thallas-Bonke V, Penfold S, Andrikopoulos S, et al. Disparate effects on renal and oxidative parameters following RAGE deletion, AGE accumulation inhibition, or dietary AGE control in experimental diabetic nephropathy. Am J Physiol Renal Physiol. 2010;298(3):F763-70.

76. Yamamoto Y, Kato I, Doi T, Yonekura H, Ohashi S, Takeuchi M, et al. Development and prevention of advanced diabetic nephropathy in RAGE-overexpressing mice. J Clin Invest. 2001;108(2):261-8.

77. Vallon V, Komers R. Pathophysiology of the diabetic kidney. Compr Physiol. 2011;1(3):1175-232.

78. Noh H, King GL. The role of protein kinase C activation in diabetic nephropathy. Kidney Int Suppl. 2007(106):S49-53.

79. Menne J, Park JK, Boehne M, Elger M, Lindschau C, Kirsch T, et al. Diminished loss of proteoglycans and lack of albuminuria in protein kinase C-alpha-deficient diabetic mice. Diabetes. 2004;53(8):2101-9.

80. Menne J, Meier M, Park JK, Boehne M, Kirsch T, Lindschau C, et al. Nephrin loss in experimental diabetic nephropathy is prevented by deletion of protein kinase C alpha signaling in-vivo. Kidney International. 2006;70(8):1456-62.

81. Koya D, Jirousek MR, Lin YW, Ishii H, Kuboki K, King GL. Characterization of protein kinase C beta isoform activation on the gene expression of transforming growth factor-beta, extracellular matrix components, and prostanoids in the glomeruli of diabetic rats. J Clin Invest. 1997;100(1):115-26.

82. Tuttle KR, Bakris GL, Toto RD, McGill JB, Hu K, Anderson PW. The effect of ruboxistaurin on nephropathy in type 2 diabetes. Diabetes Care. 2005;28(11):2686-90.

83. Ma RC, Tam CH, Wang Y, Luk AO, Hu C, Yang X, et al. Genetic variants of the protein kinase C-beta 1 gene and development of end-stage renal disease in patients with type 2 diabetes. Jama. 2010;304(8):881-9.

84. Meier M, Menne J, Park JK, Holtz M, Gueler F, Kirsch T, et al. Deletion of protein kinase C-epsilon signaling pathway induces glomerulosclerosis and tubulointerstitial fibrosis in vivo. J Am Soc Nephrol. 2007;18(4):1190-8.

85. Das Evcimen N, King GL. The role of protein kinase C activation and the vascular complications of diabetes. Pharmacological Research. 2007;55(6):498-510.

86. Tilton RG, Chang K, Pugliese G, Eades DM, Province MA, Sherman WR, et al. Prevention of hemodynamic and vascular albumin filtration changes in diabetic rats by aldose reductase inhibitors. Diabetes. 1989;38(10):1258-70.

87. Ishii H, Tada H, Isogai S. An aldose reductase inhibitor prevents glucose-induced increase in transforming growth factor-β and protein kinase C activity in cultured human mesangial cells. Diabetologia. 1998;41(3):362-4.

88. Morrisey K, Steadman R, Williams JD, Phillips AO. Renal proximal tubular cell fibronectin accumulation in response to glucose is polyol pathway dependent. Kidney International. 1999;55(1):160-7.

89. Patney V, Whaley-Connell A, Bakris G. Hypertension Management in Diabetic Kidney Disease. Diabetes Spectr. 2015;28(3):175-80.

90. Van Buren PN, Toto R. Hypertension in diabetic nephropathy: epidemiology, mechanisms, and management. Adv Chronic Kidney Dis. 2011;18(1):28-41.

91. Ohishi M. Hypertension with diabetes mellitus: physiology and pathology. Hypertension research : official journal of the Japanese Society of Hypertension. 2018;41(6):389-93.

92. Neal B, Perkovic V, Mahaffey KW, de Zeeuw D, Fulcher G, Erondu N, et al. Canagliflozin and Cardiovascular and Renal Events in Type 2 Diabetes. New England Journal of Medicine. 2017;377(7):644-57.

93. Zinman B, Wanner C, Lachin JM, Fitchett D, Bluhmki E, Hantel S, et al. Empagliflozin, Cardiovascular Outcomes, and Mortality in Type 2 Diabetes. New England Journal of Medicine. 2015;373(22):2117-28.

94. Wanner C, Lachin JM, Inzucchi SE, Fitchett D, Mattheus M, George J, et al. Empagliflozin and Clinical Outcomes in Patients With Type 2 Diabetes Mellitus, Established Cardiovascular Disease, and Chronic Kidney Disease. Circulation. 2018;137(2):119-29.

95. Yamazaki D, Hitomi H, Nishiyama A. Hypertension with diabetes mellitus complications. Hypertension research : official journal of the Japanese Society of Hypertension. 2018;41(3):147-56.

96. Garud MS, Kulkarni YA. Hyperglycemia to nephropathy via transforming growth factor beta. Current diabetes reviews. 2014;10(3):182-9.

97. Chang AS, Hathaway CK, Smithies O, Kakoki M. Transforming growth factor-beta1 and diabetic nephropathy. Am J Physiol Renal Physiol. 2016;310(8):F689-f96.

98. McGaraughty S, Davis-Taber RA, Zhu CZ, Cole TB, Nikkel AL, Chhaya M, et al. Targeting Anti-TGF-beta Therapy to Fibrotic Kidneys with a Dual Specificity Antibody Approach. J Am Soc Nephrol. 2017;28(12):3616-26.

99. Ziyadeh FN, Hoffman BB, Han DC, Iglesias-De La Cruz MC, Hong SW, Isono M, et al. Long-term prevention of renal insufficiency, excess matrix gene expression, and glomerular mesangial matrix expansion by treatment with monoclonal antitransforming growth factor-beta antibody in db/db diabetic mice. Proceedings of the National Academy of Sciences of the United States of America. 2000;97(14):8015-20.

100. Traykova-Brauch M, Schönig K, Greiner O, Miloud T, Jauch A, Bode M, et al. An efficient and versatile system for acute and chronic modulation of renal tubular function in transgenic mice. Nature medicine. 2008;14(9):979-84.

101. Ronco P, Chatziantoniou C. Matrix metalloproteinases and matrix receptors in progression and reversal of kidney disease: therapeutic perspectives. Kidney International. 2008;74(7):873-8.

102. Zeisberg EM, Potenta SE, Sugimoto H, Zeisberg M, Kalluri R. Fibroblasts in kidney fibrosis emerge via endothelial-to-mesenchymal transition. J Am Soc Nephrol. 2008;19(12):2282-7.

103. Zeisberg EM, Tarnavski O, Zeisberg M, Dorfman AL, McMullen JR, Gustafsson E, et al. Endothelial-to-mesenchymal transition contributes to cardiac fibrosis. Nat Med. 2007;13(8):952-61.

104. LeBleu VS, Taduri G, O'Connell J, Teng Y, Cooke VG, Woda C, et al. Origin and Function of Myofibroblasts in Kidney Fibrosis. Nature medicine. 2013;19(8):1047-53.

105. Wang A, Ziyadeh FN, Lee EY, Pyagay PE, Sung SH, Sheardown SA, et al. Interference with TGF-beta signaling by Smad3-knockout in mice limits diabetic glomerulosclerosis without affecting albuminuria. Am J Physiol Renal Physiol. 2007;293(5):F1657-65.

106. Jha JC, Banal C, Chow BSM, Cooper ME, Jandeleit-Dahm K. Diabetes and Kidney Disease: Role of Oxidative Stress. Antioxidants & Redox Signaling. 2016;25(12):657-84.

107. Holmström KM, Finkel T. Cellular mechanisms and physiological consequences of redox-dependent signalling. Nature Reviews Molecular Cell Biology. 2014;15:411.

108. Schulz E, Jansen T, Wenzel P, Daiber A, Munzel T. Nitric oxide, tetrahydrobiopterin, oxidative stress, and endothelial dysfunction in hypertension. Antioxid Redox Signal. 2008;10(6):1115-26.

109. Giacco F, Brownlee M. Oxidative stress and diabetic complications. Circulation research. 2010;107(9):1058-70.

110. Susztak K, Raff AC, Schiffer M, Böttinger EP. Glucose-Induced Reactive Oxygen Species Cause Apoptosis of Podocytes and Podocyte Depletion at the Onset of Diabetic Nephropathy. Diabetes. 2006;55(1):225-33.

111. Sharma K. Mitochondrial Dysfunction in the Diabetic Kidney. In: Santulli G, editor. Mitochondrial Dynamics in Cardiovascular Medicine. Cham: Springer International Publishing; 2017. p. 553-62.
112. Declèves A-E, Mathew AV, Cunard R, Sharma K. AMPK Mediates the Initiation of Kidney Disease Induced by a High-Fat Diet. Journal of the American Society of Nephrology : JASN. 2011;22(10):1846-55.
113. Dugan LL, You Y-H, Ali SS, Diamond-Stanic M, Miyamoto S, DeCleves A-E, et al. AMPK dysregulation promotes diabetes-related reduction of superoxide and mitochondrial function. The Journal of Clinical Investigation. 2013;123(11):4888-99.
114. Sharma K, Karl B, Mathew AV, Gangoiti JA, Wassel CL, Saito R, et al. Metabolomics reveals signature of mitochondrial dysfunction in diabetic kidney disease. J Am Soc Nephrol. 2013;24(11):1901-12.
115. Touyz RM, Briones AM, Sedeek M, Burger D, Montezano AC. NOX isoforms and reactive oxygen species in vascular health. Molecular interventions. 2011;11(1):27-35.
116. You YH, Okada S, Ly S, Jandeleit-Dahm K, Barit D, Namikoshi T, et al. Role of Nox2 in diabetic kidney disease. Am J Physiol Renal Physiol. 2013;304(7):F840-8.
117. Rhee EP. NADPH Oxidase 4 at the Nexus of Diabetes, Reactive Oxygen Species, and Renal Metabolism. Journal of the American Society of Nephrology. 2016;27(2):337-9.
118. Yang Q, Wu F-r, Wang J-n, Gao L, Jiang L, Li H-D, et al. Nox4 in renal diseases: An update. Free Radical Biology and Medicine. 2018;124:466-72.
119. Gorin Y, Block K, Hernandez J, Bhandari B, Wagner B, Barnes JL, et al. Nox4 NAD(P)H oxidase mediates hypertrophy and fibronectin expression in the diabetic kidney. The Journal of biological chemistry. 2005;280(47):39616-26.
120. Thallas-Bonke V, Jha JC, Gray SP, Barit D, Haller H, Schmidt HHHW, et al. Nox-4 deletion reduces oxidative stress and injury by PKC-α-associated mechanisms in diabetic nephropathy. Physiological Reports. 2014;2(11):e12192.
121. Jha JC, Gray SP, Barit D, Okabe J, El-Osta A, Namikoshi T, et al. Genetic targeting or pharmacologic inhibition of NADPH oxidase nox4 provides renoprotection in long-term diabetic nephropathy. J Am Soc Nephrol. 2014;25(6):1237-54.

122. Jha JC, Thallas-Bonke V, Banal C, Gray SP, Chow BS, Ramm G, et al. Podocyte-specific Nox4 deletion affords renoprotection in a mouse model of diabetic nephropathy. Diabetologia. 2016;59(2):379-89.
123. Babelova A, Avaniadi D, Jung O, Fork C, Beckmann J, Kosowski J, et al. Role of Nox4 in murine models of kidney disease. Free Radic Biol Med. 2012;53(4):842-53.
124. You YH, Quach T, Saito R, Pham J, Sharma K. Metabolomics Reveals a Key Role for Fumarate in Mediating the Effects of NADPH Oxidase 4 in Diabetic Kidney Disease. J Am Soc Nephrol. 2016;27(2):466-81.
125. Safety and Efficacy of Oral GKT137831 in Patient With Type 2 Diabetes and Albuminuria. https://ClinicalTrials.gov/show/NCT02010242.
126. Teixeira G, Szyndralewiez C, Molango S, Carnesecchi S, Heitz F, Wiesel P, et al. Therapeutic potential of NADPH oxidase 1/4 inhibitors. British Journal of Pharmacology. 2017;174(12):1647-69.
127. Montezano AC, Burger D, Paravicini TM, Chignalia AZ, Yusuf H, Almasri M, et al. Nicotinamide adenine dinucleotide phosphate reduced oxidase 5 (Nox5) regulation by angiotensin II and endothelin-1 is mediated via calcium/calmodulin-dependent, rac-1-independent pathways in human endothelial cells. Circulation research. 2010;106(8):1363-73.
128. Holterman CE, Thibodeau J-F, Towaij C, Gutsol A, Montezano AC, Parks RJ, et al. Nephropathy and Elevated BP in Mice with Podocyte-Specific NADPH Oxidase 5 Expression. Journal of the American Society of Nephrology. 2014;25(4):784-97.
129. Jha JC, Banal C, Okabe J, Gray SP, Hettige T, Chow BSM, et al. NADPH Oxidase Nox5 Accelerates Renal Injury in Diabetic Nephropathy. Diabetes. 2017;66(10):2691-703.
130. Yu P, Han W, Villar VAM, Yang Y, Lu Q, Lee H, et al. Unique role of NADPH oxidase 5 in oxidative stress in human renal proximal tubule cells. Redox biology. 2014;2:570-9.
131. Quiroga B, Arroyo D, de Arriba G. Present and Future in the Treatment of Diabetic Kidney Disease. Journal of Diabetes Research. 2015;2015:801348.
132. Sesso HD, Buring JE, Christen WG, Kurth T, Belanger C, MacFadyen J, et al. Vitamins E and C in the prevention of cardiovascular disease in men: the Physicians' Health Study II randomized controlled trial. Jama. 2008;300(18):2123-33.

133. Akbar S, Bellary S, Griffiths HR. Dietary antioxidant interventions in type 2 diabetes patients: a meta-analysis. The British Journal of Diabetes & Vascular Disease. 2011;11(2):62-8.

134. Yusuf S, Dagenais G, Pogue J, Bosch J, Sleight P. Vitamin E supplementation and cardiovascular events in high-risk patients. The Heart Outcomes Prevention Evaluation Study Investigators. The New England journal of medicine. 2000;342(3):154-60.

135. Marchioli R, Levantesi G, Macchia A, Marfisi RM, Nicolosi GL, Tavazzi L, et al. Vitamin E increases the risk of developing heart failure after myocardial infarction: Results from the GISSI-Prevenzione trial. Journal of cardiovascular medicine (Hagerstown, Md). 2006;7(5):347-50.

136. Fukai T, Ushio-Fukai M. Superoxide Dismutases: Role in Redox Signaling, Vascular Function, and Diseases. Antioxidants & Redox Signaling. 2011;15(6):1583-606.

137. Fujita H, Fujishima H, Chida S, Takahashi K, Qi Z, Kanetsuna Y, et al. Reduction of Renal Superoxide Dismutase in Progressive Diabetic Nephropathy. Journal of the American Society of Nephrology : JASN. 2009;20(6):1303-13.

138. DeRubertis FR, Craven PA, Melhem MF. Acceleration of diabetic renal injury in the superoxide dismutase knockout mouse: effects of tempol. Metabolism. 2007;56(9):1256-64.

139. DeRubertis FR, Craven PA, Melhem MF, Salah EM. Attenuation of renal injury in db/db mice overexpressing superoxide dismutase: evidence for reduced superoxide-nitric oxide interaction. Diabetes. 2004;53(3):762-8.

140. Craven PA, Melhem MF, Phillips SL, DeRubertis FR. Overexpression of Cu2+/Zn2+ superoxide dismutase protects against early diabetic glomerular injury in transgenic mice. Diabetes. 2001;50(9):2114-25.

141. Safo MK, Musayev FN, Wu S-H, Abraham DJ, Ko T-P. Structure of tetragonal crystals of human erythrocyte catalase. Acta Crystallographica Section D. 2001;57(1):1-7.

142. Zhou Z, Kang YJ. Cellular and Subcellular Localization of Catalase in the Heart of Transgenic Mice. Journal of Histochemistry & Cytochemistry. 2000;48(5):585-94.

143. Sadi G, Eryilmaz N, Tütüncüoğlu E, Cingir Ş, Güray T. Changes in expression profiles of antioxidant enzymes in diabetic rat kidneys. Diabetes/Metabolism Research and Reviews. 2012;28(3):228-35.

144. Hwang I, Lee J, Huh JY, Park J, Lee HB, Ho Y-S, et al. Catalase Deficiency Accelerates Diabetic Renal Injury Through Peroxisomal Dysfunction. Diabetes. 2012;61(3):728-38.

145. Godin N, Liu F, Lau GJ, Brezniceanu M-L, Chénier I, Filep JG, et al. Catalase overexpression prevents hypertension and tubular apoptosis in angiotensinogen transgenic mice. Kidney International. 2010;77(12):1086-97.

146. Shi Y, Lo CS, Chenier I, Maachi H, Filep JG, Ingelfinger JR, et al. Overexpression of catalase prevents hypertension and tubulointerstitial fibrosis and normalization of renal angiotensin-converting enzyme-2 expression in Akita mice. American journal of physiology Renal physiology. 2013;304(11):F1335-46.

147. Rojo de la Vega M, Chapman E, Zhang DD. NRF2 and the Hallmarks of Cancer. Cancer Cell. 2018;34(1):21-43.

148. Motohashi H, Yamamoto M. Nrf2–Keap1 defines a physiologically important stress response mechanism. Trends in Molecular Medicine. 2004;10(11):549-57.

149. Rada P, Rojo AI, Chowdhry S, McMahon M, Hayes JD, Cuadrado A. SCF/{beta}-TrCP promotes glycogen synthase kinase 3-dependent degradation of the Nrf2 transcription factor in a Keap1-independent manner. Molecular and cellular biology. 2011;31(6):1121-33.

150. Wang H, Liu K, Geng M, Gao P, Wu X, Hai Y, et al. RXRalpha inhibits the NRF2-ARE signaling pathway through a direct interaction with the Neh7 domain of NRF2. Cancer research. 2013;73(10):3097-108.

151. Boutten A, Goven D, Artaud-Macari E, Boczkowski J, Bonay M. NRF2 targeting: a promising therapeutic strategy in chronic obstructive pulmonary disease. Trends in Molecular Medicine. 2011;17(7):363-71.

152. Tao S, Liu P, Luo G, Rojo de la Vega M, Chen H, Wu T, et al. p97 Negatively Regulates NRF2 by Extracting Ubiquitylated NRF2 from the KEAP1-CUL3 E3 Complex. Molecular and cellular biology. 2017.

153. McMahon M, Lamont DJ, Beattie KA, Hayes JD. Keap1 perceives stress via three sensors for the endogenous signaling molecules nitric oxide, zinc, and alkenals. Proceedings of the National Academy of Sciences. 2010;107(44):18838-43.

154. Baird L, Llères D, Swift S, Dinkova-Kostova AT. Regulatory flexibility in the Nrf2-mediated stress response is conferred by conformational cycling of the Keap1-Nrf2 protein complex. Proceedings of the National Academy of Sciences. 2013;110(38):15259-64.

155. Sun Z, Zhang S, Chan JY, Zhang DD. Keap1 controls postinduction repression of the Nrf2-mediated antioxidant response by escorting nuclear export of Nrf2. Molecular and cellular biology. 2007;27(18):6334-49.

156. Sun Z, Wu T, Zhao F, Lau A, Birch CM, Zhang DD. KPNA6 (Importin {alpha}7)-mediated nuclear import of Keap1 represses the Nrf2-dependent antioxidant response. Molecular and cellular biology. 2011;31(9):1800-11.

157. Ichimura Y, Waguri S, Sou YS, Kageyama S, Hasegawa J, Ishimura R, et al. Phosphorylation of p62 activates the Keap1-Nrf2 pathway during selective autophagy. Mol Cell. 2013;51(5):618-31.

158. Komatsu M, Kurokawa H, Waguri S, Taguchi K, Kobayashi A, Ichimura Y, et al. The selective autophagy substrate p62 activates the stress responsive transcription factor Nrf2 through inactivation of Keap1. Nature Cell Biology. 2010;12:213.

159. Ni HM, Woolbright BL, Williams J, Copple B, Cui W, Luyendyk JP, et al. Nrf2 promotes the development of fibrosis and tumorigenesis in mice with defective hepatic autophagy. Journal of hepatology. 2014;61(3):617-25.

160. Son TG, Camandola S, Mattson MP. Hormetic dietary phytochemicals. Neuromolecular Med. 2008;10(4):236-46.

161. Huang H-C, Nguyen T, Pickett CB. Phosphorylation of Nrf2 at Ser-40 by Protein Kinase C Regulates Antioxidant Response Element-mediated Transcription. Journal of Biological Chemistry. 2002;277(45):42769-74.

162. Hayes John D, Chowdhry S, Dinkova-Kostova Albena T, Sutherland C. Dual regulation of transcription factor Nrf2 by Keap1 and by the combined actions of β-TrCP and GSK-3. Biochemical Society Transactions. 2015;43(4):611-20.

163. Kaspar JW, Jaiswal AK. Antioxidant-induced phosphorylation of tyrosine 486 leads to rapid nuclear export of Bach1 that allows Nrf2 to bind to the antioxidant response element and activate defensive gene expression. The Journal of biological chemistry. 2010;285(1):153-62.

164. Merrell MD, Jackson JP, Augustine LM, Fisher CD, Slitt AL, Maher JM, et al. The Nrf2 activator oltipraz also activates the constitutive androstane receptor. Drug Metab Dispos. 2008;36(8):1716-21.

165. Zhang Y, Gordon GB. A strategy for cancer prevention: stimulation of the Nrf2-ARE signaling pathway. Mol Cancer Ther. 2004;3(7):885-93.

166. Ramos-Gomez M, Kwak MK, Dolan PM, Itoh K, Yamamoto M, Talalay P, et al. Sensitivity to carcinogenesis is increased and chemoprotective efficacy of enzyme inducers is lost in nrf2 transcription factor-deficient mice. Proceedings of the National Academy of Sciences of the United States of America. 2001;98(6):3410-5.
167. Iida K, Itoh K, Kumagai Y, Oyasu R, Hattori K, Kawai K, et al. Nrf2 is essential for the chemopreventive efficacy of oltipraz against urinary bladder carcinogenesis. Cancer research. 2004;64(18):6424-31.
168. Pietsch EC, Chan JY, Torti FM, Torti SV. Nrf2 mediates the induction of ferritin H in response to xenobiotics and cancer chemopreventive dithiolethiones. The Journal of biological chemistry. 2003;278(4):2361-9.
169. Kwak MK, Egner PA, Dolan PM, Ramos-Gomez M, Groopman JD, Itoh K, et al. Role of phase 2 enzyme induction in chemoprotection by dithiolethiones. Mutat Res. 2001;480-481:305-15.
170. Antras-Ferry J, Maheo K, Chevanne M, Dubos MP, Morel F, Guillouzo A, et al. Oltipraz stimulates the transcription of the manganese superoxide dismutase gene in rat hepatocytes. Carcinogenesis. 1997;18(11):2113-7.
171. Kelley MJ, Glaser EM, Herndon JE, 2nd, Becker F, Bhagat R, Zhang YJ, et al. Safety and efficacy of weekly oral oltipraz in chronic smokers. Cancer Epidemiol Biomarkers Prev. 2005;14(4):892-9.
172. Le Ferrec E, Lagadic-Gossmann D, Rauch C, Bardiau C, Maheo K, Massiere F, et al. Transcriptional induction of CYP1A1 by oltipraz in human Caco-2 cells is aryl hydrocarbon receptor- and calcium-dependent. The Journal of biological chemistry. 2002;277(27):24780-7.
173. Arlt A, Sebens S, Krebs S, Geismann C, Grossmann M, Kruse ML, et al. Inhibition of the Nrf2 transcription factor by the alkaloid trigonelline renders pancreatic cancer cells more susceptible to apoptosis through decreased proteasomal gene expression and proteasome activity. Oncogene. 2012;32:4825.
174. Boettler U, Sommerfeld K, Volz N, Pahlke G, Teller N, Somoza V, et al. Coffee constituents as modulators of Nrf2 nuclear translocation and ARE (EpRE)-dependent gene expression. J Nutr Biochem. 2011;22(5):426-40.
175. Zhao S, Ghosh A, Lo CS, Chenier I, Scholey JW, Filep JG, et al. Nrf2 Deficiency Upregulates Intrarenal Angiotensin-Converting Enzyme-2 and Angiotensin 1-7 Receptor

Expression and Attenuates Hypertension and Nephropathy in Diabetic Mice. Endocrinology. 2018;159(2):836-52.

176. Abdo S, Shi Y, Otoukesh A, Ghosh A, Lo CS, Chenier I, et al. Catalase overexpression prevents nuclear factor erythroid 2-related factor 2 stimulation of renal angiotensinogen gene expression, hypertension, and kidney injury in diabetic mice. Diabetes. 2014;63(10):3483-96.

177. Zhou J, Chan L, Zhou S. Trigonelline: a plant alkaloid with therapeutic potential for diabetes and central nervous system disease. Curr Med Chem. 2012;19(21):3523-31.

178. van Dijk AE, Olthof MR, Meeuse JC, Seebus E, Heine RJ, van Dam RM. Acute effects of decaffeinated coffee and the major coffee components chlorogenic acid and trigonelline on glucose tolerance. Diabetes Care. 2009;32(6):1023-5.

179. Hilal-Dandan R. Renin and Angiotensin. In: Brunton LL, Chabner BA, Knollmann BC, editors. Goodman & Gilman's: The Pharmacological Basis of Therapeutics, 12e. New York, NY: McGraw-Hill Education; 2015.

180. Paul M, Mehr AP, Kreutz R. Physiology of Local Renin-Angiotensin Systems. Physiological Reviews. 2006;86(3):747-803.

181. Zhuo JL, Ferrao FM, Zheng Y, Li XC. New Frontiers in the Intrarenal Renin-Angiotensin System: A Critical Review of Classical and New Paradigms. Frontiers in Endocrinology. 2013;4:166.

182. Kobori H, Nangaku M, Navar LG, Nishiyama A. The Intrarenal Renin-Angiotensin System: From Physiology to the Pathobiology of Hypertension and Kidney Disease. Pharmacological Reviews. 2007;59(3):251-87.

183. Burns KD, Homma T, Harris RC. The intrarenal renin-angiotensin system. Semin Nephrol. 1993;13(1):13-30.

184. Ingelfinger JR, Zuo WM, Fon EA, Ellison KE, Dzau VJ. In situ hybridization evidence for angiotensinogen messenger RNA in the rat proximal tubule. An hypothesis for the intrarenal renin angiotensin system. J Clin Invest. 1990;85(2):417-23.

185. Wang TT, Wu XH, Zhang SL, Chan JS. Effect of glucose on the expression of the angiotensinogen gene in opossum kidney cells. Kidney Int. 1998;53(2):312-9.

186. Seikaly MG, Arant BS, Jr., Seney FD, Jr. Endogenous angiotensin concentrations in specific intrarenal fluid compartments of the rat. J Clin Invest. 1990;86(4):1352-7.

187. Braam B, Mitchell KD, Fox J, Navar LG. Proximal tubular secretion of angiotensin II in rats. Am J Physiol. 1993;264(5 Pt 2):F891-8.
188. Lai KN, Leung JC, Lai KB, To WY, Yeung VT, Lai FM. Gene expression of the renin-angiotensin system in human kidney. J Hypertens. 1998;16(1):91-102.
189. Navar LG, Kobori H, Prieto-Carrasquero M. Intrarenal angiotensin II and hypertension. Curr Hypertens Rep. 2003;5(2):135-43.
190. Navar LG. The role of the kidneys in hypertension. J Clin Hypertens (Greenwich). 2005;7(9):542-9.
191. Sparks MA, Crowley SD, Gurley SB, Mirotsou M, Coffman TM. Classical Renin-Angiotensin system in kidney physiology. Compr Physiol. 2014;4(3):1201-28.
192. Nguyen G, Delarue F, Burckle C, Bouzhir L, Giller T, Sraer JD. Pivotal role of the renin/prorenin receptor in angiotensin II production and cellular responses to renin. J Clin Invest. 2002;109(11):1417-27.
193. Nguyen G, Burckle CA, Sraer JD. Renin/prorenin-receptor biochemistry and functional significance. Curr Hypertens Rep. 2004;6(2):129-32.
194. Ichihara A, Hayashi M, Kaneshiro Y, Suzuki F, Nakagawa T, Tada Y, et al. Inhibition of diabetic nephropathy by a decoy peptide corresponding to the "handle" region for nonproteolytic activation of prorenin. J Clin Invest. 2004;114(8):1128-35.
195. Kobori H, Ozawa Y, Suzaki Y, Prieto-Carrasquero MC, Nishiyama A, Shoji T, et al. Young Scholars Award Lecture: Intratubular angiotensinogen in hypertension and kidney diseases. Am J Hypertens. 2006;19(5):541-50.
196. Kobori H, Nishiyama A, Harrison-Bernard LM, Navar LG. Urinary angiotensinogen as an indicator of intrarenal Angiotensin status in hypertension. Hypertension. 2003;41(1):42-9.
197. Sachetelli S, Liu Q, Zhang SL, Liu F, Hsieh TJ, Brezniceanu ML, et al. RAS blockade decreases blood pressure and proteinuria in transgenic mice overexpressing rat angiotensinogen gene in the kidney. Kidney international. 2006;69(6):1016-23.
198. Liu F, Brezniceanu M-L, Wei C-C, Chénier I, Sachetelli S, Zhang S-L, et al. Overexpression of Angiotensinogen Increases Tubular Apoptosis in Diabetes. Journal of the American Society of Nephrology : JASN. 2008;19(2):269-80.

199. Yamamoto T, Hayashi K, Matsuda H, Kubota E, Tanaka H, Ogasawara Y, et al. In vivo visualization of angiotensin II- and tubuloglomerular feedback-mediated renal vasoconstriction. Kidney Int. 2001;60(1):364-9.
200. Loon N, Shemesh O, Morelli E, Myers BD. Effect of angiotensin II infusion on the human glomerular filtration barrier. Am J Physiol. 1989;257(4 Pt 2):F608-14.
201. Pagtalunan ME, Rasch R, Rennke HG, Meyer TW. Morphometric analysis of effects of angiotensin II on glomerular structure in rats. Am J Physiol. 1995;268(1 Pt 2):F82-8.
202. Hoffmann S, Podlich D, Hahnel B, Kriz W, Gretz N. Angiotensin II type 1 receptor overexpression in podocytes induces glomerulosclerosis in transgenic rats. J Am Soc Nephrol. 2004;15(6):1475-87.
203. Whaley-Connell AT, Chowdhury NA, Hayden MR, Stump CS, Habibi J, Wiedmeyer CE, et al. Oxidative stress and glomerular filtration barrier injury: role of the renin-angiotensin system in the Ren2 transgenic rat. Am J Physiol Renal Physiol. 2006;291(6):F1308-14.
204. Kota SK, Meher LK, Jammula S, Kota SK, Modi KD. ACE inhibitors or ARBs for diabetic nephropathy: the unrelenting debate. Diabetes Metab Syndr. 2012;6(4):215-7.
205. Wolf G, Neilson EG. Angiotensin II as a renal growth factor. J Am Soc Nephrol. 1993;3(9):1531-40.
206. Weigert C, Brodbeck K, Klopfer K, Haring HU, Schleicher ED. Angiotensin II induces human TGF-beta 1 promoter activation: similarity to hyperglycaemia. Diabetologia. 2002;45(6):890-8.
207. Marrero MB, Banes-Berceli AK, Stern DM, Eaton DC. Role of the JAK/STAT signaling pathway in diabetic nephropathy. Am J Physiol Renal Physiol. 2006;290(4):F762-8.
208. Pupilli C, Lasagni L, Romagnani P, Bellini F, Mannelli M, Misciglia N, et al. Angiotensin II stimulates the synthesis and secretion of vascular permeability factor/vascular endothelial growth factor in human mesangial cells. J Am Soc Nephrol. 1999;10(2):245-55.
209. Williams B, Baker AQ, Gallacher B, Lodwick D. Angiotensin II increases vascular permeability factor gene expression by human vascular smooth muscle cells. Hypertension. 1995;25(5):913-7.
210. Yang HY, Erdos EG, Levin Y. A dipeptidyl carboxypeptidase that converts angiotensin I and inactivates bradykinin. Biochim Biophys Acta. 1970;214(2):374-6.

211. Mann S, O'Brien KP. Once daily lisinopril and captopril in hypertension: a double blind comparison using ambulatory monitoring. N Z Med J. 1994;107(987):391-4.
212. Donoghue M, Hsieh F, Baronas E, Godbout K, Gosselin M, Stagliano N, et al. A novel angiotensin-converting enzyme-related carboxypeptidase (ACE2) converts angiotensin I to angiotensin 1-9. Circulation research. 2000;87(5):E1-9.
213. Tipnis SR, Hooper NM, Hyde R, Karran E, Christie G, Turner AJ. A human homolog of angiotensin-converting enzyme. Cloning and functional expression as a captopril-insensitive carboxypeptidase. The Journal of biological chemistry. 2000;275(43):33238-43.
214. Varagic J, Trask AJ, Jessup JA, Chappell MC, Ferrario CM. New angiotensins. J Mol Med (Berl). 2008;86(6):663-71.
215. Ye M, Wysocki J, Naaz P, Salabat MR, LaPointe MS, Batlle D. Increased ACE 2 and decreased ACE protein in renal tubules from diabetic mice: a renoprotective combination? Hypertension. 2004;43(5):1120-5.
216. Tikellis C, Johnston CI, Forbes JM, Burns WC, Burrell LM, Risvanis J, et al. Characterization of renal angiotensin-converting enzyme 2 in diabetic nephropathy. Hypertension. 2003;41(3):392-7.
217. Karnik SS, Unal H, Kemp JR, Tirupula KC, Eguchi S, Vanderheyden PML, et al. International Union of Basic and Clinical Pharmacology. XCIX. Angiotensin Receptors: Interpreters of Pathophysiological Angiotensinergic Stimuli. Pharmacological Reviews. 2015;67(4):754-819.
218. de Gasparo M, Catt KJ, Inagami T, Wright JW, Unger T. International Union of Pharmacology. XXIII. The Angiotensin II Receptors. Pharmacological Reviews. 2000;52(3):415-72.
219. Kaschina E, Unger T. Angiotensin AT1/AT2 receptors: regulation, signalling and function. Blood pressure. 2003;12(2):70-88.
220. Jones ES, Vinh A, McCarthy CA, Gaspari TA, Widdop RE. AT2 receptors: functional relevance in cardiovascular disease. Pharmacology & therapeutics. 2008;120(3):292-316.
221. Miura S, Karnik SS, Saku K. Constitutively active homo-oligomeric angiotensin II type 2 receptor induces cell signaling independent of receptor conformation and ligand stimulation. The Journal of biological chemistry. 2005;280(18):18237-44.

222. AbdAlla S, Lother H, Abdel-tawab AM, Quitterer U. The angiotensin II AT2 receptor is an AT1 receptor antagonist. The Journal of biological chemistry. 2001;276(43):39721-6.
223. Jin XH, Siragy HM, Carey RM. Renal interstitial cGMP mediates natriuresis by direct tubule mechanism. Hypertension. 2001;38(3):309-16.
224. Siragy HM, Inagami T, Ichiki T, Carey RM. Sustained hypersensitivity to angiotensin II and its mechanism in mice lacking the subtype-2 (AT₂) angiotensin receptor. Proceedings of the National Academy of Sciences. 1999;96(11):6506-10.
225. Santos RA, Ferreira AJ, Verano-Braga T, Bader M. Angiotensin-converting enzyme 2, angiotensin-(1-7) and Mas: new players of the renin-angiotensin system. J Endocrinol. 2013;216(2):R1-r17.
226. Xu P, Costa-Goncalves AC, Todiras M, Rabelo LA, Sampaio WO, Moura MM, et al. Endothelial dysfunction and elevated blood pressure in MAS gene-deleted mice. Hypertension. 2008;51(2):574-80.
227. Umanath K, Lewis JB. Update on Diabetic Nephropathy: Core Curriculum 2018. Am J Kidney Dis. 2018;71(6):884-95.
228. Dusing R. Mega clinical trials which have shaped the RAS intervention clinical practice. Ther Adv Cardiovasc Dis. 2016;10(3):133-50.
229. Galluzzi L, Vitale I, Aaronson SA, Abrams JM, Adam D, Agostinis P, et al. Molecular mechanisms of cell death: recommendations of the Nomenclature Committee on Cell Death 2018. Cell Death & Differentiation. 2018;25(3):486-541.
230. Gibert B, Mehlen P. Dependence Receptors and Cancer: Addiction to Trophic Ligands. Cancer research. 2015;75(24):5171-5.
231. Hotchkiss RS, Strasser A, McDunn JE, Swanson PE. Cell Death. New England Journal of Medicine. 2009;361(16):1570-83.
232. Nagata S. Fas ligand-induced apoptosis. Annu Rev Genet. 1999;33:29-55.
233. Adams JM. Ways of dying: multiple pathways to apoptosis. Genes & development. 2003;17(20):2481-95.
234. Delbridge AR, Grabow S, Strasser A, Vaux DL. Thirty years of BCL-2: translating cell death discoveries into novel cancer therapies. Nature reviews Cancer. 2016;16(2):99-109.
235. Doerflinger M, Glab JA, Puthalakath H. BH3-only proteins: a 20-year stock-take. The FEBS Journal. 2015;282(6):1006-16.

236. Delbridge ARD, Grabow S, Strasser A, Vaux DL. Thirty years of BCL-2: translating cell death discoveries into novel cancer therapies. Nature Reviews Cancer. 2016;16:99.

237. Chen ZX, Pervaiz S. Bcl-2 induces pro-oxidant state by engaging mitochondrial respiration in tumor cells. Cell death and differentiation. 2007;14(9):1617-27.

238. Velaithan R, Kang J, Hirpara JL, Loh T, Goh BC, Le Bras M, et al. The small GTPase Rac1 is a novel binding partner of Bcl-2 and stabilizes its antiapoptotic activity. Blood. 2011;117(23):6214-26.

239. Lindsten T, Ross AJ, King A, Zong WX, Rathmell JC, Shiels HA, et al. The combined functions of proapoptotic Bcl-2 family members bak and bax are essential for normal development of multiple tissues. Mol Cell. 2000;6(6):1389-99.

240. Wei MC, Zong WX, Cheng EH, Lindsten T, Panoutsakopoulou V, Ross AJ, et al. Proapoptotic BAX and BAK: a requisite gateway to mitochondrial dysfunction and death. Science. 2001;292(5517):727-30.

241. Chipuk JE, Moldoveanu T, Llambi F, Parsons MJ, Green DR. The BCL-2 Family Reunion. Molecular cell. 2010;37(3):299-310.

242. Doerflinger M, Glab JA, Puthalakath H. BH3-only proteins: a 20-year stock-take. FEBS J. 2015;282(6):1006-16.

243. Wei MC, Lindsten T, Mootha VK, Weiler S, Gross A, Ashiya M, et al. tBID, a membrane-targeted death ligand, oligomerizes BAK to release cytochrome c. Genes & development. 2000;14(16):2060-71.

244. Kang S, Song J, Kang J, Kang H, Lee D, Lee Y, et al. Suppression of the alpha-isoform of class II phosphoinositide 3-kinase gene expression leads to apoptotic cell death. Biochemical and biophysical research communications. 2005;329(1):6-10.

245. Happo L, Strasser A, Cory S. BH3-only proteins in apoptosis at a glance. Journal of cell science. 2012;125(Pt 5):1081-7.

246. Coultas L, Bouillet P, Stanley EG, Brodnicki TC, Adams JM, Strasser A. Proapoptotic BH3-Only Bcl-2 Family Member Bik/Blk/Nbk Is Expressed in Hemopoietic and Endothelial Cells but Is Redundant for Their Programmed Death. Molecular and cellular biology. 2004;24(4):1570-81.

247. Mebratu YA, Dickey BF, Evans C, Tesfaigzi Y. The BH3-only protein Bik/Blk/Nbk inhibits nuclear translocation of activated ERK1/2 to mediate IFNγ-induced cell death. The Journal of cell biology. 2008;183(3):429-39.
248. Moran C, Sanz-Rodriguez A, Jimenez-Pacheco A, Martinez-Villareal J, McKiernan RC, Jimenez-Mateos EM, et al. Bmf upregulation through the AMP-activated protein kinase pathway may protect the brain from seizure-induced cell death. Cell death & disease. 2013;4(4):e606.
249. Lau GJ, Godin N, Maachi H, Lo CS, Wu SJ, Zhu JX, et al. Bcl-2-modifying factor induces renal proximal tubular cell apoptosis in diabetic mice. Diabetes. 2012;61(2):474-84.
250. Puthalakath H, Villunger A, O'Reilly LA, Beaumont JG, Coultas L, Cheney RE, et al. Bmf: a proapoptotic BH3-only protein regulated by interaction with the myosin V actin motor complex, activated by anoikis. Science (New York, NY). 2001;293(5536):1829-32.
251. Labi V, Erlacher M, Kiessling S, Manzl C, Frenzel A, O'Reilly L, et al. Loss of the BH3-only protein Bmf impairs B cell homeostasis and accelerates γ irradiation–induced thymic lymphoma development. The Journal of Experimental Medicine. 2008;205(3):641-55.
252. Pinon JD, Labi V, Egle A, Villunger A. Bim and Bmf in tissue homeostasis and malignant disease. Oncogene. 2008;27 Suppl 1:S41-52.
253. Lei K, Davis RJ. JNK phosphorylation of Bim-related members of the Bcl2 family induces Bax-dependent apoptosis. Proceedings of the National Academy of Sciences of the United States of America. 2003;100(5):2432-7.
254. Girnius N, Davis RJ. JNK Promotes Epithelial Cell Anoikis by Transcriptional and Post-translational Regulation of BH3-Only Proteins. Cell Rep. 2017;21(7):1910-21.
255. Shao Y, Aplin AE. ERK2 phosphorylation of serine 77 regulates Bmf pro-apoptotic activity. Cell death & disease. 2012;3:e253.
256. Hubner A, Cavanagh-Kyros J, Rincon M, Flavell RA, Davis RJ. Functional cooperation of the proapoptotic Bcl2 family proteins Bmf and Bim in vivo. Molecular and cellular biology. 2010;30(1):98-105.
257. Zhang Y, Adachi M, Kawamura R, Imai K. Bmf is a possible mediator in histone deacetylase inhibitors FK228 and CBHA-induced apoptosis. Cell death and differentiation. 2006;13(1):129-40.

258. Schmelzle T, Mailleux AA, Overholtzer M, Carroll JS, Solimini NL, Lightcap ES, et al. Functional role and oncogene-regulated expression of the BH3-only factor Bmf in mammary epithelial anoikis and morphogenesis. Proceedings of the National Academy of Sciences of the United States of America. 2007;104(10):3787-92.
259. Labi V, Erlacher M, Kiessling S, Manzl C, Frenzel A, O'Reilly L, et al. Loss of the BH3-only protein Bmf impairs B cell homeostasis and accelerates gamma irradiation-induced thymic lymphoma development. The Journal of experimental medicine. 2008;205(3):641-55.
260. Gramantieri L, Fornari F, Ferracin M, Veronese A, Sabbioni S, Calin GA, et al. MicroRNA-221 targets Bmf in hepatocellular carcinoma and correlates with tumor multifocality. Clin Cancer Res. 2009;15(16):5073-81.
261. Xia HF, He TZ, Liu CM, Cui Y, Song PP, Jin XH, et al. MiR-125b expression affects the proliferation and apoptosis of human glioma cells by targeting Bmf. Cell Physiol Biochem. 2009;23(4-6):347-58.
262. Guo X, Xiang C, Zhang Z, Zhang F, Xi T, Zheng L. Displacement of Bax by BMF Mediates STARD13 3'UTR-Induced Breast Cancer Cells Apoptosis in an miRNA-Depedent Manner. Molecular pharmaceutics. 2018;15(1):63-71.
263. Morales AA, Olsson A, Celsing F, Osterborg A, Jondal M, Osorio LM. Expression and transcriptional regulation of functionally distinct Bmf isoforms in B-chronic lymphocytic leukemia cells. Leukemia. 2004;18(1):41-7.
264. Ramjaun AR, Tomlinson S, Eddaoudi A, Downward J. Upregulation of two BH3-only proteins, Bmf and Bim, during TGF beta-induced apoptosis. Oncogene. 2007;26(7):970-81.
265. Geuens T, Bouhy D, Timmerman V. The hnRNP family: insights into their role in health and disease. Hum Genet. 2016;135(8):851-67.
266. Abdo S, Lo CS, Chenier I, Shamsuyarova A, Filep JG, Ingelfinger JR, et al. Heterogeneous nuclear ribonucleoproteins F and K mediate insulin inhibition of renal angiotensinogen gene expression and prevention of hypertension and kidney injury in diabetic mice. Diabetologia. 2013;56(7):1649-60.
267. Ghosh A, Abdo S, Zhao S, Wu CH, Shi Y, Lo CS, et al. Insulin Inhibits Nrf2 Gene Expression via Heterogeneous Nuclear Ribonucleoprotein F/K in Diabetic Mice. Endocrinology. 2017;158(4):903-19.

268. Lo CS, Chang SY, Chenier I, Filep JG, Ingelfinger JR, Zhang SL, et al. Heterogeneous nuclear ribonucleoprotein F suppresses angiotensinogen gene expression and attenuates hypertension and kidney injury in diabetic mice. Diabetes. 2012;61(10):2597-608.
269. Lo CS, Shi Y, Chang SY, Abdo S, Chenier I, Filep JG, et al. Overexpression of heterogeneous nuclear ribonucleoprotein F stimulates renal Ace-2 gene expression and prevents TGF-beta1-induced kidney injury in a mouse model of diabetes. Diabetologia. 2015;58(10):2443-54.
270. Lo CS, Shi Y, Chenier I, Ghosh A, Wu CH, Cailhier JF, et al. Heterogeneous Nuclear Ribonucleoprotein F Stimulates Sirtuin-1 Gene Expression and Attenuates Nephropathy Progression in Diabetic Mice. Diabetes. 2017;66(7):1964-78.
271. Wei CC, Guo DF, Zhang SL, Ingelfinger JR, Chan JS. Heterogenous nuclear ribonucleoprotein F modulates angiotensinogen gene expression in rat kidney proximal tubular cells. J Am Soc Nephrol. 2005;16(3):616-28.
272. Wei CC, Zhang SL, Chen YW, Guo DF, Ingelfinger JR, Bomsztyk K, et al. Heterogeneous nuclear ribonucleoprotein K modulates angiotensinogen gene expression in kidney cells. The Journal of biological chemistry. 2006;281(35):25344-55.
273. Han SP, Tang YH, Smith R. Functional diversity of the hnRNPs: past, present and perspectives. Biochem J. 2010;430(3):379-92.
274. Bomsztyk K, Denisenko O, Ostrowski J. hnRNP K: One protein multiple processes. BioEssays. 2004;26(6):629-38.
275. Matunis MJ, Michael WM, Dreyfuss G. Characterization and primary structure of the poly(C)-binding heterogeneous nuclear ribonucleoprotein complex K protein. Molecular and cellular biology. 1992;12(1):164-71.
276. Siomi H, Matunis MJ, Michael WM, Dreyfuss G. The pre-mRNA binding K protein contains a novel evolutionarily conserved motif. Nucleic Acids Res. 1993;21(5):1193-8.
277. Matunis MJ, Xing J, Dreyfuss G. The hnRNP F protein: unique primary structure, nucleic acid-binding properties, and subcellular localization. Nucleic Acids Res. 1994;22(6):1059-67.
278. Dominguez C, Fisette JF, Chabot B, Allain FH. Structural basis of G-tract recognition and encaging by hnRNP F quasi-RRMs. Nat Struct Mol Biol. 2010;17(7):853-61.

279. Martinez-Contreras R, Fisette J-F, Nasim F-uH, Madden R, Cordeau M, Chabot B. Intronic Binding Sites for hnRNP A/B and hnRNP F/H Proteins Stimulate Pre-mRNA Splicing. PLOS Biology. 2006;4(2):e21.

280. Lee J, Pilch PF. The insulin receptor: structure, function, and signaling. Am J Physiol. 1994;266(2 Pt 1):C319-34.

281. Vienberg SG, Bouman SD, Sorensen H, Stidsen CE, Kjeldsen T, Glendorf T, et al. Receptor-isoform-selective insulin analogues give tissue-preferential effects. Biochem J. 2011;440(3):301-8.

282. White MF. Insulin Signaling in Health and Disease. Science. 2003;302(5651):1710-1.

283. Artunc F, Schleicher E, Weigert C, Fritsche A, Stefan N, Häring H-U. The impact of insulin resistance on the kidney and vasculature. Nature Reviews Nephrology. 2016;12:721.

284. Zhang W, Liu HT. MAPK signal pathways in the regulation of cell proliferation in mammalian cells. Cell Research. 2002;12:9.

285. Brosius FC, Alpers CE, Bottinger EP, Breyer MD, Coffman TM, Gurley SB, et al. Mouse Models of Diabetic Nephropathy. Journal of the American Society of Nephrology : JASN. 2009;20(12):2503-12.

286. Breyer MD, Bottinger E, Brosius FC, 3rd, Coffman TM, Harris RC, Heilig CW, et al. Mouse models of diabetic nephropathy. J Am Soc Nephrol. 2005;16(1):27-45.

287. Wang J, Takeuchi T, Tanaka S, Kubo SK, Kayo T, Lu D, et al. A mutation in the insulin 2 gene induces diabetes with severe pancreatic beta-cell dysfunction in the Mody mouse. J Clin Invest. 1999;103(1):27-37.

288. Alpers CE, Hudkins KL. Mouse models of diabetic nephropathy. Curr Opin Nephrol Hypertens. 2011;20(3):278-84.

289. Hummel KP, Dickie MM, Coleman DL. Diabetes, a new mutation in the mouse. Science. 1966;153(3740):1127-8.

290. Sharma K, McCue P, Dunn SR. Diabetic kidney disease in the db/db mouse. Am J Physiol Renal Physiol. 2003;284(6):F1138-44.

291. Lee SM, Bressler R. Prevention of diabetic nephropathy by diet control in the db/db mouse. Diabetes. 1981;30(2):106-11.

292. Deji N, Kume S, Araki S, Soumura M, Sugimoto T, Isshiki K, et al. Structural and functional changes in the kidneys of high-fat diet-induced obese mice. Am J Physiol Renal Physiol. 2009;296(1):F118-26.
293. Brosius FC, 3rd, Alpers CE, Bottinger EP, Breyer MD, Coffman TM, Gurley SB, et al. Mouse models of diabetic nephropathy. J Am Soc Nephrol. 2009;20(12):2503-12.
294. Betz B, Conway BR. An Update on the Use of Animal Models in Diabetic Nephropathy Research. Current diabetes reports. 2016;16:18.
295. Kakoki M, Takahashi N, Jennette JC, Smithies O. Diabetic nephropathy is markedly enhanced in mice lacking the bradykinin B2 receptor. Proceedings of the National Academy of Sciences of the United States of America. 2004;101(36):13302-5.
296. Thibodeau JF, Holterman CE, Burger D, Read NC, Reudelhuber TL, Kennedy CR. A novel mouse model of advanced diabetic kidney disease. PLoS One. 2014;9(12):e113459.
297. Gilbert RE. Proximal Tubulopathy: Prime Mover and Key Therapeutic Target in Diabetic Kidney Disease. Diabetes. 2017;66(4):791-800.
298. Gilbert RE, Cooper ME. The tubulointerstitium in progressive diabetic kidney disease: more than an aftermath of glomerular injury? Kidney Int. 1999;56(5):1627-37.
299. Bonventre JV. Can we target tubular damage to prevent renal function decline in diabetes? Semin Nephrol. 2012;32(5):452-62.
300. Drummond K, Mauer M. The early natural history of nephropathy in type 1 diabetes: II. Early renal structural changes in type 1 diabetes. Diabetes. 2002;51(5):1580-7.
301. Retinopathy and Nephropathy in Patients with Type 1 Diabetes Four Years after a Trial of Intensive Therapy. New England Journal of Medicine. 2000;342(6):381-9.
302. Remuzzi G, Macia M, Ruggenenti P. Prevention and Treatment of Diabetic Renal Disease in Type 2 Diabetes: The BENEDICT Study. Journal of the American Society of Nephrology. 2006;17(4 suppl 2):S90-S7.
303. Zhang SL, Filep JG, Hohman TC, Tang SS, Ingelfinger JR, Chan JS. Molecular mechanisms of glucose action on angiotensinogen gene expression in rat proximal tubular cells. Kidney Int. 1999;55(2):454-64.
304. Zhang SL, Tang SS, Chen X, Filep JG, Ingelfinger JR, Chan JS. High levels of glucose stimulate angiotensinogen gene expression via the P38 mitogen-activated protein kinase pathway in rat kidney proximal tubular cells. Endocrinology. 2000;141(12):4637-46.

305. Hsieh TJ, Fustier P, Zhang SL, Filep JG, Tang SS, Ingelfinger JR, et al. High glucose stimulates angiotensinogen gene expression and cell hypertrophy via activation of the hexosamine biosynthesis pathway in rat kidney proximal tubular cells. Endocrinology. 2003;144(10):4338-49.
306. Hsieh TJ, Zhang SL, Filep JG, Tang SS, Ingelfinger JR, Chan JS. High glucose stimulates angiotensinogen gene expression via reactive oxygen species generation in rat kidney proximal tubular cells. Endocrinology. 2002;143(8):2975-85.
307. Liu F, Brezniceanu ML, Wei CC, Chenier I, Sachetelli S, Zhang SL, et al. Overexpression of angiotensinogen increases tubular apoptosis in diabetes. J Am Soc Nephrol. 2008;19(2):269-80.
308. Lo CS, Liu F, Shi Y, Maachi H, Chenier I, Godin N, et al. Dual RAS blockade normalizes angiotensin-converting enzyme-2 expression and prevents hypertension and tubular apoptosis in Akita angiotensinogen-transgenic mice. Am J Physiol Renal Physiol. 2012;302(7):F840-52.
309. Brezniceanu ML, Liu F, Wei CC, Tran S, Sachetelli S, Zhang SL, et al. Catalase overexpression attenuates angiotensinogen expression and apoptosis in diabetic mice. Kidney Int. 2007;71(9):912-23.
310. Brezniceanu ML, Liu F, Wei CC, Chenier I, Godin N, Zhang SL, et al. Attenuation of interstitial fibrosis and tubular apoptosis in db/db transgenic mice overexpressing catalase in renal proximal tubular cells. Diabetes. 2008;57(2):451-9.
311. Kim HJ, Sato T, Rodriguez-Iturbe B, Vaziri ND. Role of intrarenal angiotensin system activation, oxidative stress, inflammation, and impaired nuclear factor-erythroid-2-related factor 2 activity in the progression of focal glomerulosclerosis. The Journal of pharmacology and experimental therapeutics. 2011;337(3):583-90.
312. Tan SM, Sharma A, Stefanovic N, Yuen DY, Karagiannis TC, Meyer C, et al. Derivative of bardoxolone methyl, dh404, in an inverse dose-dependent manner lessens diabetes-associated atherosclerosis and improves diabetic kidney disease. Diabetes. 2014;63(9):3091-103.
313. Wu QQ, Wang Y, Senitko M, Meyer C, Wigley WC, Ferguson DA, et al. Bardoxolone methyl (BARD) ameliorates ischemic AKI and increases expression of protective genes Nrf2, PPARγ, and HO-12011 2011-05-01 00:00:00. F1180-F92 p.
314. Zhao S, Ghosh A, Lo CS, Chenier I, Scholey JW, Filep JG, et al. Nrf2 Deficiency Upregulates Intrarenal Angiotensin-converting Enzyme-2 and Angiotensin 1-7 Receptor

Expression and Attenuates Hypertension and Nephropathy in Diabetic Mice. Endocrinology. 2017.

315. Zoja C, Corna D, Nava V, Locatelli M, Abbate M, Gaspari F, et al. Analogs of bardoxolone methyl worsen diabetic nephropathy in rats with additional adverse effects. Am J Physiol Renal Physiol. 2013;304(6):F808-19.

316. de Zeeuw D, Akizawa T, Audhya P, Bakris GL, Chin M, Christ-Schmidt H, et al. Bardoxolone methyl in type 2 diabetes and stage 4 chronic kidney disease. The New England journal of medicine. 2013;369(26):2492-503.

317. Chen X, Zhang SL, Pang L, Filep JG, Tang SS, Ingelfinger JR, et al. Characterization of a putative insulin-responsive element and its binding protein(s) in rat angiotensinogen gene promoter: regulation by glucose and insulin. Endocrinology. 2001;142(6):2577-85.

318. Grespi F, Soratroi C, Krumschnabel G, Sohm B, Ploner C, Geley S, et al. BH3-only protein Bmf mediates apoptosis upon inhibition of CAP-dependent protein synthesis. Cell death and differentiation. 2010;17(11):1672-83.

319. Venugopal R, Jaiswal AK. Nrf1 and Nrf2 positively and c-Fos and Fra1 negatively regulate the human antioxidant response element-mediated expression of NAD(P)H:quinone oxidoreductase1 gene. Proceedings of the National Academy of Sciences of the United States of America. 1996;93(25):14960-5.

320. Motohashi H, Yamamoto M. Nrf2-Keap1 defines a physiologically important stress response mechanism. Trends in molecular medicine. 2004;10(11):549-57.

321. Surh YJ, Kundu JK, Na HK. Nrf2 as a master redox switch in turning on the cellular signaling involved in the induction of cytoprotective genes by some chemopreventive phytochemicals. Planta medica. 2008;74(13):1526-39.

322. Jiang T, Huang Z, Lin Y, Zhang Z, Fang D, Zhang DD. The protective role of Nrf2 in streptozotocin-induced diabetic nephropathy. Diabetes. 2010;59(4):850-60.

323. Zheng H, Whitman SA, Wu W, Wondrak GT, Wong PK, Fang D, et al. Therapeutic potential of Nrf2 activators in streptozotocin-induced diabetic nephropathy. Diabetes. 2011;60(11):3055-66.

324. Yore MM, Liby KT, Honda T, Gribble GW, Sporn MB. The synthetic triterpenoid 1-[2-cyano-3,12-dioxooleana-1,9(11)-dien-28-oyl]imidazole blocks nuclear factor-kappaB

activation through direct inhibition of IkappaB kinase beta. Molecular cancer therapeutics. 2006;5(12):3232-9.

325. Liby K, Voong N, Williams CR, Risingsong R, Royce DB, Honda T, et al. The synthetic triterpenoid CDDO-Imidazolide suppresses STAT phosphorylation and induces apoptosis in myeloma and lung cancer cells. Clinical cancer research : an official journal of the American Association for Cancer Research. 2006;12(14 Pt 1):4288-93.

326. Pergola PE, Raskin P, Toto RD, Meyer CJ, Huff JW, Grossman EB, et al. Bardoxolone methyl and kidney function in CKD with type 2 diabetes. The New England journal of medicine. 2011;365(4):327-36.

327. de Zeeuw D, Akizawa T, Audhya P, Bakris GL, Chin M, Christ-Schmidt H, et al. Bardoxolone methyl in type 2 diabetes and stage 4 chronic kidney disease. The New England journal of medicine. 2013;369(26):2492-503.

328. Coletta DK, Balas B, Chavez AO, Baig M, Abdul-Ghani M, Kashyap SR, et al. Effect of acute physiological hyperinsulinemia on gene expression in human skeletal muscle in vivo. American journal of physiology Endocrinology and metabolism. 2008;294(5):E910-7.

329. Korsheninnikova E, Voshol PJ, Baan B, van der Zon GC, Havekes LM, Romijn JA, et al. Dynamics of insulin signalling in liver during hyperinsulinemic euglycaemic clamp conditions in vivo and the effects of high-fat feeding in male mice. Archives of physiology and biochemistry. 2007;113(4-5):173-85.

330. Hsieh TJ, Fustier P, Wei CC, Zhang SL, Filep JG, Tang SS, et al. Reactive oxygen species blockade and action of insulin on expression of angiotensinogen gene in proximal tubular cells. J Endocrinol. 2004;183(3):535-50.

331. Chan JS, Chan AH, Jiang Q, Nie ZR, LaChance S, Carriere S. Molecular cloning and expression of the rat angiotensinogen gene. Pediatric nephrology. 1990;4(4):429-35.

332. Wang L, Lei C, Zhang SL, Roberts KD, Tang SS, Ingelfinger JR, et al. Synergistic effect of dexamethasone and isoproterenol on the expression of angiotensinogen in immortalized rat proximal tubular cells. Kidney Int. 1998;53(2):287-95.

333. Alquier T, Peyot ML, Latour MG, Kebede M, Sorensen CM, Gesta S, et al. Deletion of GPR40 impairs glucose-induced insulin secretion in vivo in mice without affecting intracellular fuel metabolism in islets. Diabetes. 2009;58(11):2607-15.

334. Godin N, Liu F, Lau GJ, Brezniceanu ML, Chenier I, Filep JG, et al. Catalase overexpression prevents hypertension and tubular apoptosis in angiotensinogen transgenic mice. Kidney Int. 2010;77(12):1086-97.
335. Tang SS, Jung F, Diamant D, Brown D, Bachinsky D, Hellman P, et al. Temperature-sensitive SV40 immortalized rat proximal tubule cell line has functional renin-angiotensin system. Am J Physiol. 1995;268(3 Pt 2):F435-46.
336. The Diabetes Control and Complications Trial Research Group. The effect of intensive treatment of diabetes on the development and progression of long-term complications in insulin-dependent diabetes mellitus. The Diabetes Control and Complications Trial Research Group. The New England journal of medicine. 1993;329(14):977-86.
337. The Diabetes Control and Complications Trial/Epidemiology of Diabetes Interventions and Complications Research Groups. Retinopathy and nephropathy in patients with type 1 diabetes four years after a trial of intensive insulin therapy. The New England journal of medicine. 2000;342:381-89.
338. de Boer IH, Rue TC, Cleary PA, Lachin JM, Molitch ME, Steffes MW, et al. Long-term renal outcomes of patients with type 1 diabetes mellitus and microalbuminuria: an analysis of the Diabetes Control and Complications Trial/Epidemiology of Diabetes Interventions and Complications cohort. Arch Intern Med. 2011;171(5):412-20.
339. Dzau VJ, Ingelfinger JR. Molecular biology and pathophysiology of the intrarenal renin-angiotensin system. J Hypertens Suppl. 1989;7(7):S3-8.
340. Johnston CI, Fabris B, Jandeleit K. Intrarenal renin-angiotensin system in renal physiology and pathophysiology. Kidney international Supplement. 1993;42:S59-63.
341. Loghman-Adham M, Rohrwasser A, Helin C, Zhang S, Terreros D, Inoue I, et al. A conditionally immortalized cell line from murine proximal tubule. Kidney international. 1997;52(1):229-39.
342. Wolf G, Neilson EG. Angiotensin II as a hypertrophogenic cytokine for proximal tubular cells. Kidney international Supplement. 1993;39:S100-7.
343. Yoshioka M, Kayo T, Ikeda T, Koizumi A. A novel locus, Mody4, distal to D7Mit189 on chromosome 7 determines early-onset NIDDM in nonobese C57BL/6 (Akita) mutant mice. Diabetes. 1997;46(5):887-94.

344. Lizotte F, Denhez B, Guay A, Gevry N, Cote AM, Geraldes P. Persistent Insulin Resistance in Podocytes Caused by Epigenetic Changes of SHP-1 in Diabetes. Diabetes. 2016;65(12):3705-17.
345. Salem ES, Grobe N, Elased KM. Insulin treatment attenuates renal ADAM17 and ACE2 shedding in diabetic Akita mice. American journal of physiology Renal physiology. 2014;306(6):F629-39.
346. Sun Z, Huang Z, Zhang DD. Phosphorylation of Nrf2 at multiple sites by MAP kinases has a limited contribution in modulating the Nrf2-dependent antioxidant response. PLoS One. 2009;4(8):e6588.
347. Zhang SL, Chen X, Filep JG, Tang SS, Ingelfinger JR, Chan JS. Insulin inhibits angiotensinogen gene expression via the mitogen-activated protein kinase pathway in rat kidney proximal tubular cells. Endocrinology. 1999;140(11):5285-92.
348. Zhang SL, Chen X, Wei CC, Filep JG, Tang SS, Ingelfinger JR, et al. Insulin inhibits dexamethasone effect on angiotensinogen gene expression and induction of hypertrophy in rat kidney proximal tubular cells in high glucose. Endocrinology. 2002;143(12):4627-35.
349. Huang HC, Nguyen T, Pickett CB. Phosphorylation of Nrf2 at Ser-40 by protein kinase C regulates antioxidant response element-mediated transcription. The Journal of biological chemistry. 2002;277(45):42769-74.
350. Niture SK, Jain AK, Jaiswal AK. Antioxidant-induced modification of INrf2 cysteine 151 and PKC-delta-mediated phosphorylation of Nrf2 serine 40 are both required for stabilization and nuclear translocation of Nrf2 and increased drug resistance. Journal of cell science. 2009;122(Pt 24):4452-64.
351. Hu S, Xie Z, Onishi A, Yu X, Jiang L, Lin J, et al. Profiling the human protein-DNA interactome reveals ERK2 as a transcriptional repressor of interferon signaling. Cell. 2009;139(3):610-22.
352. Kwak MK, Itoh K, Yamamoto M, Kensler TW. Enhanced expression of the transcription factor Nrf2 by cancer chemopreventive agents: role of antioxidant response element-like sequences in the nrf2 promoter. Molecular and cellular biology. 2002;22(9):2883-92.
353. Chen Y, Schnetz MP, Irarrazabal CE, Shen RF, Williams CK, Burg MB, et al. Proteomic identification of proteins associated with the osmoregulatory transcription factor

TonEBP/OREBP: functional effects of Hsp90 and PARP-1. American journal of physiology Renal physiology. 2007;292(3):F981-92.

354. Wang E, Aslanzadeh V, Papa F, Zhu H, de la Grange P, Cambi F. Global profiling of alternative splicing events and gene expression regulated by hnRNPH/F. PLoS One. 2012;7(12):e51266.

355. Chin MP, Reisman SA, Bakris GL, O'Grady M, Linde PG, McCullough PA, et al. Mechanisms contributing to adverse cardiovascular events in patients with type 2 diabetes mellitus and stage 4 chronic kidney disease treated with bardoxolone methyl. American journal of nephrology. 2014;39(6):499-508.

356. Chin MP, Wrolstad D, Bakris GL, Chertow GM, de Zeeuw D, Goldsberry A, et al. Risk factors for heart failure in patients with type 2 diabetes mellitus and stage 4 chronic kidney disease treated with bardoxolone methyl. Journal of cardiac failure. 2014;20(12):953-8.

357. Van Laecke S, Van Biesen W, Vanholder R. The paradox of bardoxolone methyl: a call for every witness on the stand? Diabetes, obesity & metabolism. 2015;17(1):9-14.

358. Mann JF, Green D, Jamerson K, Ruilope LM, Kuranoff SJ, Littke T, et al. Avosentan for overt diabetic nephropathy. J Am Soc Nephrol. 2010;21(3):527-35.

359. Schainuck LI, Striker GE, Cutler RE, Benditt EP. Structural-functional correlations in renal disease. II. The correlations. Human pathology. 1970;1(4):631-41.

360. Javaid B, Olson JL, Meyer TW. Glomerular injury and tubular loss in adriamycin nephrosis. Journal of the American Society of Nephrology : JASN. 2001;12(7):1391-400.

361. Marcussen N. Tubulointerstitial damage leads to atubular glomeruli: significance and possible role in progression. Nephrology, dialysis, transplantation : official publication of the European Dialysis and Transplant Association - European Renal Association. 2000;15 Suppl 6:74-5.

362. Lindop GB, Gibson IW, Downie TT, Vass D, Cohen EP. The glomerulo-tubular junction: a target in renal diseases. The Journal of pathology. 2002;197(1):1-3.

363. Najafian B, Kim Y, Crosson JT, Mauer M. Atubular glomeruli and glomerulotubular junction abnormalities in diabetic nephropathy. Journal of the American Society of Nephrology : JASN. 2003;14(4):908-17.

364. Najafian B, Crosson JT, Kim Y, Mauer M. Glomerulotubular junction abnormalities are associated with proteinuria in type 1 diabetes. Journal of the American Society of Nephrology : JASN. 2006;17(4 Suppl 2):S53-60.

365. Nagata S. Apoptosis by death factor. Cell. 1997;88(3):355-65.

366. Kang BP, Frencher S, Reddy V, Kessler A, Malhotra A, Meggs LG. High glucose promotes mesangial cell apoptosis by oxidant-dependent mechanism. American journal of physiology Renal physiology. 2003;284(3):F455-66.

367. Allen DA, Harwood S, Varagunam M, Raftery MJ, Yaqoob MM. High glucose-induced oxidative stress causes apoptosis in proximal tubular epithelial cells and is mediated by multiple caspases. FASEB J. 2003;17(8):908-10.

368. Kumar D, Zimpelmann J, Robertson S, Burns KD. Tubular and interstitial cell apoptosis in the streptozotocin-diabetic rat kidney. Nephron Experimental nephrology. 2004;96(3):e77-88.

369. Kumar D, Robertson S, Burns KD. Evidence of apoptosis in human diabetic kidney. Molecular and cellular biochemistry. 2004;259(1-2):67-70.

370. Mishra R, Emancipator SN, Kern T, Simonson MS. High glucose evokes an intrinsic proapoptotic signaling pathway in mesangial cells. Kidney international. 2005;67(1):82-93.

371. de Boer IH, Kestenbaum B, Rue TC, Steffes MW, Cleary PA, Molitch ME, et al. Insulin therapy, hyperglycemia, and hypertension in type 1 diabetes mellitus. Arch Intern Med. 2008;168(17):1867-73.

372. Puthalakath H, Strasser A. Keeping killers on a tight leash: transcriptional and post-translational control of the pro-apoptotic activity of BH3-only proteins. Cell Death Differ. 2002;9(5):505-12.

373. Legouis D, Bataille A, Hertig A, Vandermeersch S, Simon N, Rondeau E, et al. Ex vivo analysis of renal proximal tubular cells. BMC cell biology. 2015;16:12.

374. Day CL, Puthalakath H, Skea G, Strasser A, Barsukov I, Lian LY, et al. Localization of dynein light chains 1 and 2 and their pro-apoptotic ligands. The Biochemical journal. 2004;377(Pt 3):597-605.

375. Pfeiffer S, Halang L, Düssmann H, Byrne MM, Prehn JHM. BH3-Only protein bmf is required for the maintenance of glucose homeostasis in an in vivo model of HNF1α-MODY diabetes. Cell Death Discovery. 2015;1:15041.

376. Grgic I, Campanholle G, Bijol V, Wang C, Sabbisetti VS, Ichimura T, et al. Targeted proximal tubule injury triggers interstitial fibrosis and glomerulosclerosis. Kidney Int. 2012;82(2):172-83.

377. Afsar B, Afsar RE, Dagel T, Kaya E, Erus S, Ortiz A, et al. Capillary rarefaction from the kidney point of view. Clinical Kidney Journal. 2018;11(3):295-301.

378. Schelling JR. Tubular atrophy in the pathogenesis of chronic kidney disease progression. Pediatric nephrology (Berlin, Germany). 2016;31(5):693-706.

379. Ding Y, Sigmund CD. Androgen-dependent regulation of human angiotensinogen expression in KAP-hAGT transgenic mice. Am J Physiol Renal Physiol. 2001;280(1):F54-60.

380. Veniant M, Heudes D, Clozel JP, Bruneval P, Menard J. Calcium blockade versus ACE inhibition in clipped and unclipped kidneys of 2K-1C rats. Kidney Int. 1994;46(2):421-9.

381. Weibel E. Numerical density: shape and size of particles. Stereological Methods. 1980;2:149-52.

382. Gundersen HJG. The nucleator. Journal of Microscopy. 1988;151(1):3-21.

383. Haseyama T, Fujita T, Hirasawa F, Tsukada M, Wakui H, Komatsuda A, et al. Complications of IgA nephropathy in a non-insulin-dependent diabetes model, the Akita mouse. Tohoku J Exp Med. 2002;198(4):233-44.

384. Ueno Y, Horio F, Uchida K, Naito M, Nomura H, Kato Y, et al. Increase in oxidative stress in kidneys of diabetic Akita mice. Biosci Biotechnol Biochem. 2002;66(4):869-72.

385. Schein PS, Loftus S. Streptozotocin: depression of mouse liver pyridine nucleotides. Cancer research. 1968;28(8):1501-6.

386. Schacht RG, Feiner HD, Gallo GR, Lieberman A, Baldwin DS. Nephrotoxicity of nitrosoureas. Cancer. 1981;48(6):1328-34.

387. Palm F, Ortsater H, Hansell P, Liss P, Carlsson PO. Differentiating between effects of streptozotocin per se and subsequent hyperglycemia on renal function and metabolism in the streptozotocin-diabetic rat model. Diabetes Metab Res Rev. 2004;20(6):452-9.

388. Gilbert SJ, Weiner DE, Gipson DS, Perazella MA, Tonelli M, National Kidney F. National Kidney Foundation's primer on kidney diseases. Sixth edition.. ed: Philadelphia : Elsevier/Saunders; 2014.

389. Tay YC, Wang Y, Kairaitis L, Rangan GK, Zhang C, Harris DC. Can murine diabetic nephropathy be separated from superimposed acute renal failure? Kidney Int. 2005;68(1):391-8.

390. Navar LG, Harrison-Bernard LM, Nishiyama A, Kobori H. Regulation of intrarenal angiotensin II in hypertension. Hypertension. 2002;39(2 Pt 2):316-22.

391. Saito T, Urushihara M, Kotani Y, Kagami S, Kobori H. Increased urinary angiotensinogen is precedent to increased urinary albumin in patients with type 1 diabetes. The American journal of the medical sciences. 2009;338(6):478-80.

392. Kobori H, Urushihara M, Xu JH, Berenson GS, Navar LG. Urinary angiotensinogen is correlated with blood pressure in men (Bogalusa Heart Study). Journal of hypertension. 2010;28(7):1422-8.

393. Navar LG, Prieto MC, Satou R, Kobori H. Intrarenal angiotensin II and its contribution to the genesis of chronic hypertension. Current opinion in pharmacology. 2011;11(2):180-6.

394. Saccomani G, Mitchell KD, Navar LG. Angiotensin II stimulation of Na(+)-H+ exchange in proximal tubule cells. Am J Physiol. 1990;258(5 Pt 2):F1188-95.

395. Navar LG, Harrison-Bernard LM, Wang CT, Cervenka L, Mitchell KD. Concentrations and actions of intraluminal angiotensin II. J Am Soc Nephrol. 1999;10 Suppl 11:S189-95.

396. Batlle D, Wysocki J, Soler MJ, Ranganath K. Angiotensin-converting enzyme 2: enhancing the degradation of angiotensin II as a potential therapy for diabetic nephropathy. Kidney Int. 2012;81(6):520-8.

397. Ingelfinger JR. Angiotensin-converting enzyme 2: implications for blood pressure and kidney disease. Curr Opin Nephrol Hypertens. 2009;18(1):79-84.

398. Koka V, Huang XR, Chung AC, Wang W, Truong LD, Lan HY. Angiotensin II up-regulates angiotensin I-converting enzyme (ACE), but down-regulates ACE2 via the AT1-ERK/p38 MAP kinase pathway. Am J Pathol. 2008;172(5):1174-83.

399. Mizuiri S, Hemmi H, Arita M, Ohashi Y, Tanaka Y, Miyagi M, et al. Expression of ACE and ACE2 in individuals with diabetic kidney disease and healthy controls. Am J Kidney Dis. 2008;51(4):613-23.

400. Liu F, Wei C-C, Wu S-J, Chenier I, Zhang S-L, Filep JG, et al. Apocynin attenuates tubular apoptosis and tubulointerstitial fibrosis in transgenic mice independent of hypertension. Kidney Int. 2008;75(2):156-66.

401. Yusuf S, Dagenais G, Pogue J, Bosch J, Sleight P. Vitamin E supplementation and cardiovascular events in high-risk patients. The New England journal of medicine. 2000;342(3):154-60.
402. Akizawa T, Asano Y, Morita S, Wakita T, Onishi Y, Fukuhara S, et al. Effect of a Carbonaceous Oral Adsorbent on the Progression of CKD: A Multicenter, Randomized, Controlled Trial. American Journal of Kidney Diseases. 2009;54(3):459-67.
403. Schulman G, Berl T, Beck GJ, Remuzzi G, Ritz E, Arita K, et al. Randomized Placebo-Controlled EPPIC Trials of AST-120 in CKD. Journal of the American Society of Nephrology : JASN. 2015;26(7):1732-46.
404. Ristow M. Unraveling the truth about antioxidants: mitohormesis explains ROS-induced health benefits. Nat Med. 2014;20(7):709-11.
405. Chen J, Siriki R. Antioxidants Therapy for Patients with Chronic Kidney Disease: A Question of Balance. American journal of nephrology. 2015;42(4):318-9.
406. Nezu M, Suzuki N, Yamamoto M. Targeting the KEAP1-NRF2 System to Prevent Kidney Disease Progression. American journal of nephrology. 2017;45(6):473-83.
407. Ho YS, Xiong Y, Ma W, Spector A, Ho DS. Mice lacking catalase develop normally but show differential sensitivity to oxidant tissue injury. The Journal of biological chemistry. 2004;279(31):32804-12.
408. Kang YJ, Chen Y, Epstein PN. Suppression of doxorubicin cardiotoxicity by overexpression of catalase in the heart of transgenic mice. The Journal of biological chemistry. 1996;271(21):12610-6.
409. Kobayashi M, Sugiyama H, Wang DH, Toda N, Maeshima Y, Yamasaki Y, et al. Catalase deficiency renders remnant kidneys more susceptible to oxidant tissue injury and renal fibrosis in mice. Kidney Int. 2005;68(3):1018-31.
410. Ungvari Z, Bailey-Downs L, Gautam T, Jimenez R, Losonczy G, Zhang C, et al. Adaptive induction of NF-E2-related factor-2-driven antioxidant genes in endothelial cells in response to hyperglycemia. American journal of physiology Heart and circulatory physiology. 2011;300(4):H1133-40.
411. Aleksunes LM, Goedken MJ, Rockwell CE, Thomale J, Manautou JE, Klaassen CD. Transcriptional regulation of renal cytoprotective genes by Nrf2 and its potential use as a

therapeutic target to mitigate cisplatin-induced nephrotoxicity. The Journal of pharmacology and experimental therapeutics. 2010;335(1):2-12.

412. Dodson M, de la Vega MR, Cholanians AB, Schmidlin CJ, Chapman E, Zhang DD. Modulating NRF2 in Disease: Timing Is Everything. Annual review of pharmacology and toxicology. 2018.

413. Han HJ, Lee YJ, Park SH, Lee JH, Taub M. High glucose-induced oxidative stress inhibits Na+/glucose cotransporter activity in renal proximal tubule cells. Am J Physiol Renal Physiol. 2005;288(5):F988-96.

414. Genet S, Kale RK, Baquer NZ. Alterations in antioxidant enzymes and oxidative damage in experimental diabetic rat tissues: effect of vanadate and fenugreek (Trigonellafoenum graecum). Molecular and cellular biochemistry. 2002;236(1-2):7-12.

415. Osorio H, Coronel I, Arellano A, Pacheco U, Bautista R, Franco M, et al. Sodium-glucose cotransporter inhibition prevents oxidative stress in the kidney of diabetic rats. Oxid Med Cell Longev. 2012;2012:542042.

416. Sait Celik HA.

Total Antioxidant Capacity, Catalase and Superoxide Dismutase on Rats Before and After Diabetes. Journal of Animal and Veterinary Advances. 2009;8(8):1503-8.

417. Chan JSD, Chan AHH, Jiang Q, Nie Z-R, LaChance S, Carrière S. Molecular cloning and expression of the rat angiotensinogen gene. Pediatric Nephrology. 1990;4(4):429-35.

418. Cui W, Bai Y, Miao X, Luo P, Chen Q, Tan Y, et al. Prevention of diabetic nephropathy by sulforaphane: possible role of Nrf2 upregulation and activation. Oxid Med Cell Longev. 2012;2012:821936.

419. Yoh K, Hirayama A, Ishizaki K, Yamada A, Takeuchi M, Yamagishi S, et al. Hyperglycemia induces oxidative and nitrosative stress and increases renal functional impairment in Nrf2-deficient mice. Genes to cells : devoted to molecular & cellular mechanisms. 2008;13(11):1159-70.

420. Uruno A, Furusawa Y, Yagishita Y, Fukutomi T, Muramatsu H, Negishi T, et al. The Keap1-Nrf2 system prevents onset of diabetes mellitus. Molecular and cellular biology. 2013;33(15):2996-3010.

421. Yu Z, Shao W, Chiang Y, Foltz W, Zhang Z, Ling W, et al. Oltipraz upregulates the nuclear factor (erythroid-derived 2)-like 2 [corrected](NRF2) antioxidant system and prevents

insulin resistance and obesity induced by a high-fat diet in C57BL/6J mice. Diabetologia. 2011;54(4):922-34.

422. He HJ, Wang GY, Gao Y, Ling WH, Yu ZW, Jin TR. Curcumin attenuates Nrf2 signaling defect, oxidative stress in muscle and glucose intolerance in high fat diet-fed mice. World J Diabetes. 2012;3(5):94-104.

423. Shin S, Wakabayashi J, Yates MS, Wakabayashi N, Dolan PM, Aja S, et al. Role of Nrf2 in prevention of high-fat diet-induced obesity by synthetic triterpenoid CDDO-imidazolide. Eur J Pharmacol. 2009;620(1-3):138-44.

424. Saha PK, Reddy VT, Konopleva M, Andreeff M, Chan L. The triterpenoid 2-cyano-3,12-dioxooleana-1,9-dien-28-oic-acid methyl ester has potent anti-diabetic effects in diet-induced diabetic mice and Lepr(db/db) mice. The Journal of biological chemistry. 2010;285(52):40581-92.

425. Xu J, Kulkarni SR, Donepudi AC, More VR, Slitt AL. Enhanced Nrf2 Activity Worsens Insulin Resistance, Impairs Lipid Accumulation in Adipose Tissue, and Increases Hepatic Steatosis in Leptin-Deficient Mice. Diabetes. 2012;61(12):3208-18.

426. More VR, Xu J, Shimpi PC, Belgrave C, Luyendyk JP, Yamamoto M, et al. Keap1 knockdown increases markers of metabolic syndrome after long-term high fat diet feeding. Free Radic Biol Med. 2013;61:85-94.

427. Dodson M, de la Vega MR, Cholanians AB, Schmidlin CJ, Chapman E, Zhang DD. Modulating NRF2 in Disease: Timing Is Everything. Annual review of pharmacology and toxicology. 2018.

428. Vaziri ND, Liu S, Farzaneh SH, Nazertehrani S, Khazaeli M, Zhao YY. Dose-dependent deleterious and salutary actions of the Nrf2 inducer dh404 in chronic kidney disease. Free Radic Biol Med. 2015;86:374-81.

429. Chin M, Lee CY, Chuang JC, Bumeister R, Wigley WC, Sonis ST, et al. Bardoxolone methyl analogs RTA 405 and dh404 are well tolerated and exhibit efficacy in rodent models of Type 2 diabetes and obesity. Am J Physiol Renal Physiol. 2013;304(12):F1438-46.

430. Hong DS, Kurzrock R, Supko JG, He X, Naing A, Wheler J, et al. A phase I first-in-human trial of bardoxolone methyl in patients with advanced solid tumors and lymphomas. Clin Cancer Res. 2012;18(12):3396-406.

431. Pergola PE, Krauth M, Huff JW, Ferguson DA, Ruiz S, Meyer CJ, et al. Effect of bardoxolone methyl on kidney function in patients with T2D and Stage 3b-4 CKD. American journal of nephrology. 2011;33(5):469-76.
432. Pergola PE, Raskin P, Toto RD, Meyer CJ, Huff JW, Grossman EB, et al. Bardoxolone Methyl and Kidney Function in CKD with Type 2 Diabetes. New England Journal of Medicine. 2011;365(4):327-36.
433. de Zeeuw D, Akizawa T, Audhya P, Bakris GL, Chin M, Christ-Schmidt H, et al. Bardoxolone Methyl in Type 2 Diabetes and Stage 4 Chronic Kidney Disease. The New England journal of medicine. 2013;369(26):2492-503.
434. Van Laecke S, Van Biesen W, Vanholder R. The paradox of bardoxolone methyl: a call for every witness on the stand? Diabetes, Obesity and Metabolism. 2015;17(1):9-14.
435. Kovac S, Angelova PR, Holmström KM, Zhang Y, Dinkova-Kostova AT, Abramov AY. Nrf2 regulates ROS production by mitochondria and NADPH oxidase. Biochimica et Biophysica Acta. 2015;1850(4):794-801.
436. Sogawa Y, Nagasu H, Iwase S, Ihoriya C, Itano S, Uchida A, et al. Infiltration of M1, but not M2, macrophages is impaired after unilateral ureter obstruction in Nrf2-deficient mice. Scientific Reports. 2017;7(1):8801.
437. Suzuki T, Seki S, Hiramoto K, Naganuma E, Kobayashi EH, Yamaoka A, et al. Hyperactivation of Nrf2 in early tubular development induces nephrogenic diabetes insipidus. Nature Communications. 2017;8:14577.
438. Yamawaki K, Kanda H, Shimazaki R. Nrf2 activator for the treatment of kidney diseases. Toxicology and applied pharmacology. 2018;360:30-7.
439. Rojo de la Vega M, Dodson M, Chapman E, Zhang DD. NRF2-targeted therapeutics: New targets and modes of NRF2 regulation. Current Opinion in Toxicology. 2016;1:62-70.
440. Shoemaker AH. NRF2 much of a good thing. Science Translational Medicine. 2017;9(420).
441. Miller KM, Foster NC, Beck RW, Bergenstal RM, DuBose SN, DiMeglio LA, et al. Current state of type 1 diabetes treatment in the U.S.: updated data from the T1D Exchange clinic registry. Diabetes Care. 2015;38(6):971-8.
442. Davies M. The reality of glycaemic control in insulin treated diabetes: defining the clinical challenges. Int J Obes Relat Metab Disord. 2004;28 Suppl 2:S14-22.

443. Pafili K, Maltezos E, Papanas N. Dapagliflozin for the treatment of type 1 diabetes mellitus. Expert Opinion on Investigational Drugs. 2017;26(7):873-81.
444. Salazar M, Rojo AI, Velasco D, de Sagarra RM, Cuadrado A. Glycogen synthase kinase-3beta inhibits the xenobiotic and antioxidant cell response by direct phosphorylation and nuclear exclusion of the transcription factor Nrf2. The Journal of biological chemistry. 2006;281(21):14841-51.
445. Keum YS, Yu S, Chang PP, Yuan X, Kim JH, Xu C, et al. Mechanism of action of sulforaphane: inhibition of p38 mitogen-activated protein kinase isoforms contributing to the induction of antioxidant response element-mediated heme oxygenase-1 in human hepatoma HepG2 cells. Cancer research. 2006;66(17):8804-13.
446. Cross DA, Alessi DR, Cohen P, Andjelkovich M, Hemmings BA. Inhibition of glycogen synthase kinase-3 by insulin mediated by protein kinase B. Nature. 1995;378(6559):785-9.
447. Decorsiere A, Cayrel A, Vagner S, Millevoi S. Essential role for the interaction between hnRNP H/F and a G quadruplex in maintaining p53 pre-mRNA 3'-end processing and function during DNA damage. Genes & development. 2011;25(3):220-5.
448. Dominguez C, Allain FH. NMR structure of the three quasi RNA recognition motifs (qRRMs) of human hnRNP F and interaction studies with Bcl-x G-tract RNA: a novel mode of RNA recognition. Nucleic Acids Res. 2006;34(13):3634-45.
449. DeFronzo RA, Tobin JD, Andres R. Glucose clamp technique: a method for quantifying insulin secretion and resistance. Am J Physiol. 1979;237(3):E214-23.
450. Tam CS, Xie W, Johnson WD, Cefalu WT, Redman LM, Ravussin E. Defining insulin resistance from hyperinsulinemic-euglycemic clamps. Diabetes Care. 2012;35(7):1605-10.
451. Gallo LA, Ward MS, Fotheringham AK, Zhuang A, Borg DJ, Flemming NB, et al. Once daily administration of the SGLT2 inhibitor, empagliflozin, attenuates markers of renal fibrosis without improving albuminuria in diabetic db/db mice. Scientific Reports. 2016;6:26428.
452. Su S, Cao M, Wu G, Long Z, Cheng X, Fan J, et al. Hordenine protects against hyperglycemia-associated renal complications in streptozotocin-induced diabetic mice. Biomedicine & Pharmacotherapy. 2018;104:315-24.
453. Kilbride SM, Farrelly AM, Bonner C, Ward MW, Nyhan KC, Concannon CG, et al. AMP-activated Protein Kinase Mediates Apoptosis in Response to Bioenergetic Stress through

Activation of the Pro-apoptotic Bcl-2 Homology Domain-3-only Protein BMF. The Journal of biological chemistry. 2010;285(46):36199-206.

454. Alkhalifah F, Pfeiffer SL, Halang L, Dussman H, Prehn JHM. The role of BH3-only protein Bmf in the pathogenesis of dominant negative hepatocyte nuclear factor-1 –induced mature-onset diabetes of the young in transgenic mice. BMC Proceedings. 2015;9(Suppl 7):A25-A.

455. Tang SC, Lai KN. The pathogenic role of the renal proximal tubular cell in diabetic nephropathy. Nephrology, dialysis, transplantation : official publication of the European Dialysis and Transplant Association - European Renal Association. 2012;27(8):3049-56.

456. Hasegawa K, Wakino S, Simic P, Sakamaki Y, Minakuchi H, Fujimura K, et al. Renal tubular Sirt1 attenuates diabetic albuminuria by epigenetically suppressing Claudin-1 overexpression in podocytes. Nat Med. 2013;19(11):1496-504.

457. Romagnani P, Remuzzi G. Renal progenitors in non-diabetic and diabetic nephropathies. Trends Endocrinol Metab. 2013;24(1):13-20.

458. Lo C-S, Chang S-Y, Chenier I, Filep JG, Ingelfinger JR, Zhang SL, et al. Heterogeneous Nuclear Ribonucleoprotein F Suppresses Angiotensinogen Gene Expression and Attenuates Hypertension and Kidney Injury in Diabetic Mice. Diabetes. 2012;61(10):2597-608.

459. Ghosh A, Abdo S, Zhao S, Wu CH, Shi Y, Lo CS, et al. Insulin Inhibits Nrf2 Gene Expression via Heterogeneous Nuclear Ribonucleoprotein F/K in Diabetic Mice. Endocrinology. 2017.

460. Miani M, Elvira B, Gurzov EN. Sweet Killing in Obesity and Diabetes: The Metabolic Role of the BH3-only Protein BIM. Journal of Molecular Biology. 2018;430(18, Part B):3041-50.

461. Hornsveld M, Tenhagen M, van de Ven RA, Smits AM, van Triest MH, van Amersfoort M, et al. Restraining FOXO3-dependent transcriptional BMF activation underpins tumour growth and metastasis of E-cadherin-negative breast cancer. Cell death and differentiation. 2016;23(9):1483-92.

462. Contreras AU, Mebratu Y, Delgado M, Montano G, Hu CA, Ryter SW, et al. Deacetylation of p53 induces autophagy by suppressing Bmf expression. The Journal of cell biology. 2013;201(3):427-37.

463. Chan G, Gu S, Neel BG. Erk1 and Erk2 are required for maintenance of hematopoietic stem cells and adult hematopoiesis. Blood. 2013;121(18):3594-8.

Annex 1: List of Publications

1. Ghosh A, Zhao S, Lo CS, Maachi H, Chenier I, Lateef MA, Abdo S, Filep J, Ingelfinger JR, Zhang SL, Chan JSD. Heterogeneous Nuclear Ribonucleoprotein F Mediates Insulin Inhibition of Bcl2-Modifying Factor Expression and Tubulopathy in Diabetic Kidney. Scientific Reports. 2019, SREP-18-36519B (Manuscript accepted for publication, Feb 4th 2019)

2. Ghosh A, Abdo S, Zhao S, Wu CH, Shi Y, Lo CS, Chenier I, Alquier T, Filep JG, Ingelfinger JR, Zhang SL, Chan JSD. Insulin Inhibits Nrf2 Gene Expression via Heterogeneous Nuclear Ribonucleoprotein F/K in Diabetic Mice. Endocrinology (2017) 158 (4): 903-919.

3. Zhao S, Ghosh A, Lo CS, Chenier I, Scholey JW, Filep JG, Ingelfinger JR, Zhang SL, Chan JS. Nrf2 Deficiency Upregulates Intrarenal Angiotensin-Converting Enzyme-2 and Angiotensin 1-7 Receptor Expression and Attenuates Hypertension and Nephropathy in Diabetic Mice. Endocrinology. 2018;159(2):836-852.

4. Lo CS, Y. Shi, I. Chenier, A. Ghosh, CH. Wu, JF. Cailhier, J. Ethier, J-B. Lattouf, JG. Filep, JR. Ingelfinger, SL Zhang, JS Chan. Heterogeneous Nuclear Ribonucleoprotein F Stimulates Sirtuin-1 Gene Expression and Attenuates Nephropathy Progression in Diabetic Mice. Diabetes, 2017, (66(7):1964-1978).

5. Abdo S, Shi Y, Otoukesh A, Ghosh A, Lo CS, Chenier I, Filep JG, Ingelfinger JR, Zhang SL, Chan JSD. Catalase Overexpression Prevents Nuclear Factor Erythroid 2-Related Factor 2 Stimulation of Renal Angiotensinogen Gene Expression, Hypertension and Kidney Injury in Diabetic Mice. Diabetes, 2014. (63:3483-3496)